DYNAMICS AND OPTIMAL CONTROL OF FLEXIBLE HEAT-EXCHANGER NETWORKS

by

V. CANTÜRK BOYACI

B. S. in Ch. E., Boğaziçi University, 1993

Submitted to the Institute for Graduate Studies in
Science and Engineering in partial fulfillment of
the requirements for the degree of
Master of Science
in
Chemical Engineering

Boğaziçi University

1995

ACKNOWLEDGMENT

I would like to express my deepest appreciation to Doç. Dr. Uğur Akman for his invaluable guidance, understanding and encouragement throughout my study. I am also grateful to Prof. Dr. Öner Hortaçsu and Prof. Dr. Osman Türkay for the time they devoted to reading and commenting on my thesis.

Graduate assistantship granted throughout my studies by the Department of Chemical Engineering is gratefully acknowledged.

I would also like to extend my thanks to Nihat Baysal and Alp Er Ş. Konukman for their help and interest in my work. Heartfelt thanks are due to Mine Kaplan, Özlem Keskin, Özge Güney, Mehmet Karaaslan, Derya Uztürk and Bülent Turgay for their continuous encouragement, willingness to help and kinship, and to all my friends in the Department for their support and friendship.

Special thanks are due to Serkan Sağlam for his endless help and kind support, and for the cheerful times we spent.

Last but not the least, I would also thank to Nihan Eren, to whom I am deeply indebted, for her everlasting encouragement, enthusiasm and support in completion of this work.

Finally, this thesis is dedicated to my family for their support and confidence.

ABSTRACT

In this work, the dynamics, controllability and resiliency of Heat-Exchanger Networks (HENs) are investigated.

A rigorous distributed-parameter model of typical countercurrent shell-and-tube (multi-tube) heat exchangers constituting the HENs to be studied was developed. The model consists of four coupled partial-differential equations (PDEs) for each exchanger and includes energy balances for the shell (cold) and tube (hot) fluids, and for the shell and tube walls. The advanced numerical-solution algorithm eliminated the steady-state offset problem mentioned in encountered literature.

Dynamic models of the HENs were constructed by connecting the exchanger models through boundary conditions in accordance with the network structure. Flow rates of bypass streams around exchangers were considered as the only manipulated variables, and the target streams of the HEN, were considered as the controlled variables.

Two centralized optimal-control algorithms were developed and tested for various HENs, for different sets of disturbances in source-stream temperatures, and for different control-range constraints on target-stream-temperatures. In both of the algorithms, first, the values of the optimal bypass openings are determined by an optimizer which satisfies the control-precision constraints (hard or soft) imposed on the target streams by referring to the algebraic model of the HEN. The optimizer, thus, finds a feasible and optimal post-disturbance steady-state operating point around the pre-disturbance operating point. In cases where the HEN structure allows, the post-disturbance feasible operating point may as well be the nominal (pre-disturbance) operating point.

In the centralized open-loop (without state feed back) control algorithm, the bypasses were opened from their nominal values (which may be zero) up to their optimal values as a function of time. The use of ramp functions resulted in very satisfactory dynamic response of the HENs, and temporal violation of the control-range constraints were prevented by optimal tuning of the rate with which the bypasses were opened.

In the centralized closed-loop (with state feedback) control algorithm, bypasses were opened from their nominal values up to their optimal values as dependent on the pseudo-controlled target-stream temperatures. The use of state feedback resulted in smoother dynamic response for a sample HEN. However, the closed-loop algorithm, in its presented form, cannot always prevent temporal violation of the control-range constraints.

Overall, both of the proposed centralized (hierarchical) model-based optimal-control algorithms proved to be promising in control of HENs.

ÖZET

Bu çalışmada ısı değiştirici ağlarının (IDA) dinamiği, denetlenebilirliği ve dinamik esnekliği incelenmiştir.

İncelenecek IDA'ları oluşturan ters akımlı, kabuklu borulu tipik ısı değiştiricilerin (çok borulu) (dağıtımlı-parametre) modeli geliştirilmiştir. Bu model, her bir ısı değiştiricisi için, bileşkeli dört kısmi diferansiyel denklemden oluşmuş olup, kabuk (soğuk akım) ile boru (sıcak akım) akışkanlarının ve kabuk ile boru metal kısımlarının enerji dengelerini kapsamaktadır. Literatürde sıkça karşılaşılan yatışkın durum uyumsuzluğu, ileri bir sayısal çözüm algoritması kullanılarak aşılmıştır.

Isı değiştirici modelleri, ağ yapısına uygun olacak şekilde, sınır değerleri vasıtasıyla birbirine bağlanarak IDA'ların dinamik modeli elde edilmiştir. Isı değiştiricilerin etrafındaki yangeçit akımlarının debileri IDA'ların tek karar değişkeni, hedef akım sıcaklıkları ise kontrol değişkenleri olarak ele alınmıştır.

İki farklı merkezi eniyi denetim algoritmaları geliştirilmiş ve bu algoritmalar çeşitli IDA'larda, kaynak akım sıcaklıklarında farklı bozucu etki değerleri ve hedef akım sıcaklıklarında farklı denetim sınırları kısıtları için denenmiştir. Her iki modelde de önce, IDA modelini göz önünde bulundurarak hedef akımı sıcaklıklarının denetim sınırı kısıtlarını sağlayan yangeçit oranları eniyileme yöntemiyle bulunmuştur. Bu eniyileme ile bozucu etki öncesi çalışılan nokta (yatışkın durum) etrafında uygun ve eniyi yeni bir bozucu etki sonrası çalışma noktası bulunmuştur. Bazı durumlarda, IDA yapısının elverdiği ölçüde, bozucu etki sonrası uygun çalışma noktası, nominal (bozucu etki öncesi) çalışma noktası ile çakışabilir.

Merkezi açık döngü (geri beslemeli olmayan) denetim algoritmasında, yangeçitler nominal değerlerinden (bu nominal değerler sıfır olabilir) eniyi değerlerine kadar zamanın bir fonksiyonu olarak açılmışlardır. Yangeçitlerin zamanla doğrusal olarak açılması, IDA'ların dinamik tepkilerinin çok tatmin edici olmasıyla sonuçlanmıştır. Denetim sınır kısıtlarının geçici olarak aşılmaları ise yangeçitlerin zaman içinde eniyi açılma oranlarının ayarlanmasıyla engellenmiştir.

Merkezil kapalı döngü (geri beslemeli) denetim algoritmasında, yangeçitler nominal değerlerinden eniyi değerlerine görünürde denetlenen hedef akım sıcaklıklarına bağlı olarak açılmışlardır. Bu geri beslemeli uygulama sonucunda aynı IDA örneğinin dinamik tepkisinin açık döngü algoritmasına göre daha düzgün olduğu gözlenmiştir. Ancak bu kapalı çevrim denetim algoritması burada açıklandığı şekliyle denetim sınır kısıtlarını her zaman sağlayamaz.

Genel olarak merkezil modeli temel alan her iki eniyi denetim algoritması da, IDA' ların denetimi için umut vericidir.

TABLE OF CONTENTS

LIST OF FIGURES

Page

Page

Page

Page

LIST OF TABLES

LIST OF SYMBOLS

a ,b	Parameters in temperature-dependent property relationships
A	Heat-transfer area, m^2
a_C	Outer surface area of a single tube per unit length, m^2
A_C	Crossectional flow area of shell fluid, m^2
a_H	Inner surface area of a single tube per unit length, m^2
A_H	Inner Crossectional area of a single tube, m^2
A_n	Heat-transfer area of n^{th} heat exchanger, m^2
A_{req}	Required heat transfer area for specified heat duty, m^2
a_S	Inner surface area of shell wall per unit length, m^2
A_S	Crossectional area of shell wall material, m^2
A_T	Crossectional area of tube wall material, m^2
c	Vector of control ranges for target streams, K
C_p	Heat capacity, J/kg K
C_{P_C}	Heat capacity of cold fluid, J/kg K
C_{P_H}	Heat capacity of hot fluid, J/kg K
C_{pi}	Heat capacity of tube fluid, J/kg K
C_{po}	Heat capacity of shell fluid, J/kg K
C_{P_S}	Heat capacity of shell-wall material, J/kg K
C_{P_T}	Heat capacity of tube-wall material, J/kg K
Cl	Diametrical shell-bundle clearance, m
d	Vector of disturbances imposed on supply-temperatures, K
D_b	Tube-bundle diameter, m
d_i	Inner tube diameter, m

$\mathbf{d}_n$	N^{th} Vector of Disturbances imposed on supply-temperatures, K
d_o	Outer tube diameter, m
d_{otl}	Shell outer tube limit, m
D_s	Inside diameter of shell, m
F_{bp}	Fraction of crossflow area available for bypass flow, m^2
F_T	Correction factor for deviation from countercurrent flow
F_{tc}	Fraction of total tubes in crossflow
G_i	Mass velocity, kg/m^2 s
G_o	Mass velocity of shell fluid, kg/m^2s
Gz	Graetz Number
h_C	Heat-transfer coefficient for shell-side cold fluid, W/m^2K
h_H	Heat-transfer coefficient for tube-side hot fluid, W/m^2 K
h_i	Inside heat-transfer coefficient, W/m^2K
h_o	Outside heat-transfer coefficient, W/m^2K
$h_{o,ideal}$	Actual outside heat-transfer coefficient, W/m^2K
h_S	Heat-transfer coefficient of shell wall, W/m^2K
j_H	Correction factor for outside heat-transfer coefficient
k	Thermal Conductivity, W/m K
K_1	Parameter of tube-bundle equation
k_i	Thermal conductivity of tube fluid, W/m K
k_o	Thermal conductivity of shell fluid, W/m K
k_w	Thermal conductivity of tube- and shell-wall material, W/m K
L	Length of heat-exchanger, m
L^0	Initial guess of heat exchanger length, m
l_b	Baffle spacing, m
l_c	Baffle cut, m
$l_{in,out}$	Inlet and outlet baffle spacing, m
l_s	Tube sheet thickness, m
n	Heat exchanger number
n_1	Parameter of tube-bundle equation
N_b	Number of baffles in the exchanger
N_c	Number of tube rows crossed in one crossflow section

NCS	Number of cold streams
N_{cw}	Number of effective crossflows in each window
N_{HEX}	Number of heat exchangers
NHS	Number of hot streams
N_{ODE}	Number of ordinary differential equations
N_{PDE}	Number of partial differential equations
N_{ss}	Number of pairs of sealing strips
N_T	Total number of tubes in the assembly
N_{TP}	Number of tube passes in the bundle
N_T^0	Initial guess of number of tubes
Nu	Nusselt Number
N_Z	Number of grid points
p_n	Tube pitch normal to flow,m
p_P	Tube pitch parallel to flow, m
Pr_i	Prandtl Number of tube fluid
Pr_o	Prandtl Number of shell fluid
p_T	Tube pitch, m
Re	Reynold's Number
Q	Heat-transfer rate, W
R_{di}	Inner fouling resistance, m^2K/W
R_{do}	Outer fouling resistance, m^2K/W
S_m	Crossflow area at center line for one crossflow section, m^2
S_{sb}	Shell to baffle leakage area for one baffle, m^2
S_{tb}	Tube bundle leakage area for one baffle spacing, m^2
t	time, s
T	Temperature, K
$\Delta T_{a,n}$	Minimum approach temperature, K
T_C	Temperature of cold fluid, K
T_C^0	Initial temperature of cold fluid, K
T_C^b	Bulk temperature of cold fluid, K
T_C^i	Inlet temperature of cold stream to heat-exchanger, K

T_C^o	Outlet temperature of cold stream from heat-exchanger, K
$T_{C,n}^e$	Effluent temperature of cold stream (before bypass mixing) from n^{th} heat exchanger, K
$T_{C,n}^i$	Inlet temperature of cold stream of n^{th} heat exchanger, K
$T_{C,n}^o$	Outlet temperature of cold stream (after bypass mixing) of n^{th} heat exchanger, K
$\overline{T}_{C,n}^o$	Nominal outlet temperature of cold stream (after bypass mixing) from n^{th} heat exchanger, K
$\Delta T_{C,n}^o$	Cold-stream outlet-temperature deviation of n^{th} heat exchanger, K
$T_{C,n}^s$	Supply temperature of cold stream of n^{th} heat exchanger, K
$\overline{T}_{C,n}^s$	Nominal supply temperature of cold stream of n^{th} heat exchanger, K
$\Delta T_{C,n}^s$	Cold-stream supply-temperature deviation of n^{th} heat exchanger, K
$T_{C,n}^t$	Target temperature of cold stream of n^{th} heat exchanger, K
$\overline{T}_{C,n}^t$	Nominal cold-stream target temperature of n^{th} heat exchanger, K
$\Delta T_{C,n}^t$	Cold-stream target-temperature deviation of n^{th} heat exchanger, K
T_H	Temperature of hot fluid, K
T_H^0	Initial temperature of hot fluid, K
T_H^b	Bulk temperature of hot fluid, K
T_H^i	Inlet temperature of hot stream to heat-exchanger, K
T_H^o	Outlet temperature of hot stream from heat-exchanger, K
$T_{H,n}^e$	Effluent temperature of hot stream (before bypass mixing) from n^{th} heat exchanger, K
$T_{H,n}^i$	Inlet temperature of hot stream of n^{th} heat exchanger, K
$T_{H,n}^o$	Outlet temperature of hot stream (after bypass mixing) from n^{th} heat exchanger, K

$\overline{T}^{o}_{H,n}$	Nominal outlet temperature of hot stream (after bypass mixing) from n^{th} heat exchanger, K
$\Delta T^{o}_{H,n}$	Hot-stream outlet-temperature deviation of n^{th} heat exchanger, K
$T^{s}_{H,n}$	Supply Temperature of hot stream of n^{th} heat exchanger, K
$\overline{T}^{s}_{H,n}$	Nominal supply temperature of hot stream of n^{th} heat exchanger, K
$\Delta T^{s}_{H,n}$	Hot-stream supply-temperature deviation of n^{th} heat exchanger, K
$T^{t}_{H,n}$	Target temperature of hot stream of n^{th} heat exchanger, K
$\overline{T}^{t}_{H,n}$	Nominal hot-stream target temperature of n^{th} heat exchanger, K
$\Delta T^{t}_{H,n}$	Hot-stream target-temperature deviation of n^{th} heat exchanger, K
ΔT_{lm}	Log-mean temperature difference, K
T^{e}_{n}	Effluent temperature (before bypass mixing) from n^{th} heat exchanger, K
$T^{e}_{n}(0)$	Effluent temperature (before bypass mixing) from n^{th} heat exchanger at t=0, K
$T^{e}_{n}(\infty)$	Effluent temperature (before bypass mixing) from n^{th} heat exchanger at steady state, K
T^{i}_{n}	Inlet temperature of n^{th} heat exchanger, K
T^{t}_{n}	Target temperature of n^{th} heat exchanger, K
T^{0}_{S}	Initial temperature of shell wall, K
T_{ref}	Reference temperature for fluid properties, K
T_{S}	Temperature of shell wall, K
T_{T}	Temperature of tube wall, K
T^{0}_{T}	Initial temperature of tube wall, K
$\overline{T}^{t}$	Nominal target temperature, K
ΔT^{t}	Target temperature deviation, K
T_{w}	Tube wall temperature, K
T^{i}	Inlet temperature to heat exchanger, K
T^{o}	Outlet temperature from heat exchanger, K

t^{∞}	Steady state time, s
U	Overall heat-transfer coefficient, W/m^2 K
$\mathbf{u}_C$	Vector of bypass stream fractions on cold stream
$\mathbf{u}_C^{opt}$	Optimal vector of bypass fractions on cold fluids
$u_{C,n}$	Bypass stream fraction on cold stream of n^{th} heat exchanger
$\mathbf{u}_H$	Vector of bypass stream fractions on hot stream
$\mathbf{u}_H^{opt}$	Optimal vector of bypass fractions on hot fluids
$u_{H,n}$	Bypass stream fractions on hot stream of n^{th} heat exchanger
$\mathbf{u}_n$	Vector of bypass stream openings of bypasses of n^{th} heat-exchanger
$\bar{\mathbf{u}}_n$	Nominal vector of bypass stream openings of bypasses of n^{th} heat-exchanger
$\mathbf{u}_n^{opt}$	Optimum bypass stream opening vector of bypasses of n^{th} heat-exchanger
U_n	Overall heat-transfer coefficient of n^{th} heat exchanger
U_o	Heat-transfer coefficient based on outside tube area, W/m^2 K
u^{max}	Maximum allowable bypass stream fraction
$\mathbf{u}^{opt}$	Optimal vector of bypass stream fractions
v	velocity, m/s
v_C	Velocity of cold fluid, m/s
v_H	Velocity of hot fluid, m/s
W	Heat capacity flowrate, J/s K
w_C	Mass flowrate of cold fluid, kg/s
	W_C Heat capacity flowrate of cold fluid, J/s K
$w_{C,n}$	Mass flowrate of cold fluid of n^{th} heat exchanger, kg/s
w_H	Mass flowrate of hot fluid, kg/s
W_C	Heat capacity flowrate of hot fluid, J/s K
$w_{H,n}$	Mass flowrate of hot fluid of n^{th} heat exchanger, kg/s
w_i	Mass flowrate of tube fluid, kg/s
w_o	Mass flowrate of shell fluid, kg/s
z	Axial direction
δ_{sb}	Diametrical shell-baffle clearance, m
ε	Incremental length, m

ε_1	Sum of deviations of target temperatures from their nominal values, K
ε_2	Sum of deviations of target temperatures from their final target values, K
ε_M	Mismatch error between physical and required heat-transfer area, m^2
ϕ_l	Correction factor for baffle-leakage effects
ϕ_b	Correction factor for bundle-bypassing effects
ϕ_c	Correction factor for baffle-configuration effects
ϕ_r	Correction factor for-adverse temperature-gradient built-up at low Re
ϕ_s	Correction factor for unequal baffle spacing at inlet and outlet
μ	viscosity, Ns/m^2
μ_i	Viscosity of tube fluid, Ns/m^2
μ_o	Viscosity of shell fluid, Ns/m^2
μ_{ow}	Viscosity of water in shell-side, Ns/m^2
μ_w	Viscosity of water, Ns/m^2
ρ	Density, kg/m^3
ρ_C	Density of cold fluid, kg/m^3
ρ_H	Density of hot fluid, kg/m^3
ρ_i	Density of tube fluid, kg/m^3
ρ_o	Density of shell fluid, kg/m^3
ρ_S	Density of shell-wall material, kg/m^3
ρ_T	Density of tube-wall material, kg/m^3
τ	Vector of opening times of bypass streams, s
τ_i	Opening time of i^{th} bypass stream, s
τ_i^{opt}	Optimal bypass stream opening time of i^{th} bypass stream, s

1. INTRODUCTION

Heat Exchanger Networks (HENs) are among the major components of chemical processing systems because they determine to a large extent the energy efficiency of processes. In HENs, thermal preparation of various hot and cold stream are accomplished by matching them in order to reduce the utility consumption and/or total heat-transfer area.

Most HEN synthesis algorithms [1, 2, 3, 4], which have been developed as a result of extensive research carried out over two decades, decompose the synthesis problem into at least two stages: i) targeting of minimum utility consumption and minimum number of units (exchangers, heaters, and coolers), ii) synthesis of a HEN structure with minimum utility consumption and with a minimum or close to a minimum number of units. However, such algorithms, since they generate HENs for fixed (nominal) values of the stream supply temperatures, flow rates, and heat-transfer coefficients, do not account for the possible disturbances due to changes in inlet temperatures, flow rates, and heat-transfer coefficients of the supply streams. Both the temperatures and flow rates of the incoming streams may introduce disturbances to a HEN owing to uncontrolled upsets in the upstream process units and affect the target stream(s), and, in turn, affects the operations carried out in the downstream process units. The target temperatures of the outgoing streams of the HEN should be tightly controlled for the safety of operations carried out in the downstream process units.

The synthesized HEN must be both flexible (ability to meet the requirements of changing/desired conditions; *static resilience*), and resilient (ability to tolerate and recover from undesired changes; *dynamic resilience*) [5] to the possible changes mentioned above to be able to control the network outlet (target) temperatures at desired values or within a given permissible range. The degrees of freedom to achieve the control objectives are

owing to the bypass streams which are not considered in traditional static HEN synthesis methods, and to stream-split ratios which are not frequently encountered in traditionally synthesized HENs.

Quite a few authors have looked at the flexibility and controllability of HENs simultaneously. Mathisen et al. [6] reviewed different controllability measures and showed how these measures might be used to select bypasses and appropriate pairings among controlled variables (target temperatures) and manipulated variables (bypass-stream flow rates). They concluded that structural designs and bypass selections where all critical targets are controlled by either utility streams or bypasses with a direct effect should be preferred. These authors also found that flow-rate dependence of heat-transfer coefficients had significant effect on control. Mathisen et al. [7, 8] and Mathisen [9] also, suggested several optimization problems and proposed to take controllability into account by adding control-related constraints to the flexibility-problem formulation. They also derived a target for the number of bypasses. The same authors argued that the use of multi-bypasses (bypassing more than one exchanger) might increase both flexibility and controllability, when both outlet temperatures of one exchanger were controlled outputs. Konukman et al. [5] have investigated the effects of bypass streams on disturbance propagation paths via formulating the problem as constrained nonlinear optimization (minimization of total bypass flows subject to target-stream temperature constraints and minimization of target-temperature deviations subject to target-stream temperature constraints) for typical pre-designed HENs. In each case, different range constraints on the hot and cold targets are imposed in order to demonstrate the possibility of creation of alternate disturbance-propagation paths via bypass-stream manipulations. Later, Konukman et al. [10] developed a method for simultaneous optimization and retrofit design (by the addition of bypass streams and the manipulation of the exchanger areas) of HENs. The authors argued that such retrofit HEN designs are both flexible and controllable for a predefined retrofit design resiliency index, called RDRI, which is a measure of the disturbance magnitudes pre-specified in all possible directions. The optimization framework (minimum cost for the specified RDRI) of Konukman et al. [10] enables simultaneous testing and comparison of retrofit design costs and design resiliency of alternative HEN structures.

The aims of this thesis are to develop rigorous distributed-parameter-based dynamic models of heat exchangers to investigate the relationships among flexibility, controllability, resiliency, and dynamic behavior of HENs, and to develop and apply an optimal-control algorithm such that the HENs having static resilience will have dynamic resilience as well.

In Chapter 2, a detailed design algorithm of individual heat exchangers constituting the HEN is demonstrated. Single-tube-pass shell-and-tube heat exchangers are chosen as the exchanger type. The design parameters are selected such that the resulting exchangers are close to off-the-shelf-type heat exchangers.

Chapter 3 deals with developing a rigorous distributed-parameter model (partial differential equations) for the heat exchanger designed in Chapter 2. To be as realistic as possible, the partial differential equations of the tube and shell walls are also included in the model. These partial differential equations models of the individual exchangers are then interconnected according to the HEN structure to investigate the dynamics of the HEN.

The concern of Chapter 4 is to find alternative feasible steady-state operating points, along with the optimal bypass-stream openings, such that the target-stream temperatures are kept exactly at the desired nominal conditions or within the specified control range when the HEN is imposed to a specified disturbance.

In Chapter 5, both the uncontrolled dynamics, and the dynamics and controllability of the HENs under an open-loop (no state feed-back) optimal-control algorithm are investigated. The ways of implementing the manipulated variables (instantaneous application or time-dependent manipulation of the optimal bypass openings) to obtain a satisfactory and smooth dynamic response are developed. Optimal-control schemes based on the control-vector-parameterization technique are developed and tested for various HEN structures.

In Chapter 6, dynamics and controllability of HENs under an optimal closed-loop control (target-temperature-dependent bypass-stream manipulation) algorithm are studied.

Some concluding remarks and recommendations for future works, are provided in Chapter 7.

2. DESIGN OF HEAT EXCHANGERS

In this chapter, a methodology for the design of individual heat exchangers constituting the HEN will be explained.

All terminal temperatures of the heat exchangers constituting the HEN to be analyzed in the subsequent chapters are known. Using this information on terminal temperatures along with the specified length of the exchanger and other related information, the individual heat-transfer coefficients, and hence the overall heat-transfer coefficient, can be calculated. These detailed design calculations enable determination of the parameters such as the number of tubes, shell diameter, crossectional flow areas etc., which are utilized in the dynamic models of the exchangers in the proceeding chapters.

To accomplish this design task, a software program, the details of which are available in [11], was used. There are six important key variables: T_C^i, T_C^o, T_H^i, T_H^o, w_C, and w_H (see Figure 2.1). The program is capable of performing the following calculations:

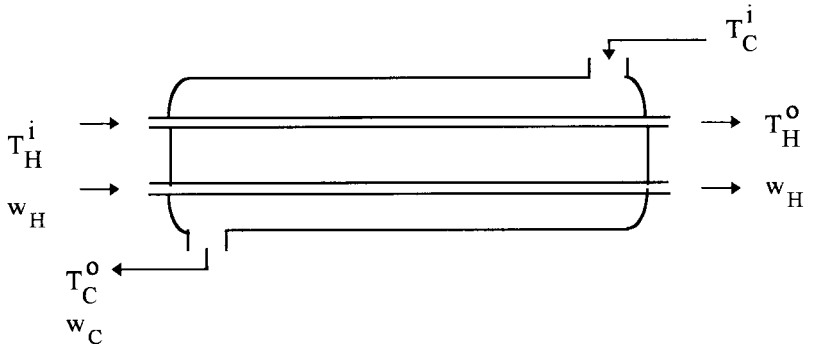

FIGURE 2.1. Nomenclature for a 1-1 (One-Shell-One-Tube Pass) Multi Tube Heat Exchanger.

a) If all the key variables are specified, the energy balance is checked for consistency. If the degree of inconsistency is high, the heat duty of the hot fluid is taken for further calculations [11].

b) If one of the key variables is not specified, this variable is determined by the energy balance [11].

c) If four variables are specified, an iterative procedure is performed to find a solution that satisfies simultaneously both the energy balance and the heat-transfer calculations [11].

In all cases, the extent of overdesign or underdesign are determined by comparing the required heat-transfer area satisfying the heat duty with the actual area (physical area) [11].

Since all of the six key variables of the exchangers of the HEN to be studied were specified in this work, the algorithm was modified so that only the consistency check option was accessible. The procedure and the equations of the modified algorithm is as follows:

The main objective in the design of an exchanger is to determine the required heat-transfer area. In order to perform the design, some of the parameters such as the inner and outer tube diameters shell-wall thickness, etc., must be specified. If these parameters are taken from standard heat-exchanger design literature, the resulting exchanger will be closer to an off-the-shelf type exchanger. The modified algorithm also contains some additional design calculations which are not present in the original algorithm [11]; such as the calculation of the diameter of the tube bundle and the inner diameter of the shell.

The equation of heat transfer across a surface is given by:

$$Q = U A \Delta T_{lm} \tag{2.1}$$

where,

$$\Delta T_{lm} = \frac{(T_H^i - T_C^o) - (T_H^o - T_C^i)}{\ln\left(\frac{T_H^i - T_C^o}{T_H^o - T_C^i}\right)} \tag{2.2}$$

In Equation (2.2), it is implicitly assumed that the flow is countercurrent, heat capacities, flow rates and overall heat-transfer coefficient are constant, and heat losses are negligible. In exchangers with multi tube passes, the flows deviate from ideal countercurrent flow. In these exchangers both countercurrent and cocurrent flows exist. In such cases, the common way of estimating the true temperature difference from the log-mean temperature is by applying a correction factor, F_T , to allow for the deviation from true countercurrent flow as:

$$\Delta T_{lm} = F_T \Delta T_{lm} \tag{2.3}$$

The correction factor, F_T , depends on the number of tube passes. Since in this work only 1-1 (one-shell-one-tube pass) multi tube exchangers were considered, the value of the correction factor was taken as unity.

Evaluation of the overall heat-transfer coefficient requires the estimation of the tube-side and shell-side heat-transfer coefficients. Overall heat-transfer coefficient is the sum of the reciprocals of several individual heat-transfer resistances. On the basis of outside tube surface, it is defined as:

$$\frac{1}{U_o} = \frac{d_o}{d_i}\frac{1}{h_i} + \frac{1}{h_o} + \frac{(d_o - d_i)}{2k_w} + R_{di} + R_{do} \tag{2.4}$$

If the parameters d_o , d_i , k_w , R_{di}, and R_{do} are specified, the remaining variables should be estimated.

2.1. Estimation of the Tube-Side Heat-Transfer Coefficient

The local heat-transfer coefficient for the tube side, h_i, can be calculated from Nusselt Number which is defined as:

$$Nu = \frac{h_i d_i}{k_i} \tag{2.5}$$

The correlations for the Nu depends on Reynold's Number, which is defined for the tube side as:

$$Re = \frac{d_i G_i}{\mu_i} \tag{2.6}$$

where, G_i is the mass velocity and is given by:

$$G_i = \frac{4W_i}{n\pi d_i^2} \tag{2.7}$$

where, W_i is the total mass flow rate in tube side and n is the number of tubes per pass.
For $Re \leq 2100$, Nu is defined as [11]:

$$Nu = 3.66 + \frac{0.085Gz}{1+0.047Gz^{2/3}}\left(\frac{\mu_i}{\mu_w}\right)^{0.14} \qquad \text{for } Gz \leq 100 \qquad (2.8)$$

$$Nu = 1.86Gz^{1/3}\left(\frac{\mu_i}{\mu_w}\right)^{0.14} \qquad \text{for } Gz > 100 \qquad (2.9)$$

where, Gz is the Graetz Number and is defined as:

$$Gz = \frac{d_i^2 G_i C_{pi}}{k_i L} \qquad (2.10)$$

For $2100 < Re < 10^4$, Nu becomes [11]

$$Nu = 0.116\,(Re^{2/3} - 125)\,Pr^{1/3}\left[1+\left(\frac{d_i}{L}\right)^{2/3}\right]\left(\frac{\mu_i}{\mu_w}\right)^{0.14} \qquad (2.11)$$

where Pr is the Prandtl Number and is defined as:

$$Pr = \frac{C_{pi}\mu_i}{k_i} \qquad (2.12)$$

For turbulent flow ($Re \geq 10^4$), Nu becomes [11],

$$Nu = 0.023\,Re^{0.8}\,Pr^{0.33}\left(\frac{\mu_i}{\mu_w}\right)^{0.14} \tag{2.13}$$

2.2. Estimation of the Shell-Side Heat-Transfer Coefficient

The determination of the shell-side heat-transfer coefficient, h_o, is more complex. It is a common way to correlate heat-transfer data in terms of j_H. An empirical equation for j_H is as follows [11]

$$j_H = a_1\,Re^{a_2}\left(\frac{1.33d_o}{p_T}\right)^{a} \tag{2.14}$$

with

$$a = \frac{a_3}{1+0.14\,Re^{a_4}} \tag{2.15}$$

where, p_T represents the tube pitch. The coefficients a_1 to a_4 can be found in [11].

The Re for the shell side is calculated according to:

$$Re = \frac{d_o W_o}{\mu_o S_m} \tag{2.16}$$

where, S_m represents the crossflow area at or near the center line for one crossflow section, which is defined as [11]:

for rotated and in-line square layouts:

$$S_m = 1_b \left[D_s - d_{otl} + \frac{d_{otl} - d_o}{p_n} \left(p_T - d_o \right) \right] \tag{2.17}$$

for triangular layouts:

$$S_m = 1_b \left[D_s - d_{otl} + \frac{d_{otl} - d_o}{p_T} \left(p_T - d_o \right) \right] \tag{2.18}$$

In these equations, p_n represents tube pitch normal to flow, which is defined as [11]:

$$p_n = p_T \quad \text{for in-line square layout} \tag{2.19}$$

$$p_n = \frac{p_T}{\sqrt{2}} \quad \text{for rotated square layout} \tag{2.20}$$

$$p_n = \frac{p_T}{2} \quad \text{for triangular layout} \tag{2.21}$$

After Re and j_H are determined, the shell-side heat-transfer coefficient for an ideal tube bank can be calculated from:

$$\frac{h_o}{C_{po} G_o} = j_H \, Pr_o^{-2/3} \left(\frac{\mu_o}{\mu_{ow}} \right)^{0.14} \tag{2.22}$$

Since there are some distortions of flow pattern introduced by the baffles, presence of leakage, and bypass flow through clearances, the calculated heat-transfer coefficient for an ideal tube bank must be corrected by the following correction factors[11]:

Baffle Configuration Factor: It accounts for the effects of the baffle configuration. It is expressed as [11]:

$$\phi_c = F_{tc} + 0.54\left(1 - F_{tc}\right)^{0.345} \tag{2.23}$$

where, F_{tc} represents the fraction of total tubes in crossflow, which is given by:

$$F_{tc} = \frac{1}{\pi}\left[\pi + 2\frac{D_s - 2l_c}{d_{otl}} \sin\left(\cos^{-1}\frac{D_s - 2l_c}{d_{otl}}\right) - 2\left(\cos^{-1}\frac{D_s - 2l_c}{d_{otl}}\right)\right] \tag{2.24}$$

Baffle Leakage Factor: It accounts for the effects of the baffle leakage. It is expressed as [11]:

$$\phi_l = \alpha + (1-\alpha)\exp\left[-2.2\frac{S_{tb}+S_{sb}}{S_m}\right] \tag{2.25}$$

with

$$\alpha = 0.44\left(1-\frac{S_{sb}}{S_{tb}+S_{sb}}\right) \tag{2.26}$$

where, S_{tb} represents the tube-to-baffle hole leakage area, which is given by [11]:

$$S_{tb} = 15.81 d_0 N_T (1+F_{tc}) \tag{2.27}$$

and where, S_{sb} represents the shell-to-baffle leakage area for one baffle, which is given by [11]:

$$S_{sb} = \frac{D_s \delta_{sb}}{2}\left[\pi - \cos^{-1}\left(1-\frac{2l_c}{D_s}\right)\right] \tag{2.28}$$

Bundle Bypassing Factor: It accounts for the effects of the bundle bypassing. It is expressed as [11]:

$$\phi_b = \exp\left[-C_{bh}F_{bp}\left\{1-2\left(\frac{N_{ss}}{N_c}\right)^{1/3}\right\}\right] \tag{2.29}$$

with

$$C_{bh} = 1.35 \quad \text{for } Re \leq 100 \tag{2.30}$$

$$C_{bh} = 1.25 \quad \text{for } Re > 100 \tag{2.31}$$

In above relation, F_{bp} represents the fraction of crossflow area available for bypass flow, which is formulated as [11]:

$$F_{bp} = \frac{D_s - d_{otl}}{S_m} l_b \tag{2.32}$$

where, N_{ss} represent the number of sealing pairs, and N_c represents the number of tube rows crossed in one crossflow section, which is defined as [11]:

$$N_c = \frac{D_s}{p_p}\left(1-2\frac{l_c}{D_s}\right) \tag{2.33}$$

where, p_p represents the tube pitch parallel to flow, which is defined as [11]:

$$p_p = \frac{\sqrt{3}}{2} p_T \qquad \text{for triangular layout} \qquad (2.34)$$

$$p_p = p_T \qquad \text{for in-line square layout} \qquad (2.35)$$

$$p_p = \frac{p_T}{\sqrt{2}} \qquad \text{for rotated square layout} \qquad (2.36)$$

If the ratio N_{ss}/N_c is less than 0.5 then the bundle bypassing factor ϕ_b becomes 1.

Adverse Temperature Gradient Build-Up Factor: It accounts for the effects of adverse temperature gradient build-up. It is expressed as [11]:

$$\phi_r = 1 \qquad \text{Re} > 100 \qquad (2.37)$$

$$= 1-(1-\phi_r^*)(1.24-0.0124\text{Re}) \qquad 20 \leq \text{Re} \leq 100 \qquad (2.38)$$

$$= \phi^*_r \qquad \text{Re} < 20 \qquad (2.39)$$

where ,

$$\phi^*_r = 3.76[\ln(N_c+N_{cw})]^{-0.15} N_b^{-0.174} \qquad (2.40)$$

Here, N_{cw} represents the number of effective crossflow rows in each window, which is formulated as [11]:

$$N_{cw} = \frac{0.8\,1_c}{p_p} \tag{2.41}$$

where, N_b is the number of baffles, which is obtained from [11]:

$$N_b = \frac{L}{1_b} - 1 \tag{2.42}$$

Unequal Baffle Spacing Factor: It accounts for the effects of unequal baffle spacing at inlet and outlet and is defined as [11]:

$$\phi_s = \frac{\left(N_b - 1\right) + 1_{in}^{*(1-n)} + 1_{out}^{*(1-n)}}{\left(N_b - 1\right) + 1_{in}^{*} + 1_{out}^{*}} \tag{2.43}$$

with

$$1^* = 1_c/1_b \tag{2.44}$$

and

$$n = 0.333 \qquad \text{for } Re \leq 100 \tag{2.45}$$

$$n = 0.6 \qquad \text{for } Re > 100 \tag{2.46}$$

After all correction factors are evaluated, the actual shell-side heat-transfer coefficient can be calculated from the relation [11]:

$$h_o = h_{o,ideal}\phi_c\phi_l\phi_b\phi_r\phi_s \tag{2.47}$$

Since both the tube-side and shell-side heat-transfer coefficients are known, the overall heat transfer coefficient can be calculated from equation (4).

2.3. Estimation of the Crossectional-Flow Area

In order to find the free crossectional area of the shell which is required by the dynamic model of the exchangers (in Chapter 3), the inner shell diameter must be evaluated. Inner shell diameter is obtained by adding the tube-bundle diameter and shell-bundle clearance. Bundle diameter can be estimated from the empirical equation [12]:

$$D_b = d_o\,(N_T/K_1)^{1/n_1} \tag{2.48}$$

The constants K_1 and n_1, which can be found in [12], depend on the tube arrangement, tube pitch, and number of tube passes.

In order to reduce bypassing around the outside of the tube-bundle, the shell diameter must be as close to the tube bundle as possible; in other words, the shell-bundle clearance should be very small. It can be estimated by the following relation which was

derived in this thesis from the data [12] relating the bundle diameter to shell-bundle clearance for 1-1 heat exchangers:

$$Cl_{shell\text{-}bundle} = (D_b * 10^{-3}) + 8 \tag{2.49}$$

After the bundle diameter, D_b ,and clearance, Cl, is determined, the shell diameter can be easily obtained by adding them up.

2.4. The Modified Design Algorithm

The design algorithm modified for this thesis which satisfies the given terminal temperatures and flowrates of the heat exchanger is as follows :

1. The tube-side and shell-side heat-transfer coefficients are evaluated by using the related correlations mentioned above (initially, viscosity correction factor μ_i/μ_w is set to unity).

2. The tube-wall temperature is estimated from:

$$T_w = T_H^b + \frac{h_o}{h_i + h_o}\left(T_C^b - T_H^b\right) \tag{2.50}$$

where, T^b_C and T^b_H are the bulk temperatures of the shell and tube fluids respectively and obtained as:

$$T_H^b = \frac{T_H^i + T_H^o}{2} \tag{2.51}$$

$$T_C^b = \frac{T_C^i + T_C^o}{2} \tag{2.52}$$

3. The viscosity correction factor is calculated and the steps 2-3 are repeated until T_w converges.

4. The overall heat-transfer coefficient and the log-mean temperature difference are determined.

5. The required heat-transfer area is calculated from the known heat duty using

$$A_{req} = \frac{Q}{U\Delta T_{lm}} \tag{2.53}$$

The overcapacity or undercapacity of the exchanger was determined by comparing the actual area (physical area as calculated from tube dimensions) and required heat transfer area (calculated from Equation (2.53)).

During the calculations, the temperature-dependent parameters were evaluated using the following correlations on the basis of two different reference temperatures:

viscosity,

$$\mu = a \exp(b / T) \tag{2.54}$$

conductivity,

$$k = a+bT \tag{2.55}$$

heat capacity,

$$C_p = a+bT \tag{2.56}$$

density,

$$\rho = a+bT \tag{2.57}$$

2.5. Determination of the Length and the Number of Tubes

In order to make the heat exchangers of the HEN comparable to each other, in this work, it was preferred that each exchanger to have more or less the same length. To make the length of heat exchangers close to each others, the behavior of the mismatch error, ε_M, (extent of overcapacity or undercapacity; i.e., actual heat-transfer area calculated from Equation (2.53) minus the physical area calculated from tube dimensions) was studied. It was observed that the error increased as the number of tubes was increased at a constant length. If the initial number of tubes was suitably selected, the error began at a negative value and changed sign as the number of tubes was increased. The same behaviors was also

observed when the length was increased at constant number of tubes. In order to adjust the length of the exchangers close to the desired value, the desired length was selected as the initial length in input parameters. The number of tubes of an exchanger in the HEN was increased or decreased at this initial length until the mismatch error changed sign (at this point the value of the error was very small). After setting the number of tubes at this value, the length was varied, usually in the range of ± 5 per cent of the initial length, either by increasing or decreasing so that the mismatch error was negligibly small. Thus, with this procedure the minimum number of tubes that yields an exchanger length very close to predefined length could be determined.

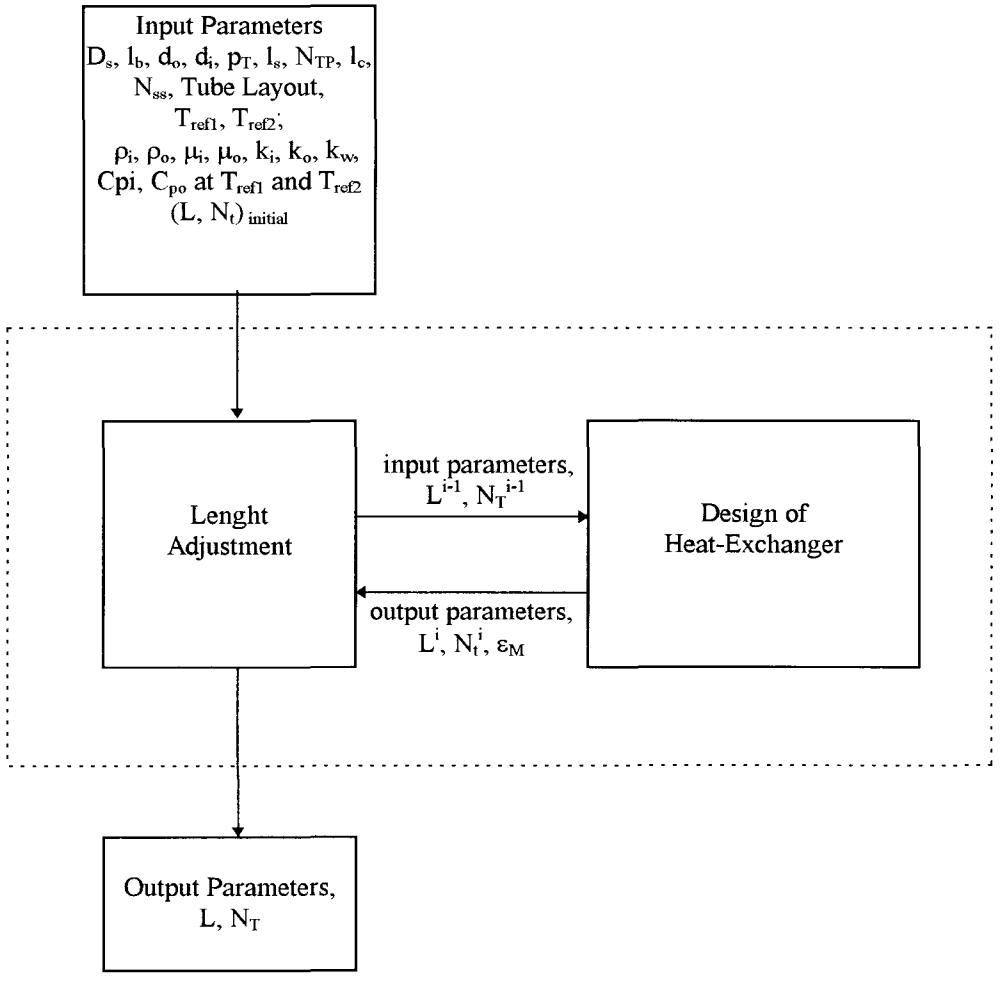

FIGURE 2.2. Logic for the Adjustment of Length and Number of Tubes.

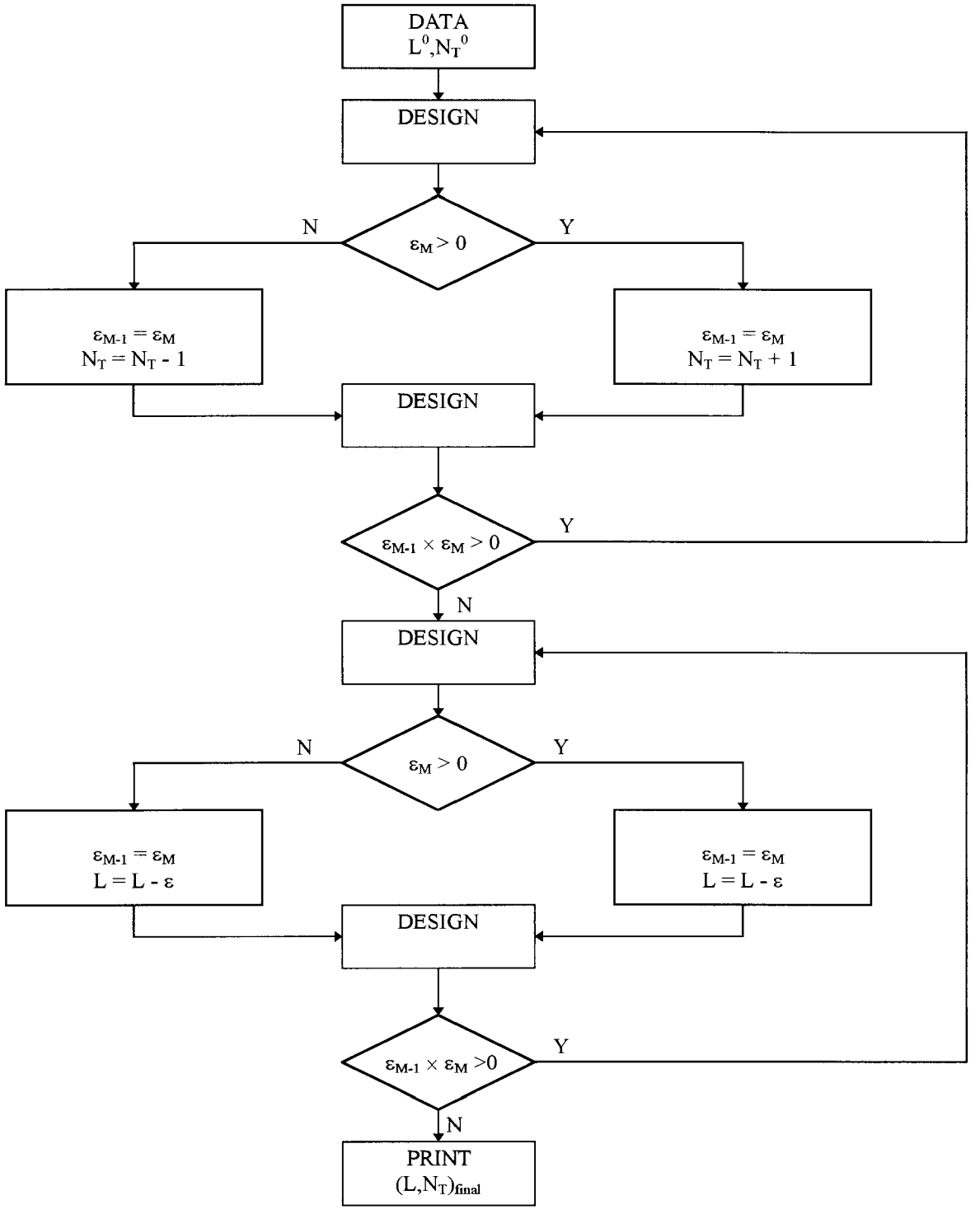

FIGURE 2.3. Flowchart of the Heat Exchanger Design Program.

This procedure is converted to a software program which uses the previous design program as a subroutine. The general logic and the flowchart of the program is shown in Figure 2.2 and Figure 2.3, respectively. If this procedure is applied for all exchangers of the HEN, the resulting exchangers will have different number of tubes but very close exchanger lengths. The listing of the design program can be found in Appendix A.

To illustrate the above algorithm consider the heat exchanger shown in Figure 2.4 [11]. The physical properties of the fluids are given in Table 2.1.

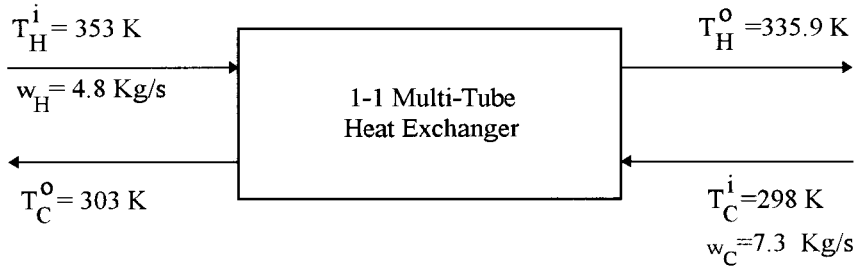

FIGURE 2.4. Heat Exchanger with Specified Inlet and Outlet Conditions.

TABLE 2.1. Physical Properties of the Fluids [11].

	Tube Fluid		Shell Fluid	
Reference Temperature, K	323	283	375	289
Density, kg/m^3	988.1	999.7	798	885
Viscosity, mNs/m^2	0.6	1.26	0.258	0.679
Thermal Conductivity, W/m K	0.640	0.603	0.126	0.163
Heat Capacity, J/kg K	4183	4195	1980	1675

The specified geometry of the exchanger is as follows: d_o=25.4 mm; d_i=19.86 mm; initial N_T=80; triangular pitch; pitch ratio=1.25; tube roughness=0.025 mm; initial L=2 m; l_s=27 mm; D_s=305 mm; d_{otl}=294 mm; δ_{sb}=4.45 mm; N_{ss}=0; l_{bc}=450 mm; l_{in}=l_{out}=100 mm; baffle cut=25 per cent; thermal conductivity of wall metal= 45 W m^{-1} K^{-1}; fouling resistances are

0.00036 and 0.00018 $m^2K\ W^{-1}$ for the tube-side and shell-side, respectively. The resulting design is summarized in Table 2.2.

TABLE 2.2. Results of the Design of the HEX.

Number of Tubes	:	77
Length (m)	:	1.97933
Shell Diameter (mm)	:	376.15199
Velocity (HOT) (m/s)	:	0.307352
Velocity (COLD) (m/s)	:	8.03098×10^{-2}
Heat Transfer Area (HOT) (m^2/tube)	:	0.123494
Heat Transfer Area (COLD) (m^2)	:	12.16163
Heat Transfer Area (SHELL-WALL) (m^2)	:	2.33900
Crossectional Inner Area (HOT) (m^2/tube)	:	3.09776×10^{-4}
Crossectional Inner Area (COLD) (m^2)	:	7.21097×10^{-2}
Crossectional Tube Wall Area (m^2/tube)	:	1.96931×10^{-4}
Crossectional Shell Wall Area (m^2)	:	9.03959×10^{-3}
Heat Transfer Coefficient (HOT) (W/m^2K)	:	5428.32529
Heat Transfer Coefficient (COLD) (W/m^2K)	:	378.20823
Overall Heat Transfer Coefficient (W/m^2K)	:	287.25653

3. MODELING AND DYNAMICS OF HEAT EXCHANGERS

In this chapter, a distributed-parameter model for the individual heat exchangers constituting the HEN is developed and a numerical solution technique of the resulting partial-differential equations (PDEs) is presented.

3.1. Dynamic Model of Heat Exchangers

In order to derive the dynamic model of the multi-tube shown in Figure 3.1, 1-1 shell-and-tube heat exchangers, the energy balance is applied over the differential volume element covering the tube and shell fluids, and the tube and shell wall [13].

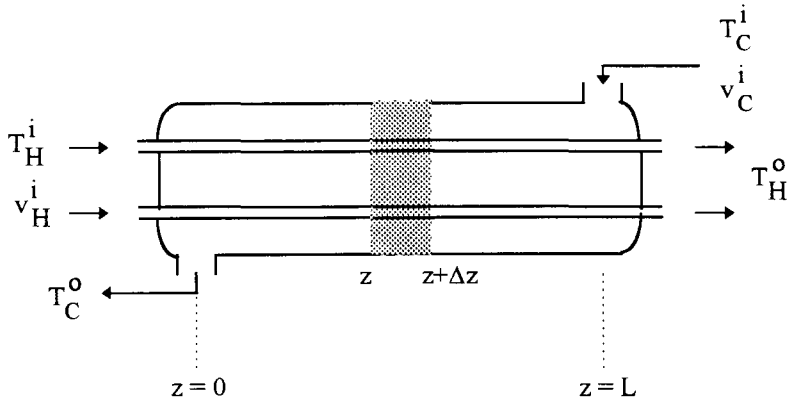

FIGURE 3.1. A 1-1 Shell-and-Tube Exchanger in Countercurrent Flow.

The basic assumptions in modeling are as follows [13]:

a) Fluids are in plug flow with velocities independent of the axial position (z).

b) There are no radial temperature gradients in tube- and shell-side fluids, and the tube and shell walls.

c) Physical properties such as densities and heat capacities are constant.

d) Heat conduction in axial direction is negligible.

e) The shell is insulated.

f) The heat transfer can be represented by Newton's law of cooling with a constant heat-transfer coefficient.

After these assumptions, the PDEs describing the system are as follows [13]:

For the hot-side (tube fluid):

$$\frac{\partial \left(A \rho C_P T\right)_H}{\partial t} = -\frac{\partial \left(v A \rho C_P T\right)_H}{\partial z} + h_H a_H \left(T_T - T_H\right) \tag{3.1}$$

For the cold-side (shell fluid):

$$\frac{\partial \left(A \rho C_P T\right)_C}{\partial t} = +\frac{\partial \left(v A \rho C_P T\right)_C}{\partial z} + h_C \left(\sum^{N_T} a_C\right) \left(T_T - T_C\right) + h_S a_S \left(T_S - T_C\right) \tag{3.2}$$

For the tube-wall:

$$\frac{\partial \left(A \rho C_P T\right)_T}{\partial t} = h_H a_H \left(T_H - T_T\right) + h_C a_C \left(T_C - T_T\right) \tag{3.3}$$

For the shell-wall:

$$\frac{\partial \left(A \rho C_P T\right)_S}{\partial t} = h_S a_S \left(T_C - T_S\right) \tag{3.4}$$

In these equations, the h represents the local heat-transfer coefficients, a represents the heat-transfer area per unit length, and $\sum^{N_T} a_C$ the heat-transfer area based on the outer surface of all tubes per unit length.

With the assumptions mentioned above, the differential energy balances can be further simplified to [13]:

$$\frac{\partial T_H}{\partial t} = -v_H \frac{\partial T_H}{\partial z} + b_H \left(T_T - T_H\right) \tag{3.5}$$

$$\frac{\partial T_C}{\partial t} = +v_C \frac{\partial T_C}{\partial z} + b_C \left(T_T - T_C\right) + b_S \left(T_S - T_C\right) \tag{3.6}$$

$$\frac{\partial T_T}{\partial t} = b'_H \left(T_H - T_T\right) + b'_C \left(T_C - T_T\right) \tag{3.7}$$

$$\frac{\partial T_S}{\partial t} = b'_S \left(T_C - T_S\right) \tag{3.8}$$

where,

$$b_H = \frac{h_H a_H}{A_H \rho_H C_{P_H}} \tag{3.9}$$

$$b_C = \frac{h_C \left(\sum_{}^{N_T} a_C \right)}{A_C \rho_C C_{P_C}} \tag{3.10}$$

$$b_S = \frac{h_S a_S}{A_C \rho_C C_{P_C}} \tag{3.11}$$

$$b'_H = \frac{h_H a_H}{A_T \rho_T C_{P_T}} \tag{3.12}$$

$$b'_C = \frac{h_C a_C}{A_T \rho_T C_{P_T}} \tag{3.13}$$

$$b'_S = \frac{h_S a_S}{A_S \rho_S C_{P_S}} \tag{3.14}$$

The initial conditions (at t = 0) are:

$$T_H(0, z) = T_H^0(z) \tag{3.15}$$

$$T_C(0,z) = T_C^0(z) \tag{3.16}$$

$$T_S(0,z) = T_S^0(z) \tag{3.17}$$

$$T_T(0,z) = T_T^0(z) \tag{3.18}$$

The boundary conditions are the specified inlet temperatures of the hot and cold streams [13]:

$$\text{at } z = 0 \qquad T_H(t,0) = T_H^i(t) \tag{3.19}$$

$$\text{at } z = L \qquad T_C(t,L) = T_C^i(t) \tag{3.20}$$

3.2. The Steady-State Solution of the Dynamic Model

The steady-state solution of the PDEs can be obtained by setting the time derivatives to zero [13],

$$\frac{\partial T_H}{\partial t} = \frac{\partial T_C}{\partial t} = \frac{\partial T_T}{\partial t} = \frac{\partial T_S}{\partial t} = 0 \tag{3.21}$$

The steady state solution is as follows [13]:

$$T_H(z) = T_H^i e^{mz} + A\left(1 - e^{mz}\right) \tag{3.22}$$

$$T_C(z) = \frac{v_H U_C A_C}{v_C U_H A_H} T_H^i e^{mz} + A\left(1 - \frac{v_H U_C A_C}{v_C U_H A_H} e^{mz}\right) \tag{3.23}$$

$$T_T(z) = \frac{b'_H}{b'_H + b'_C} T_H(z) + \frac{b'_C}{b'_H + b'_C} T_C(z) \tag{3.24}$$

$$T_S(z) = T_C(z) \tag{3.25}$$

where,

$$m = \frac{U_C a_C}{v_C} - \frac{U_H a_H}{v_H} \tag{3.26}$$

$$U_H a_H = \frac{b_H b'_C}{b'_H + b'_C} \tag{3.27}$$

$$U_C a_C = \frac{b_C b'_H}{b'_H + b'_C} \tag{3.28}$$

$$A = \frac{T_C^i - \left(\frac{v_H}{v_C}\right)\left(\frac{U_C a_C}{U_H a_H}\right) T_H^i e^{mL}}{1 - \left(\frac{v_H}{v_C}\right)\left(\frac{U_C a_C}{U_H a_H}\right) e^{mL}} \tag{3.29}$$

3.3. Numerical Solution of the Dynamic Model

There is no analytical solution to the unsteady-state model of the system. Therefore, the unsteady-state model requires a numerical solution technique. The distributed model in Equations (3.5) to (3.8) involves four coupled PDEs. The temperatures of the fluids and of the tube and shell walls are the dependent variables. The "method of lines" numerical technique can be conveniently used for the solution of the PDEs. In this technique, the PDEs are discretized in the z-direction using finite-difference approximation of the spatial derivatives and thus converted into -usually stiff- set of ordinary differential equations (ODEs). The resulting set of ODEs are then integrated in time domain using standard and well-established techniques. To accomplish this task, the exchanger was divided into (N_Z-1) intervals with N_Z grid points along the z-direction, as shown in Figure 3.2.

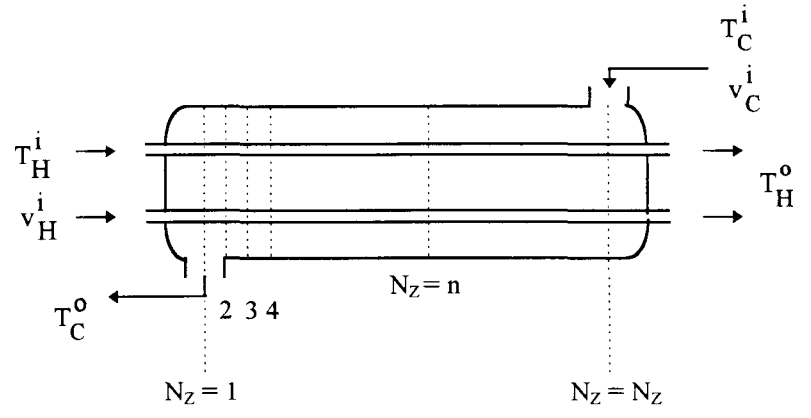

FIGURE 3.2. Discretized Heat Exchanger.

The ODEs were discretized in the spatial domain (z-direction) by using "five-point biased-upwind" finite-difference formulas [14]. The differentiation formulas have been derived from the Lagrange interpolation polynomials and provide fourth-order accuracy [14]. The resulting stiff set of ODEs were then integrated in time domain using the software package LSODES, which uses the Gear's implicit algorithm and has the capability of handling sparse-Jacobian systems.

The number of ODEs, N_{ODE}, to be integrated is given by

$$N_{ODE} = N_{PDE} \times N_Z - 2 \tag{3.30}$$

where N_{PDE} is the number of PDEs (which is equal to four for 1-1 heat exchangers considered in this work), N_Z is the number of grid points in the z-direction, and two ODEs corresponding to the specified boundary conditions at $z=0$ ($N_Z = 1$) and $z=L$ ($N_Z = N_Z$) are subtracted. Thus, for the type of exchangers considered in this work, $N_{ODE} = 4 \times N_Z - 2$ ODEs had to be integrated simultaneously.

3.4. Dynamic Behavior of a Sample Heat Exchanger

To examine its dynamics consider the heat exchanger shown in Figure 3.3 [15]. The specified geometry of the exchanger is the same as the exchanger in Figure 2.4 of Chapter 2 (d_o, 25.4 mm; d_i, 19.86 mm; initial N_T, 80; triangualar pitch; pitch ratio, 1.25; tube roughness, 0.025 mm; initial L, 2 m; l_s, 27 mm; D_s, 305 mm; d_{otl}, 294 mm; δ_{sb}, 4.45 mm; N_{ss}, 0; l_{bc}, 450 mm; l_{in}, l_{out}, 100 mm; baffle cut, 25 per cent [11]), except the fouling resistances 3.522×10^{-4} $m^2K\ W^{-1}$ for both the tube- and shell-side [16]. The physical

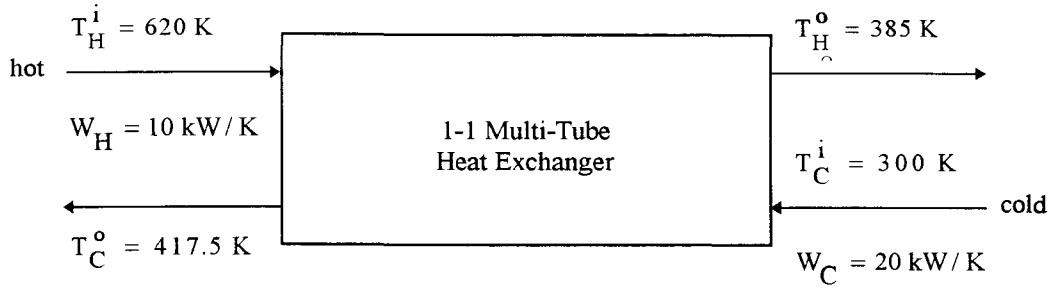

FIGURE 3.3. A Sample Single Heat Exchanger.

properties of the streams are shown in Table 3.1. Due to the relatively high inlet and outlet stream temperatures, sodium-potassium alloy (56 Na- 44 K weight per cent) is selected as the sample heat-transfer liquids for both the hot and cold streams [16], and steel (1 per cent C) is selected as the tube- and shell-wall material for the same reason, of which the heat capacity and density is 502.44 J kg^{-1} K^{-1} and 7833.78 kg m^3 [16] respectively.

TABLE 3.1. Physical Properties of Hot and Cold Streams [16].

	Tube and Shell Fluids
Density, kg/m^3	840
Viscosity, mNs/m^2	0.24×10^{-3}
Thermal Conductivity, W/m K	26.99
Heat Capacity, J/kg K	1046.7

The exchanger was designed by the algorithm developed in Chapter 2, and thus the required parameters of the PDEs in Equations (3.5) to (3.8) were determined as shown in Table 3.2. However, in order to be consistent with the heat-exchanger parameters used in Konukman et al. [10], the local and overall heat-transfer coefficients were fixed at the specified values [10], given in Table 3.2. It was further assumed that the properties of the streams do not vary with temperature.

TABLE 3.2. Results of the Heat Exchanger Design.

Number of Tubes	:	111
Length (m)	:	1.96014
Shell Diameter (mm)	:	402.16504
Velocity (HOT) (m/s)	:	0.33077
Velocity (COLD) (m/s)	:	0.32136
Heat-Transfer Area (HOT) (m^2/tube)	:	0.12229
Heat-Transfer Area (COLD) (m^2)	:	17.36177
Heat-Transfer Area (SHELL-WALL) (m^2)	:	2.47652
Crossectional Inner Area (HOT) (m^2/tube)	:	3.09776×10^{-4}
Crossectional Inner Area (COLD) (m^2)	:	7.07832×10^{-2}
Crossectional Tube Wall Area (m^2/tube)	:	1.96931×10^{-4}
Crossectional Shell Wall Area (m^2)	:	9.65250×10^{-3}
Heat-Transfer Coefficient (TUBE) (W/m^2K)	:	2557.905
Heat-Transfer Coefficient (SHELL) (W/m^2K)	:	2000
Overall Heat-Transfer Coefficient (W/m^2K)	:	1000

Initially the heat exchanger ia assumed to operate at steady state. The initial steady-state temperature profiles along the z-direction were obtained from the analytical steady-state solution given by Equations (3.22) - (3.25).

In this chapter, the dynamic behavior of the exchanger was investigated for the following set of disturbances:

a) an upset of +10 K in inlet temperature of the hot stream
b) an upset of -10 K in inlet temperature of the cold stream
c) an upset of +10 K in inlet temperature of the hot stream and an upset of -10 K in inlet temperature of the cold stream, simultaneously

The set of PDEs in Equations (3.5) to (3.8) were integrated numerically using the method mentioned above. N_Z=51 grid points were used in finite-difference discretization, and thus N_{ODE}=202 ODEs were integrated.

Figure 3.4 shows the dynamic response of the exchanger for +10 K upset in inlet temperature of the hot stream. Figure 3.5 shows the dynamic response of the exchanger for -10 K upset in inlet temperature of the cold stream. Figure 3.6 shows the dynamic response of the exchanger for +10 K upset in inlet temperature of the hot stream and -10 K in inlet temperature of the cold stream. In these figures, the plotted variables are the effluent temperatures of the hot (at z = L) and cold (at z = 0) fluids, and the temperatures of the tube (at z = L) and shell (z = 0) walls, as deviations from their steady-state (before disturbance) values.

There is no steady-state offset in numerical simulation; i.e., steady-state solution and dynamic response at steady-state perfectly match. This 'zero offset' was achieved by the use of 'five-point biased-upwind' finite-difference approximations. It is known, and was also observed in this work, that the 'tanks-in-series' approximation (corresponds to 'two-point forward/backward' finite differencing) as well as 'central' finite-difference formulation (e.g. 'five-point central' finite differencing) do not eliminate steady-state offset problem even for very large number of grid points [17].

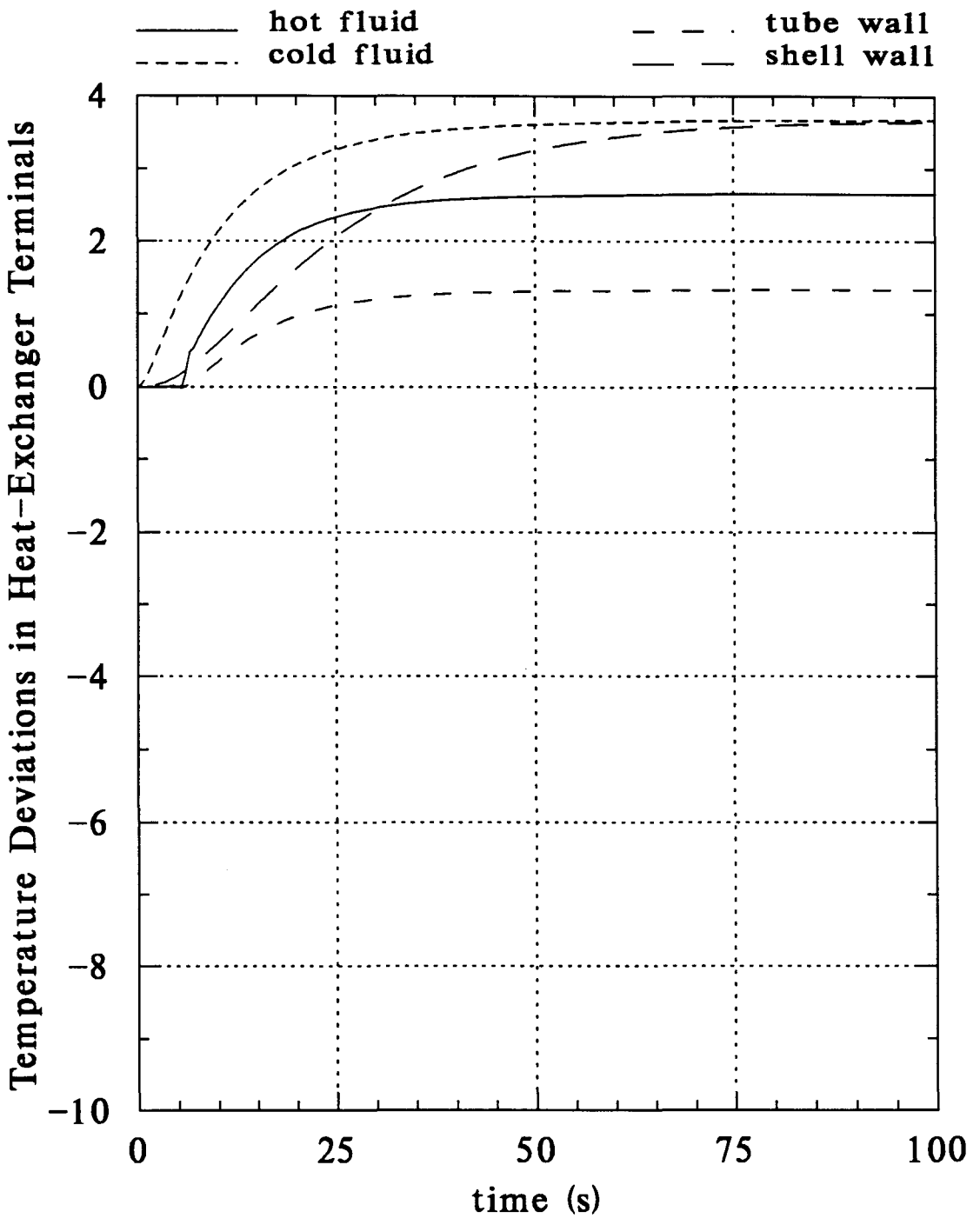

FIGURE 3.4. Response of the Exchanger for +10 K Upset in Inlet Temperature of the Hot Stream.

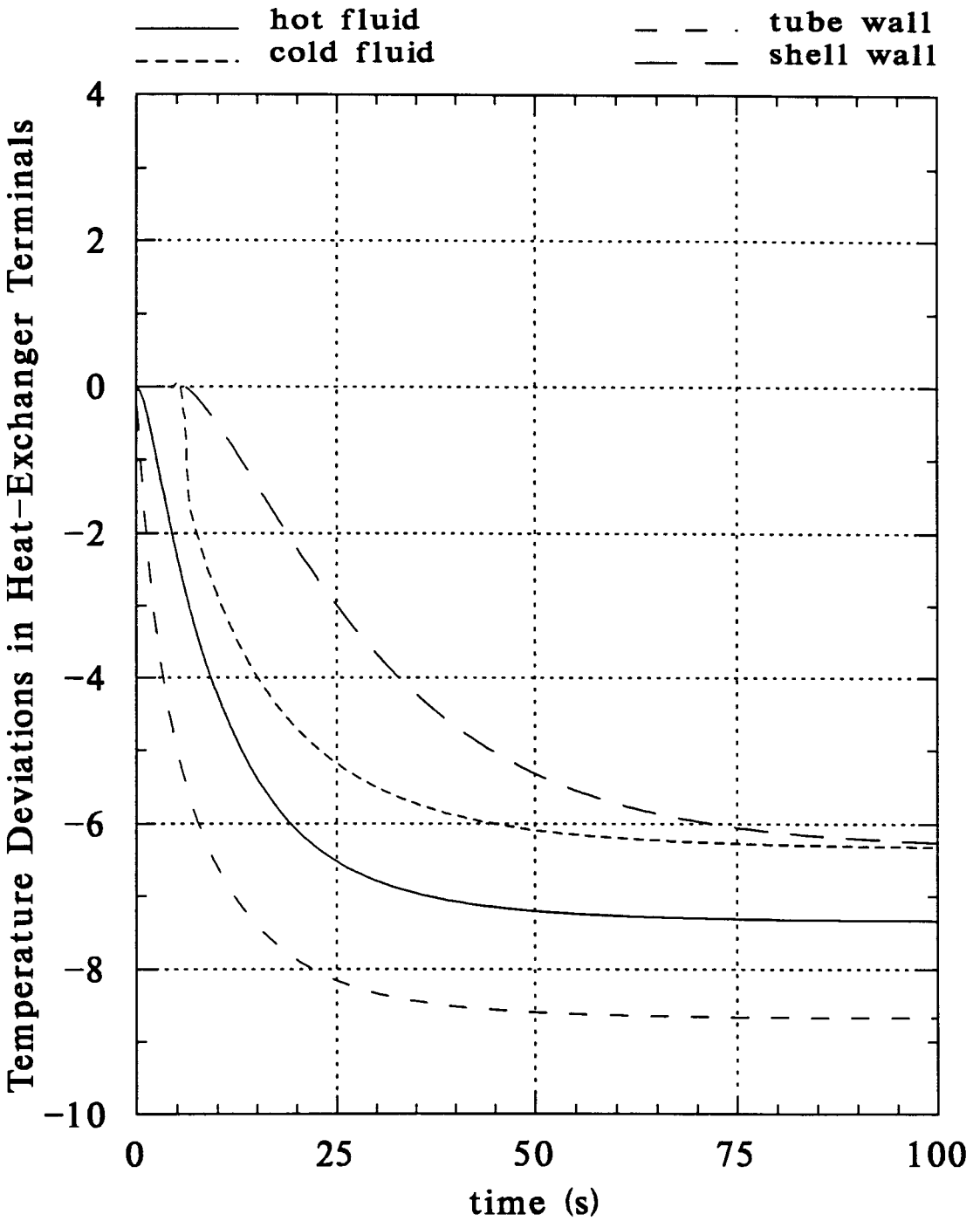

FIGURE 3.5. Response of the Exchanger for -10 K Upset in Inlet Temperature of the Cold Stream.

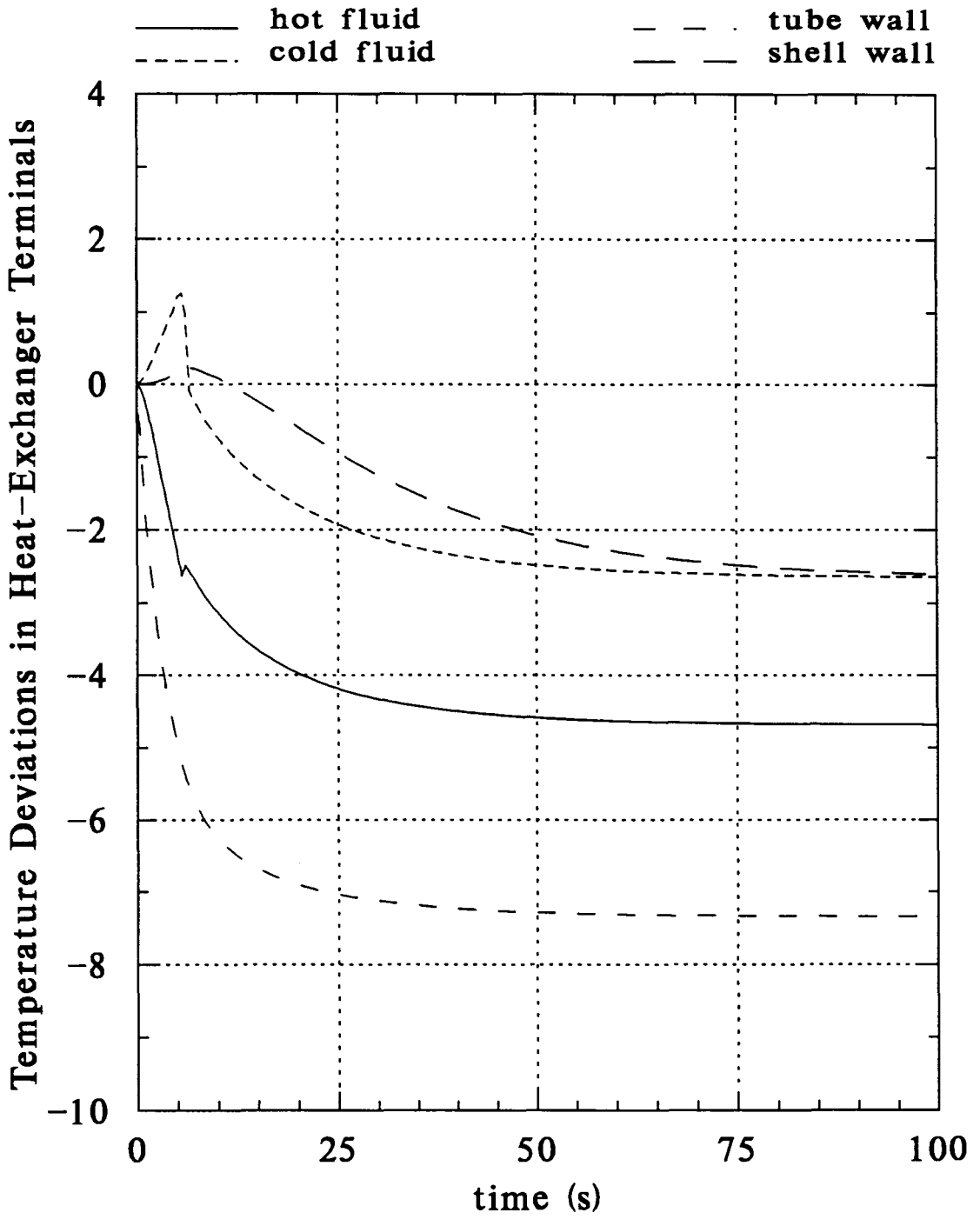

FIGURE 3.6. Response of the Exchanger for +10 K Upset in Inlet Temperature of the Hot Stream and -10 K Upset in Inlet Temperature of the Cold Stream.

4. STATIC OPTIMIZATION OF HEAT-EXCHANGER NETWORKS

As briefly mentioned in Chapter 1, the objective of this thesis is to investigate the dynamics, controllability, and resiliency of HENs when they receive an external disturbance while operating at an economically/thermodynamically feasible point (nominal operating conditions) for which they have been designed. Usually, the objective is to keep (control) the target-stream temperatures exactly at these nominal conditions (hard targets) or as close as possible to the nominal conditions (soft targets). Generally, for an arbitrary disturbance, all of the hard targets cannot be satisfied since during the traditional steady-state (static) design of HENs, flexibility (disturbance-rejection ability) at/around this nominal design point is not taken into consideration.

Therefore, in most cases, the control of HENs exactly at the nominal operating conditions is not possible. Instead, an alternative operating point around the nominal operating conditions should be chosen as the target. However, not all operating points around the nominal conditions are thermodynamically feasible. Therefore, for a specified/measured disturbance, new, but feasible, targets could be selected. Once this new feasible (optimal) operating point is identified, the remaining control task is to drive the system from its nominal operating conditions to the new operating point as smoothly and quickly as possible. It should also be made possible to drive the HEN to its nominal operating conditions soon after the disturbance disappears.

In this Chapter, we describe how to find an alternative feasible steady-state operating point for a specified disturbance around the nominal operating point for which a HEN has been designed.

4.1. Flexibility and Control Problems of HENs

The algorithmic static (steady-state) synthesis methods generate HENs for fixed (nominal) values of stream supply temperatures, flow rates, and target temperatures. In practice, however, stream supply temperatures and flowrates can vary. Thus, a HEN must cope with desired or undesired variations in operating conditions. A HEN synthesized for the nominal conditions must be flexible and resilient to desired and undesired changes in supply temperatures, flow rates, and to uncertainties in design variables (e.g., heat-transfer coefficients). However, decisions made during static structural design of a HEN may put severe limitations on achievable dynamic performance (controllability) of the resulting HEN [10, 5].

The major problem in the control of HENs is the lack of sufficient degrees of freedom; i.e., there may not be enough number of variables to manipulate in order to achieve the control objectives. As seen in Figure 4.1, the hot and the cold process streams (source streams) come to the HEN from upstream process units, and, after proper heat exchange, they (target streams) are sent to downstream process units. Both the temperatures and the flow rates of the incoming streams may introduce disturbances to the HEN owing to uncontrolled upsets in the upstream process units. The target temperatures (target enthalpies) of the outgoing streams of the HEN should be tightly controlled for the safety of operations carried out in the downstream process units. The static HEN synthesis methods (e.g., minimum-utility or minimum-area algorithms) do not necessarily accommodate utility exchangers (heaters or coolers) for each of the target streams. Therefore, since the flow rates of the source streams cannot be manipulated for the safety of the operations carried out in the upstream process units, all necessary control actions in order to satisfy target-temperature (target-enthalpy) constraints should be taken using the manipulated variables that may/should be present in the pre-designed HEN structure (based

on steady-state conditions of the complete plant). Only, stream splits and bypasses that may/should be present in the HEN structure can provide the degrees of freedom necessary to achieve the control objectives. Unfortunately, algorithmic/evolutionary static HEN synthesis methods never consider bypass of one or multiple exchangers and generally yield HEN structures which do not contain any or enough number of stream splits [5].

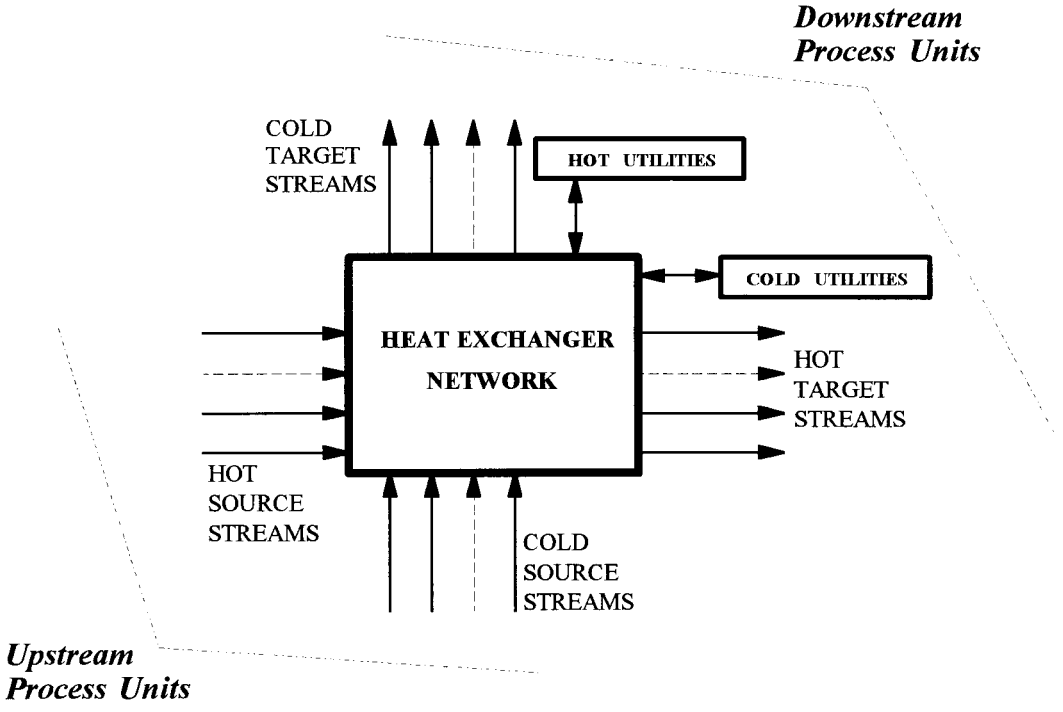

FIGURE 4.1. Process Heat Exchanger Network [5].

Controllability of HENs is investigated only by a few authors. Mathisen et al. [6] reviewed different controllability measures and showed how these measures might be used to select bypasses and appropriate pairings among controlled variables (target temperatures) and manipulated variables (bypass-stream flow rates). They concluded that structural designs and bypass selections where all critical targets are controlled by either utility streams or bypasses with a direct effect should be preferred. The authors also found that flowrate dependence of heat-transfer coefficients had significant effect on control. Mathisen et al. [7, 8] suggested several optimization problems and proposed to take controllability into account by adding control-related constraints to the flexibility-problem

formulation. They also derived a target for the number of bypasses. The authors argued that the use of multi-bypasses (bypassing more than one exchanger) might increase both flexibility; for a given number of bypasses, and controllability; when both outlet temperatures of one exchanger were controlled outputs. Recently, Konukman et al. [10] presented an optimization method for developing resilient (flexible and controllable) retrofit HEN designs starting with a known structure obtained from a static synthesis method.

4.2. Steady-State Optimization and Control of HENs

Consider the HEN structure given in Figure 4.2. The nominal values of the source and target temperatures, and the nominal flow rates are indicated in the figure. The design has been based on a constant overall heat-transfer coefficient, U_n, of 1000 W/m^2-K for all the exchangers [5]. The bypass streams are shown with dashed lines since the original design does not contain bypass streams; without any disturbance their values are zero (nominal bypass fractions are zero) [5].

The static optimization and steady-state control problem is defined as follows: When the HEN experiences a set of source-temperature disturbance ($\Delta T^s_{H,n}$ of +5 K for both of the hot source streams and $\Delta T^s_{C,n}$ of –5 K for both of the cold source streams), find a set of bypass fractions, $u_{H,n}$ and $u_{C,n}$, that will minimize the total deviations in the hot- and cold-stream target temperatures, $\sum_{j}^{NHS} \left|\Delta T^t_{H,n}\right| + \sum_{k}^{NCS} \left|\Delta T^t_{C,n}\right|$, subject to the hot and cold target-stream-temperature control ranges (soft constraints), $\Delta T^t_{H,n}$ and $\Delta T^t_{C,n}$, respectively, and subject to a minimum approach temperature, $\Delta T_{a,n}$, of +10 K for both

terminals of all the exchangers, so that the HEN remains feasible, both under the nominal operating conditions and under the specified disturbances.

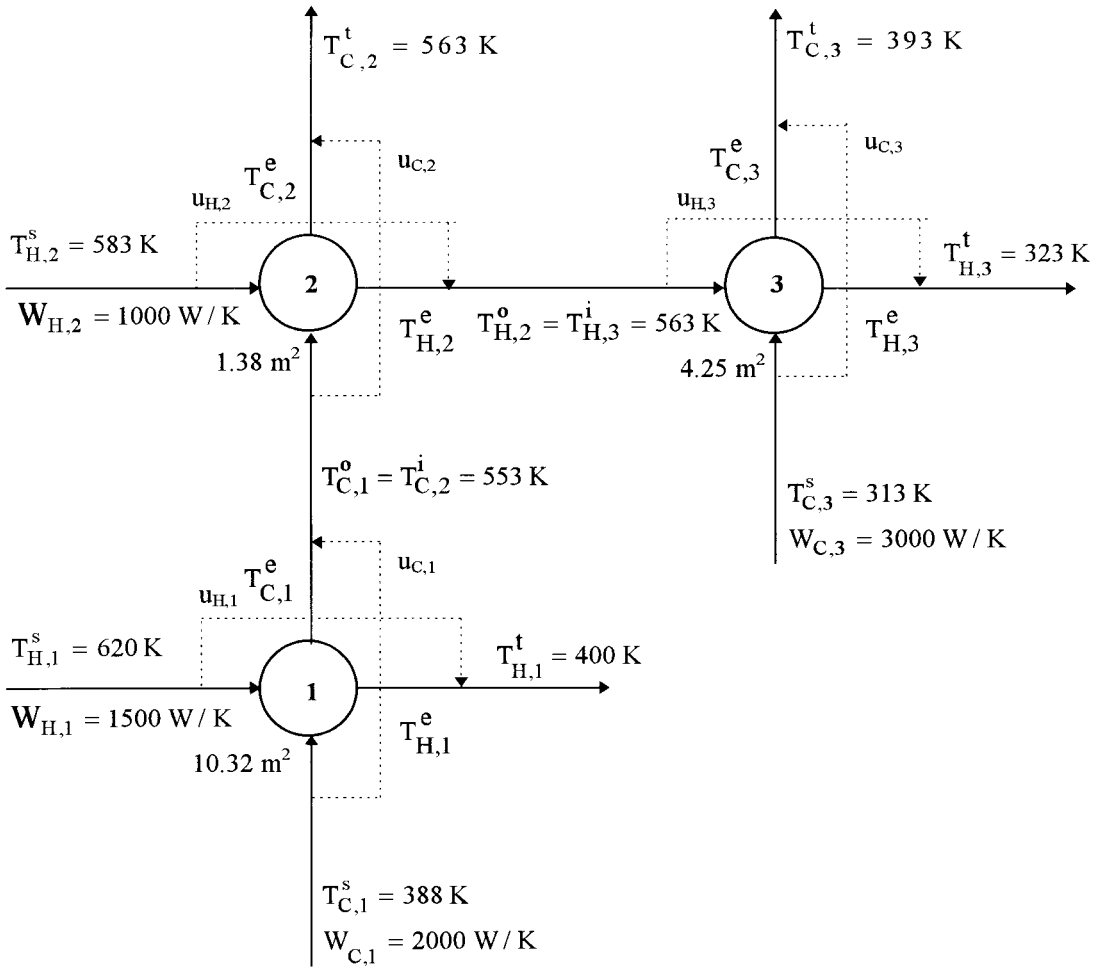

FIGURE 4.2. The Nominal Operating Conditions of the Heat Exchanger Network [5].

The constrained nonlinear optimization problem for the HEN depicted in Figure 4.2 may be stated in the most general notation by considering the single heat exchanger shown in Figure 4.3 [5]:

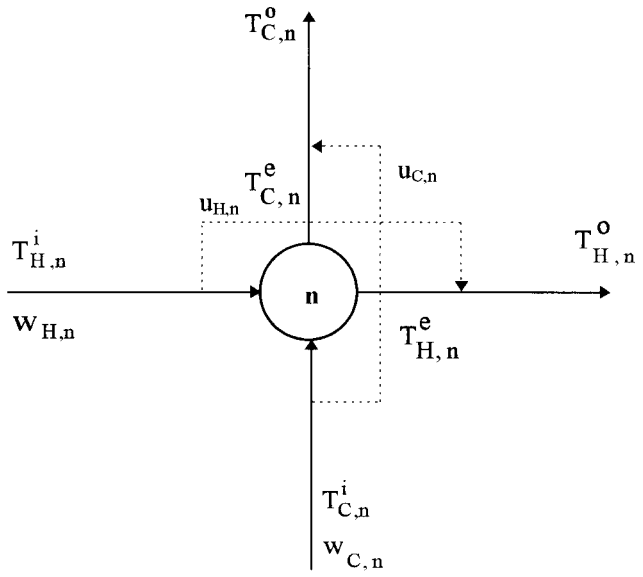

FIGURE 4.3. Notation for a Single Heat Exchanger [5].

The static optimization problem has been formulated using the infeasible-path approach [18] by Konukman et al. [5]. However, in this thesis, we present the static optimization problem using the feasible-path approach [18]. The mathematical formulation is as follows:

Objective Function :

$$\underset{u_{H,n},u_{C,n}}{minimize}\left\{\sum_{n}^{NHS}\left|\Delta T^{t}_{H,n}\right|+\sum_{n}^{NCS}\left|\Delta T^{t}_{C,n}\right|\right\} \tag{4.1}$$

Inequality Constraints (minimum approach-temperature constraints) :

$$T^{e}_{C,n}-T^{i}_{H,n}+\Delta T_{a,n}\leq 0 \tag{4.2}$$

$$T^{i}_{C,n} - T^{o}_{H,n} + \Delta T_{a,n} \leq 0 \tag{4.3}$$

Inequality Constraints (target-temperature range constraints) :

$$\left(T^{t}_{H,n} - \Delta T^{t}_{H,n}\right) \leq T^{o}_{H,n} \leq \left(T^{t}_{H,n} + \Delta T^{t}_{H,n}\right) \tag{4.4}$$

$$\left(T^{t}_{C,n} - \Delta T^{t}_{C,n}\right) \leq T^{o}_{C,n} \leq \left(T^{t}_{C,n} + \Delta T^{t}_{C,n}\right) \tag{4.5}$$

Inequality Constraints (manipulated-variable range constraints) :

$$0 \leq u_{H,n} \leq u^{max} \tag{4.6}$$

$$0 \leq u_{C,n} \leq u^{max} \tag{4.7}$$

where

$$\Delta T^{t}_{H,n} = T^{o}_{H,n} - T^{t}_{H,n} \tag{4.8}$$

$$\Delta T^{t}_{C,n} = T^{o}_{C,n} - T^{t}_{C,n} \tag{4.9}$$

The energy balances for the mixing points of the bypass streams are as follows:

$$T^{o}_{H,n} = u_{H,n}\, T^{i}_{H,n} + \left(1 - u_{H,n}\right) T^{e}_{H,n} \tag{4.10}$$

$$T^{o}_{C,n} = u_{C,n}\, T^{i}_{C,n} + \left(1 - u_{C,n}\right) T^{e}_{C,n} \tag{4.11}$$

The effluent temperatures can be calculated from the analytical solution derived in Chapter 3:

$$T^{e}_{H,n} = T^{o}_{H,n} e^{r_n} + R_n\left(1 - e^{r_n}\right) \tag{4.12}$$

$$T^{e}_{C,n} = T^{o}_{C,n} \Omega_n + R_n\left(1 - \Omega_n\right) \tag{4.13}$$

where

$$r_n = u_n A_n \left(\frac{1}{W_{C,n}} - \frac{1}{W_{H,n}}\right) \tag{4.14}$$

$$\Omega_n = \frac{W_{H,n}}{W_{C,n}} \tag{4.15}$$

$$R_n = \frac{T^o_{C,n} - \Omega_n T^o_{H,n} e^{r_n}}{1 - \Omega_n e^{r_n}} \tag{4.16}$$

For the HEN structure shown in Figure 4.2, the following identities are valid:

$T^s_{H,1} = T^i_{H,1} = 620\,K$ $\quad T^s_{H,2} = T^i_{H,2} = 583\,K$

$T^s_{C,1} = T^i_{C,1} = 388\,K$ $\quad T^s_{C,3} = T^i_{C,3} = 313\,K$

$T^t_{H,1} = T^o_{H,1} = 400\,K$ $\quad T^t_{H,3} = T^o_{H,3} = 323\,K$

$T^t_{C,2} = T^o_{C,2} = 563\,K$ $\quad T^t_{C,3} = T^o_{C,3} = 393\,K$

$T^o_{H,2} = T^i_{H,3}$ $\quad T^o_{C,1} = T^i_{C,2}$

$W_{H,2} = W_{H,3}$ $\quad W_{C,1} = W_{C,2}$

Three different target-temperature range constraints were tested. In the first case, the hot- and cold-stream target temperatures were constrained within ±2 K, i.e., the disturbance was allowed to affect both the hot-and the cold-target streams equally. In the second case, the hot-stream target temperatures were constrained within ±4 K and the cold ones within ±0.5 K, i.e. propagation direction of the disturbance was forced towards the hot end of the HEN. In the third case, the hot-stream target temperatures were constrained within ±0.5 K and the cold ones within ±4 K, i.e. propagation direction of the bi-directional disturbance was forced towards the cold end of the HEN [5].

The optimization problem were solved using the package ADS (a FORTRAN program for Automated Design Synthesis) [19] on a PC-486 machine using double-precision arithmetic and by overriding some of the default ADS parameters (the following ADS options were used: in the strategy level, sequential unconstrained minimization using the exterior penalty function method; in the optimizer level, Broyden-Fletcher-Goldfarb-Shanno (BFGS) variable-metric method for unconstrained optimization; in the one-dimensional search, polynomial interpolation with bounds). The listing of the program can be found in Appendix B.

Table 4.1 shows the heat-capacity-flow-rate of the bypass streams and the target-temperature values for the three different disturbance-propagation scenarios mentioned above when the objective was to minimize the sum of target-temperature deviations when a source-temperature disturbance of $\Delta T^{s}_{H,n}$= +5 K in both of the hot source streams and $\Delta T^{s}_{C,n}$ = –5 K in both of the cold source streams. In the first and the third cases, the minimum approach temperature constraint of type Equation (4.5) was active for the second exchanger, but no minimum approach temperature constraint was active in the second scenario. (in each scenario, some target-temperature range constraints were active as well, as can be seen in the table) [5].

The results summarized in Table 4.1 were obtained when the optimization procedure was started using zero as the starting values for all bypass fractions. Initial-guess dependence of the optimal solution is demonstrated in Table 4.2 for the first case (± 2 K), where the optimization procedure was started using 0.5 as the initial guess for all bypass fractions. Although the values of the respective objective functions for the cases considered in Table 4.1 (first column) and Table 4.2 are identical, the resulting bypass-fraction sets are different [5].

TABLE 4.1 Optimal Heat-Capacity-Flow-Rate Values of the Bypass Streams and the Target Temperatures [5].

	$\Delta T^{t}_{H,n} = \pm 2$ K $\Delta T^{t}_{C,n} = \pm 2$ K	$\Delta T^{t}_{H,n} = \pm 4$ K $\Delta T^{t}_{C,n} = \pm 0.5$ K	$\Delta T^{t}_{H,n} = \pm 0.5$ K $\Delta T^{t}_{C,n} = \pm 4$ K
$W_{H,1}\ u_{H,1}$	18.2685	0.0059	29.6581
$W_{C,1}\ u_{C,1}$	40.6165	24.0836	61.1656
$W_{H,2}\ u_{H,2}$	359.9931	327.3805	142.8566
$W_{C,2}\ u_{C,2}$	1264.8895	1263.0901	63.8367
$W_{H,3}\ u_{H,3}$	17.8859	1.9692	16.6708
$W_{C,3}\ u_{C,3}$	17.4276	0.0000	211.0502
$T^{t}_{H,1}$	398.334	396.000	399.999
$T^{t}_{H,3}$	322.999	319.000	322.500
$T^{t}_{C,2}$	561.000	562.500	563.000
$T^{t}_{C,3}$	391.000	392.500	389.000

Even though there may exist multiple (or, in some cases infinite) solutions to the HEN optimization problem presented, the results demonstrate that propagation direction of a disturbance set can be forced towards either the hot or the cold end of a pre-designed HEN with minimum target-temperature deviations using different (optimal) sets of bypass fractions [5]. This implies that the method guarantees the steady-state feasibility of the new alternative control targets; i.e., soft target-temperature constraints are satisfied when the optimal bypass fractions (manipulated variables) are applied.

TABLE 4.2. Nonuniqueness of the Optimal Heat-Capacity-Flow-Rate Values of the Bypass Streams and the Target Temperatures [5].

$W_{H,1}\ u_{H,1}$	5.7316
$W_{C,1}\ u_{C,1}$	101.7055
$W_{H,2}\ u_{H,2}$	321.0090
$W_{C,2}\ u_{C,2}$	1314.7966
$W_{H,3}\ u_{H,3}$	2.8206
$W_{C,3}\ u_{C,3}$	750.6835
$T^t_{H,1}$	398.334
$T^t_{H,3}$	322.999
$T^t_{C,2}$	561.000
$T^t_{C,3}$	391.000

5. OPTIMAL OPEN-LOOP CONTROL OF HEAT-EXCHANGER NETWORKS

As a result of the optimization formulation described in Chapter 4, optimal values of the target temperatures and bypass openings that guarantee the steady-state feasibility of the new operating point after a disturbance can be calculated. From Chapter 4, we know that, when a set of external disturbances enters a HEN, we can meet the target streams constraints (more likely for soft constraints but less likely for hard constraints), as much as the network structure allows, by applying the values of bypass openings calculated from the solution of the optimization problem.

What is left is to determine how to apply in time the set of optimal bypass openings (controls) so that the HEN's dynamic response in reaching the final steady-state operating point is acceptable.

Figure 5.1 is a schematic of an optimal control logic of HENs which is to be tested in this chapter. According to this scheme, the temperatures of the source streams entering the HEN (I) are measured (II) at discrete time intervals (sampled). These measurements are fed to the optimizer (III) which refers to the steady-state algebraic model (IV) of the exchangers constituting the HEN, as described in Chapter 4. According to the target-temperature constraints (which may be hard or soft), the optimizer finds the optimal values of the bypass fractions, $\mathbf{u}^{opt}$, such that the target-temperature constraints which define the exact location (hard target) and/or allowable range of the desired (and feasible) new steady-state operating point (soft target). Assuming that there is no mismatch between the model and the process (HEN), the remaining task at this point, is to find how to implement (V) these optimal bypass opening as a function of time.

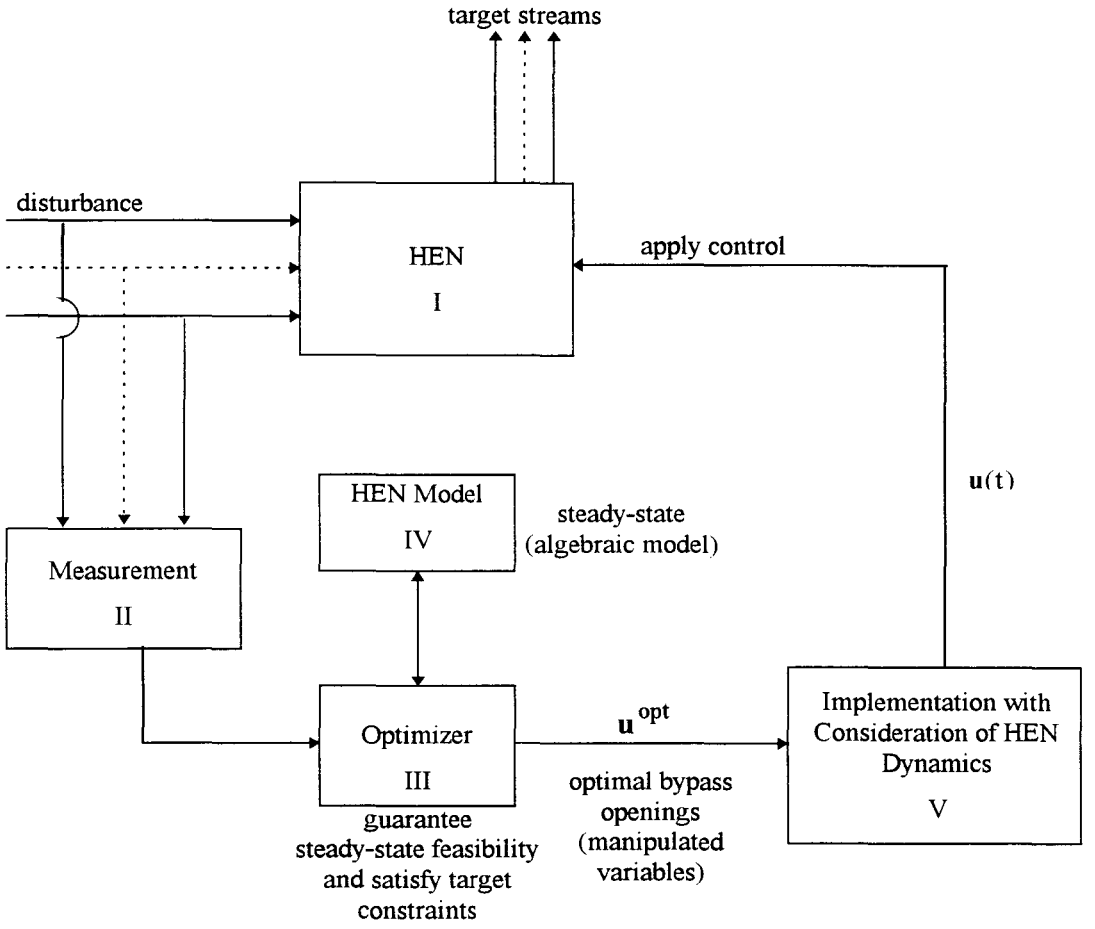

FIGURE 5.1. Schematic of an Optimal Open-Loop Control Logic of Heat Exchanger Networks.

In an open-loop control there is no feedback of the state variables (target-stream temperatures). Since there is no offset between the predictions of the algebraic and dynamic models at steady-state, the bypasses can be opened up to their optimal values either instantaneously (assuming that there is no time delay in measurement and optimization procedures) or as a function of time (e.g., as a ramp starting from their nominal values, $\bar{\mathbf{u}}$, which may be zero, towards their optimal values, $\mathbf{u}^{opt}$).

In this chapter, the dynamics and controllability of HENs will be tested for these two types of open-loop implementation of the optimal controls, i.e., instantaneous implementation and implementation as a ramp function in time.

5.1. Instantaneous Application of Optimal Bypass Stream Openings

Consider, for example, the HEN depicted in Figure 5.2 [10]. The nominal flow rates and temperatures of the streams are indicated in the figure, and Table 5.1 shows the key design specifications obtained as described in Chapter 2.

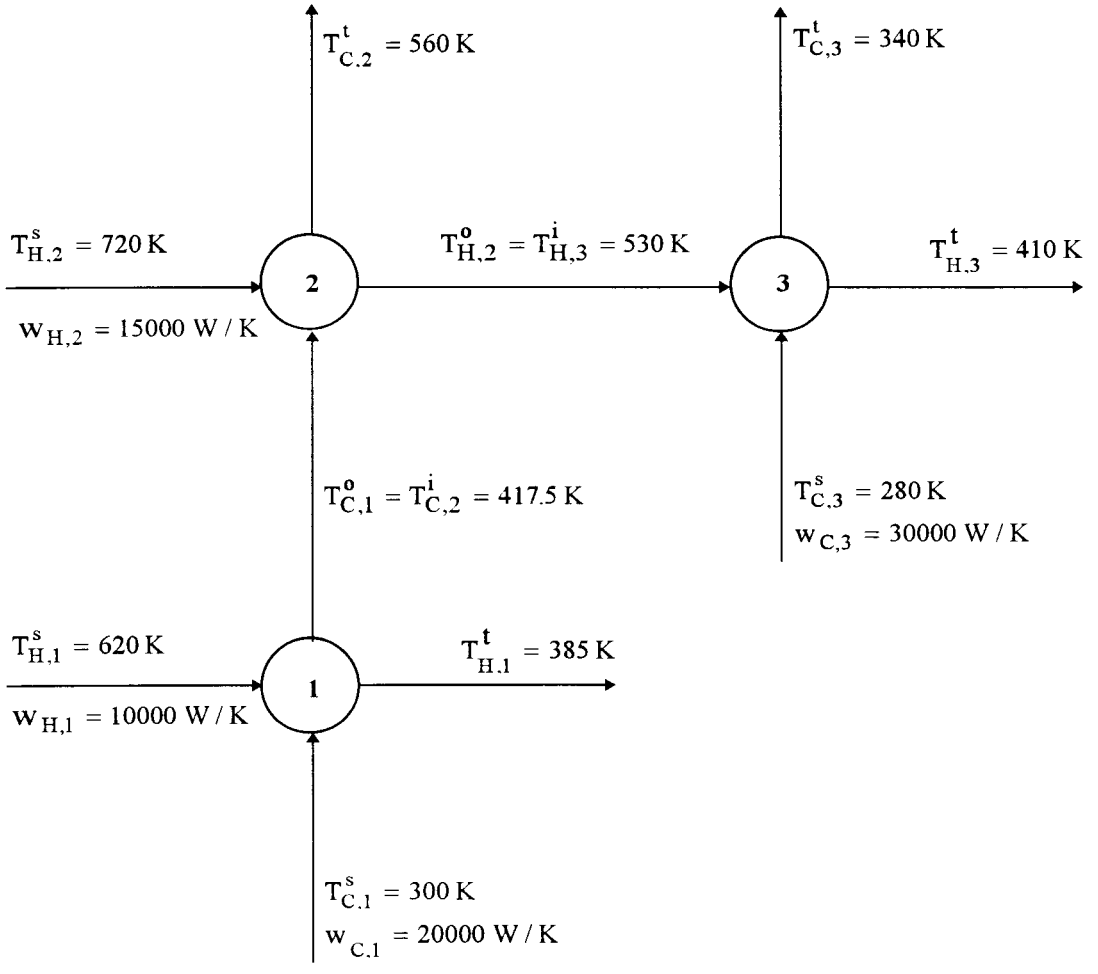

FIGURE 5.2. Sample Heat Exchanger Network [10].

TABLE 5.1. Key Design Specifications of the Heat Exchangers of the HEN.

	HEX-1	HEX-2	HEX-3
Number of Tubes	111	136	72
Length (m)	1.96014	1.94735	1.98155
Shell Diameter (mm)	402.16504	441.37316	330.04318
Velocity (HOT) (m/s)	0.33077	0.40495	0.76491
Velocity (COLD) (m/s)	0.32136	0.27051	0.69536
Heat-Transfer Area (HOT) (m^2/tube)	0.12229	0.12149	0.12363
Heat-Transfer Area (COLD) (m^2)	17.36177	21.13324	11.38469
Heat-Transfer Area (SHELL-WALL) (m^2)	2.47652	2.70022	2.05459
Crossectional Inner Area (HOT) (m^2/tube)	3.09776×10^{-4}	3.09776×10^{-4}	3.09776×10^{-4}
Crossectional Inner Area (COLD) (m^2)	7.07832×10^{-2}	8.40914×10^{-2}	4.90693×10^{-2}
Crossectional Tube Wall Area (m^2/tube)	1.96931×10^{-4}	1.96931×10^{-4}	1.96931×10^{-4}
Crossectional Shell Wall Area (m^2)	9.65250×10^{-3}	1.05763×10^{-2}	7.95317×10^{-3}
Heat-Transfer Coefficient (TUBE) (W/m^2K)	2557.905	2557.905	2557.905
Heat-Transfer Coefficient (SHELL) (W/m^2K)	2000	2000	2000
Overall Heat-Transfer Coefficient (W/m^2K)	1000	1000	1000

First, let us examine the open-loop (uncontrolled) dynamics of this HEN for the disturbance set (vector) **d** given below:

$$\mathbf{d} = \begin{bmatrix} \Delta T^{S}_{H,1} \\ \Delta T^{S}_{H,2} \\ \Delta T^{S}_{C,1} \\ \Delta T^{S}_{C,3} \end{bmatrix} = \begin{bmatrix} T^{S}_{H,1} - \overline{T}^{S}_{H,1} \\ T^{S}_{H,2} - \overline{T}^{S}_{H,2} \\ T^{S}_{C,1} - \overline{T}^{S}_{C,1} \\ T^{S}_{C,3} - \overline{T}^{S}_{C,3} \end{bmatrix} = \begin{bmatrix} 0 \\ 0 \\ -4 \\ 0 \end{bmatrix} \tag{5.1}$$

That means, no disturbance is applied on supply temperatures of the hot streams entering the first and second exchangers, and the cold stream entering the third exchanger. However, the supply temperature of cold stream to the first exchanger is decreased by 4 K, according to the disturbance vector in Equation 5.1.

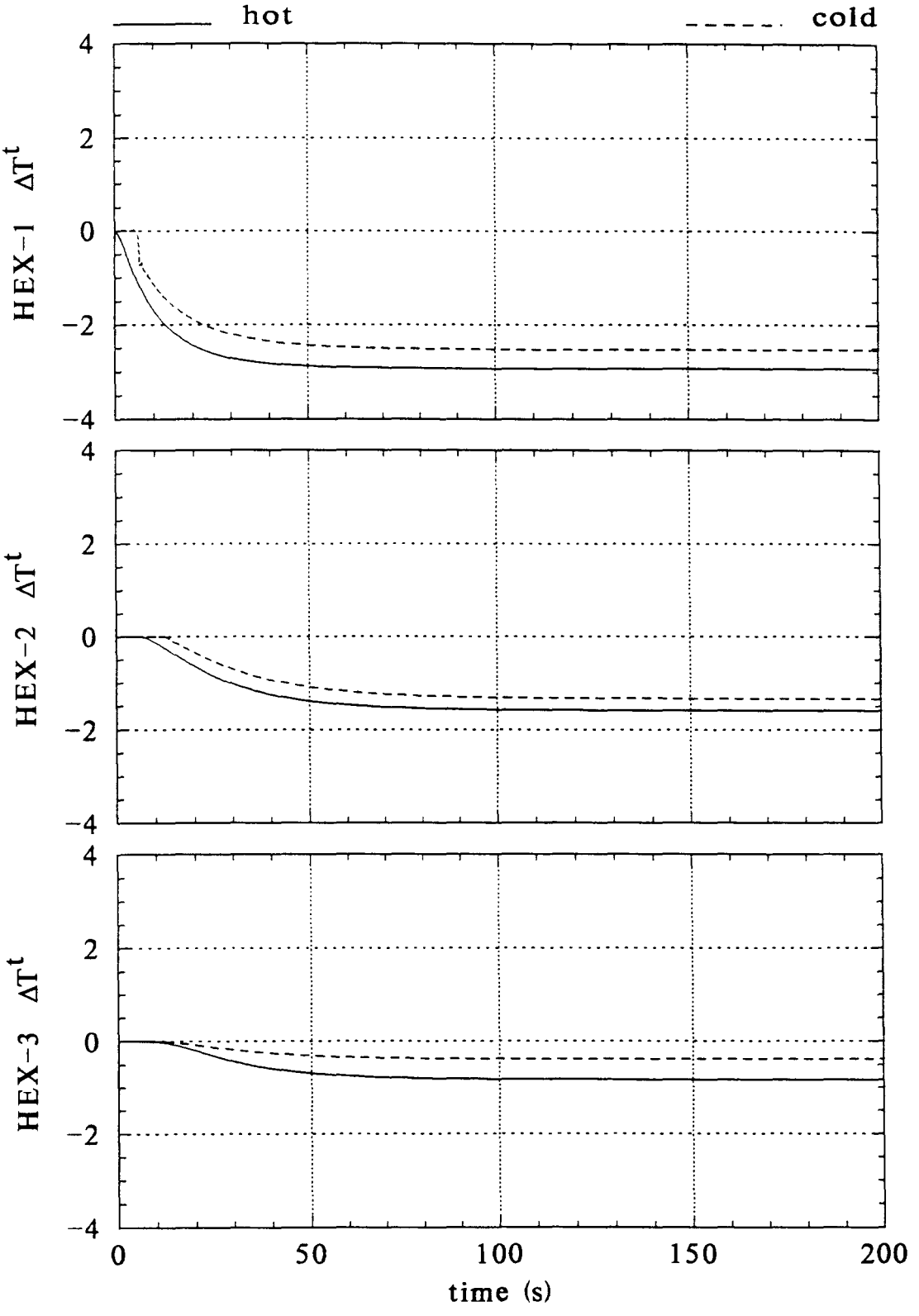

FIGURE 5.3. Openloop (Uncontrolled) Response of the HEN.

To obtain the uncontrolled dynamics of the HEN, the distributed-parameter models of the individual exchangers given in Chapter 3 were interconnected through boundary conditions. The set of partial differential equations ($4\times N_{HEX}$) were discretized in the spatial domain using "five-point biased-upwind" finite difference as explained in Chapter 3. The total number of ordinary differential equations after "method of lines" discretization is $[4\times N_Z\text{-}2]\times N_{HEX}$ (with N_Z=101 and N_{HEX}=3, the number of ODE's adds up to 1206). This stiff set of ODEs were integrated using the software package LSODES as explained in Chapter 3.

The open-loop (uncontrolled) response of the HEN is shown in Figure 5.3. The curves show the temperatures of the effluent hot (solid) and cold (dashed) streams as deviations from the nominal (zero disturbance) values given in Figure 5.2; $\Delta T^o_{H,n} = T^o_{H,n} - \overline{T}^o_{H,n}$ and $\Delta T^o_{C,n} = T^o_{C,n} - \overline{T}^o_{C,n}$. As can be seen from the response of the first exchanger (HEX-1), the disturbance in cold stream immediately affects the hot effluent stream since the hot stream exits the exchanger at the location the cold stream (disturbance) enters (counter-current exchanger). Considering the overall fast dynamics (about 50 seconds settling time) of the exchangers, lag (which is about 15 seconds) in the hot and cold streams of the third exchanger (HEX-3) is significant. The steady-state deviation after disturbance is less than the magnitude of the disturbance and decrease as the disturbance travels through more and more exchangers. The dynamic responses of the individual exchangers, and hence of the HEN, are rapid. As it is obvious from the network structure in Figure 5.2, the disturbance in $T^s_{C,1}$ has the ability to affect all terminals of the HEN.

Now, suppose that the target stream temperatures of this HEN are to be controlled according to the control-range vector **c** defined as

$$\mathbf{c} = \begin{bmatrix} \Delta T^t_{H,1} \\ \Delta T^t_{H,3} \\ \Delta T^t_{C,2} \\ \Delta T^t_{C,3} \end{bmatrix} = \begin{bmatrix} \left| T^t_{H,1} - \overline{T}^t_{H,1} \right| \\ \left| T^t_{H,3} - \overline{T}^t_{H,3} \right| \\ \left| T^t_{C,2} - \overline{T}^t_{C,2} \right| \\ \left| T^t_{C,3} - \overline{T}^t_{C,3} \right| \end{bmatrix} = \begin{bmatrix} 1 \\ 1 \\ 2 \\ 1 \end{bmatrix} \tag{5.2}$$

The nomenclature is similar to that of disturbance vector (Equation 5.1). The first and third hot target streams are to be controlled within ±1 K, i.e., in the range [384 K-386 K] and [409 K-411 K] respectively. The third cold target stream should also be controlled within ±1 K, i.e., in the range [339 K-341 K]. The cold target stream from the second exchanger should be controlled within ±2 K, i.e.; in the range [558 K-562 K].

As can be seen from the uncontrolled dynamic response of the HEN in Figure 5.3, the hot target-stream temperature from the first heat exchanger exceeds the desired control range of ±1 K. It should be noted that the cold outlet stream of the first heat exchanger and hot outlet stream of the second heat exchanger are not target streams; they are the intermediate streams connecting the heat exchangers, and hence their temperatures do not have to be controlled.

Now, let us determine the optimal values of control variables (bypass fractions) the locations of which are shown in Figure 5.4. For the disturbance and control vectors defined in Equation 5.1 and Equation 5.2, the optimization formulation described in Chapter 4, yields the following optimal bypass fractions which guarantee the steady-state feasibility (satisfaction of the control vector):

$$\mathbf{u}_H^{opt} = \begin{bmatrix} u_{H,1} \\ u_{H,2} \\ u_{H,3} \end{bmatrix} = \begin{bmatrix} 0.019919 \\ 0 \\ 0 \end{bmatrix} \tag{5.3}$$

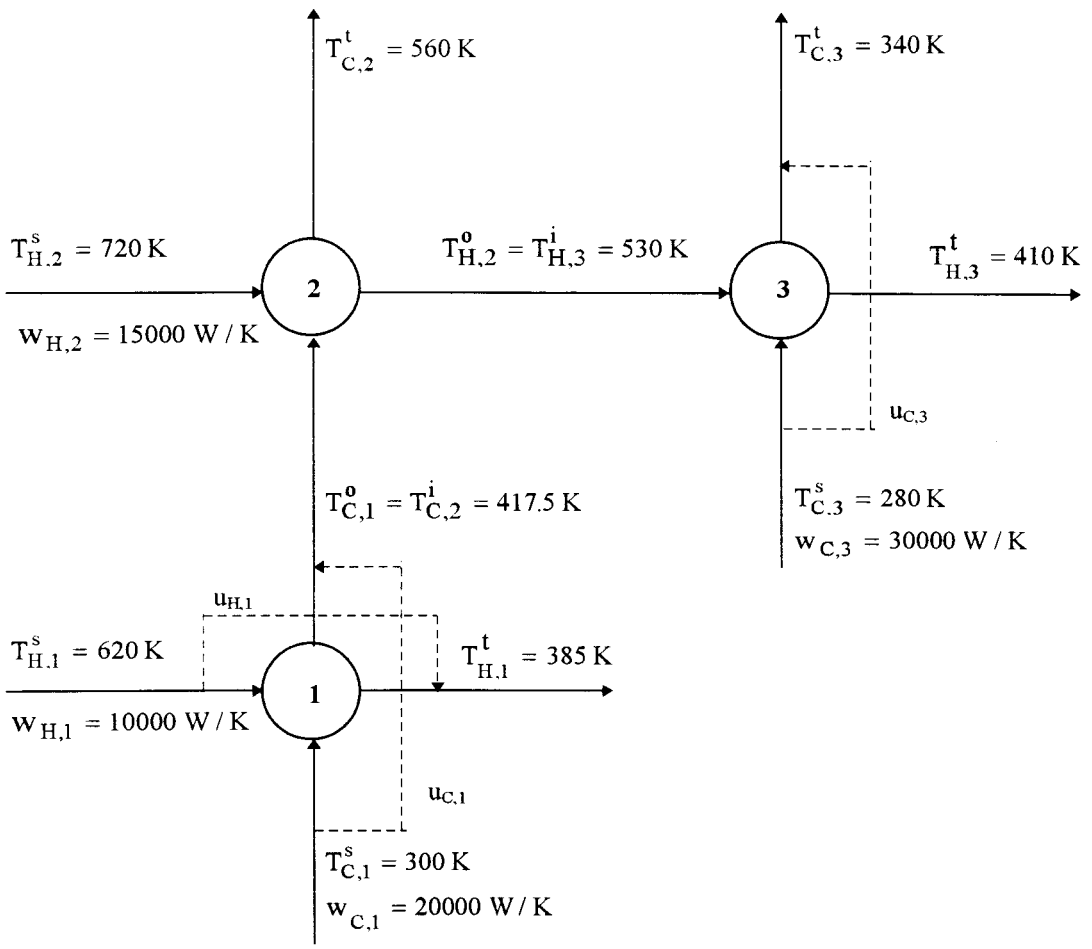

FIGURE 5.4. Locations of Bypass Streams.

$$\mathbf{u}_C^{opt} = \begin{bmatrix} u_{C,1} \\ u_{C,2} \\ u_{C,3} \end{bmatrix} = \begin{bmatrix} 0.000468 \\ 0 \\ 0.055962 \end{bmatrix} \tag{5.4}$$

Now, let us investigate the dynamics and controllability of the HEN when these optimal controls are applied instantaneously, i.e., when the optimal bypass streams are opened from their nominal values (zero) to those given in Equation 5.3 and Equation 5.4 immediately at the instant when the disturbance set, **d**, in the source streams are measured.

Figure 5.5 shows the controlled response of the HEN. As can be seen, the steady-state target temperatures are within the control range specified by the control vector, **c**. However, initially, the outlet temperature of the hot stream from the first exchanger and the outlet temperature of the cold stream from the third exchanger violate the control-range constraints. The disturbance can not be the reason for these temporary violations because it requires a certain time period to propagate through the exchangers, as can be seen in Figure 5.3. Since the initial violations do not exist in Figure 5.3, where the bypass stream were not opened, it is obvious that the initial violations are due to the immediate application of the controls. When the bypass streams are opened at the instant the disturbance is applied, the effect of the bypass streams reach the mixing points before the effect of the disturbance, and hence, causes deviations in the outlet temperatures of the mixing points. For this reason, the immediately applied controls act as an internal disturbance causing the target temperatures to violate the control-range constraints temporarily. As time passes, the effects of the disturbance propagate through the network, and, when combined with the effects of the bypass streams, the new steady-state conditions are reached without violation of the control-range constraints, as can be seen in Figure 5.5.

In order to overcome the early violations of the control-range constraints, the openings of the bypass streams should be processed in a different manner. This will be the concern of the next section.

5.2. Ramped Opening of the Bypass Streams

As it was illustrated previously, instantaneous application of the bypass streams causes the target-stream temperatures to violate the specified control-range constraints temporarily. In this section, dynamics and controllability of the HEN are investigated when the manipulated variables (bypass flows) are opened gradually (as a ramp function) in time, starting from their nominal values, $\bar{\mathbf{u}}$, up to their optimal values, $\mathbf{u}^{opt}$, within a specified

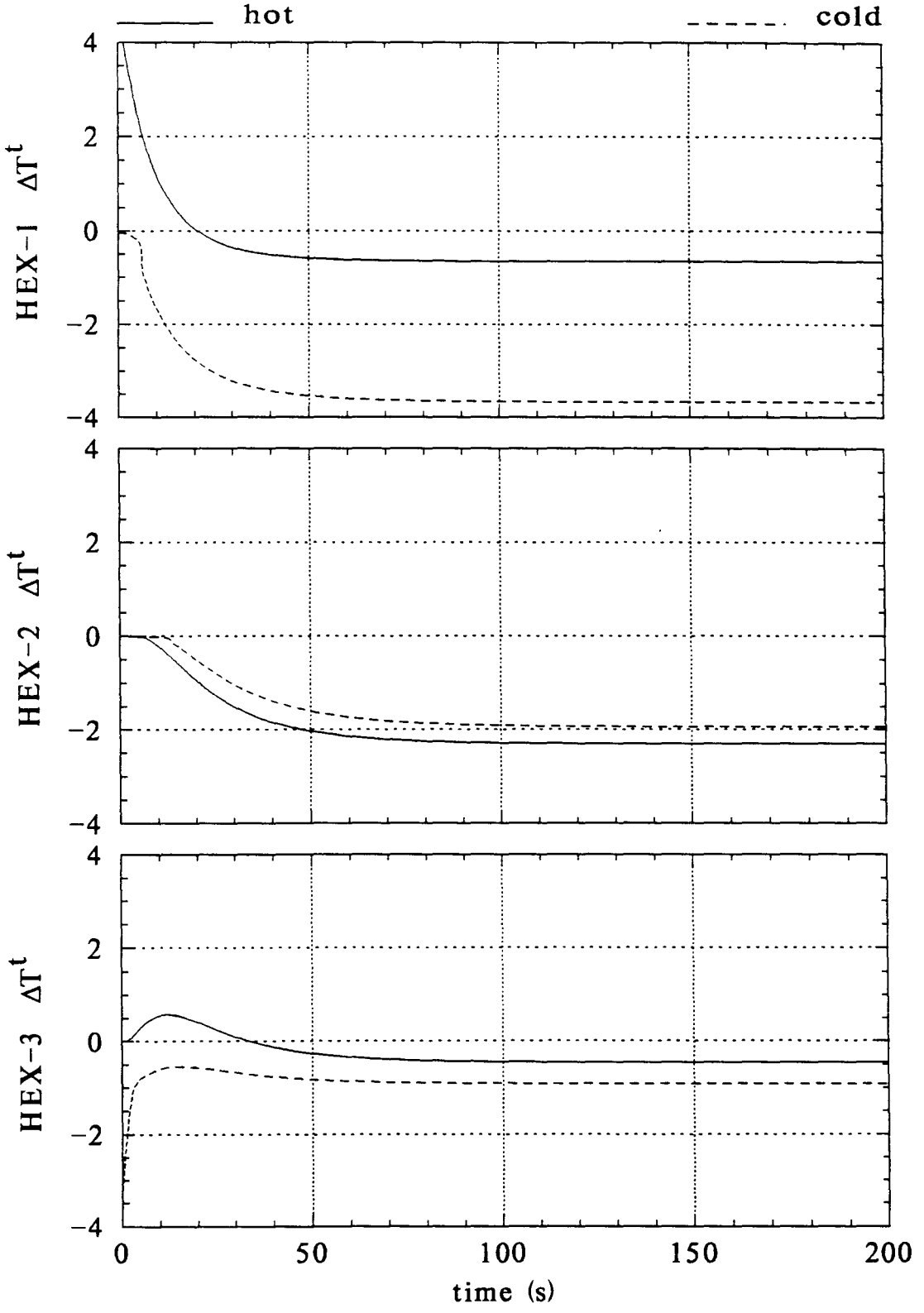

FIGURE 5.5. Response of the HEN Under Instantaneous Application of the Controls.

time interval τ. The mathematical formulation is given by Equation 5.5 and Figure 5.6 depicts this function for a single bypass.

$$u_n = \begin{cases} \bar{u}_n + \left(u_n^{opt} - \bar{u}_n\right)\left(\dfrac{t}{\tau_i}\right) & , \text{if } t < \tau_i \\ u_n^{opt} & , \text{if } t \geq \tau_i \end{cases} \tag{5.5}$$

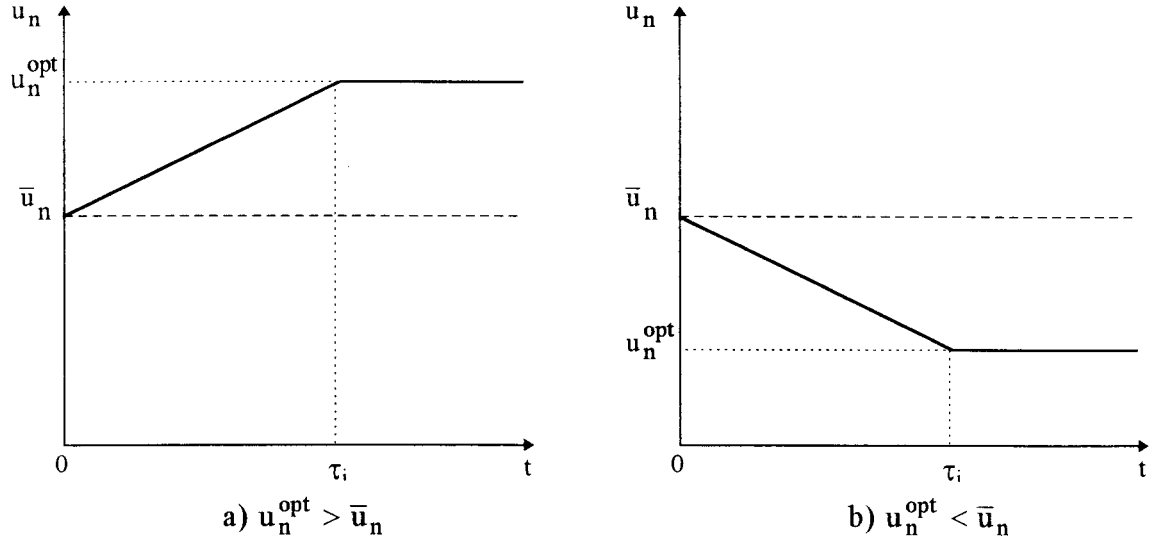

FIGURE 5.6. Two Possible Bypass Fraction Manipulations According to a Ramp Function.

The dynamic behavior of the HEN when all the bypasses were opened according to the ramp function within 20 seconds (τ_i=20) is shown in Figure 5.7. The target temperatures which violated the control range when the optimal bypasses are implemented immediately (i.e., the hot target-stream temperature exiting from the first exchanger and the cold target stream temperature exiting from the third exchanger as can be seen in Figure 5.5), do not exceed the control range. The magnitude of total target-stream temperature deviations are also small as compared to Figure 5.5. The application of the ramp function has no effect on the final steady-state conditions as can be seen in Figure

5.7. It merely alters (generally increases) the time necessary to reach the steady-state conditions.

Figures 5.8, 5.9, 5.10 and 5.11 show the dynamics of the HEN when all the bypasses were opened according to the ramp function within 30, 40 and 80 seconds (τ_i=10, τ_i=30, τ_i=40, τ_i=80), respectively. As can be seen from these figures, as the bypasses are opened more slowly (as τ_i increases), the dynamics of the HEN become smoother and slower. For τ_i = 10 seconds, the first hot target stream and third cold target stream violate the control-range constraints temporarily. For τ_i = 80 seconds, on the other hand, the hot target stream of the first exchanger violates the control-range constraints temporarily.

At this point, we know that the dynamic response of the HEN can be tuned and possible temporary violations of the control-range constraints can be eliminated by adjusting the rate with which the openings of the bypasses are done. Now, we describe a way of automatically determining the optimal rate of opening the controls (i.e., optimal value of τ_i). To do this, we select two different performance criterion which are to be minimized and are the measures of the deviations of all the target-stream temperatures from their nominal values, i.e. call it ε_1, and the deviations of all the target-stream temperatures from their final target (steady-state) values, i.e. call it ε_2. Mathematically, we define ε_1 and ε_2 as

$$\varepsilon_1 = \int_0^{t^\infty} \sum_k^{targets} \left| T_k^t(t) - \overline{T}_k^t \right| dt \tag{5.6}$$

$$\varepsilon_2 = \int_0^{t^\infty} \sum_k^{targets} \left| T_k^t(t) - T_k^{t,opt} \right| dt \tag{5.7}$$

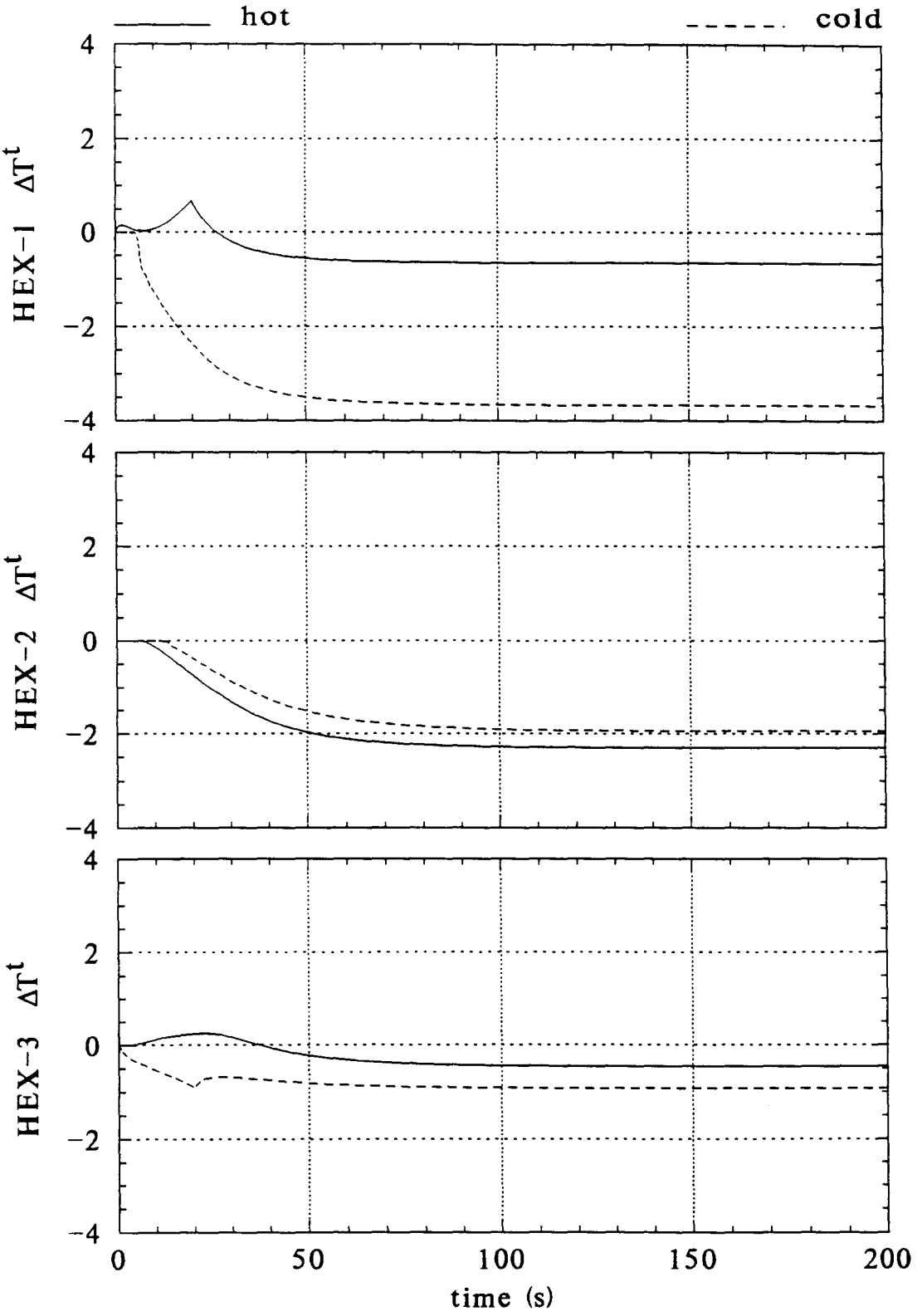

FIGURE 5.7. Response of the HEN with Bypasses Opened According to Ramp Function with τ_i = 20 seconds.

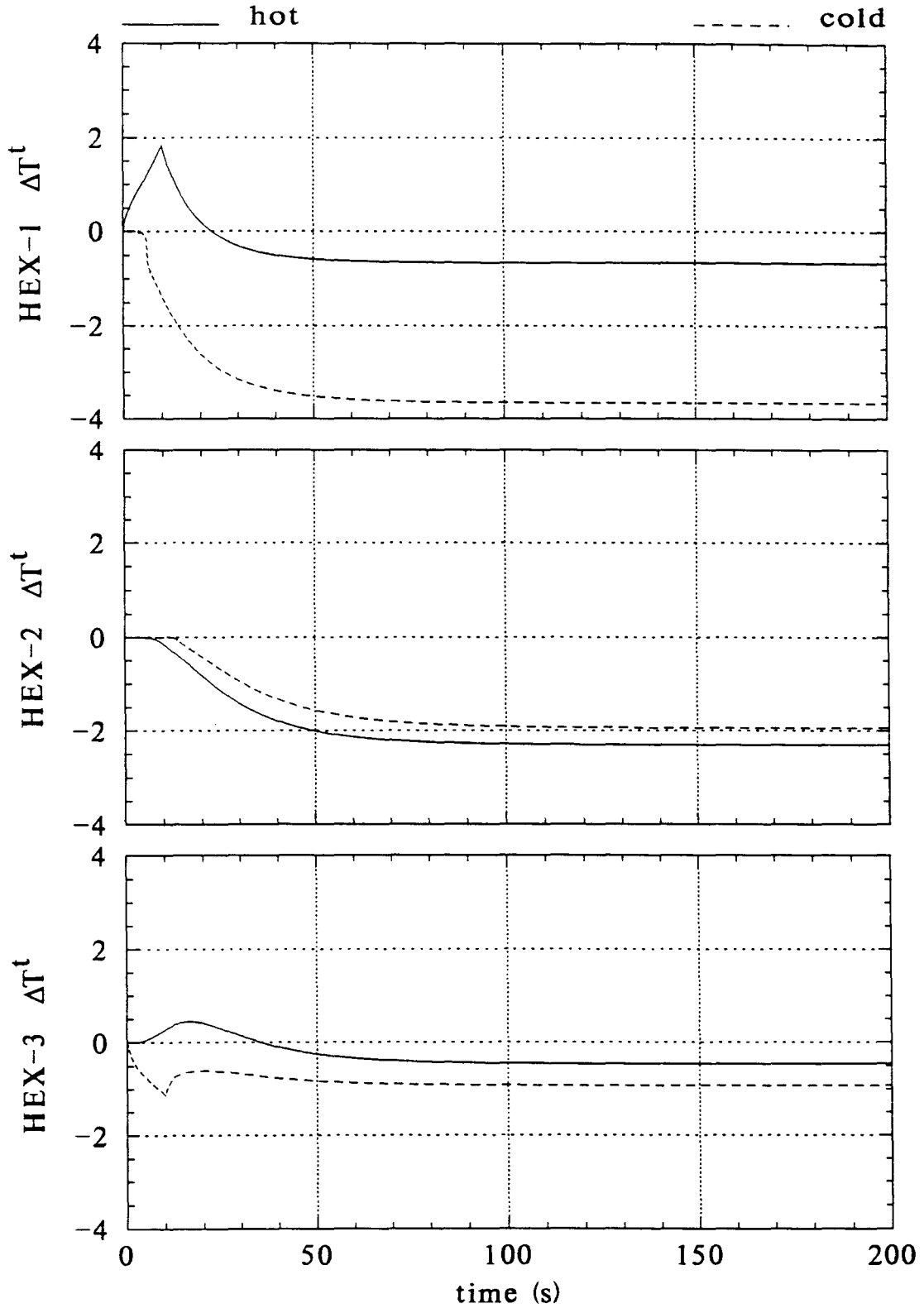

FIGURE 5.8. Response of the HEN with Bypasses Opened According to Ramp Function with τ_i = 10 seconds.

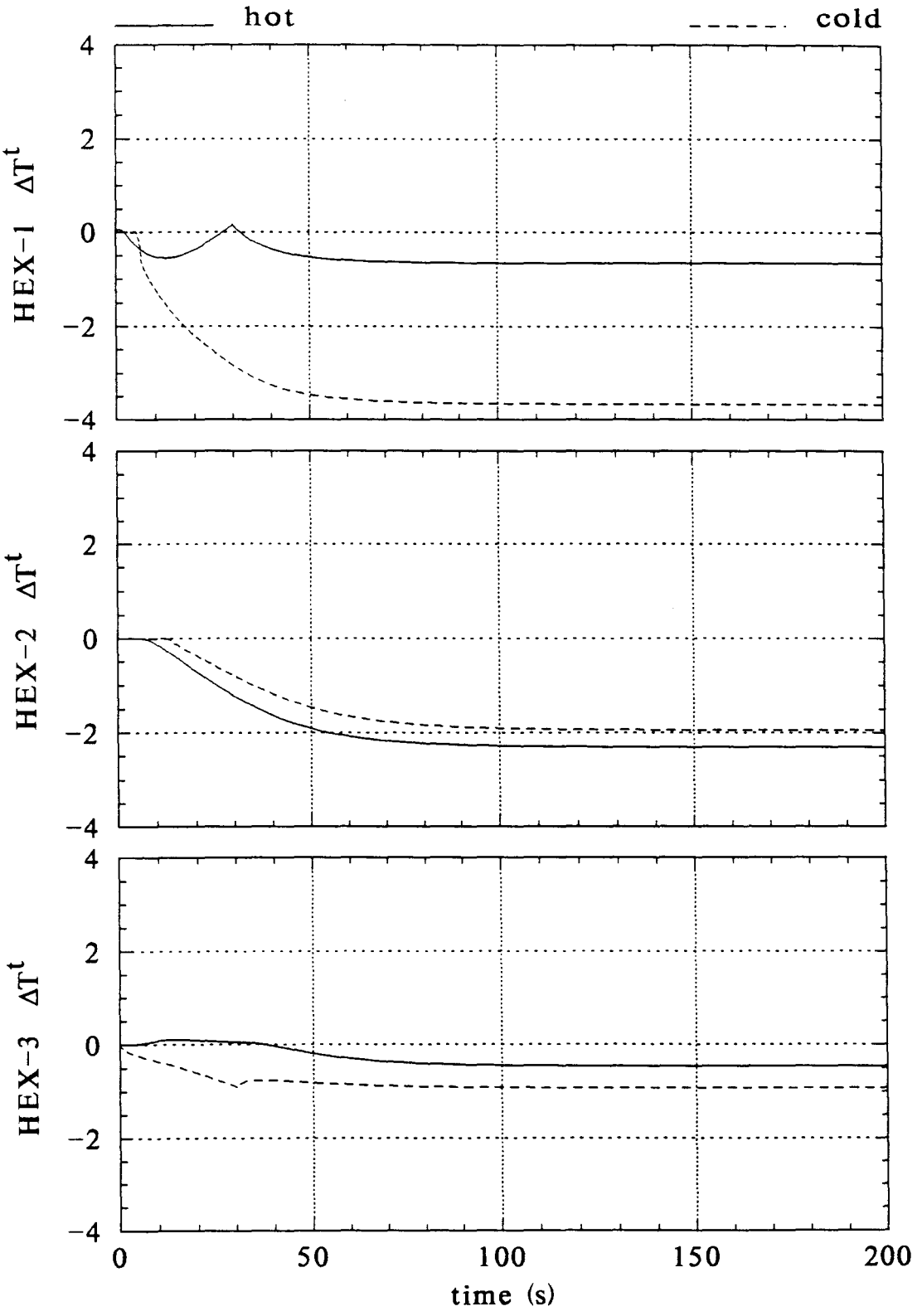

FIGURE 5.9. Response of the HEN with Bypasses Opened According to Ramp Function with τ_i = 30 seconds.

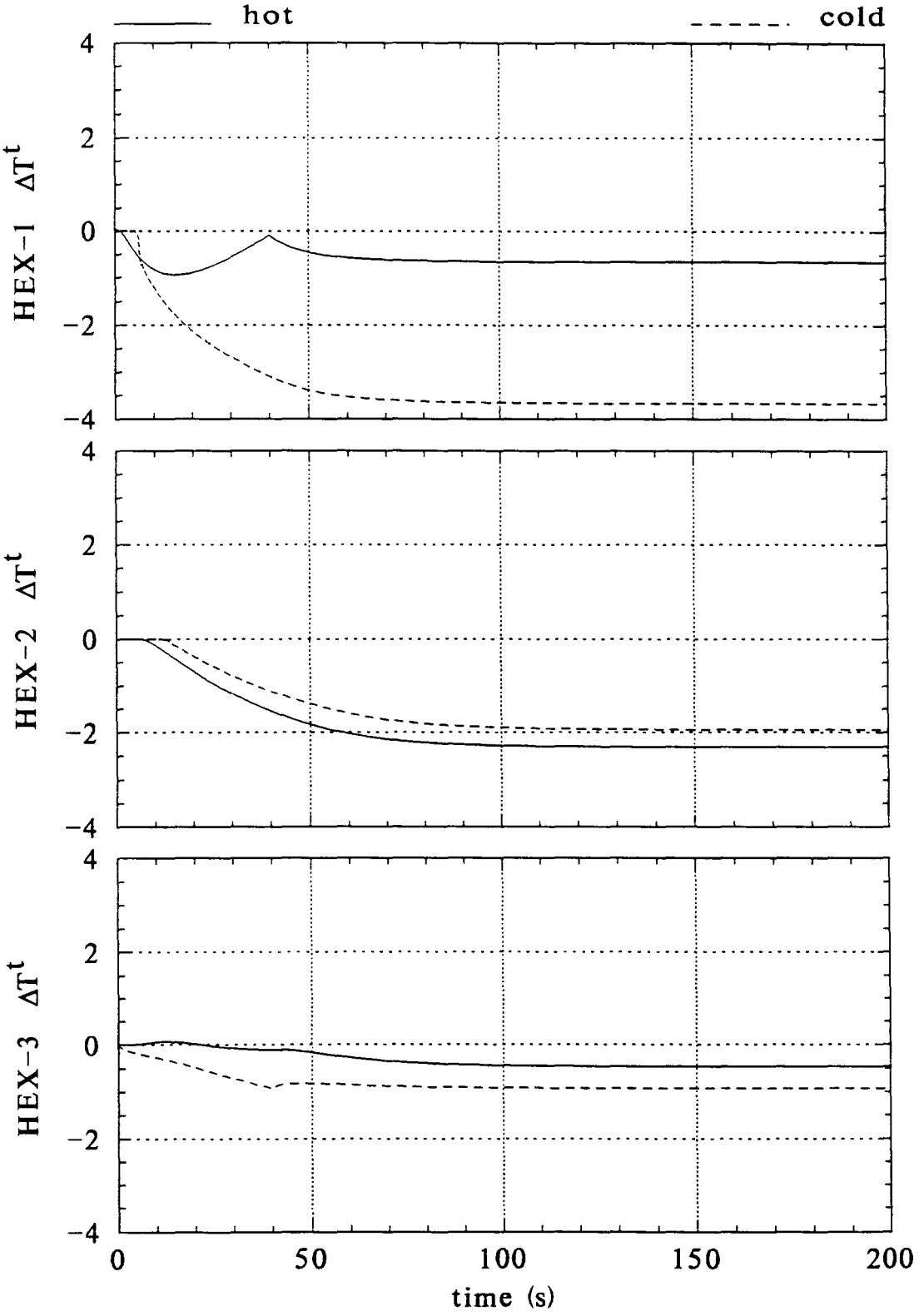

FIGURE 5.10. Response of the HEN with Bypasses Opened According to Ramp Function with τ_i = 40 seconds.

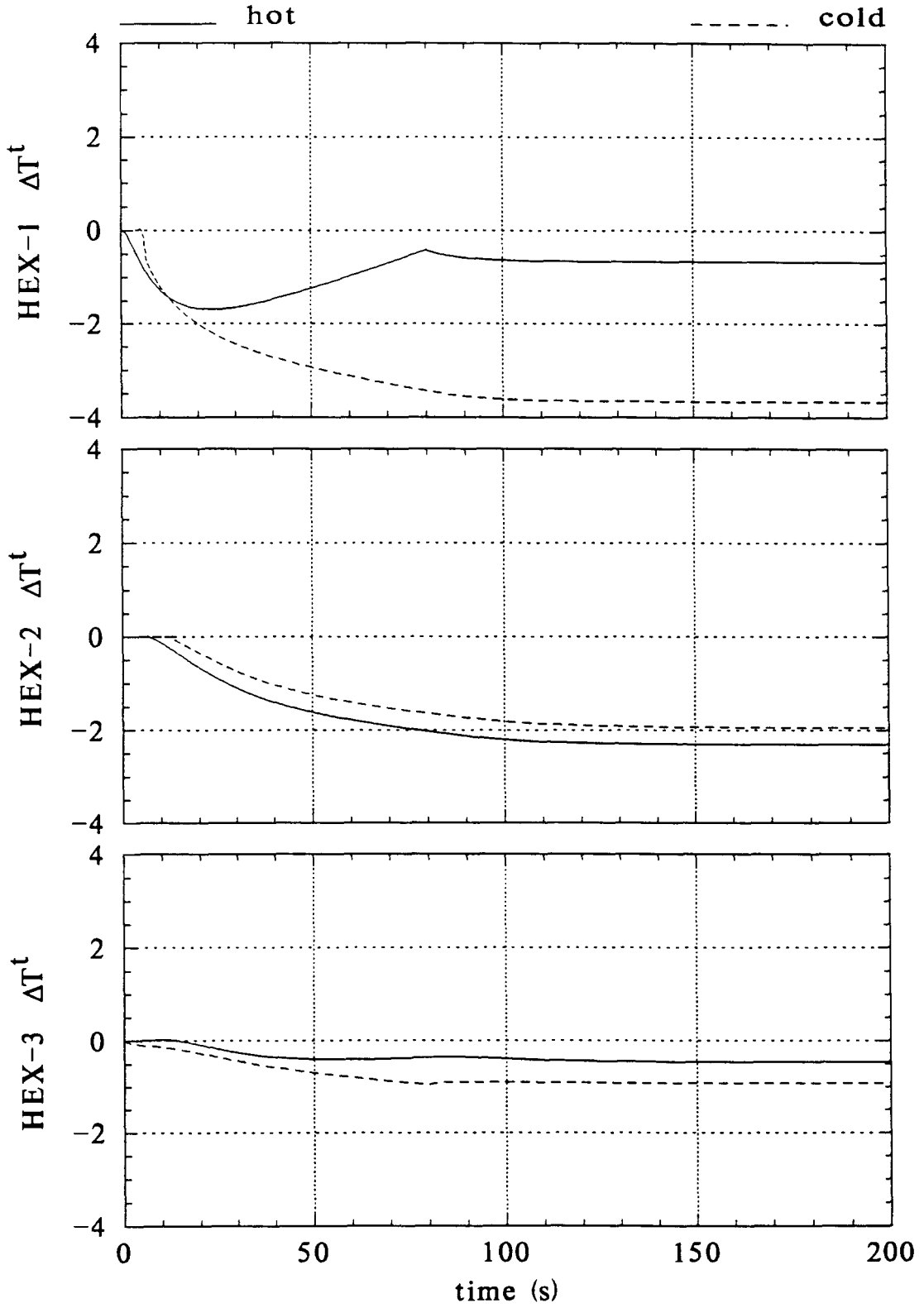

FIGURE 5.11. Response of the HEN with Bypasses Opened According to Ramp Function with τ_i = 80 seconds.

Pictorial representation of ε_1 and ε_2 (areas under and above the solid curve, respectively) for a specific target stream are shown in Figure 5.12.

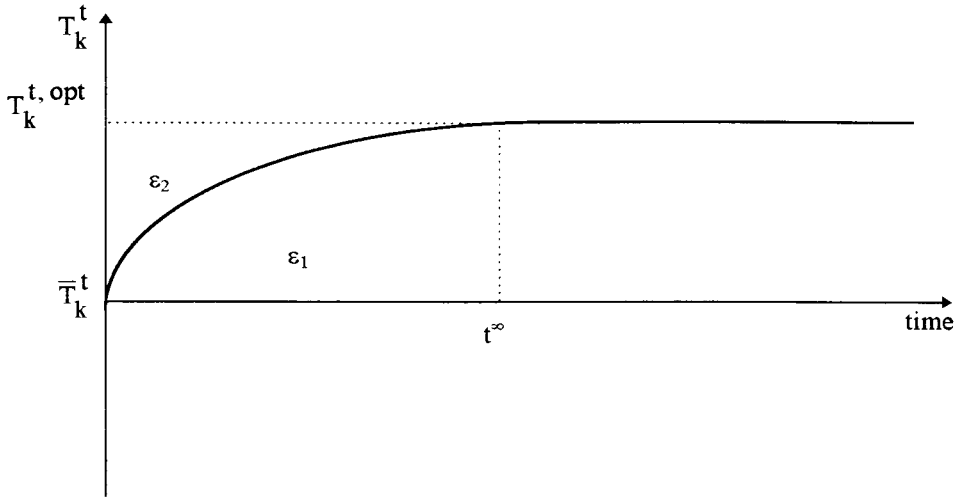

FIGURE 5.12. Description of Performance Criteria ε_1 and ε_2.

Experimentation with different HENs and with differently located bypass streams and with different disturbance directions have shown that ε_1 and ε_2 generally have the dependence on τ_i (same τ_i for all bypasses) as depicted in Figure 5.13. The left-hand-side hatched regions in these figures show the infeasible regions in which temporary violation of control-range constraints may occur since the sets of opening of the bypasses are fast. On the other hand, the right-hand-side hatched regions show the infeasible regions in which temporary violations of control-range constraints may occur since the rate of opening of the bypasses are so slow that the dynamic behavior of the HEN approaches the uncontrolled response. Since fast dynamics and quick control (settling time) of a dynamic system is generally desired, it is clear that ε_1 should be preferred as the performance index rather than ε_2.

A simplified mathematical formulation of the problem of finding an optimal τ may be expressed as follows (see Equation 5.2):

$$\underset{\tau_i}{\textit{minimize}}\ \varepsilon_1 \tag{5.8}$$

$$\text{subject to} \quad \left(\overline{T}_k^t - \Delta T_k^t(t)\right) \le T_k^t(t) \le \left(\overline{T}_k^t + \Delta T_k^t(t)\right) \quad \text{for all targets} \tag{5.9}$$

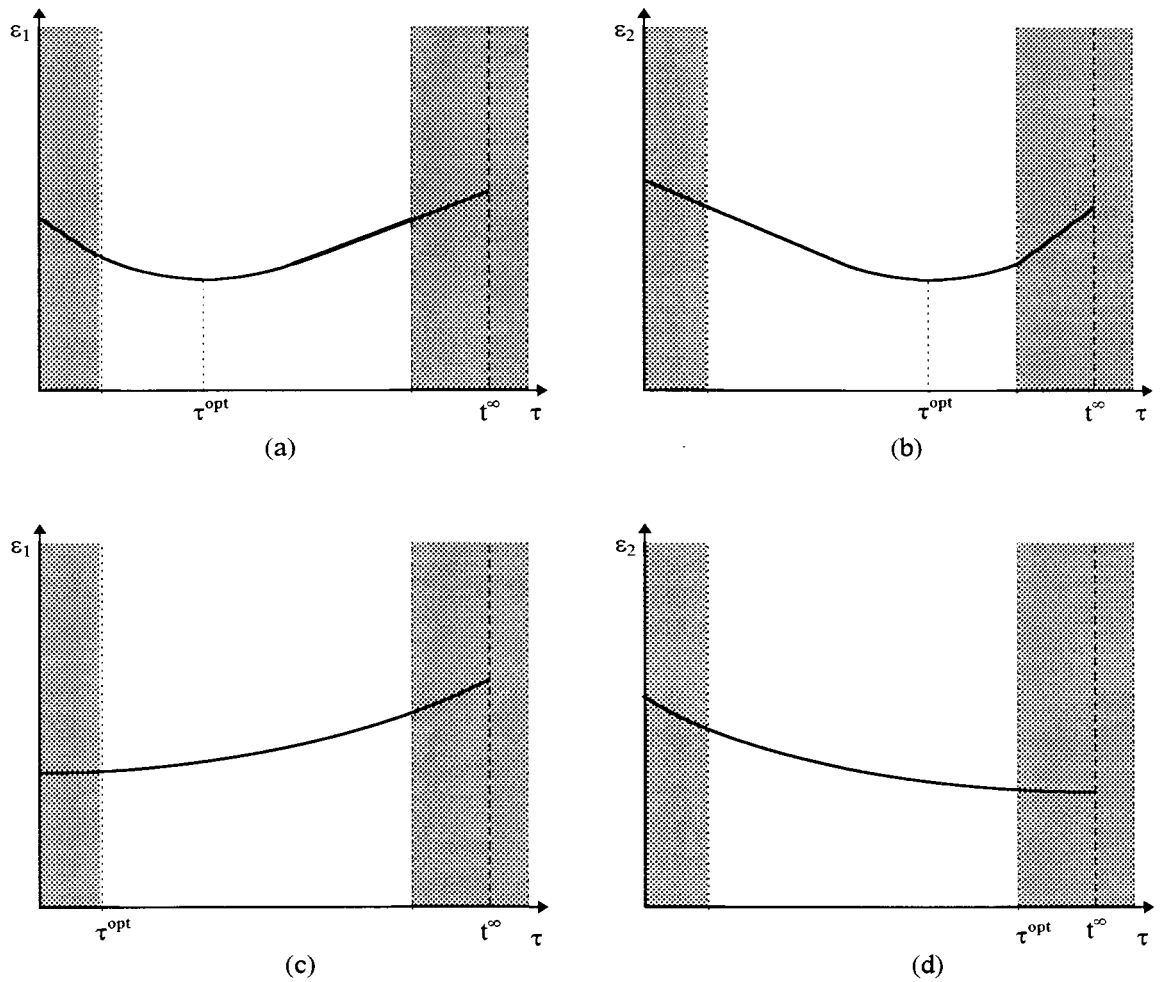

FIGURE 5.13. Dependencies of ε_1 and ε_2 on τ_i.

Figure 5.14 shows the dependence of ε_1 on τ_i (same for all bypass streams) for the HEN shown in Figure 5.4.

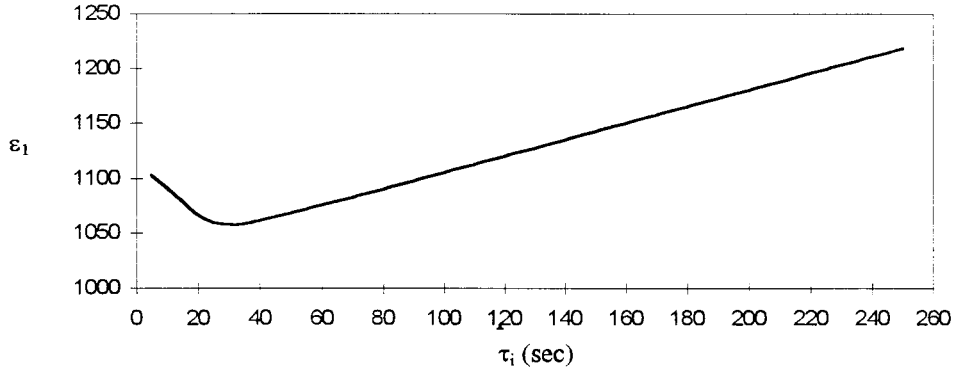

FIGURE 5.14. Dependence of ε_1 on τ_i for the Sample HEN.

The solution of the optimization problem given by Equation 5.8 and Equation 5.9 yields τ_i^{opt} as 32 seconds. Figure 5.15 shows the dynamics of the HEN when τ_i^{opt} is applied.

5.3. Consecutive Disturbances

In this part, robustness of the optimal-control algorithm is tested for consecutive disturbances.

The HEN shown in Figure 5.2 was taken as the test case, and two disturbance sets of different directions were considered. The disturbance set, $\mathbf{d}_1$, was defined as

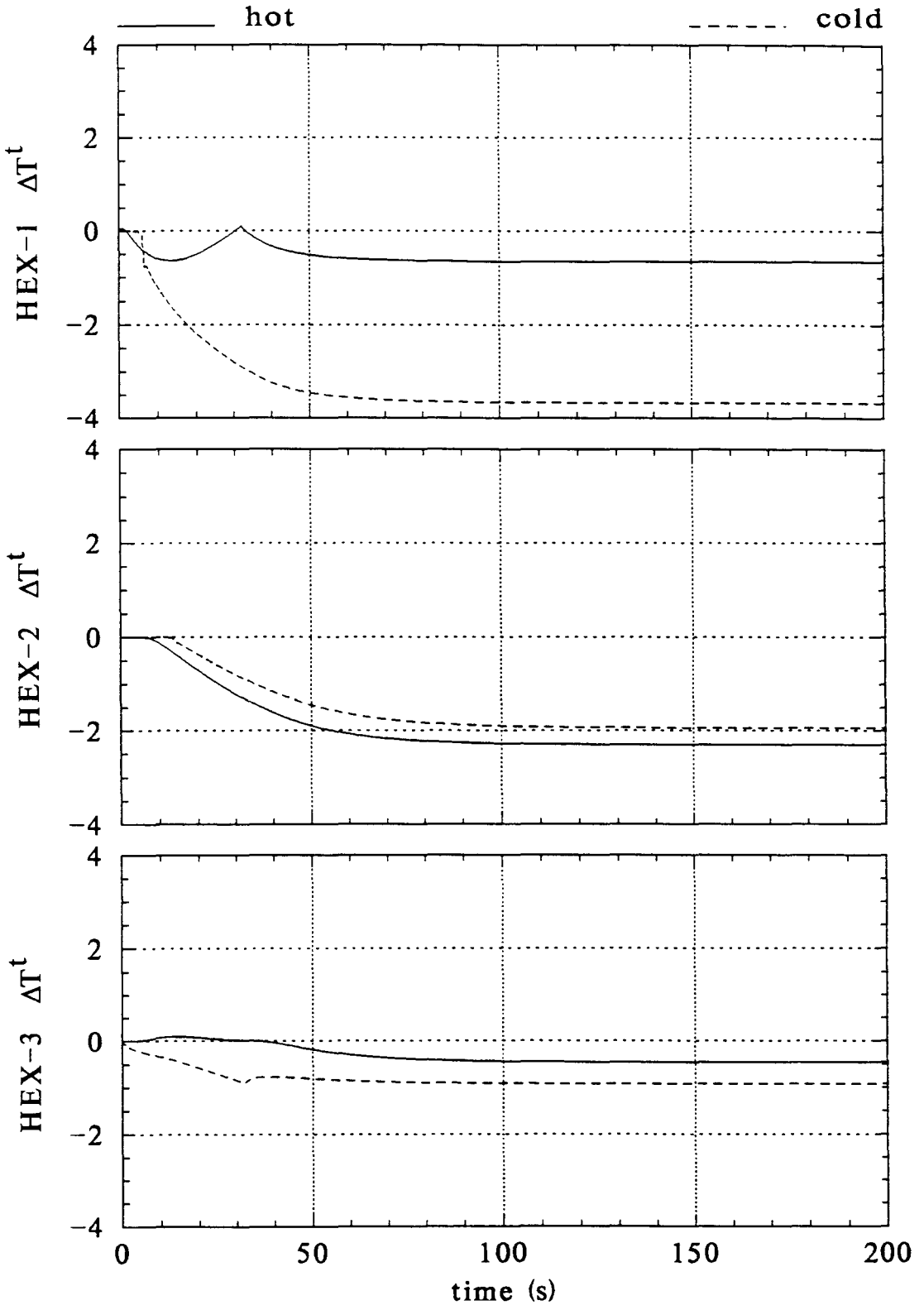

FIGURE 5.15. Response of the HEN with Bypasses Opened According to Ramp Function with τ_i^{opt} = 32 seconds.

$$\mathbf{d}_1 = \begin{bmatrix} \Delta T^s_{H,1} \\ \Delta T^s_{H,2} \\ \Delta T^s_{C,1} \\ \Delta T^s_{C,3} \end{bmatrix} = \begin{bmatrix} T^s_{H,1} - \bar{T}^s_{H,1} \\ T^s_{H,2} - \bar{T}^s_{H,2} \\ T^s_{C,1} - \bar{T}^s_{C,1} \\ T^s_{C,3} - \bar{T}^s_{C,3} \end{bmatrix} = \begin{bmatrix} 0 \\ 0 \\ 5 \\ 0 \end{bmatrix} \tag{5.10}$$

and was imposed on the HEN for $0 \leq t \leq 80$. The second disturbance set, $\mathbf{d}_2$, was defined as

$$\mathbf{d}_2 = \begin{bmatrix} \Delta T^s_{H,1} \\ \Delta T^s_{H,2} \\ \Delta T^s_{C,1} \\ \Delta T^s_{C,3} \end{bmatrix} = \begin{bmatrix} T^s_{H,1} - \bar{T}^s_{H,1} \\ T^s_{H,2} - \bar{T}^s_{H,2} \\ T^s_{C,1} - \bar{T}^s_{C,1} \\ T^s_{C,3} - \bar{T}^s_{C,3} \end{bmatrix} = \begin{bmatrix} 10 \\ 0 \\ 10 \\ -10 \end{bmatrix} \tag{5.11}$$

and was imposed on the HEN $t > 80$.

The overall control-range vector, $\mathbf{c}$, was defined as

$$\mathbf{c} = \begin{bmatrix} \Delta T^t_{H,1} \\ \Delta T^t_{H,3} \\ \Delta T^t_{C,2} \\ \Delta T^t_{C,3} \end{bmatrix} = \begin{bmatrix} \left| T^t_{H,1} - \bar{T}^t_{H,1} \right| \\ \left| T^t_{H,3} - \bar{T}^t_{H,3} \right| \\ \left| T^t_{C,2} - \bar{T}^t_{C,2} \right| \\ \left| T^t_{C,3} - \bar{T}^t_{C,3} \right| \end{bmatrix} = \begin{bmatrix} 10 \\ 5 \\ 5 \\ 5 \end{bmatrix} \tag{5.12}$$

for $t \geq 0$.

The uncontrolled dynamics of the HEN for these two consecutive disturbances is shown in Figure 5.16. As can be seen, the cold target-stream temperature from the third exchanger violates the desired control range after the second disturbance set.

The locations of the bypass streams are shown in Figure 5.17 (dashed lines represent the first set of bypass streams and the dotted lines represent the second set of bypass streams for the first and second disturbance sets, respectively). The optimal control algorithm, depicted in Figure 5.1, was applied as follows. When the first disturbance was measured in the source streams, the optimal bypass fractions, yielding minimum deviation in target temperatures and satisfying the predefined control-range constraint vector, were obtained from the solution of the static optimization problem defined in Chapter 4. The set of optimal bypass fractions were found to be:

$$\mathbf{u}_{H_{(1)}}^{opt} = \begin{bmatrix} u_{H,1} \\ u_{H,2} \\ u_{H,3} \end{bmatrix} = \begin{bmatrix} 0.01018 \\ 0 \\ 0.008363 \end{bmatrix} \tag{5.13}$$

$$\mathbf{u}_{C_{(1)}}^{opt} = \begin{bmatrix} u_{C,1} \\ u_{C,2} \\ u_{C,3} \end{bmatrix} = \begin{bmatrix} 0 \\ 0 \\ 0 \end{bmatrix} \tag{5.14}$$

As a result of this static optimization, it was found that none of the control-range constraints were active. This can also be seen from Figure 5.16; the first disturbance do not cause violation of the control-range constraints even under no control. This means that, the optimal bypasses, $\mathbf{u}_{H_{(1)}}^{opt}$ and $\mathbf{u}_{C_{(1)}}^{opt}$, simply serve to minimize the deviations of target-stream temperatures from their nominal values.

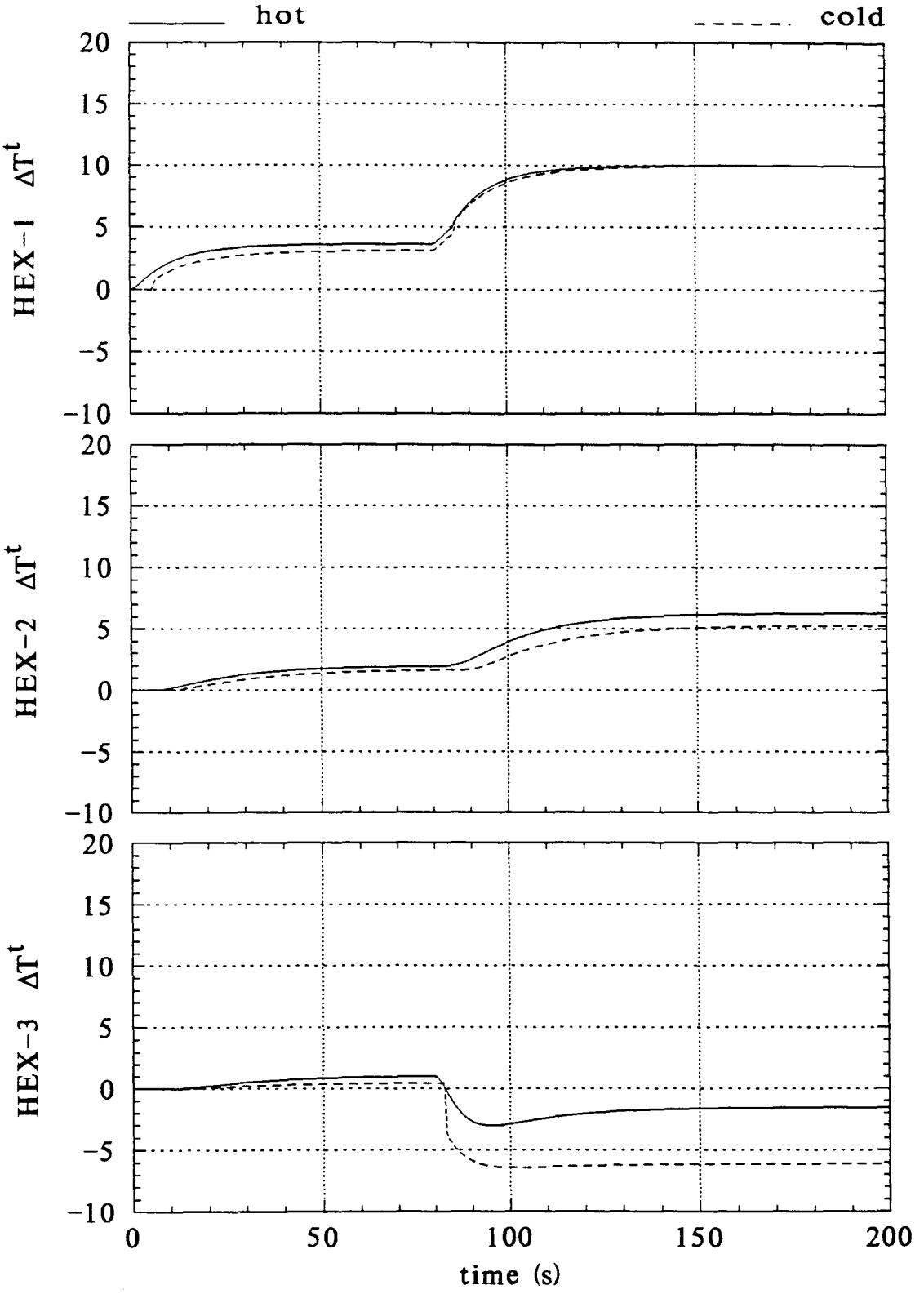

FIGURE 5.16. Uncontrolled Dynamics of the HEN with two Consecutive Disturbances.

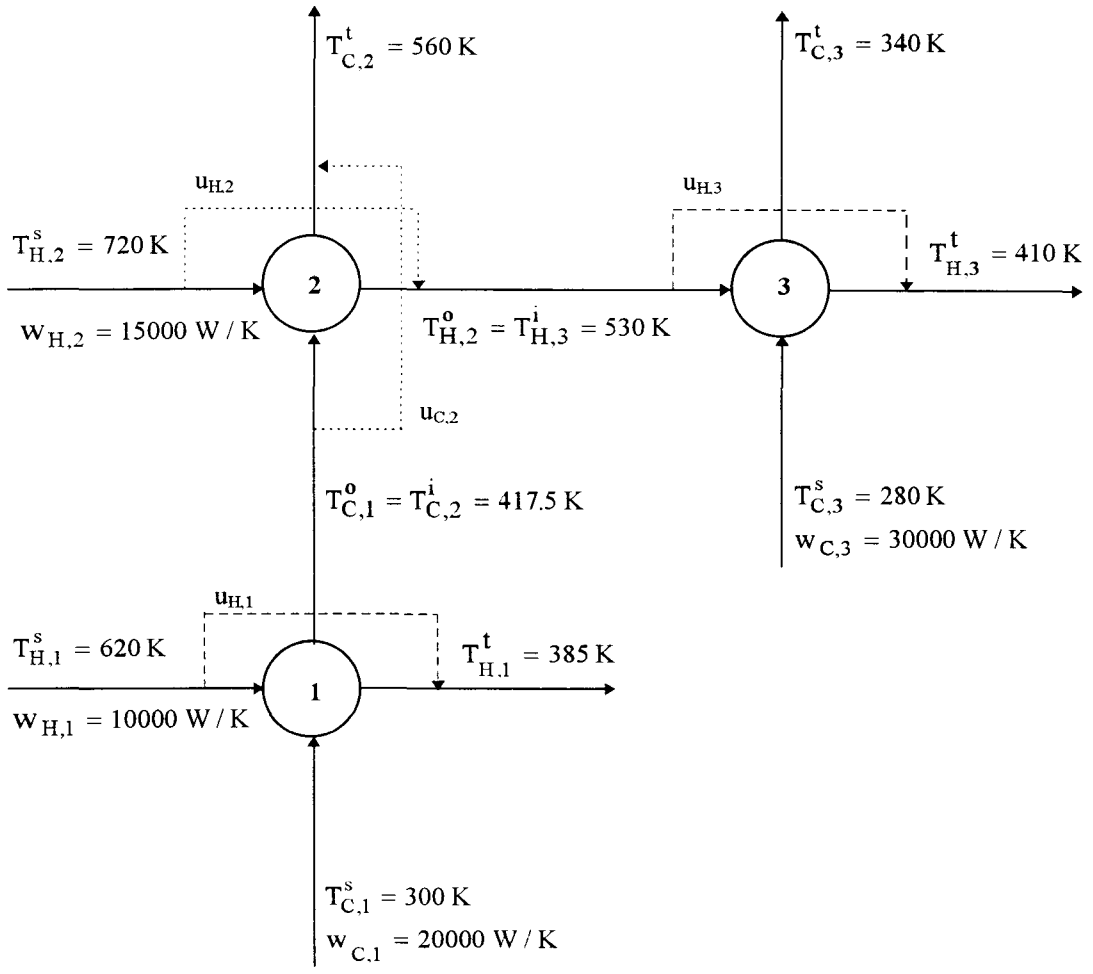

FIGURE 5.17. Bypass-Stream Locations for Consecutive Disturbances.

The dynamics of the HEN was simulated up to t = 80 seconds after which the second disturbance enters the HEN. The first set of optimal bypasses were opened following the ramp function with τ_i = 50 seconds for all the bypasses.

At t=80 seconds, the second disturbance set was measured in the source streams, and the second set of optimal bypass fractions were obtained from the solution of the optimization problem in the same way. However, in this case, the state of the system at t=80 seconds (just before the second disturbance) was taken as the nominal state and $\mathbf{d}_2$ was imposed over this state. Therefore, an intermediate control-range vector had to be defined to perform the static optimization against the second disturbance. This had to be

done in order to preserve the original overall control range, **c** (Equation 5.12), based on the original nominal state (steady-state under no disturbance) of the network. The necessity of redefining the control-range for the second disturbance is best illustrated with the Figure 5.18 for an arbitrary target stream.

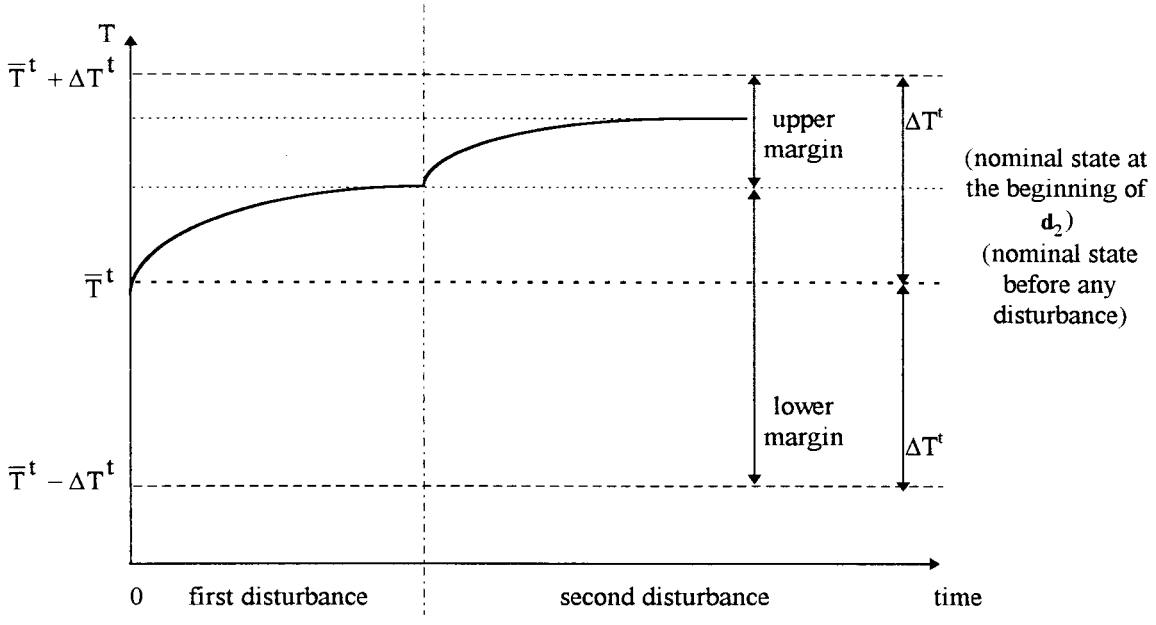

FIGURE 5.18. Description of the Modification of the Control Vector.

After the measurement of the second disturbance set and the adjustment of the control-range vector, the optimal values of the bypasses yielding minimum deviations in target temperatures and satisfying the adjusted control-range constraints were found to be:

$$\mathbf{u}_{H(2)}^{opt} = \begin{bmatrix} u_{H,1} \\ u_{H,2} \\ u_{H,3} \end{bmatrix} = \begin{bmatrix} 0 \\ 0.09469 \\ 0 \end{bmatrix} \tag{5.15}$$

$$\mathbf{u}_{C_{(2)}}^{opt} = \begin{bmatrix} u_{C,1} \\ u_{C,2} \\ u_{C,3} \end{bmatrix} = \begin{bmatrix} 0 \\ 0.08839 \\ 0 \end{bmatrix} \tag{5.16}$$

The simulation of the dynamics of the HEN was continued from t = 80 second up to steady-state conditions by opening and closing the bypasses from $\mathbf{u}_{(1)}^{opt}$ towards $\mathbf{u}_{(2)}^{opt}$ within $\tau_{H\text{-}1}$=5 and $\tau_{H\text{-}3}$=5 seconds to close $\mathbf{u}_{(1)}^{opt}$, and $\tau_{H\text{-}2}$=5 and $\tau_{C\text{-}2}$=40 seconds to open $\mathbf{u}_{(2)}^{opt}$. These τ_i's were the only set found by trial and error which prevented the temporary violations of the target-temperature constraints.

Figure 5.19 shows the overall controlled dynamics of the HEN under these two consecutive disturbances with the application of the two consecutive optimal control sets. As can be seen, none of the target-stream temperatures violate the desired overall control-range constraints given in Equation 5.12.

In this section, it was shown that the optimal control algorithm can be successfully applied for consecutive disturbances as well. The extension to more than two consecutive disturbances is straightforward.

5.4. Dynamics And Control of Alternative HEN Structures with Retrofit Designs

In this section, the dynamics and optimal control of two HENs, which are the two alternative solutions of a heat-exchanger network problem, will be investigated.

The heat-exchanger network problem is to design a HEN for the stream properties given in Table 5.2.

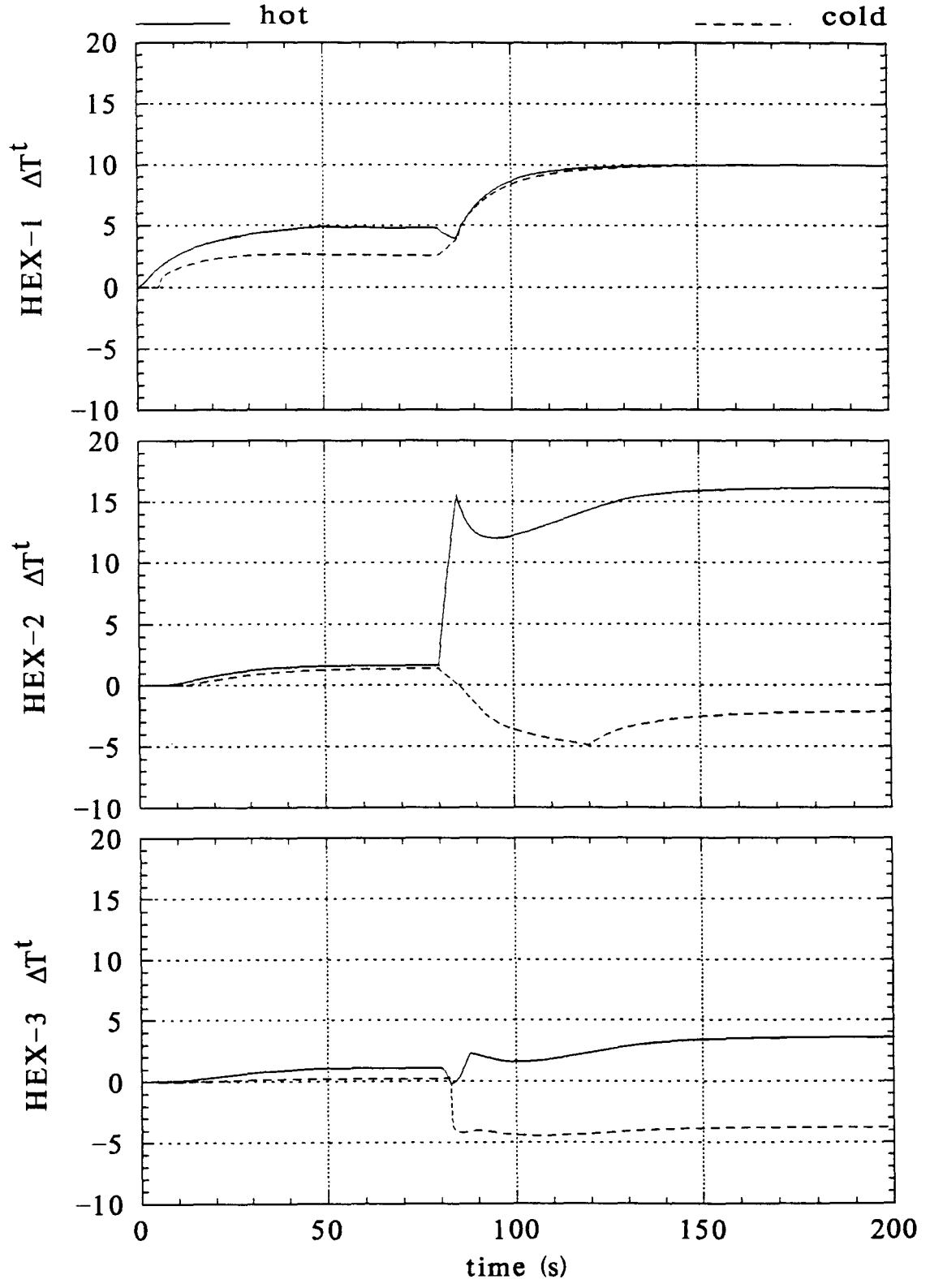

FIGURE 5.19. Controlled Response of the HEN Under Consecutive Disturbances.

TABLE 5.2. Properties of the Sample HEN Problem.

Stream	W (kW/K)	T^i (K)	T^o (K)
Hot-1	10	620	385
Hot-2	15	720	400
Cold-1	20	300	560
Cold-2	30	280	340

$U_u = 0.5$ kW/m^2-K

Two different solutions to this HEN problem exist in the literature. First solution is the HEN structure (HEN-I) obtained from the pinch method [3] and shown in Figure 5.20, and the second solution is the HEN structure (HEN-II) obtained from an MINLP algorithm [20] and shown in Figure 5.21. The original designs do not contain bypass streams (dashed lines in Figures 5.20 and 5.21).

In this section, the dynamics and controllability of the original and retrofit designs [10] of these two HENs will be studied. As briefly mentioned, 'the controllable retrofit design' methodology of Konukman et al. [10] is used to increase the flexibility, and hence, controllability of the original designs by the addition of nominal bypass streams and by optimal (minimum) addition of exchanger areas in order to meet a predefined 'retrofit-design resiliency index (RDRI)' [10].

Tables 5.3 and 5.4 show the key design specifications obtained as described in Chapter 2, for the original and retrofit designs of HEN-I and HEN-II, respectively.

The location of the nominal bypasses are shown by the dashed lines in Figure 5.20 and Figure 5.21. The values of these nominal bypass fractions for HEN-I (obtained from the Pinch Method), $\bar{u}_I$, and for HEN-II (obtained from the MINLP algorithm), $\bar{u}_{II}$, are as follows [10]:

TABLE 5.3. Key Design Specifications of the Heat Exchangers of HEN-I.

PARAMETERS	HEX-1	HEX-2	HEX-3
Original Design			
Number of Tubes	454	104	133
Length (m)	1.94698	1.9543	1.95934
Shell Diameter (mm)	768.79505	390.35871	436.88363
Velocity (HOT) (m/s)	0.12131	0.35303	0.27606
Velocity (COLD) (m/s)	0.09714	0.33961	0.41351
Heat-Transfer Area (HOT) (m^2/tube)	0.12147	0.12193	0.12225
Heat-Transfer Area (COLD) (m^2)	70.53439	16.21860	20.79441
Heat-Transfer Area (SHELL-WALL) (m^2)	4.70242	2.39668	2.68922
Crossectional Inner Area (HOT) (m^2/tube)	3.09776×10^{-4}	3.09776×10^{-4}	3.09776×10^{-4}
Crossectional Inner Area (COLD) (m^2)	0.23416	6.69813×10^{-2}	8.25147×10^{-2}
Crossectional Tube Wall Area (m^2/tube)	1.96931×10^{-4}	1.96931×10^{-4}	1.96931×10^{-4}
Crossectional Shell Wall Area (m^2)	1.82910×10^{-3}	9.37432×10^{-3}	1.04705×10^{-2}
Heat-Transfer Coefficient (TUBE) (W/m^2K)	1278.95267	1278.95267	1278.95267
Heat-Transfer Coefficient (SHELL) (W/m^2K)	1000	1000	1000
Overall Heat-Transfer Coefficient (W/m^2K)	500	500	500
Retrofit Design			
Number of Tubes	468	150	157
Length (m)	1.96014	1.95588	1.94706
Shell Diameter (mm)	779.65909	461.65711	471.42060
Velocity (HOT) (m/s)	0.11533	0.24477	0.23385
Velocity (COLD) (m/s)	0.09467	0.09750	0.17826
Heat-Transfer Area (HOT) (m^2/tube)	0.12145	0.12203	0.12148
Heat-Transfer Area (COLD) (m^2)	72.69680	23.41093	24.39287
Heat-Transfer Area (SHELL-WALL) (m^2)	4.76804	2.83669	2.88362
Crossectional Inner Area (HOT) (m^2/tube)	3.09776×10^{-4}	3.09776×10^{-4}	3.09776×10^{-4}
Crossectional Inner Area (COLD) (m^2)	0.24027	9.13836×10^{-2}	9.49917×10^{-2}
Crossectional Tube Wall Area (m^2/tube)	1.96931×10^{-4}	1.96931×10^{-4}	1.96931×10^{-4}
Crossectional Shell Wall Area (m^2)	1.85469×10^{-2}	1.10542×10^{-2}	1.12843×10^{-2}
Heat-Transfer Coefficient (TUBE) (W/m^2K)	1278.95267	1278.95267	1278.95267
Heat-Transfer Coefficient (SHELL) (W/m^2K)	1000	1000	1000
Overall Heat-Transfer Coefficient (W/m^2K)	500	500	500

TABLE 5.4. Key Design Specifications of the Heat Exchangers of HEN-II.

PARAMETERS	HEX-1	HEX-2	HEX-3
Original Design			
Number of Tubes	223	272	146
Length (m)	1.95135	194734	1.95441
Shell Diameter (mm)	553.91651	606.96147	455.96863
Velocity (HOT) (m/s)	0.16464	0.20247	0.37721
Velocity (COLD) (m/s)	0.17773	0.15012	0.38204
Heat-Transfer Area (HOT) (m^2/tube)	0.12174	0.12149	0.12193
Heat-Transfer Area (COLD) (m^2)	34.72354	42.26647	22.76937
Heat-Transfer Area (SHELL-WALL) (m^2)	3.39570	3.71325	2.79962
Crossectional Inner Area (HOT) (m^2/tube)	3.09776×10^{-4}	3.09776×10^{-4}	3.09776×10^{-4}
Crossectional Inner Area (COLD) (m^2)	0.12798	0.15151	8.93107×10^{-2}
Crossectional Tube Wall Area (m^2/tube)	1.96931×10^{-4}	1.96931×10^{-4}	1.96931×10^{-4}
Crossectional Shell Wall Area (m^2)	1.32280×10^{-2}	1.44779×10^{-2}	1.09202×10^{-2}
Heat-Transfer Coefficient (TUBE) (W/m^2K)	1278.95267	1278.95267	1278.95267
Heat-Transfer Coefficient (SHELL) (W/m^2K)	1000	1000	1000
Overall Heat-Transfer Coefficient (W/m^2K)	500	500	500
Retrofit Design			
Number of Tubes	231	289	165
Length (m)	1.94734	1.94687	1.94974
Shell Diameter (mm)	562.97370	624.15594	482.29881
Velocity (HOT) (m/s)	0.15474	0.19056	0.33778
Velocity (COLD) (m/s)	0.17249	0.12707	0.20868
Heat-Transfer Area (HOT) (m^2/tube)	0.12149	0.12146	0.12164
Heat-Transfer Area (COLD) (m^2)	35.89544	44.89714	25.67120
Heat-Transfer Area (SHELL-WALL) (m^2)	3.44414	3.81751	2.95423
Crossectional Inner Area (HOT) (m^2/tube)	3.09776×10^{-4}	3.09776×10^{-4}	3.09776×10^{-4}
Crossectional Inner Area (COLD) (m^2)	0.13187	0.15952	9.90864×10^{-2}
Crossectional Tube Wall Area (m^2/tube)	1.96931×10^{-4}	1.96931×10^{-4}	1.96931×10^{-4}
Crossectional Shell Wall Area (m^2)	1.34414×10^{-2}	1.48830×10^{-2}	1.15406×10^{-2}
Heat-Transfer Coefficient (TUBE) (W/m^2K)	1278.95267	1278.95267	1278.95267
Heat-Transfer Coefficient (SHELL) (W/m^2K)	1000	1000	1000
Overall Heat-Transfer Coefficient (W/m^2K)	500	500	500

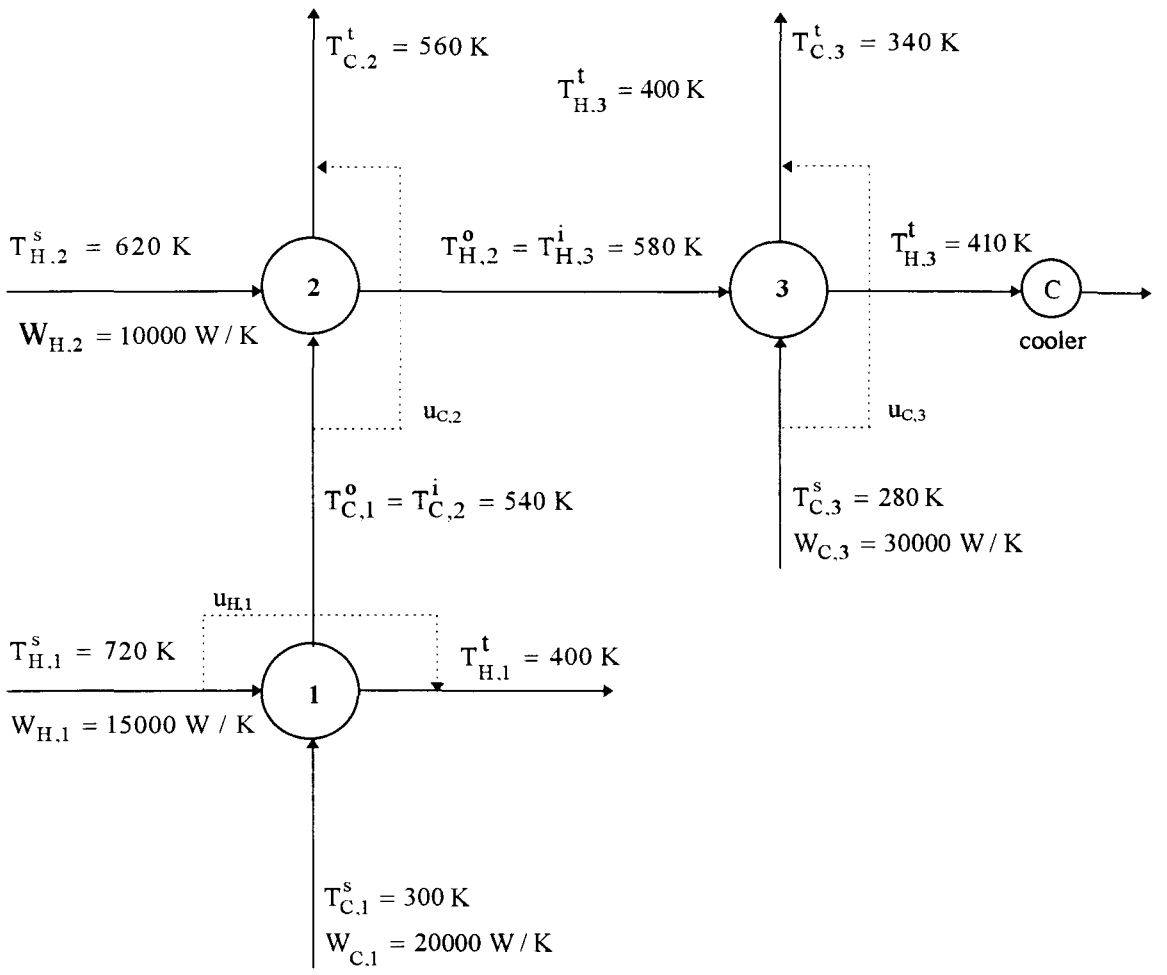

FIGURE 5.20. The Alternative HEN Generated via the Pinch Method.

$$\bar{\mathbf{u}}_{H(I)} = \begin{bmatrix} \bar{u}_{H,1} \\ \bar{u}_{H,2} \\ \bar{u}_{H,3} \end{bmatrix} = \begin{bmatrix} 0.01994 \\ 0 \\ 0 \end{bmatrix} \tag{5.17}$$

$$\bar{\mathbf{u}}_{C(I)} = \begin{bmatrix} \bar{u}_{C,1} \\ \bar{u}_{C,2} \\ \bar{u}_{C,3} \end{bmatrix} = \begin{bmatrix} 0 \\ 0.60831 \\ 0.50371 \end{bmatrix} \tag{5.18}$$

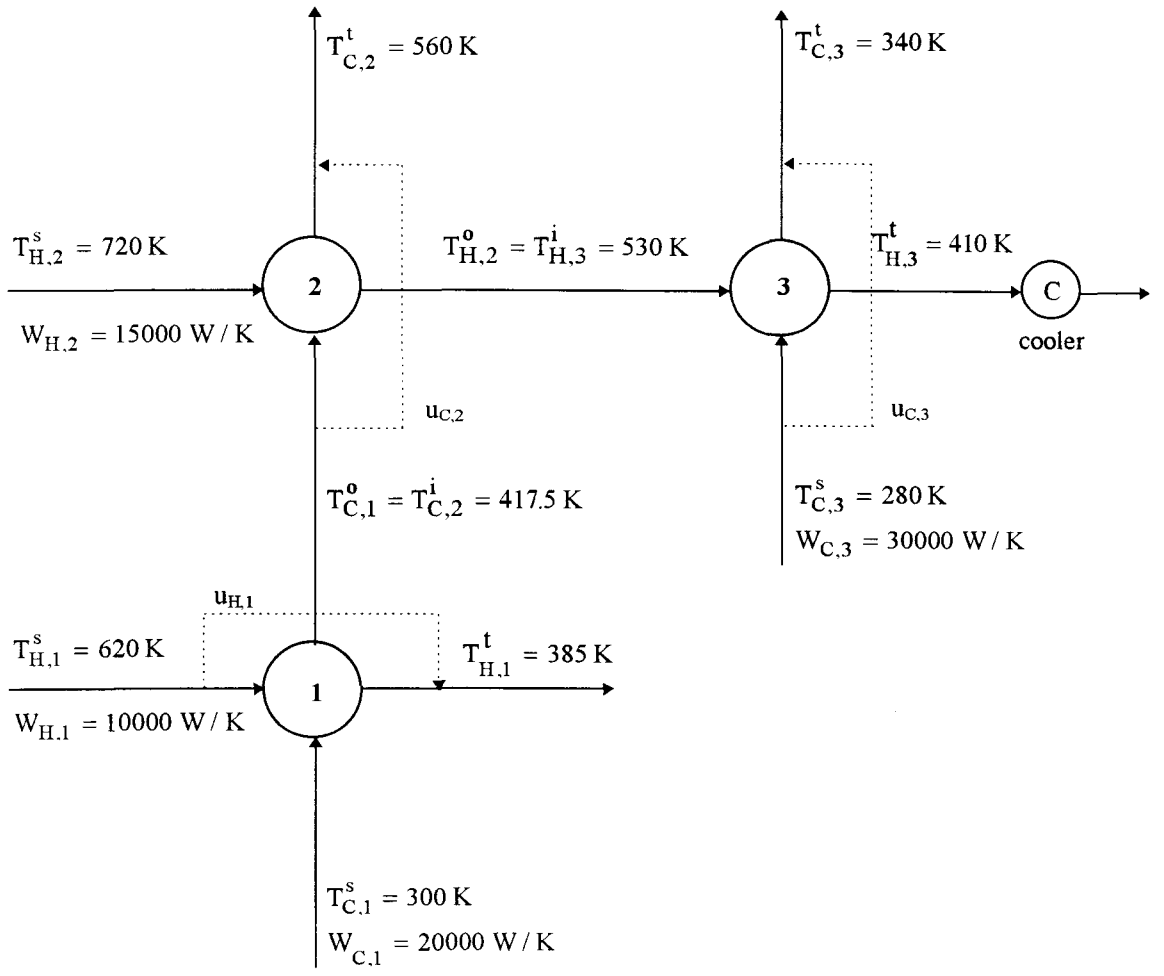

FIGURE 5.21. The Alternative HEN Generated via MINLP Algorithm.

$$\bar{\mathbf{u}}_{H(II)} = \begin{bmatrix} \bar{u}_{H,1} \\ \bar{u}_{H,2} \\ \bar{u}_{H,3} \end{bmatrix} = \begin{bmatrix} 0.06431 \\ 0 \\ 0 \end{bmatrix} \tag{5.19}$$

$$\bar{\mathbf{u}}_{C(II)} = \begin{bmatrix} \bar{u}_{C,1} \\ \bar{u}_{C,2} \\ \bar{u}_{C,3} \end{bmatrix} = \begin{bmatrix} 0 \\ 0.10881 \\ 0.39401 \end{bmatrix} \tag{5.20}$$

Konukman et al. [10] showed that HEN-I has a RDRI of 15.8 K and HEN-II 3 K. This means that the structure of HEN-1 and HEN-II, after retrofit design, can tolerate disturbances from all possible directions as long as the magnitude of the disturbances are less than or equal to 15.8 K, and 3 K, respectively. Konukman et al. [10] obtained these results for the following control-range constraints:

$$\mathbf{c} = \begin{bmatrix} \Delta T^{t}_{H,1} \\ \Delta T^{t}_{H,3} \\ \Delta T^{t}_{C,2} \\ \Delta T^{t}_{C,3} \end{bmatrix} = \begin{bmatrix} \left| T^{t}_{H,1} - \bar{T}^{t}_{H,1} \right| \\ \left| T^{t}_{H,3} - \bar{T}^{t}_{H,3} \right| \\ \left| T^{t}_{C,2} - \bar{T}^{t}_{C,2} \right| \\ \left| T^{t}_{C,3} - \bar{T}^{t}_{C,3} \right| \end{bmatrix} = \begin{bmatrix} 0 \\ \infty \\ 0 \\ 0 \end{bmatrix} \tag{5.21}$$

Note that all constraints, except hot-target from the third exchanger, are hard constraints. The allowable range for the hot-stream temperature from the third exchanger actually is not $\pm\infty$, but bounded from the lower end by the allowable cooling water temperature [10].

In this section, two different disturbance sets will be applied to these alternative original and retrofit HENs. Let us first investigate the uncontrolled and open-loop optimal control of the HENs for the disturbance $\mathbf{d}_1$

$$\mathbf{d}_1 = \begin{bmatrix} \Delta T^{s}_{H,1} \\ \Delta T^{s}_{H,2} \\ \Delta T^{s}_{C,1} \\ \Delta T^{s}_{C,3} \end{bmatrix} = \begin{bmatrix} T^{s}_{H,1} - \bar{T}^{s}_{H,1} \\ T^{s}_{H,2} - \bar{T}^{s}_{H,2} \\ T^{s}_{C,1} - \bar{T}^{s}_{C,1} \\ T^{s}_{C,3} - \bar{T}^{s}_{C,3} \end{bmatrix} = \begin{bmatrix} 0 \\ 0 \\ -3 \\ 0 \end{bmatrix} \tag{5.22}$$

Figure 5.22 and Figure 5.23 show the uncontrolled dynamic response of the original designs of HEN-I and HEN-II respectively. Figure 5.24 and Figure 5.25 show the uncontrolled dynamic response of HEN-I and HEN-II respectively. All hard targets, except $T^{t}_{H,3}$ which is not a hard target, are violated both dynamically and at the new steady-state conditions, as expected.

The dynamic resilience of the two HENs can be comparatively assessed by measuring the integral of absolute errors (deviations from nominal state), i.e., ε_I in Equation 5.6, of all the targets. The values of the performance index, ε_I, as calculated from Equation 5.6 for the original designs of HEN-I and HEN-II are 909.23 K and 1064.52 K, respectively. The values of the performance index, ε_I, for the retrofit designs of HEN-I and HEN-II are 899.46 K and 1056.68 K, respectively. According to this result, both the original and retrofit designs of HEN-I show more uncontrolled dynamic resilience to this particular disturbance. It should be noted that the retrofit designs of the alternative HENs exhibit more uncontrolled dynamic resilience compared to their original designs, for this particular disturbance.

Next, the optimal control algorithm depicted in Figure 5.1, was applied only to the retrofit designs. The disturbance was measured and the optimal bypass fractions ($\mathbf{u}_I^{opt}$ and $\mathbf{u}_{II}^{opt}$ for HEN-I and HEN-II, respectively) were obtained as a solution of the optimization problem defined in Chapter 4. The optimal bypass fraction for the two retrofit HENs are as follows:

$$\mathbf{u}^{opt}_{H(I)} = \begin{bmatrix} u_{H,1} \\ u_{H,2} \\ u_{H,3} \end{bmatrix} = \begin{bmatrix} 0.03447 \\ 0 \\ 0 \end{bmatrix} \tag{5.23}$$

$$\mathbf{u}^{opt}_{C(I)} = \begin{bmatrix} u_{C,1} \\ u_{C,2} \\ u_{C,3} \end{bmatrix} = \begin{bmatrix} 0 \\ 0.44324 \\ 0.43823 \end{bmatrix} \tag{5.24}$$

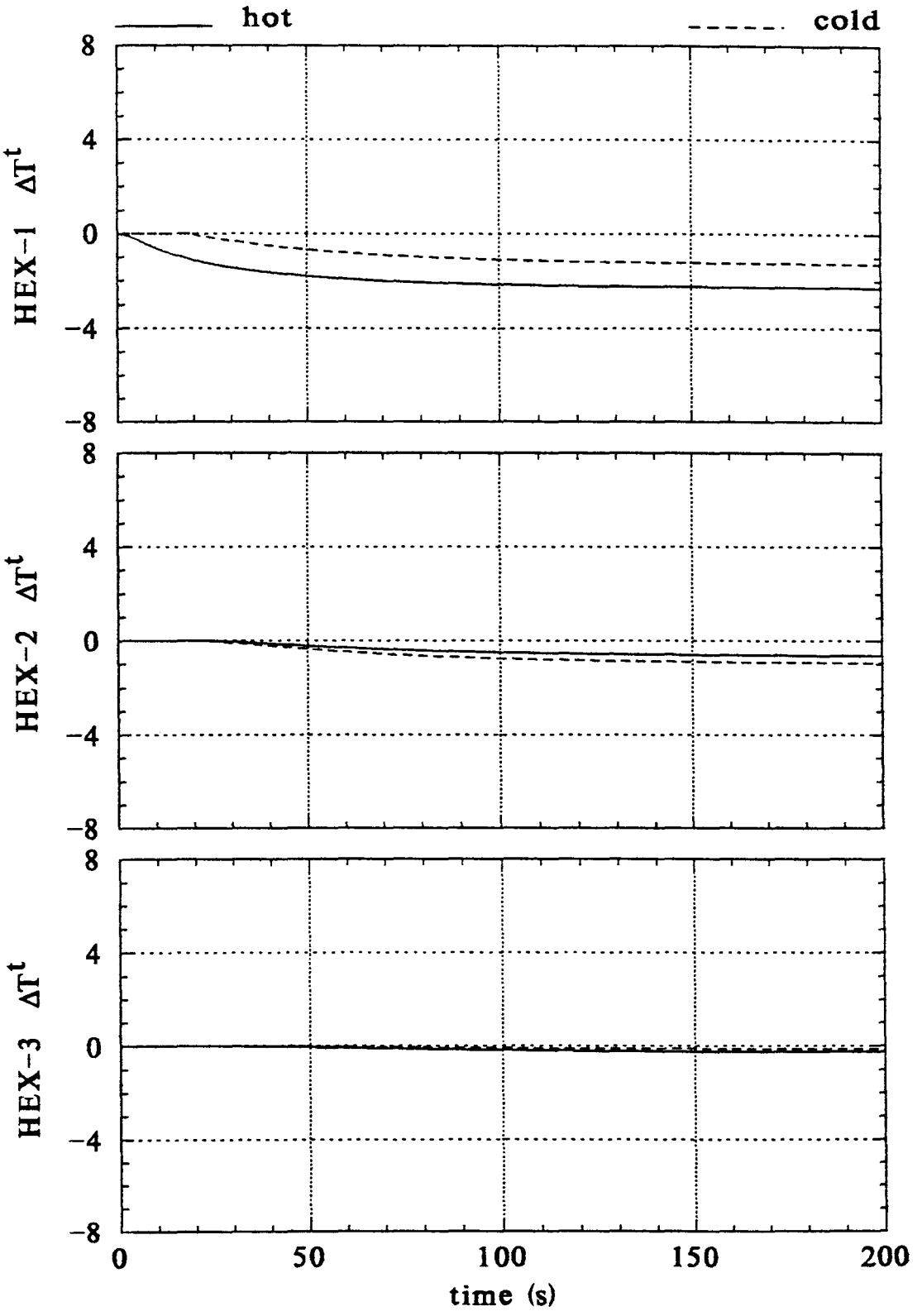

FIGURE 5.22. Uncontrolled Response of Original HEN-I After d_1.

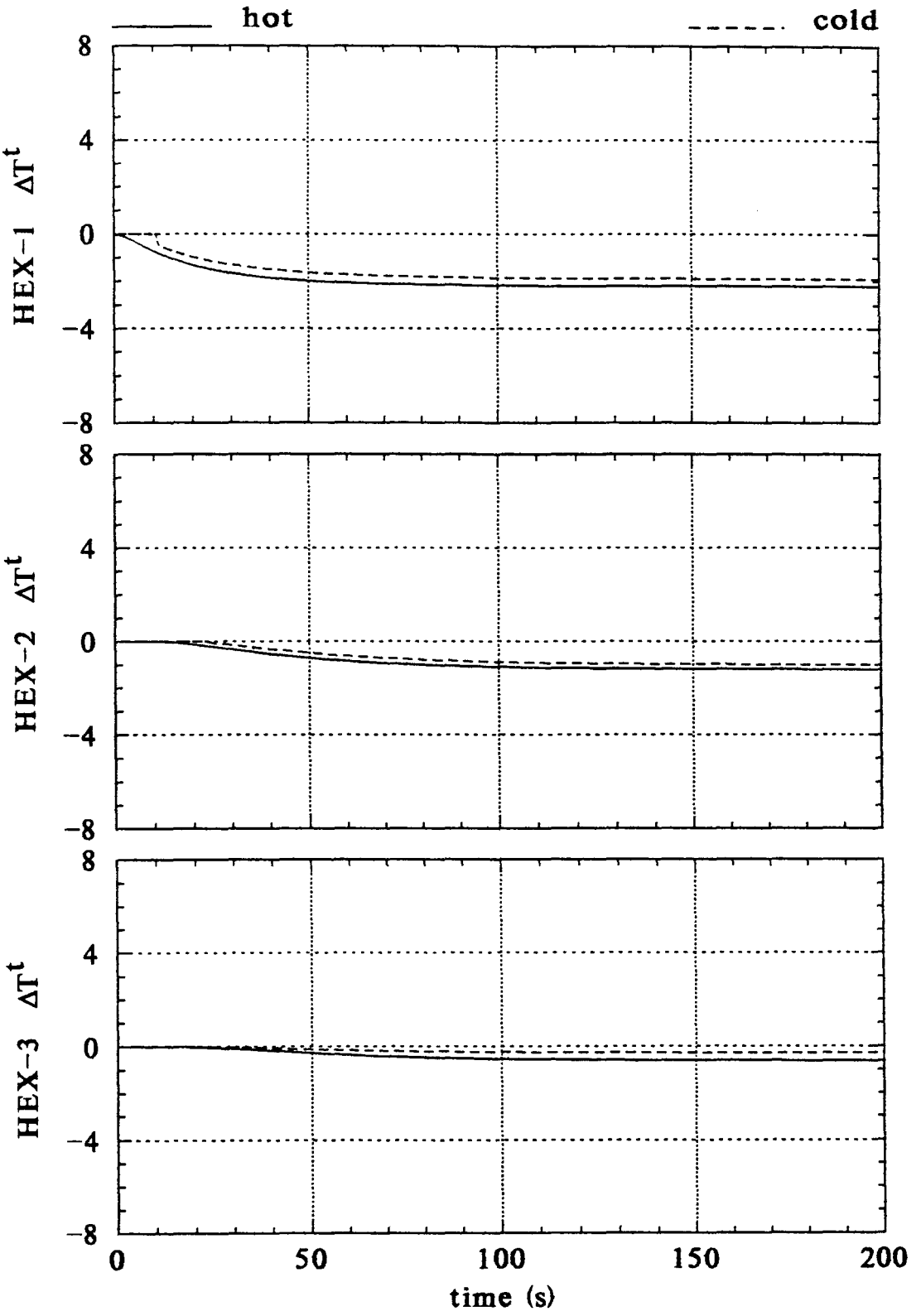

FIGURE 5.23. Uncontrolled Response of Original HEN-II After $\mathbf{d}_1$.

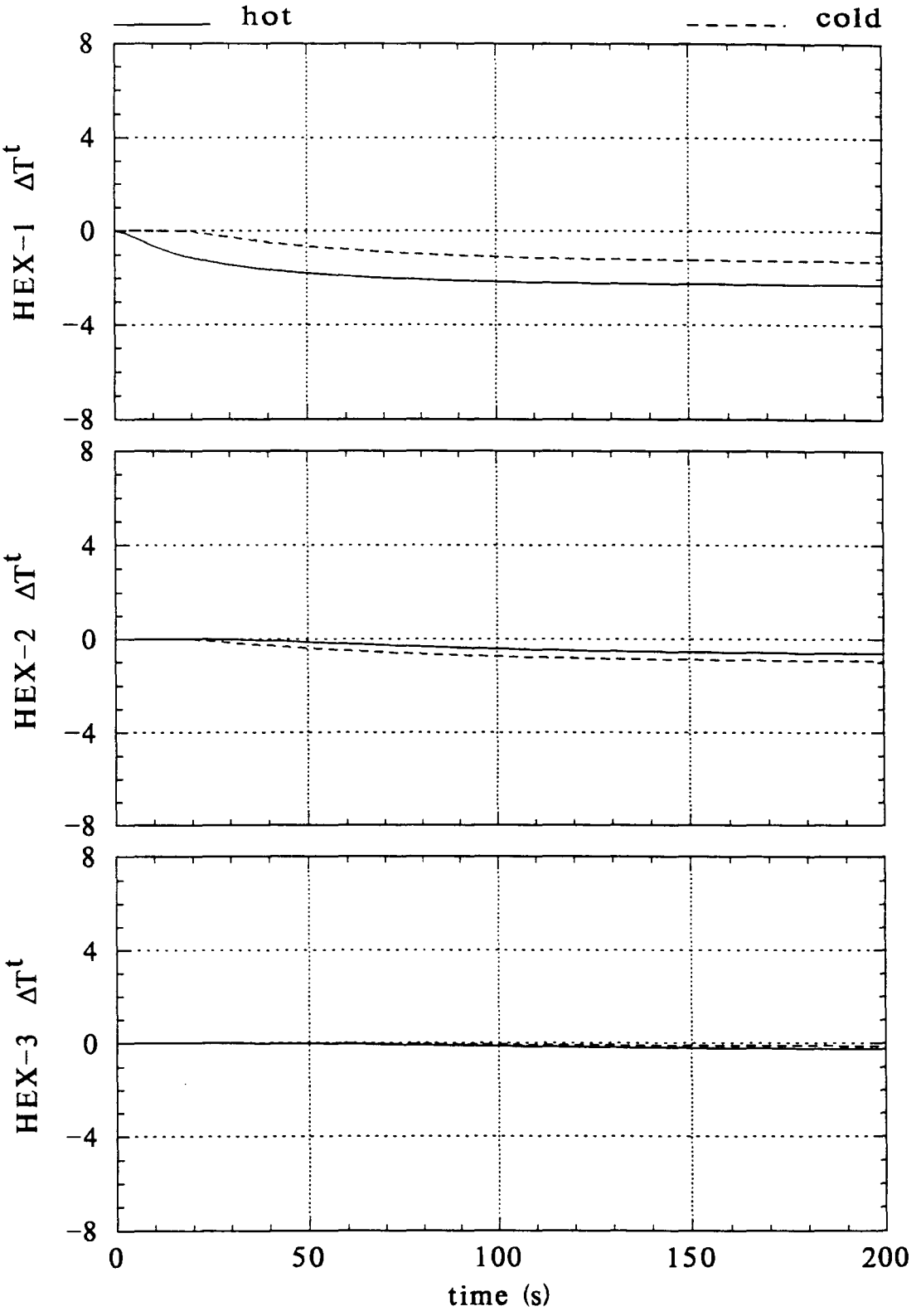

FIGURE 5.24. Uncontrolled Response of Retrofit HEN-I After $\mathbf{d}_1$.

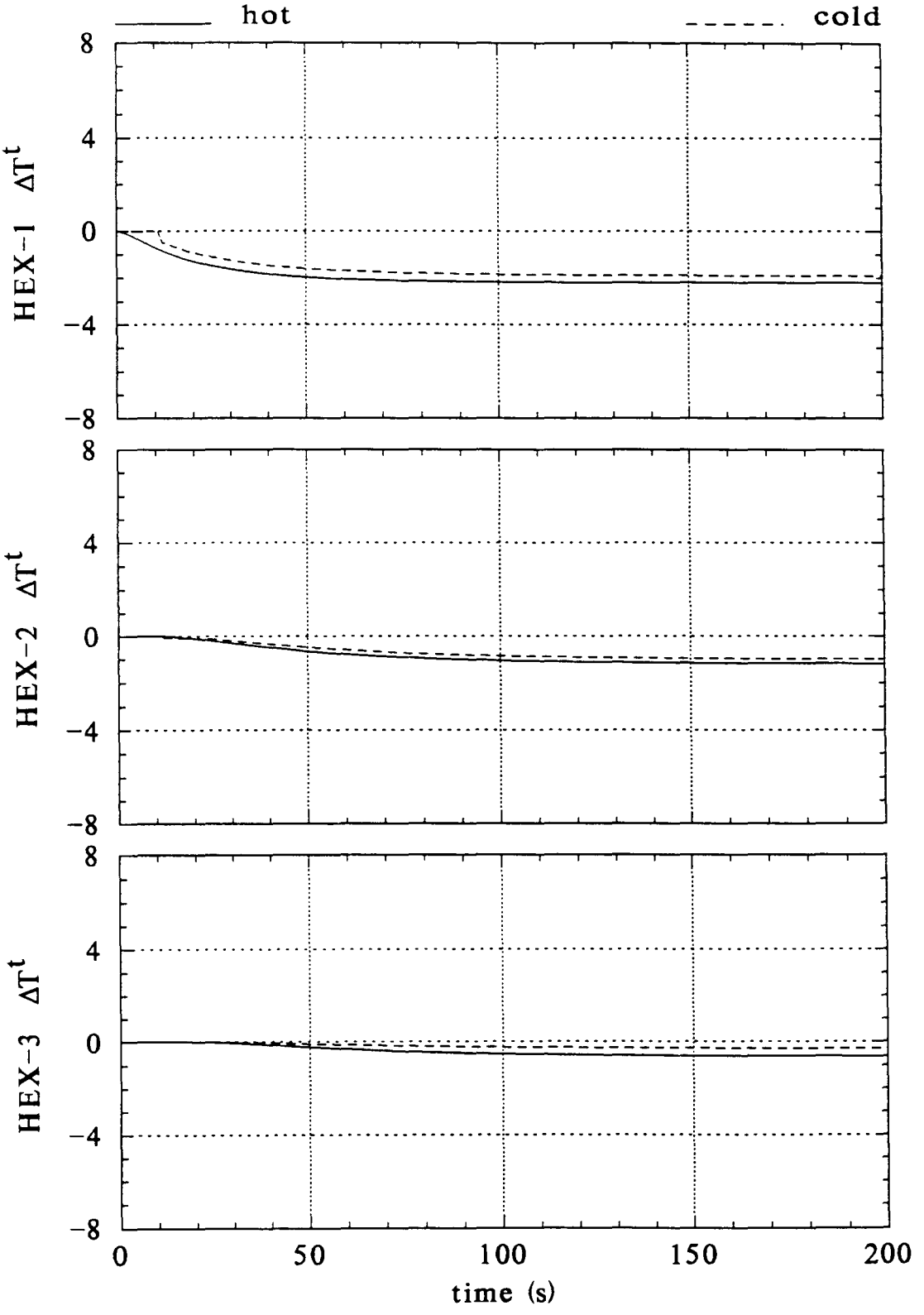

FIGURE 5.25. Uncontrolled Response of Retrofit HEN-II After $\mathbf{d}_1$.

$$\mathbf{u}_{H(II)}^{opt} = \begin{bmatrix} u_{H,1} \\ u_{H,2} \\ u_{H,3} \end{bmatrix} = \begin{bmatrix} 0.04453 \\ 0 \\ 0 \end{bmatrix} \tag{5.25}$$

$$\mathbf{u}_{C(II)}^{opt} = \begin{bmatrix} u_{C,1} \\ u_{C,2} \\ u_{C,3} \end{bmatrix} = \begin{bmatrix} 0 \\ 0.06656 \\ 0.33699 \end{bmatrix} \tag{5.26}$$

Figure 5.26 and Figure 5.27 show the dynamics of retrofit HEN-I and HEN-II, respectively, when these optimal controls are applied (changed from their nominal values, $\bar{\mathbf{u}}$, to $\mathbf{u}^{opt}$) instantaneously. As shown by these figures, the hard target constraints ($\pm$ 0) at the new final steady-state are met exactly. This shows that the HENs are resilient (hard targets can bounce back to initial/desired states). The temporal violation of the hard targets are unavoidable, but may be minimized by proper selection of the rate of application of the controls, as will be illustrated next:

To minimize the temporal deviations of all the target temperatures from their nominal values, the bypass opening rates were done according to the ramp function defined by Equation 5.5. The τ_i values for the individual bypass were obtained as a result of dynamic optimization as described by Equation 5.8 and Equation 5.9.

For HEN-I, the optimal τ_I values for the bypasses around the hot-side of the first, the cold-side of the second, and the cold side of the third exchangers, called τ_{1-H}^{opt}, τ_{2-C}^{opt} and τ_{3-C}^{opt} are 85, 150 and 150 seconds, respectively.

For HEN-II, the optimal τ_{II} values for the bypasses around the hot-side of the first, the cold-side of the second, and the cold side of the third exchangers, called τ_{1-H}^{opt}, τ_{2-C}^{opt} and τ_{3-C}^{opt} are 67, 150 and 150 seconds, respectively.

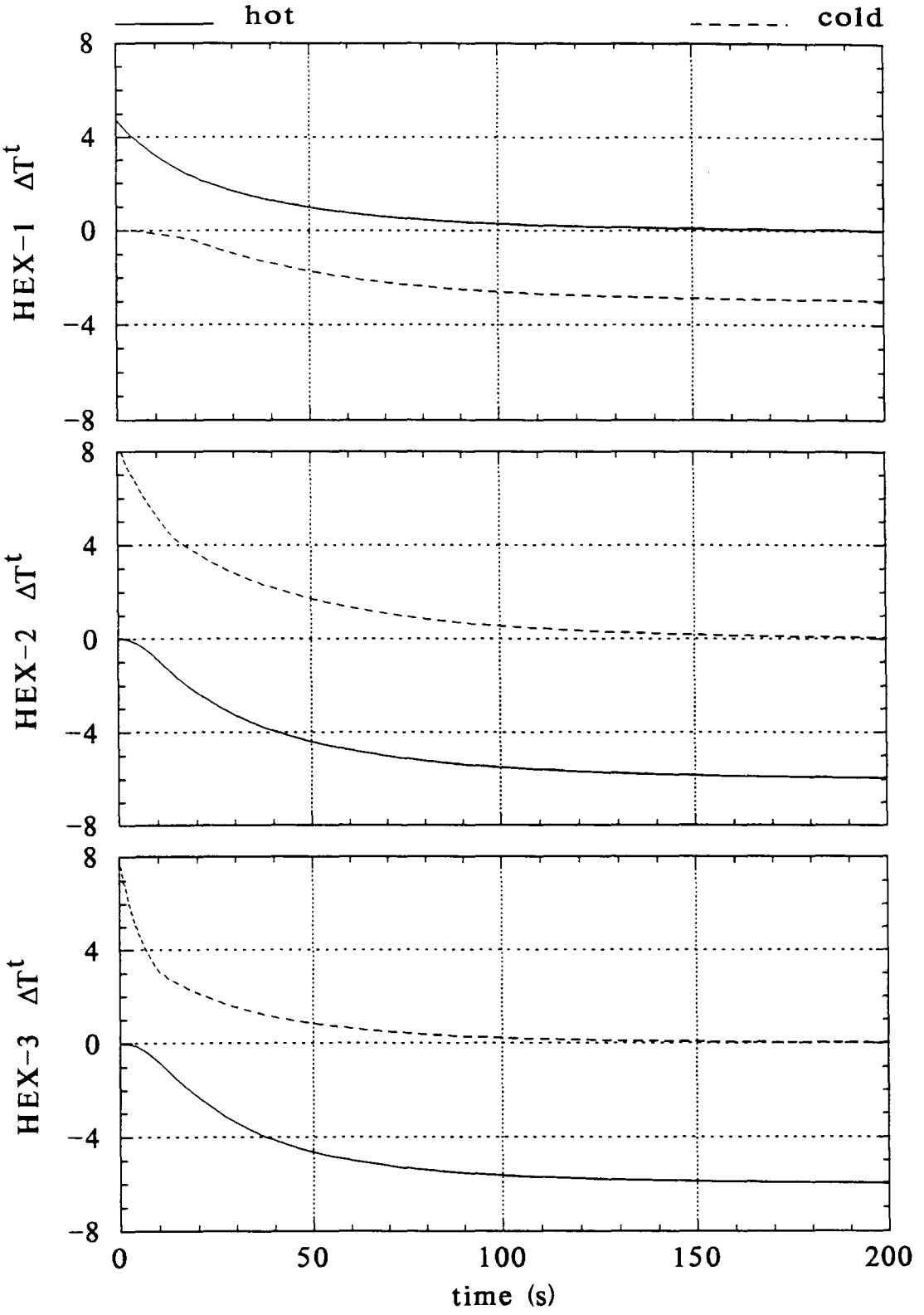

FIGURE 5.26. Response of Retrofit HEN-I with Instantaneous (τ_i=0) Application of Optimal Control.

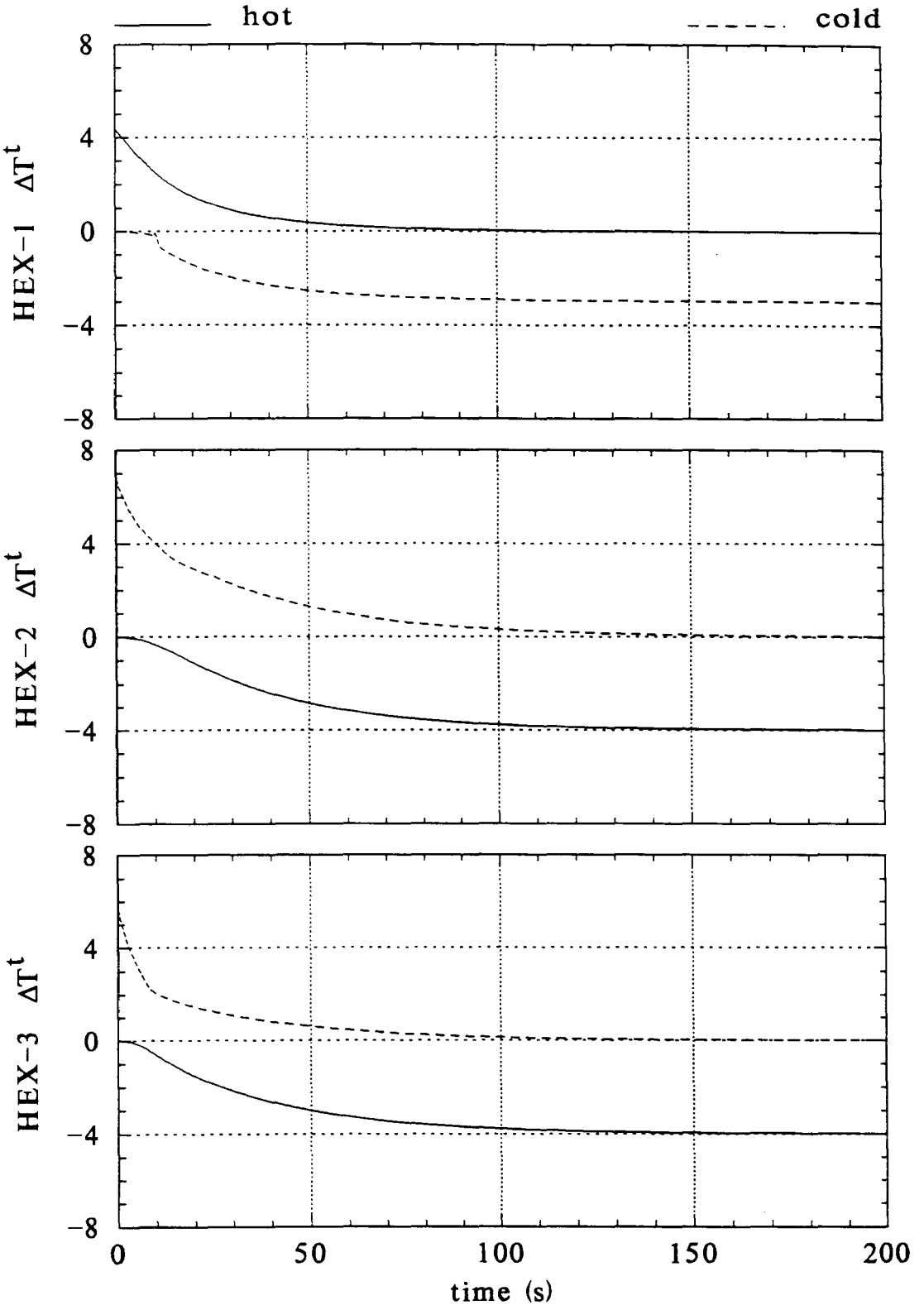

FIGURE 5.27. Response of Retrofit HEN-II with Instantaneous (τ_i=0) Application of Optimal Control.

Figure 5.28 and Figure 5.29 show the responses of the HEN-I and HEN-II, for the set of bypass openings according to τ_I^{opt} and τ_{II}^{opt} values, respectively. The performance of the optimal control algorithm can be assessed by measuring ε_1 (Equation 5.6) as mentioned before. The values of the performance index, ε_1 as calculated from Equation 5.6 for HEN-I and HEN-II are 1532.15 K and 1011.2 K, respectively. This shows that HEN-II, with its retrofit design, is more resilient/controllable as compared to HEN-I for this particular disturbance.

However, it should be remembered that HEN-I had shown more open-loop (uncontrolled) resilience than HEN-II. Therefore, it can be concluded that, the retrofit design and optimal control algorithm makes HEN-II more resilient/controllable than HEN-I.

Now, these analyses are repeated for the second disturbance (multidirectional) direction, $\mathbf{d}_2$, defined as:

$$\mathbf{d}_2 = \begin{bmatrix} \Delta T^S_{H,1} \\ \Delta T^S_{H,2} \\ \Delta T^S_{C,1} \\ \Delta T^S_{C,3} \end{bmatrix} = \begin{bmatrix} T^S_{H,1} - \overline{T}^S_{H,1} \\ T^S_{H,2} - \overline{T}^S_{H,2} \\ T^S_{C,1} - \overline{T}^S_{C,1} \\ T^S_{C,3} - \overline{T}^S_{C,3} \end{bmatrix} = \begin{bmatrix} 3 \\ 3 \\ -3 \\ -3 \end{bmatrix} \tag{5.27}$$

Figures 5.30 and 5.31 show the uncontrolled dynamic response of original designs and Figures 5.32 and 5.33 show the uncontrolled dynamic response of retrofit designs of HEN-I and HEN-II, respectively for the multidirectional disturbance.

The dynamic resilience of the two HENs can be comparatively assessed by measuring the integral of absolute errors, i.e., ε_1 of Equation 5.6 (deviations from nominal state), of all the targets for this disturbance as well. The values of the performance index, ε_1, as calculated from Equation 5.6 for the original designs of HEN-I and HEN-II are

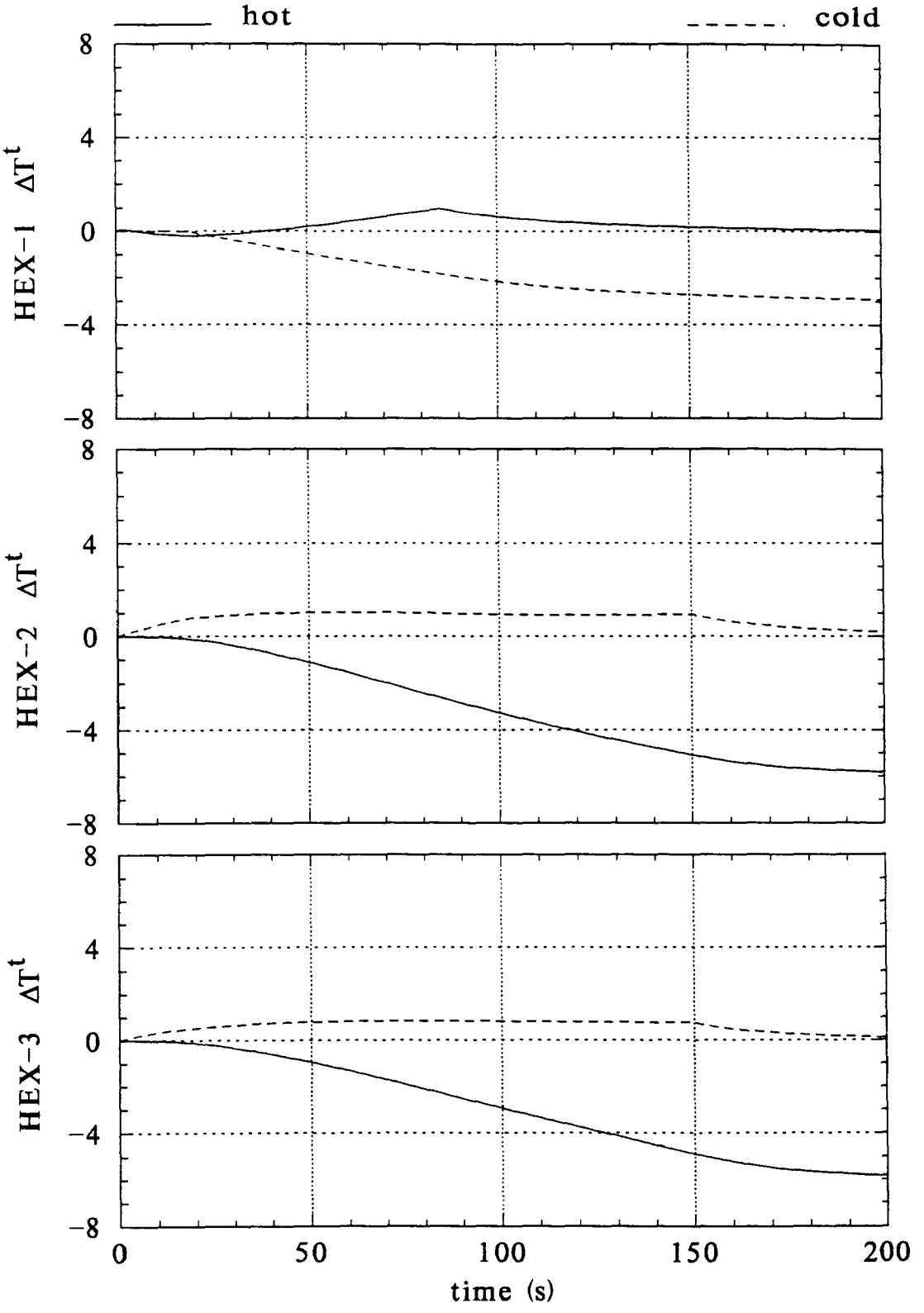

FIGURE 5.28. Controlled Response of Retrofit HEN-I with the Application of Optimal Controls According to τ_I^{opt}.

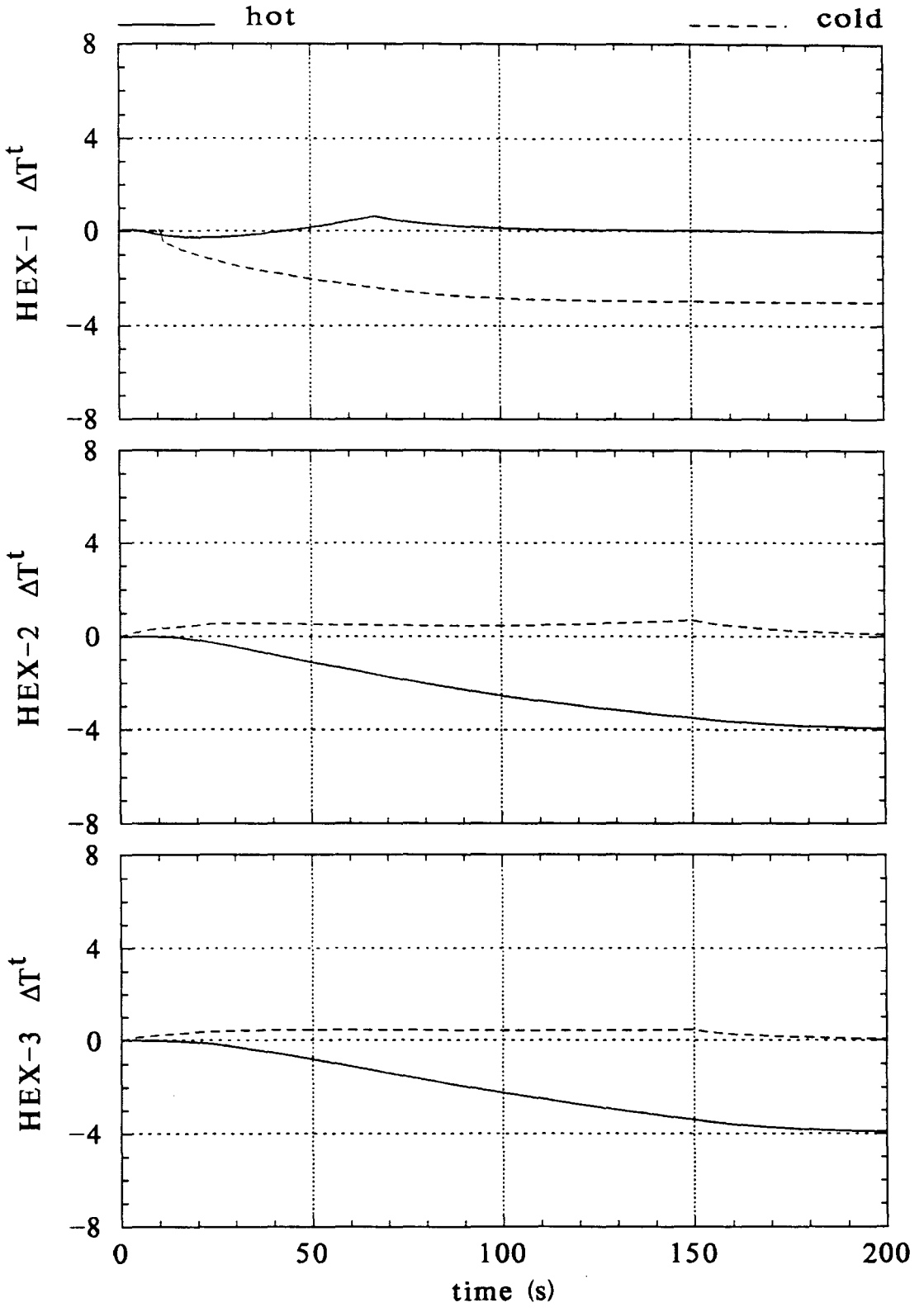

FIGURE 5.29. Controlled Response of Retrofit HEN-II with the Application of Optimal Controls According to τ_{II}^{opt}.

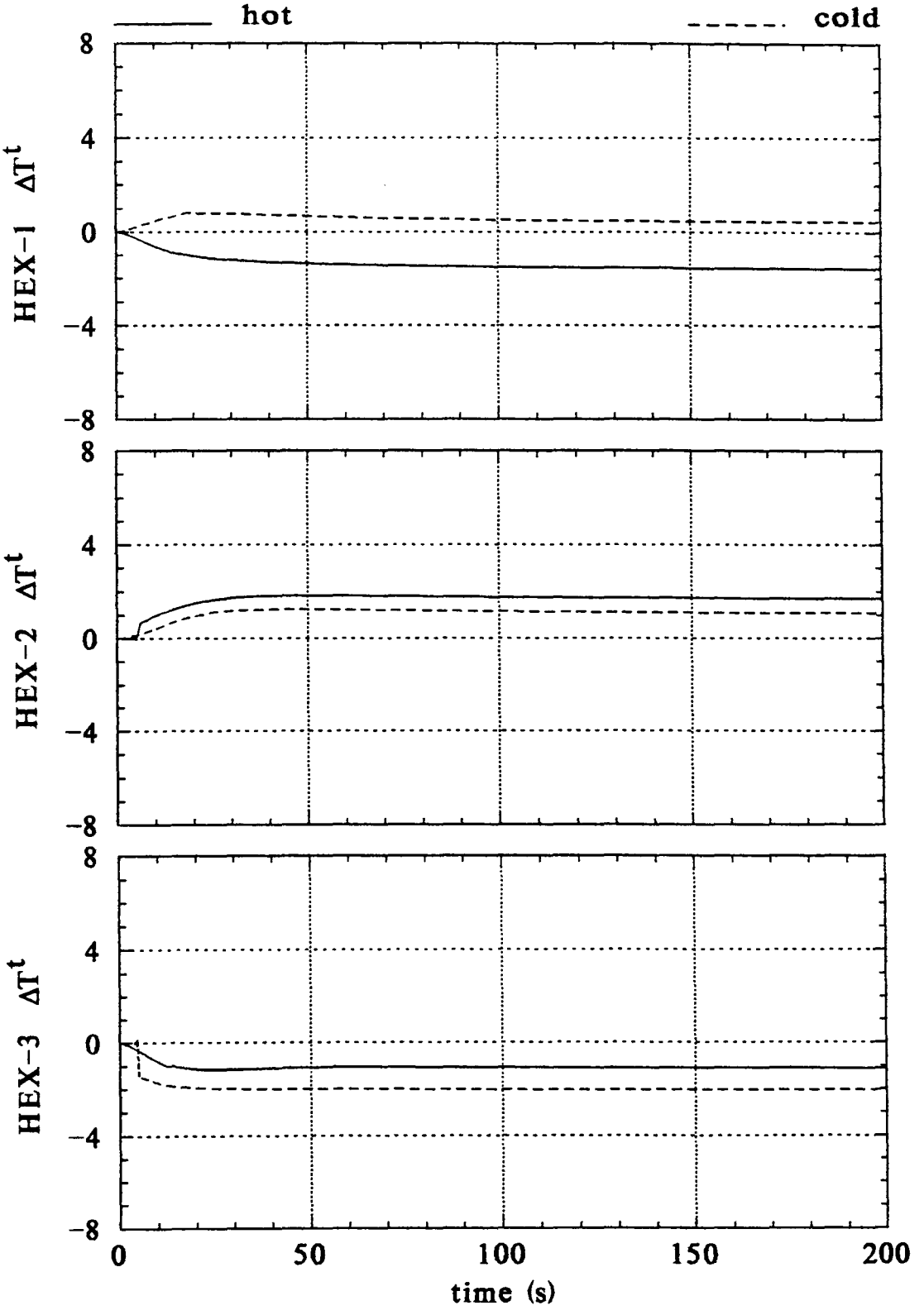

FIGURE 5.30. Uncontrolled Response of Original HEN-I After $\mathbf{d}_2$.

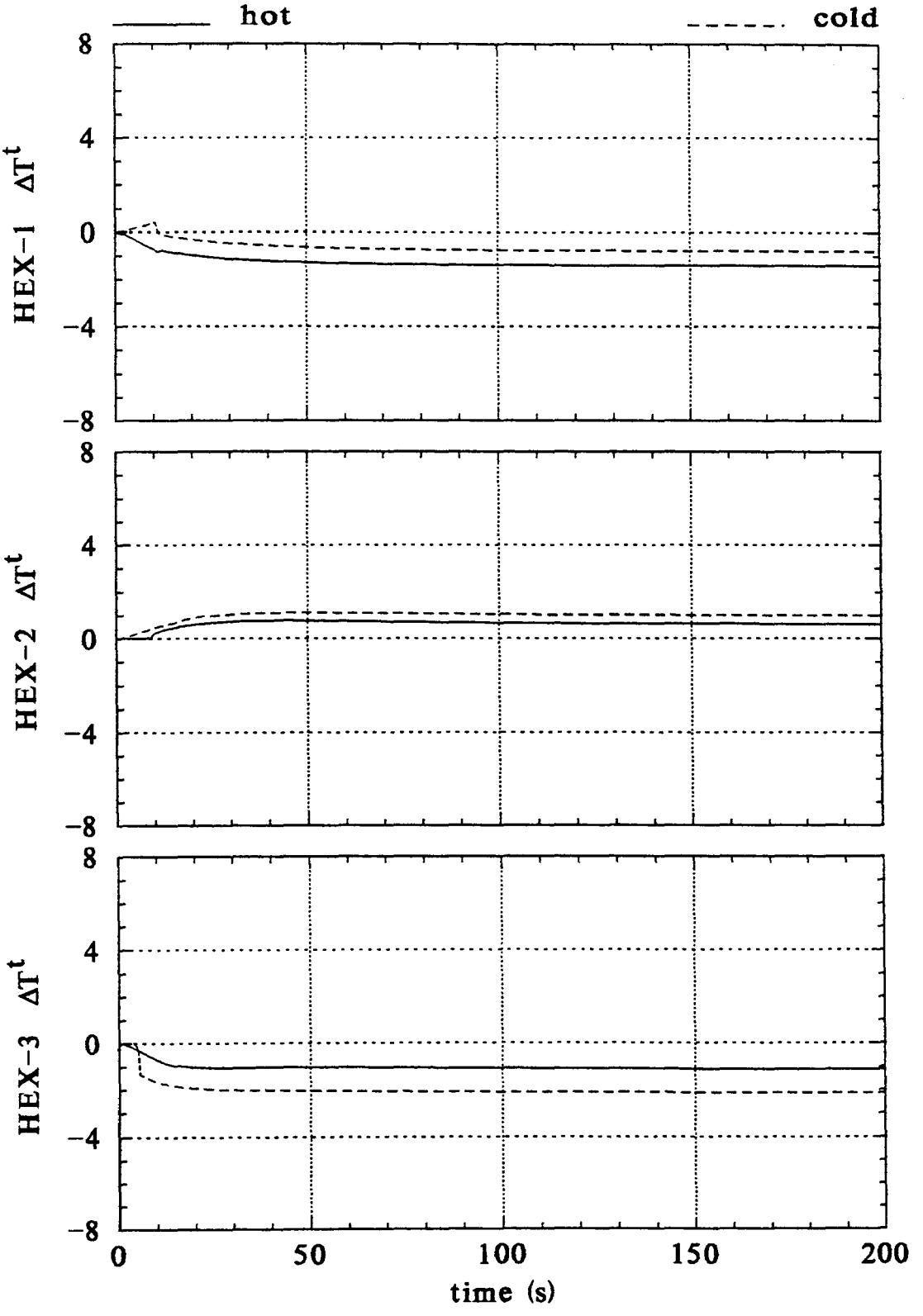

FIGURE 5.31. Uncontrolled Response of Original HEN-II After $\mathbf{d}_2$.

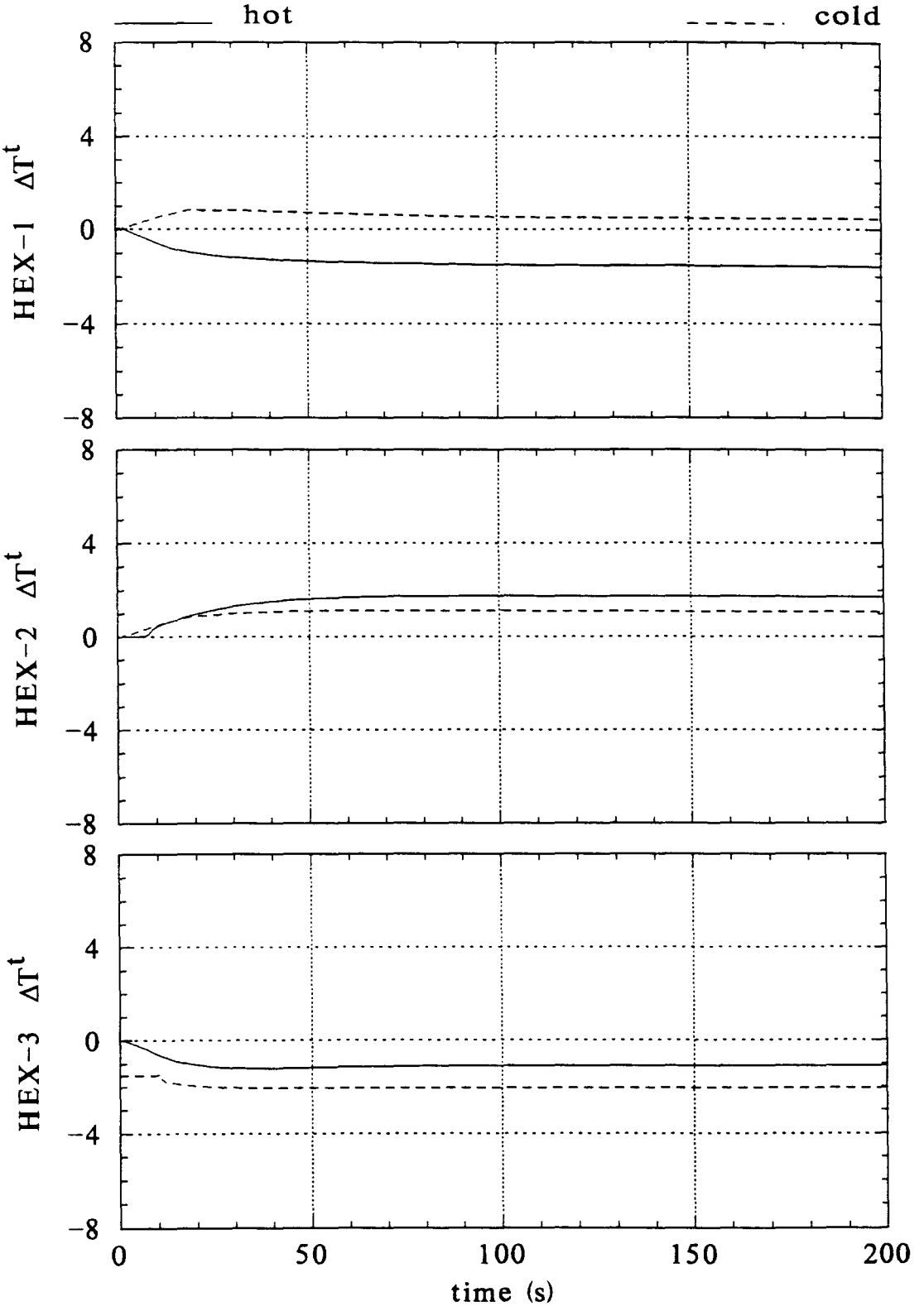

FIGURE 5.32. Uncontrolled Response of Retrofit HEN-I After $\mathbf{d}_2$.

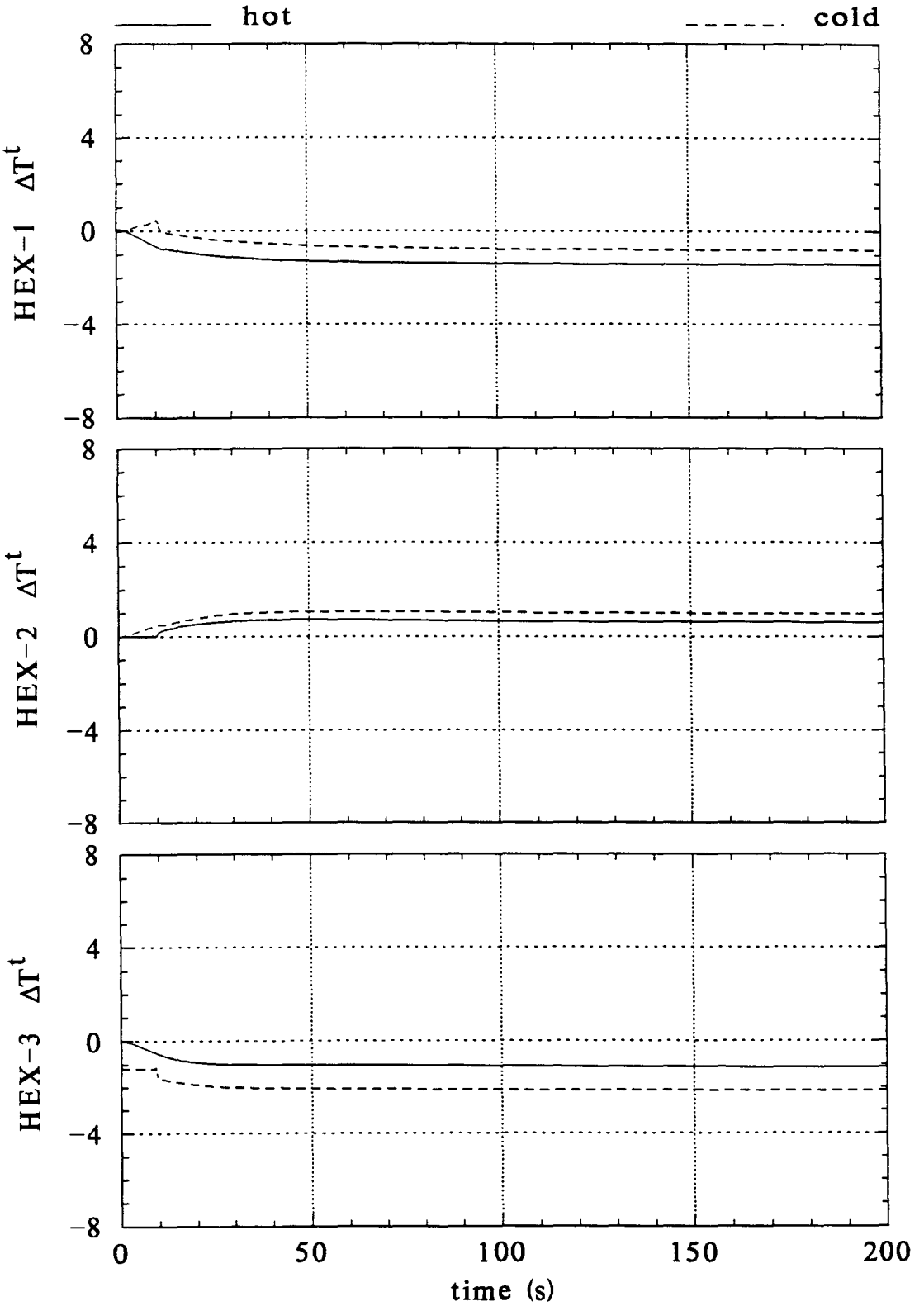

FIGURE 5.33. Uncontrolled Response of Retrofit HEN-II After $\mathbf{d}_2$.

1674.32 K and 1623.32 K, respectively. The values of the performance index, ε_1, for the retrofit designs of HEN-I and HEN-II are 1675.77 K and 1617.76 K, respectively. According to this, both the original and retrofit designs of HEN-II show more uncontrolled dynamic resilience to this particular disturbance. It should be noted that the retrofit designs of alternative HENs exhibit comparable uncontrolled dynamic resilience with respect to their original designs, for this particular disturbance.

Next, the optimal control algorithm depicted in Figure 5.1, was applied only to the retrofit HENs. The disturbance was measured and the optimal bypass fractions ($\mathbf{u}_{\mathrm{I}}^{\mathrm{opt}}$ and $\mathbf{u}_{\mathrm{II}}^{\mathrm{opt}}$ for HEN-I and HEN-II, respectively) were obtained as a solution of the optimization problem defined in Chapter 4. The optimal bypass fraction for the two retrofit HENs are as follows:

$$\mathbf{u}_{\mathrm{H(I)}}^{\mathrm{opt}} = \begin{bmatrix} u_{\mathrm{H},1} \\ u_{\mathrm{H},2} \\ u_{\mathrm{H},3} \end{bmatrix} = \begin{bmatrix} 0.02989 \\ 0 \\ 0 \end{bmatrix} \tag{5.28}$$

$$\mathbf{u}_{\mathrm{C(I)}}^{\mathrm{opt}} = \begin{bmatrix} u_{\mathrm{C},1} \\ u_{\mathrm{C},2} \\ u_{\mathrm{C},3} \end{bmatrix} = \begin{bmatrix} 0 \\ 0.61802 \\ 0.38217 \end{bmatrix} \tag{5.29}$$

$$\mathbf{u}_{\mathrm{H(II)}}^{\mathrm{opt}} = \begin{bmatrix} u_{\mathrm{H},1} \\ u_{\mathrm{H},2} \\ u_{\mathrm{H},3} \end{bmatrix} = \begin{bmatrix} 0.03794 \\ 0 \\ 0 \end{bmatrix} \tag{5.30}$$

$$\mathbf{u}_{C(II)}^{opt} = \begin{bmatrix} u_{C,1} \\ u_{C,2} \\ u_{C,3} \end{bmatrix} = \begin{bmatrix} 0 \\ 0.012423 \\ 0.26459 \end{bmatrix} \tag{5.31}$$

Figure 5.34 and Figure 5.35 show the dynamics of retrofit HEN-I and HEN-II, respectively, when these optimal controls are applied (changed from their nominal values, $\bar{\mathbf{u}}$, to $\mathbf{u}^{opt}$) instantaneously. As shown by these figures, the hard target constraints ($\pm$ 0) at the new final steady-state are met exactly. This shows that the HENs are resilient (hard targets can bounce back to initial/desired states) for this disturbance as well. The temporal violation of the hard targets are unavoidable, but may be minimized by proper selection of the rate of application of the controls, as will be illustrated next.

To minimize the temporal deviations of all the target temperatures from the nominal values, the rate of opening the bypasses were done according to the ramp function defined by Equation 5.5. The τ_i values for the individual bypass were obtained as a result of dynamic optimization as described by Equation 5.8 and Equation 5.9.

For HEN-I, the optimal τ_I values for the bypasses around the hot-side of the first, the cold-side of the second, and the cold side of the third exchangers, called τ_{1-H}^{opt}, τ_{2-C}^{opt} and τ_{3-C}^{opt} are 56, 0.05 and 150 seconds, respectively.

For HEN-II, the optimal τ_{II} values for the bypasses around the hot-side of the first, the cold-side of the second, and the cold side of the third exchangers, called τ_{1-H}^{opt}, τ_{2-C}^{opt} and τ_{3-C}^{opt} are 36, 64 and 128 seconds, respectively.

Figure 5.36 and Figure 5.37 show the responses of the HEN-I and HEN-II, respectively, for the set of bypass openings according to τ_I and τ_{II} values. The performance of the optimal-control algorithm can be assessed by measuring ε_I (Equation 5.6) as mentioned before. The values of the performance index, ε_I as calculated from Equation 5.6

for HEN-I and HEN-II are 1847.7 K and 1278.35 K, respectively. It is also worth to note that the cold target stream temperature from the second exchanger in the second HEN structure shows almost zero violation. This shows that HEN-II, with its retrofit design, is more resilient/controllable compared to HEN-I for this particular disturbance as well.

The listing of the program used for HEN-II is given as a sample in Appendix C.

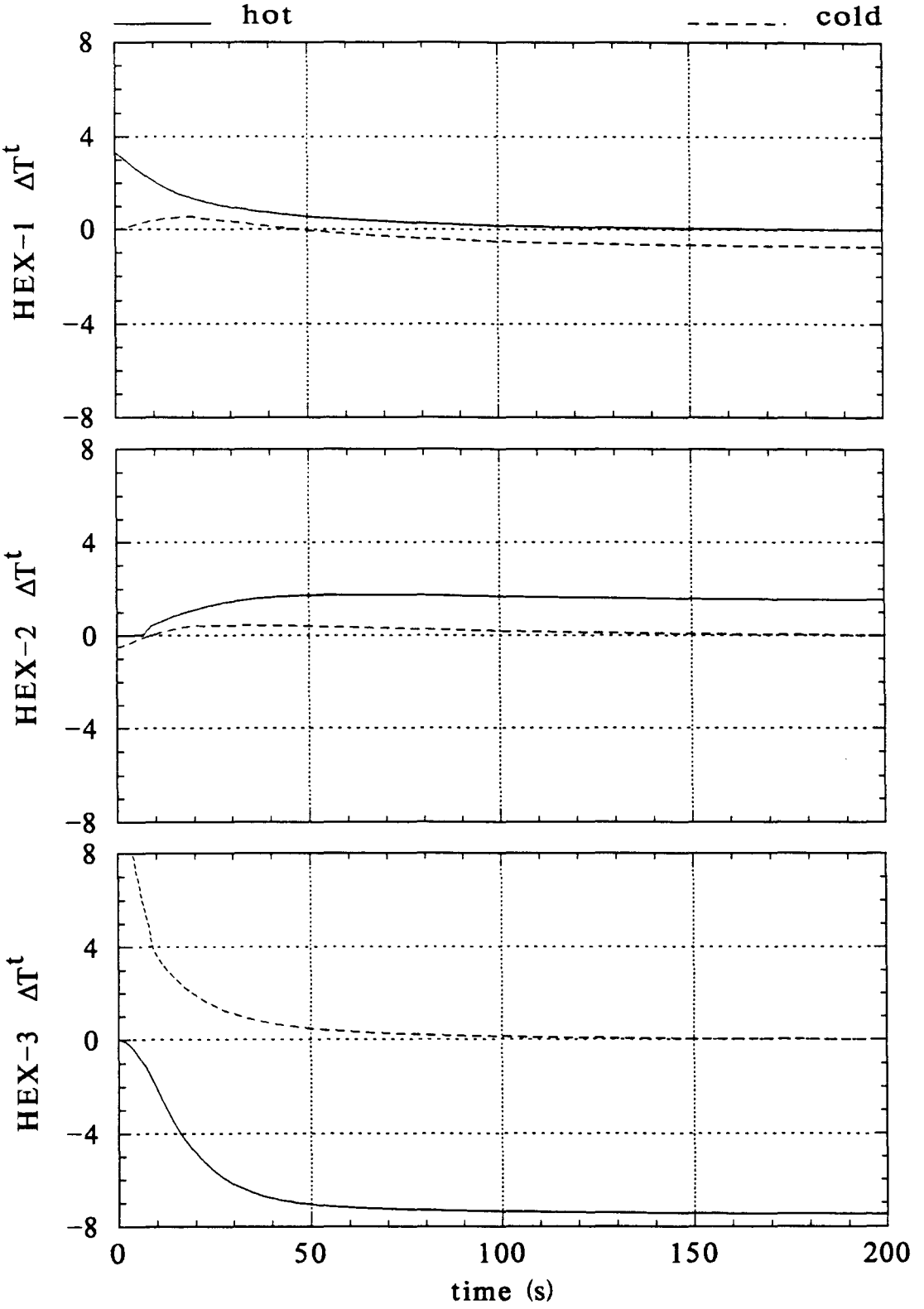

FIGURE 5.34. Response of Retrofit HEN-I with Instantaneous (τ_i=0) Application of Optimal Control.

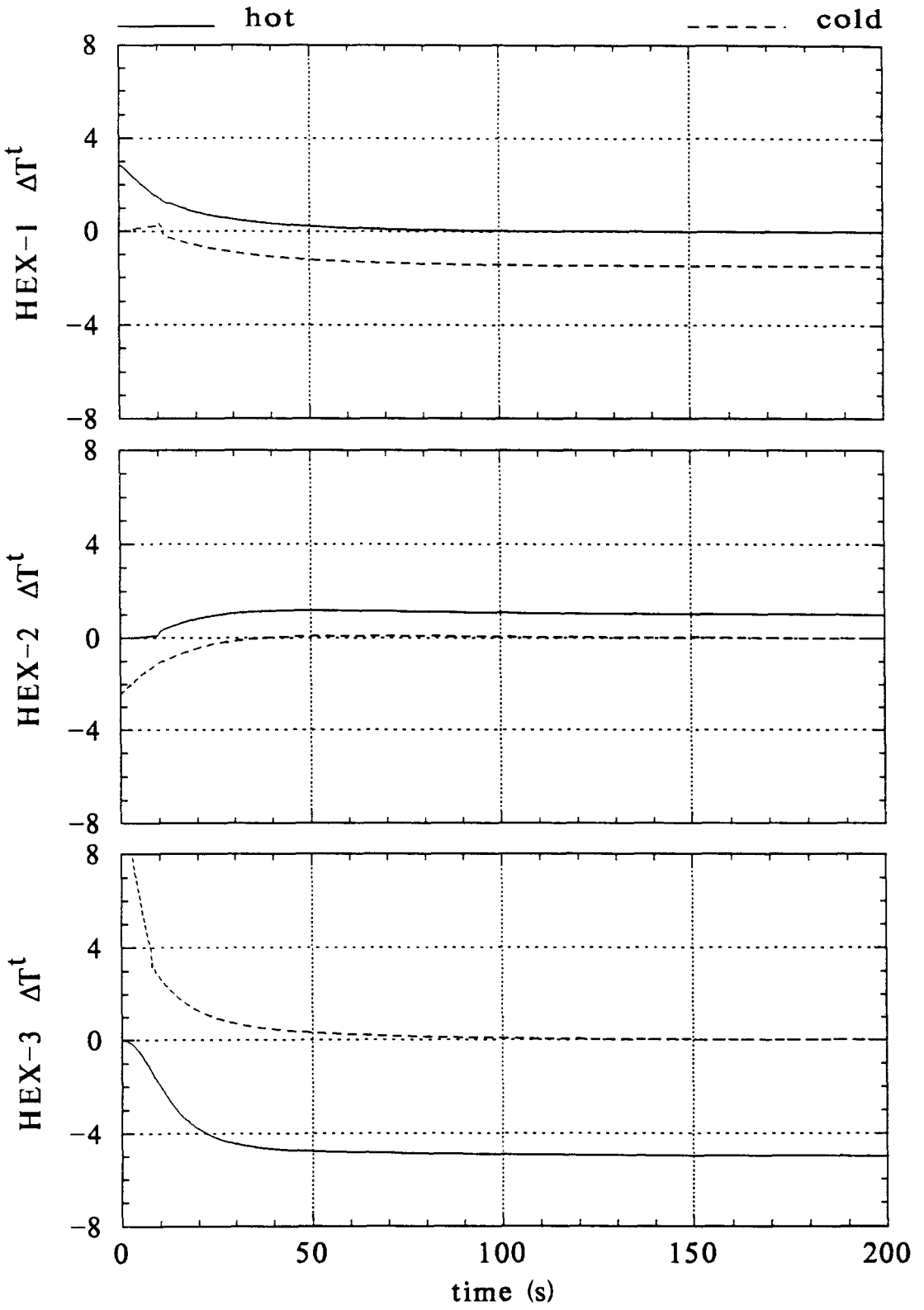

FIGURE 5.35. Response of Retrofit HEN-II with Instantaneous (τ_i=0) Application of Optimal Control.

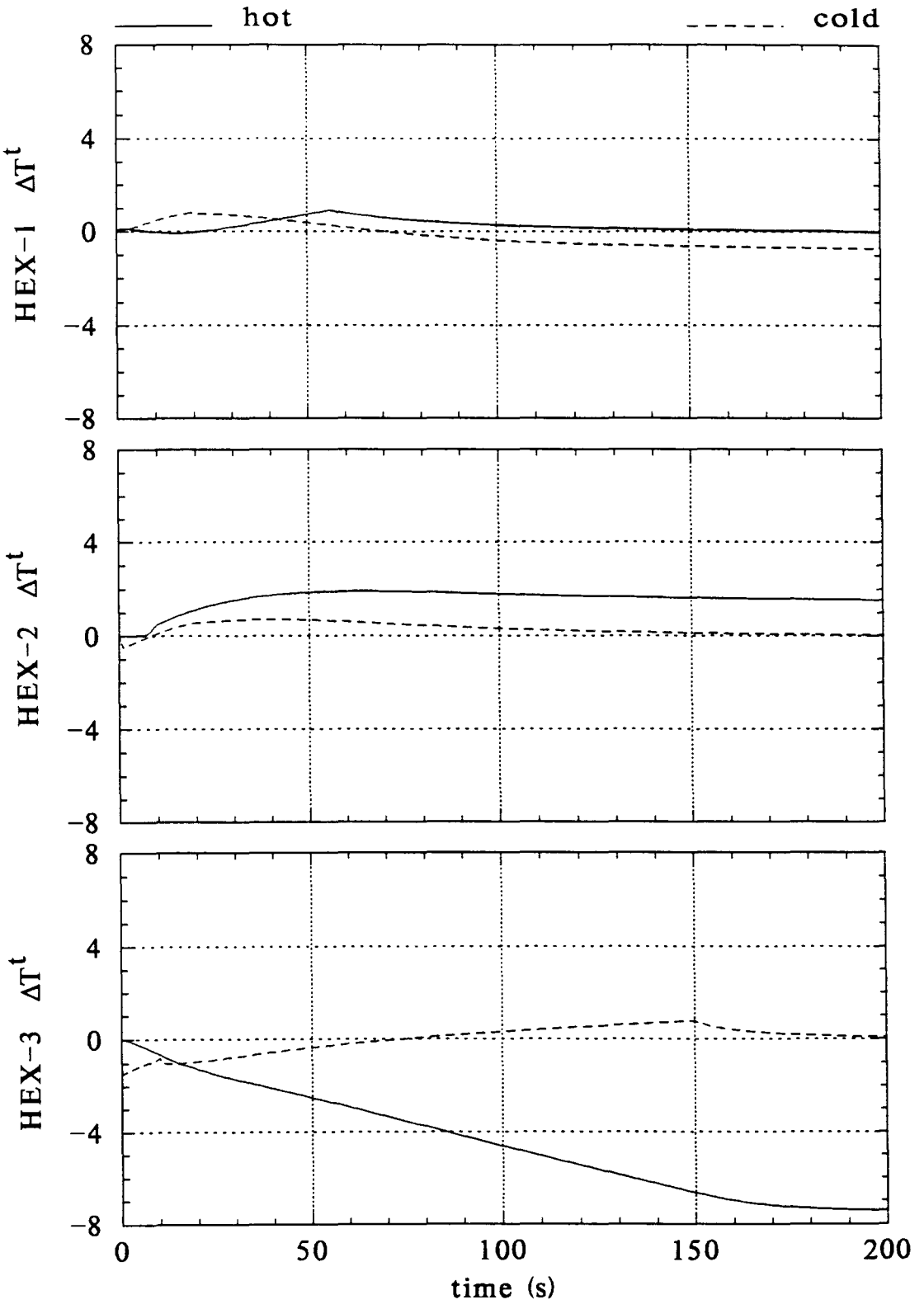

FIGURE 5.36. Controlled Response of Retrofit HEN-I with the Application of Optimal Controls According to τ_I^{opt}.

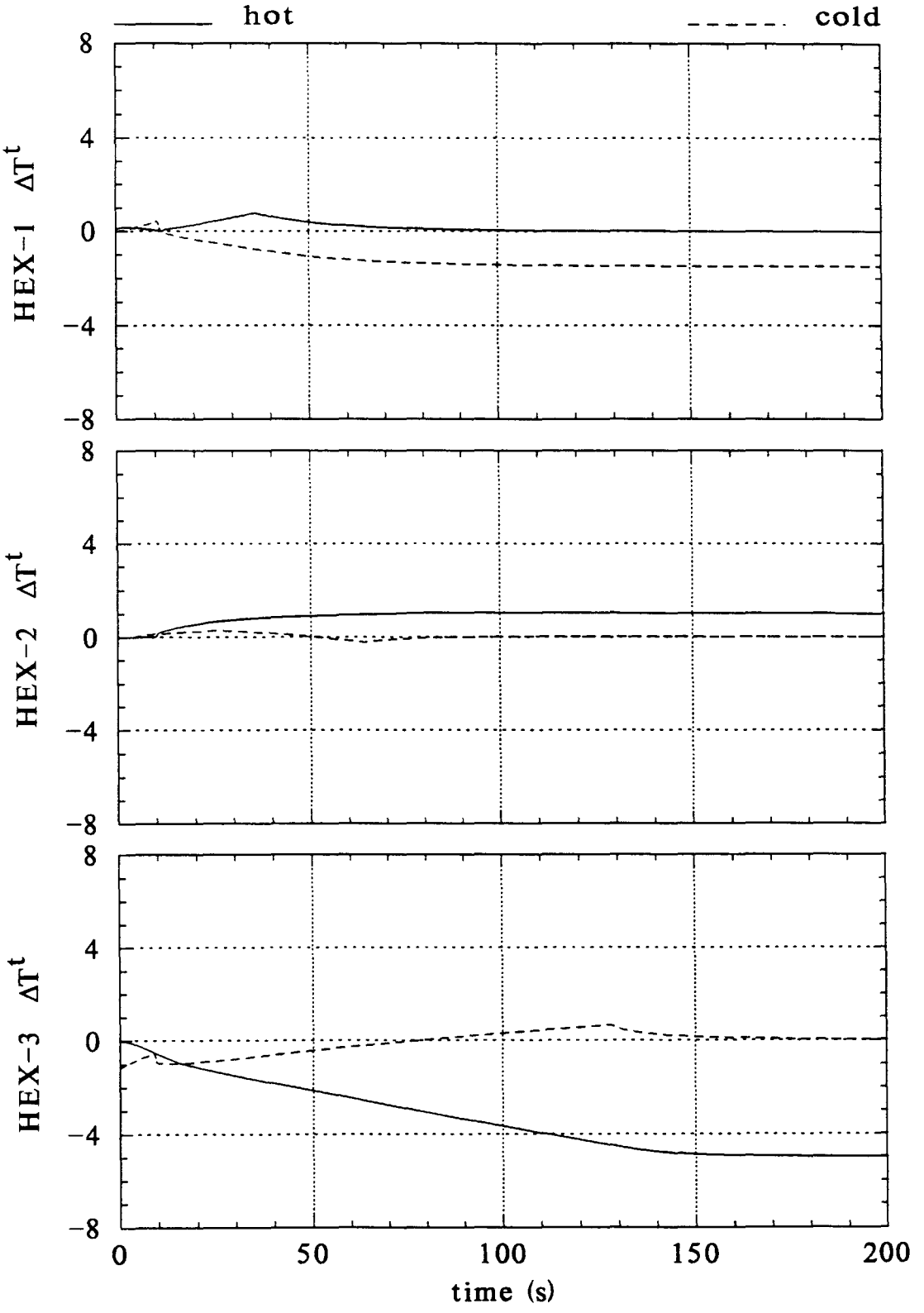

FIGURE 5.37. Controlled Response of Retrofit HEN-II with the Application of Optimal Controls According to τ_{II}^{opt}.

6. OPTIMAL CLOSED-LOOP CONTROL OF HEAT-EXCHANGER NETWORKS

In the previous chapter, the open-loop optimal control has been demonstrated (time-dependent bypass manipulation; no state feedback). According to the open-loop optimal-control algorithm, the optimal bypass openings that guarantee the steady-state feasibility of the new operating point after a disturbance, were implemented either instantaneously or gradually according to a ramp function within an optimal time period, τ_i^{opt}. It was shown that the temporary violations of the desired control-precision vector after instantaneous application of the optimal controls were overcome by the gradual implementation of the controls. In this section, a closed-loop optimal control algorithm, in which the manipulated variables (bypass openings) are handled based on the feedback of the target-stream temperatures will be presented.

The schematic of the closed-loop optimal-control algorithm is shown in Figure 6.1. The closed-loop optimal control is similar to the open-loop optimal control algorithm depicted in Fig 5.1. In the open-loop optimal-control algorithm, implementation of the optimal control was dependent on the time. In the closed-loop optimal-control algorithm, however, implementation of the optimal controls depends on the feedback information on state variables (target-stream temperatures).

In the implementation of this centralized optimal feedback control scheme, one faces with a difficult problem which was not encountered in the optimal open-loop control scheme. This problem is the pairing problem. Before the implementation of the optimal controls, the pairings among the manipulated variables (bypasses) and controlled variables (target streams) have to be selected. The question and the problem is: which bypass should

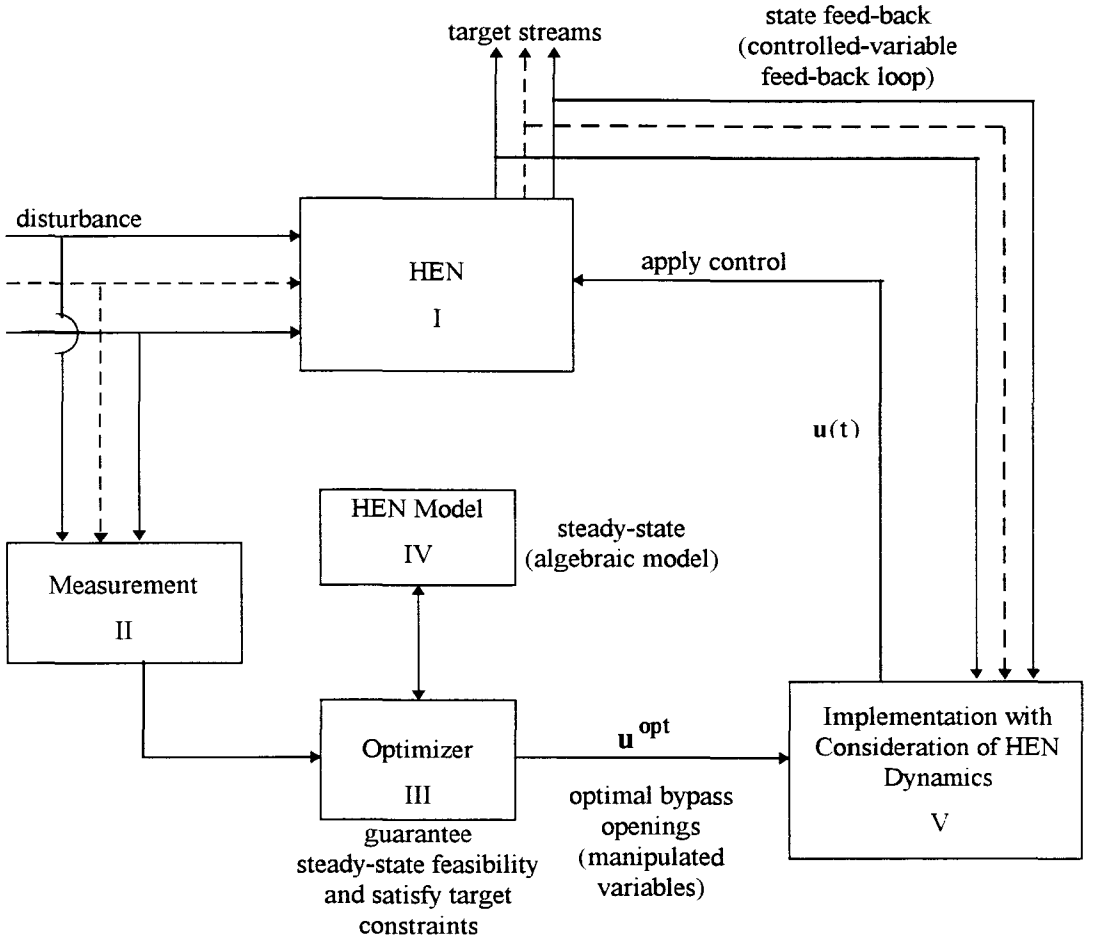

FIGURE 6.1. Schematic of an Optimal Closed-Loop Control Logic of Heat Exchanger Networks.

be matched with which target stream. As one can imagine, there may arise many pairing possibilities even for simple HEN structures. Fig 6.2 illustrates the pairing possibilities for a simple HEN. In Fig 6.2 (a) and (b), the number of controlled variables is greater than the number of manipulated variables (four target streams and three bypass streams). In Fig 6.2 (c) and (d), on the other hand, the number of control variables is less than the number of manipulated variables (four target-streams and five bypass streams).

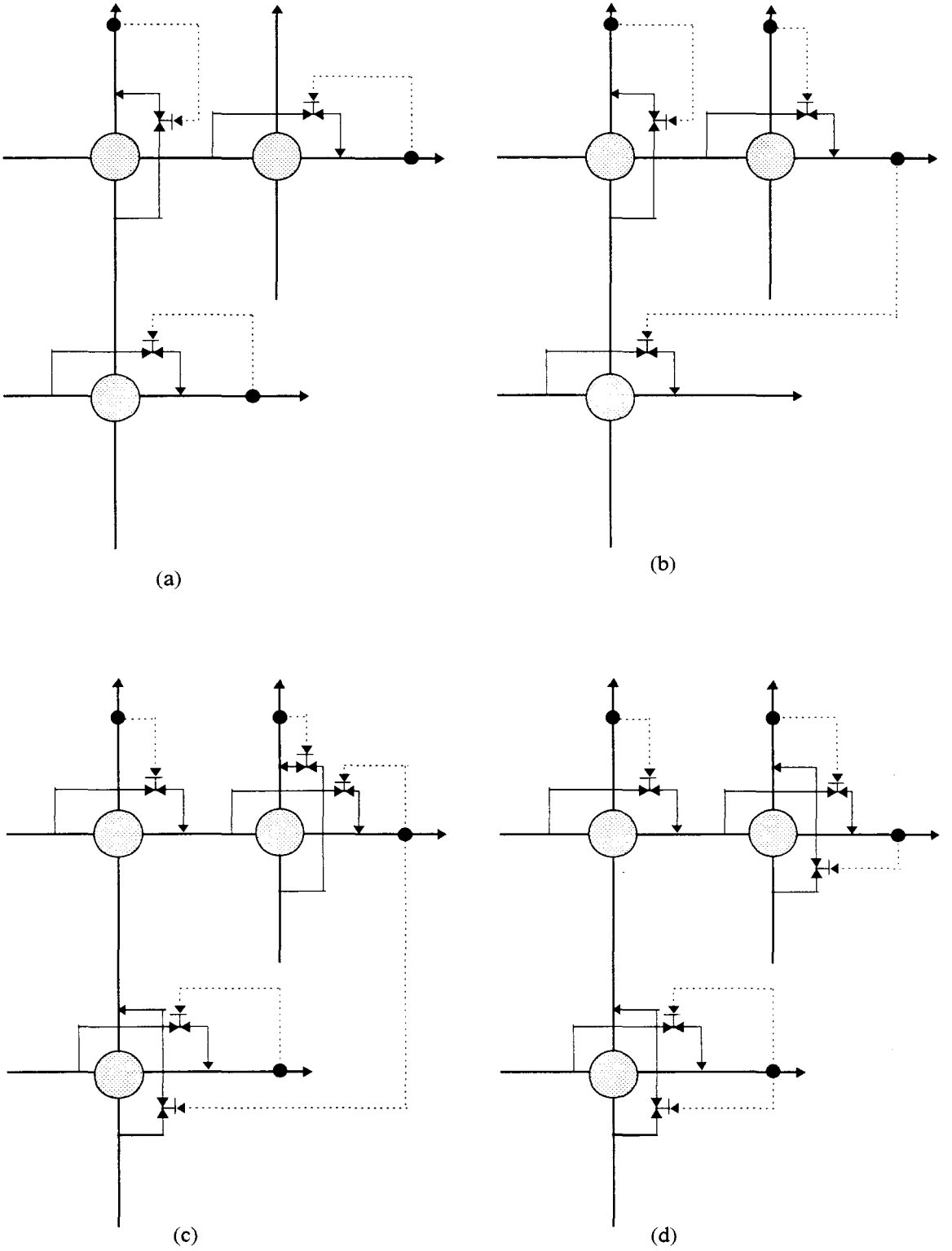

FIGURE 6.2. Some Possible Pairings Among Manipulated and Controlled Variables.

No general simple solutions exist to this kind of pairing problems even for decentralized feedback control schemes. Some heuristic rules answering the pairing problem in decentralized feedback control of HENs, including the use of RGA (Relative Gain Array) concept, are given by Mathisen [8] without verification of the suggestions via simulation of HEN dynamics.

In this thesis, we will neither go into further discussion of the pairing problem nor try to find an heuristic answer through comparative simulation of the dynamics of various HENs with alternative pairings.

Within the framework of mathematical modeling of this thesis, there is another difficulty encountered apart from the pairing problem. As can be seen in Chapter 3, in this thesis the dynamics (lag) of the bypass mixing has been neglected and, thus, the target-stream temperature, T_n^t, has been calculated from the bypass flow, u_n, and the inlet temperature, T_n^i, and the effluent temperature, T_n^e, according to the following algebraic mixing balance (refer to Figure 6.3):

$$T_n^t = T_n^i u_n + (1-u_n)T_n^e \tag{6.1}$$

According to this mixing model adopted in this thesis, temperature measurement for the feedback signal should not be made from T_n^t, but from T_n^e. This is because, there is a unique relationship between the manipulated variable, u_n, and the actual controlled variable T_n^t. If u_n were manipulated based on T_n^t, then the same variable would be both the controlled and the manipulated variable (there is a unique algebraic function, Equation (6.1), relating the two variables). Therefore, the manipulated variable, u_n, should be connected to the pseudo-controlled variable, T_n^e, for feedback information. This matching does not create a difficulty since the soft and hard constraints on T_n^e can be directly calculated/inferred from those on the actual controlled variable, T_n^t.

Figure 6.3 shows the wrong (Figure 6.3 a) and the correct (Figure 6.3 b) locations from which the feedback signal (dashed lines) is sent to the valve manipulating the bypass openings.

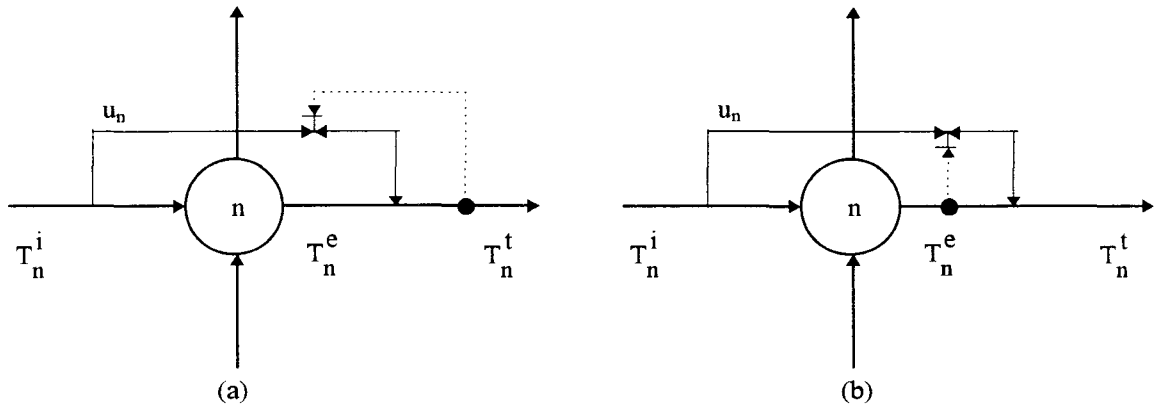

FIGURE 6.3. Alternative Measurement Locations for Feed-Back Information.

Therefore, for the centralized closed-loop optimal-control algorithm the following function is proposed for the implementation of the optimal controls:

$$u_m(t) = \bar{u}_m + \left(u_m^{opt} - \bar{u}_m\right)\left(\frac{T_n^e(t) - \bar{T}_n^e}{T_n^{e,opt}(\infty) - \bar{T}_n^e}\right) \qquad (6.2)$$

Two different subscripts, m and n, were used to designate the bypassed exchanger number (m) and the exchanger number (n) the effluent stream of which is used for feedback information.

It should be noted that, in such a centralized optimal-control scheme, all of the manipulated variables (bypasses) should be matched with at least one controlled variable (effluent of a target exchanger) This is a must since the information (optimal bypass fraction, $\mathbf{u}^{opt}$) from the optimizer is hiararchially distributed to the system, and, after the

disturbance, all bypasses -with no exception- should move from their nominal values, $\bar{u}$, to their optimal values, $\mathbf{u}^{opt}$. Failure to connect even one manipulated variable to any of the pseudo-controlled variables may drive the HEN away from the post-disturbance feasible operating point determined by the optimizer.

According to implementation function, Equation 6.2, initially (nominal operating point at t=0), the feedback temperatures, $T_n^e(0)$, are equal to their values at the nominal operating point, $\bar{T}_n^e$, and, therefore, the bypass openings, $u_m(0)$, are equal to their nominal values, $\bar{u}_m$, (which may be zero). As the effect of the disturbance propagates through the HEN, the feedback temperatures, $T_n^e(t)$, and thus, the manipulated variables, $u_m(t)$ change. As the system moves towards the feasible operating point determined by the optimizer, the feedback temperatures approach to their optimal values, $T_n^{e,opt}$. At this post-disturbance steady-state operating point (as $t \to \infty$), the feedback temperatures attain the value of $T_n^{e,opt}(\infty)$, and thus, the optimal bypasses, u_m^{opt}, are reached (the term in brackets in Equation (6.2) will have the value of unity). In this way, both the feedback temperature, $T_n^e(t)$, and bypass openings, $u_m(t)$, simultaneously reach their optimal/feasible values, $T_n^{e,opt}$ and u_m^{opt}, respectively. This simultaneous behavior of the manipulated and pseudo-controlled variables is illustrated in Figure 6.4, where the case $u_m^{opt} > \bar{u}_m$ is shown in Figure 6.4 (a), and $u_m^{opt} < \bar{u}_m$ in Figure 6.4 (b).

The centralized closed-loop optimal-control algorithm was tested on the HEN depicted in Figure 6.5. This network has the same structure and the same bypass locations with the HEN used in Chapter 5 (Figure 5.4). As can be seen in Figure 6.5, the bypass stream on the hot and cold sides of the first exchanger were both matched with the hot effluent stream from the first exchanger, and the bypass stream on the cold side of the third exchanger was matched with the hot target stream of the third exchanger.

The disturbance given to the HEN and the control-precision vector imposed on the HEN targets are identical to those used in Chapter 5, i.e., Equations (5.1) and (5.2),

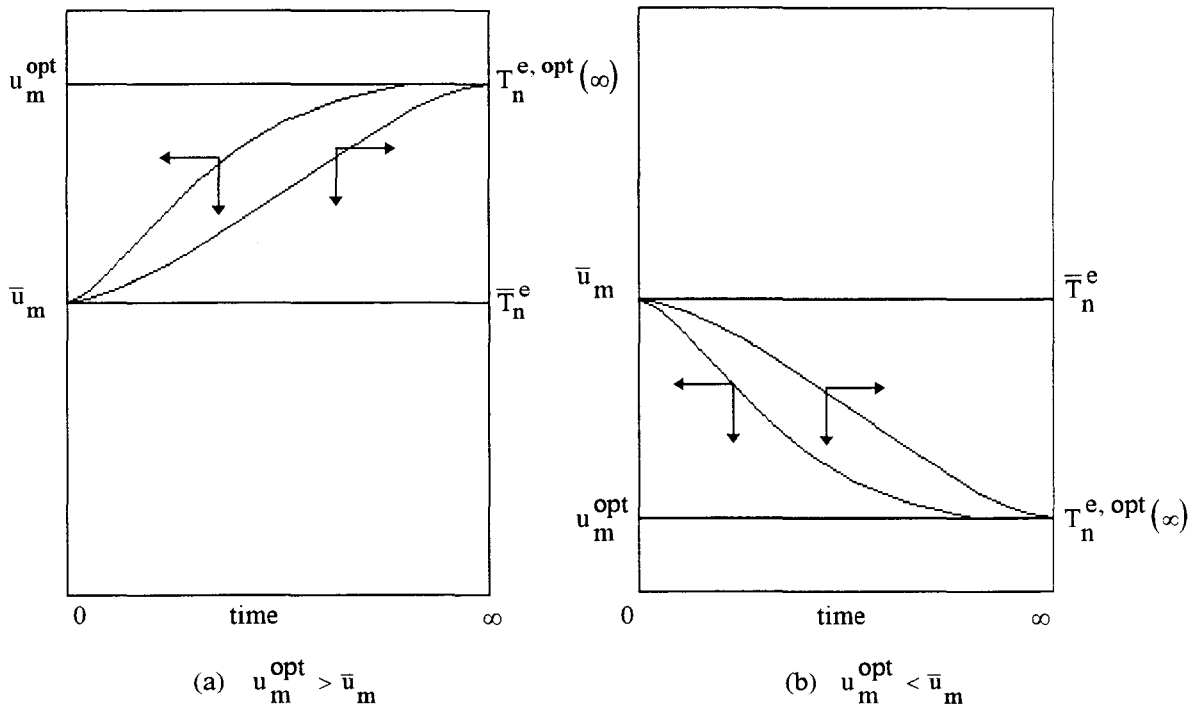

FIGURE 6.4. Illustration of the Implementation Function given by Equation (6.2).

respectively. Therefore, the optimal controls, $\mathbf{u}^{opt}$, that will drive the system to the post-disturbance feasible/optimal steady-state operating point determined by the optimizer were the same, as well, i.e., Equations (5.3) and (5.4).

The response of the HEN according to the closed-loop optimal feedback control scheme is shown in Figure 6.6. As can be seen all control-precision constraints imposed on the targets of the HEN were satisfied. Figure 6.6 shows no temporal violation of the control-range constraints. However, this is valid only for this example, and the implementation function (Equation 6.2) in its presented form, does not have a degree of freedom (a tuning parameter similar to τ of the open-loop optimal-control implementor given in Equation (5.5)) with which any possible temporary violations of the control-range constraints could be prevented.

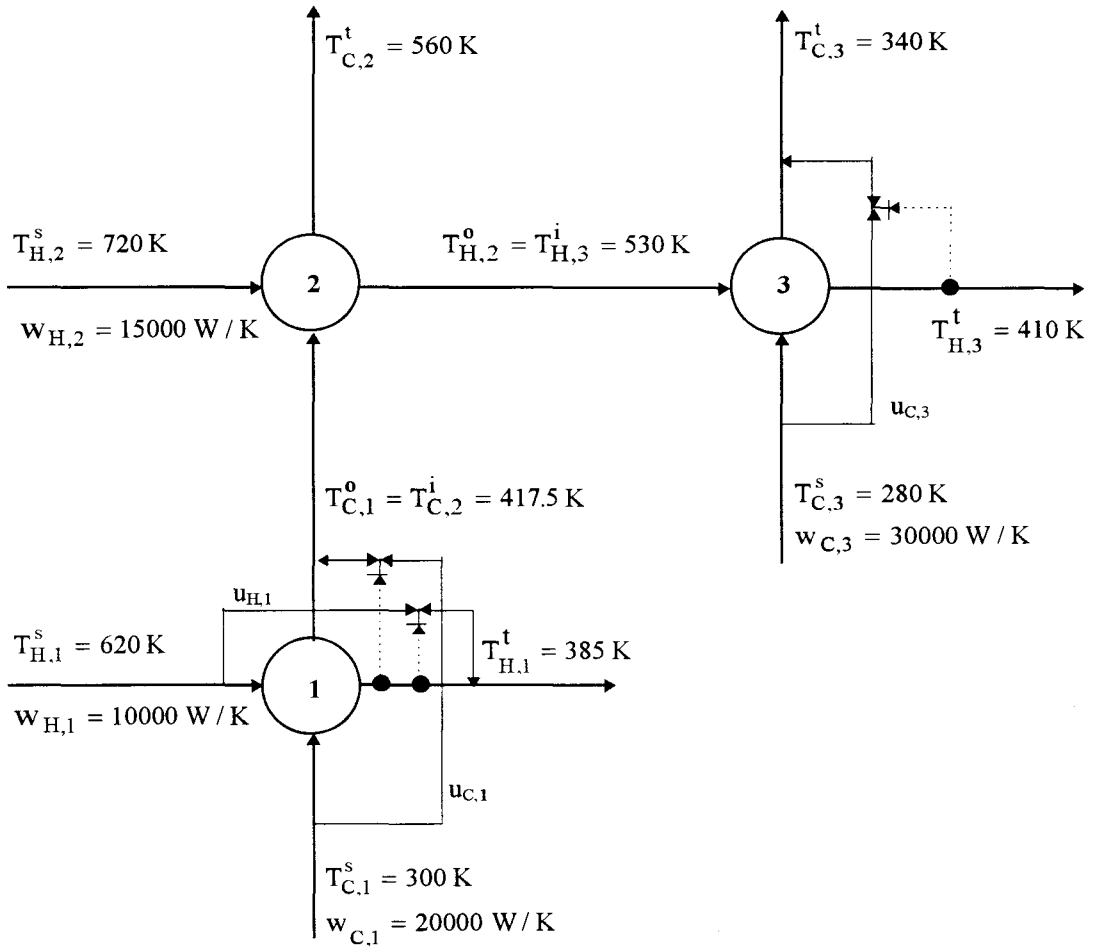

FIGURE 6.5. HEN with its Control Structure for Closed-Loop Optimal Control.

However, it is worth noting that the response of the HEN under the closed-loop optimal-control scheme is much smoother than its response under the open-loop optimal-control scheme, as can be seen by comparing Figure 6.5 with Figure 5.15 where an optimal value of $\tau_i = 32$ seconds had been used as the rate of opening of all the bypasses.

The listing of the program used for the sample HEN is given in Appendix D.

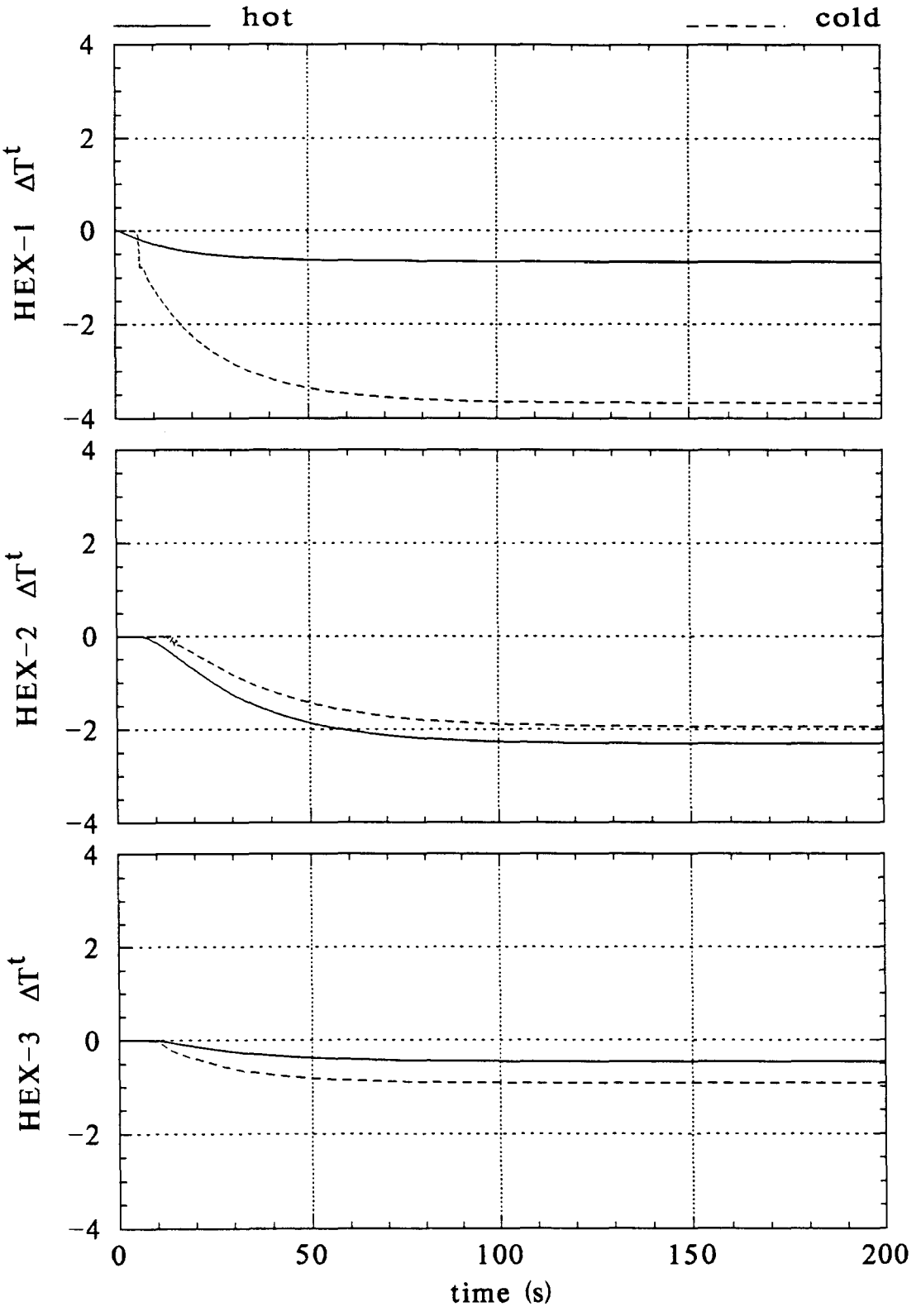

FIGURE 6.6 Response of the HEN Under Closed-Loop Optimal-Control.

7. CONCLUSIONS AND RECOMMENDATIONS

The aim of this thesis was to investigate the dynamics, controllability and resilience of Heat-Exchanger Networks (HENs), and to study the relationships between flexibility and controllability of HENs.

For this purpose, first, a rigorous distributed-parameter model for the individual heat exchangers (countercurrent, 1-1 shell-and-tube, multi-tube) constituting the HENs was developed. The model consisted of four coupled partial-differential equations (PDEs) for each exchanger and included energy balances for the shell (cold) and tube (hot) fluids, and for the shell and tube walls.

For the numerical solution of the exchanger models, the "method of lines" technique, with finite-difference discretization of the spatial derivatives, was used. Among the various finite-difference approximations tested, such as "two-point forward/backward" (corresponds to "perfectly-mixed-tanks-in-series" approximation), "five-point central", "five-point biased-upwind" finite-difference approximations, only the "five-point biased-upwind" finite-difference approximation completely eliminated the "steady-state offset" problem (the match between the steady-state algebraic solution and the dynamic response at steady state) mentioned in the literature, even with conservative number of grid points. Other finite-difference approximations could not eliminate this problem even with very large number of grids. Elimination of the steady-state offset problem allowed the use of the classical heat-exchanger design equation ($Q = U A \Delta T_{lm}$) as the steady-state model within the framework of algebraic-model-based optimal-control algorithms developed in this thesis. To the best of our knowledge, elimination of the "steady-state offset" problem, through the use of an advanced numerical solution of the PDEs constituting the exchanger's dynamic model, is a significant contribution to the literature. For future works,

it is recommended to test the numerical technique for heat exchangers with multi-tube passes to see if the results of the classical heat-exchanger design equation with well-known correction factor ($Q = U A F_T \Delta T_{lm}$) and the steady-state prediction of the numerical solution of the exchanger model do agree.

Dynamic models of the HENs investigated in the thesis were successfully constructed by connecting the individual exchanger models through their boundary conditions in accordance with the network structure. In this thesis, only the flow rates of the bypass streams around the exchangers were considered as the manipulated variables. The controlled variables were the target-stream temperatures of the HENs. For future works it is recommended to investigate HENs containing stream splits, in which case, both the bypasses and stream-split ratios could be used as manipulated variables. In this work, the dynamics at the mixing point of the bypasses, valve dynamics, and the dynamics and dead times due to transport lines connecting the exchangers were neglected. In future works, these points may be included in the analysis.

In this thesis, controllability and resilience of the HENs were investigated within the framework of two centralized steady-state-model-based optimal-control algorithms: The open-loop control scheme, in which no state-feedback information was used, and the closed-loop scheme, in which state-feedback information was used. The controllability and resilience of the HENs were studied against various set of disturbances in source-stream temperatures and for different control-range constraints imposed on the target-stream temperatures. In future studies, disturbances in flow rates (or enthalpies) of source streams could be included as well.

In both optimal-control schemes, first, the optimal bypass openings, which satisfied the control-range constraints on target-stream temperatures after a pre-defined disturbance set, (manipulated variables) were determined through the solution of a static optimization problem which referred to the algebraic steady-state model of HENs. The optimizer, thus, successfully found a feasible and optimal (minimum target-temperature deviation from nominal condition) post-disturbance steady-state operating point around the pre-disturbance (nominal) operating conditions. In principle, both the soft and/or hard

constraints on the target streams can be imposed. However, if the HEN does not have an enough flexibility margin, it is most likely that the optimizer may not be able to find a post-disturbance feasible operating point if hard constraints are imposed on all of the target-stream temperatures. Therefore, it can be concluded that HENs should be designed with consideration of their operational flexibilities, otherwise, they become quite difficult even impossible to be controlled within desired (narrow) margins.

In the centralized open-loop (without state feedback) algorithm, the bypasses were opened from their nominal values (which may be zero) up to their optimal values as a function of time. The use of ramp function resulted in very satisfactory dynamic responses of the HENs, and temporal violation of the control-range constraints were prevented by optimal tuning of the rate with which the bypasses were opened. Since the opening of the bypasses linearly in time (parameterization of the control vector linearly) proved to be satisfactory, we do not suggest testing and the use of more complicated implementation (parameterization) functions. However, we do recommend for future works to investigate if the rates of openings of the bypasses of the individual exchangers can be estimated heuristically based on the time constants of the individual exchangers of the network.

In the centralized closed-loop (with state feedback) control algorithm, the bypasses were opened from their nominal values up to their optimal values as dependent on the pseudo-controlled target-stream temperatures. The use of state feedback resulted in smoother dynamic response for a sample HEN. However, the closed-loop algorithm, in its presented form, cannot always prevent temporal violation of the control-range constraints. It is recommended for future works to develop an alternative closed-loop control scheme which can use the state-feedback information in such a way that it is capable of preventing any probable temporal violation of the control-range constraints on the target streams. It is also worth to investigate in detail the pairing problem between the manipulated (bypasses) and controlled (target temperatures) variables.

As an overall conclusion it can be said that both of the proposed centralized steady-state-model-based optimal-control algorithms have proven to be promising in controlling HENs as long as the networks have enough margin of steady-state flexibility. However,

this conclusion is valid for situations where there is no mismatch between the process (dynamic model of HEN) and the steady-state model (algebraic model used at the static optimization level). For example, if there is even a small difference in the overall heat-transfer coefficients used in the process and optimizer models, the algorithms suggested in the thesis may not perform as expected. Therefore, in future works, adequate means for eliminating or correcting the process-model mismatch should be developed.

APPENDICES

APPENDIX A

Listing of the Heat Exchanger Design Program.

```
C
C ***********************************************************************
C **                                                                   **
C **                                                                   **
C **     THIS PROGRAM FINDS THE PROPERTIES (L,NT) OF A HEX WITH        **
C **       MIN(A-AREQ), WHICH SATISFIES THE DESIRED FLOWRATE           **
C **                 AND INLET & OUTLET TEMPERATURES                   **
C **                                                                   **
C **                                                                   **
C ***********************************************************************
C **                     UĞUR AKMAN   &   CANTÜRK BOYACI               **
C ***********************************************************************
C
C
C     DIF   : MISMATCH ERROR BETWEEN PHYSICAL AND REQUIRED
C             AREAS (A-AREQ), M2
C
C     DO      : TUBE OUTSIDE DIAMETER, MM
C     DI      : TUBE INSIDE DIAMETER, MM
C     NT      : TOTAL NUMBER OF TUBES IN THE BUNDLE
C     DS      : SHELL INSIDE DIAMETER, MM
C     DSB     : DIAMETRAL SHELL-BAFFLE CLEARANCE, MM
C     RL      : TUBE LENGTH, M
C     RHOI    : REFERENCE DENSITIES FOR TUBE FLUID, KG/M3
C     RHOS    : REFERENCE DENSITIES FOR SHELL FLUID, KG/M3
C     WI      : TUBE FLUID FLOW RATE, KG/s
C     WS      : SHELL FLUID FLOW RATE, KG/s
C     TI1,TI2: INLET AND OUTLET TEMPERATURES OF TUBE FLUID, K
C     TS1,TS2: INLET AND OUTLET TEMPERATURES OF SHELL FLUID, K
C     LS      : TUBE SHEET THICKNESS, MM
C     CPIM    : MEAN HEAT CAPACITIES FOR TUBE FLUID, J/KG K
C     CPSM    : MEAN HEAT CAPACITIES FOR SHELL FLUID, J/KG K
C     LBC     : CENTRAL BAFFLE SPACING, MM
C     LBIN    : INLET BAFFLE SPACING, MM
C     LBOUT   : OUTLET BAFFLE SPACING, MM
C
C     ACH     : INNER CROSSECTIONAL AREA OF A SINGLE TUBE, M2
C     ACC     : TOTAL CROSSECTIONAL AREA OF THE SHELL, M2
C
C     AH      : INNER SURFACE AREA OF A SINGLE TUBE/LENGTH, M2
C     AC      : OUTER SURFACE AREA OF A SINGLE TUBE/LENGTH, M2
C     AS      : INNER SURFACE AREA OF THE SHELL/LENGTH, M2
```

```
C
C     VH      : VELOCITY OF THE TUBE-SIDE, M/sec
C     VC      : VELOCITY OF THE SHELL-SIDE, M/sec
C
C     ACT     : CROSSECTIONAL TUBE WALL AREA, M2
C     ACS     : CROSSECTIONAL SHELL WALL AREA, M2
C
C     VOLH    : INNER VOLUME OF A SINGLE TUBE,M3
C     VOLC    : INNER VOLUME OF THE SHELL,M3
C     VOLT    : VOLUME OF A SINGLE TUBE-WALL METAL,M3
C
C     HI      : INSIDE HEAT TRANSFER COEFFICIENT,W/M2K
C     HO      : OUTSIDE HEAT TRANSFER COEFFICIENT,W/M2K
C     U       : OVERALL HEAT TRANSFER COEFFICIENT,W/M2K
C
C
C ***************************************************************
C
      IMPLICIT REAL*8 (A-H,O-Z)
      REAL*8 LBC,L,LS,LC,LBIN,LBOUT,LDOWN,LUP,LO,DS,DO
C
      NO    = 6
      OPEN (NO,FILE=RESULTS.OUT')
C
      PI    = DACOS(-1.D0)
      TI1   = 298.D0
      TI2   = 303.D0
      TS1   = 353.D0
      TS2   = 335.9986D0
      WS    = 4.8D0
      WI    = 7.2918D0
      NT    = 86.D0
      RLS   = 2.D0
      RL    = RLS
C
C...DETERMINATION OF NUMBER OF TUBES
C
C     ----------------------------------------------------------------
      CALL DESIGN (RL,NT,DIF,DS,DO,DI,RHOS,RHOI,WS,WI,HS,HI,LS,PI,CPIM,
     &             CPSM,U,TI1,TI2,TS1,TS2)
C     ----------------------------------------------------------------
      IF (DABS(DIF).LT.1.D-10) GOTO 500
      IF (DIF.LT.0) GOTO 69
64    NT    = NT-1
      GOTO 79
69    NT    = NT+1
79    DA1   = DIF
C     ----------------------------------------------------------------
      CALL DESIGN (RL,NT,DIF,DS,DO,DI,RHOS,RHOI,WS,WI,HS,HI,LS,PI,CPIM,
     &             CPSM,U,TI1,TI2,TS1,TS2)
C     ----------------------------------------------------------------
      IF (DABS(DIF).LT.1.D-10) GOTO 500
      IF ((DIF.LT.0).AND.(DA1.LT.0)) GOTO 69
      IF ((DIF.GT.0).AND.(DA1.GT.0)) GOTO 64
      NT1   = NT-1
      NT2   = NT
      DAI   = DA1
      DAS   = DIF
      DL    = 1.D-1
```

```
C
C...DETERMINATION OF LENGTH
C
C     ------------------------------------------------------------------
      CALL FIND-L (DL,RL,NT1,DAI,DS,DO,DI,RHOS,RHOI,WS,HS,WI,HI,PI,LS,
     &             CPIM,CPSM,U,TI1,TI2,TS1,TS2)
C     ------------------------------------------------------------------
      NT    = NT1
      DAK   = DAI
      RL1   = RL
      DL    = 1.D-1
      RL    = RLS
C     ------------------------------------------------------------------
      CALL FIND-L (DL,RL,NT1,DAI,DS,DO,DI,RHOS,RHOI,WS,HS,WI,HI,PI,LS,
     &             CPIM,CPSM,U,TI1,TI2,TS1,TS2)
C     ------------------------------------------------------------------
      RL2   = RL
      IF (DABS(DAI).LT.DABS(DAS)) THEN
         NT = NT1
         RL = RL1
        ELSE
         DAK= DAS
         NT = NT2
         RL = RL2
      ENDIF
500   CONTINUE
C     ------------------------------------------------------------------
      CALL DESIGN (RL,NT,DIF,DS,DO,DI,RHOS,RHOI,WS,WI,HS,HI,LS,PI,CPIM,
     &             CPSM,U,TI1,TI2,TS1,TS2)
C     ------------------------------------------------------------------
      RHOT  =  7833.78D0
      CPT   =  502.44D0
      RL    =  RL-(2.D0*LS*1.D-3)
C
C...CALCULATION OF VELOCITIES, AREAS AND VOLUMES
C
      VH    = WI/(NT*RHOI*PI*(0.5D0*DI*1.D-3)**2)
      VC    = WS/(RHOS*PI*((0.5D0*DS*1.D-3)**2-NT*(0.5D0*DO*1.D-3)**2))
C...
      ACH   = PI*(0.5D0*DI*1.D-3)**2
      ACC   = PI*((0.5D0*DS*1.D-3)**2-NT*(0.5D0*DO*1.D-3)**2)
C...
      AH    = PI*DI*1.D-3
      AC    = PI*(DO*1.D-3)
      AS    = PI*DS*1.D-3
      AX    = AC*RL*NT
C...
      ACT   = PI*((DO*0.5D-3)**2-(DI*0.5D-3)**2)
      ST    = 15.D0
      ACS   = PI*(((DS+ST)*0.5D-3)**2-(DS*0.5D-3)**2)
C...
      VOLH  = ACH*RL
      VOLC  = ACC*RL
      VOLT  = ACT*RL
C
            WRITE(NO,*)'Number of Tubes                    : ',NT
            WRITE(NO,*)'Length (m)                         : ',RL
            WRITE(NO,*)'Shell Diameter (mm)                : ',DS
            WRITE(NO,*)
```

```
            WRITE(NO,*)'Velocity (HOT) (m/s)                    : ',VH
            WRITE(NO,*)'Velocity (COLD) (m/s)                   : ',VC
            WRITE(NO,*)
            WRITE(NO,*)'Heat Transfer Area (HOT) (m2)           : ',AH*RL
            WRITE(NO,*)'Heat Transfer Area (COLD) (m2)          : ',AX
            WRITE(NO,*)'Heat Transfer Area (SHELL-WALL) (m2)    : ',AS*RL
            WRITE(NO,*)'Crossectional Inner Area (HOT) (m2)     : ',ACH
            WRITE(NO,*)'Crossectional Inner Area (COLD) (m2)    : ',ACC
            WRITE(NO,*)
            WRITE(NO,*)'Crossectional Tube Wall Area (m2)       : ',ACT
            WRITE(NO,*)'Crossectional Shell Wall Area (m2)      : ',ACS
            WRITE(NO,*)
            WRITE(NO,*)'Heat Transfer Coef. (HOT) (W/m2K)       : ',HI
            WRITE(NO,*)'Heat Transfer Coef. (COLD) (W/m2K)      : ',HS
            WRITE(NO,*)'Overall Heat Transfer Coef. (W/m2K)     : ',U
C...
      RETURN
      END
C...
C ********************************************************************** C
      SUBROUTINE FIND-L (DL,L,NT,DIF,DS,DO,DI,RHOS,RHOI,WS,HS,WI,HI,PI,
     &                   LS,CPIM,CPSM,U,TI1,TI2,TS1,TS2)
C ********************************************************************** C
C           *                                                            *
C           *   THIS SUBROUTINE FINDS THE OPTIMAL LENGTH OF THE          *
C           *             EXCHANGER WITH MIN(A-AREQ)                     *
C           *                                                            *
C ********************************************************************** C
C
      IMPLICIT REAL*8 (A-H,O-Z)
      REAL*8 LBC,L,LS,LC,LBIN,LBOUT,LDOWN,LUP,LO,DS
C..
      LDOWN = -1000.D0
      LUP   = 10000.D0
      LO    = 0.D0
      NK    = NT
      IF (DIF.GT.0) GOTO 34
32    L     = L+DL
      GOTO 37
34    L     = L-DL
C     ------------------------------------------------------------------
37    CALL DESIGN (L,NK,DIF,DS,DO,DI,RHOS,RHOI,WS,WI,HS,HI,LS,PI,CPIM,
     &             CPSM,U,TI1,TI2,TS1,TS2)
C     ------------------------------------------------------------------
      IF (DABS(DIF).LT.1.D-10) GOTO 48
      IF (((L.EQ.LDOWN).AND.(LO.EQ.LUP)).OR.((L.EQ.LUP).AND.(LO.EQ.
     &      LDOWN))) THEN
          L = LDOWN
C     ------------------------------------------------------------------
          CALL DESIGN (L,NK,DIF,DS,DO,DI,RHOS,RHOI,WS,WI,HS,HI,LS,PI,
     &                 CPIM,CPSM,U,TI1,TI2,TS1,TS2)
C     ------------------------------------------------------------------
          DL= DL/10.D0
      ENDIF
      LO    = L
      IF (DIF.LT.0) THEN
          LDOWN = L
          GOTO 32
          ELSE
```

```
          LUP   = L
          GOTO 34
      ENDIF
48    CONTINUE
C
      RETURN
      END
C...
C ********************************************************************** C
      SUBROUTINE DESIGN (L,NT,DIF,DS,DO,DI,RHOSM,RHOIM,WS,WI,HS,HI,LS,
     &                   PI,CPIM,CPSM,U,TI1,TI2,TS1,TS2)
C ********************************************************************** C
C
C ***********************************************************************
C **                                                                   **
C **       RATING CALCULATION OF A SHELL AND TUBE EXCHANGER            **
C **            FOR HEAT TRANSFER WITHOUT PHASE CHANGE                 **
C **                                                                   **
C **                                                                   **
C **    Reference: Chemical Process Computations by Raghu Raman        **
C **                                                                   **
C ***********************************************************************
C **       UĞUR AKMAN  -  CANTÜRK BOYACI  -  DERYA UZTÜRK              **
C ***********************************************************************
C
C     RATING CALCULATIONS OF A SHELL AND TUBE EXCHANGER
C     FOR SENSIBLE HEAT TRANSFER IN SHELL AND TUBE SIDES
C     DO - TUBE OUTSIDE DIAMETER, MM
C     DI - TUBE INSIDE DIAMETER, MM
C     EPS - PIPE ROUGHNESS, MM
C     DS - SHELL INSIDE DIAMETER, MM
C     LBC - CENTRAL BAFFLE SPACING, MM
C     LBIN - INLET BAFFLE SPACING, MM
C     LBOUT - OUTLET BAFFLE SPACING, MM
C     LC - BAFFLE CUT, MM
C     DOTL - SHELL OUTER TUBE LIMIT, MM
C     DSB - DIAMETRAL SHELL-BAFFLE CLEARANCE, MM
C     PT - TUBE PITCH, MM
C     NSS - NUMBER PAIRS OF SEALING STRIPS
C     NPASS - TOTAL NUMBER OF TUBE PASSES
C     LS - TUBE SHEET THICKNESS, MM
C     LAYOUT - FLAG FOR TYPE OF TUBE LAYOUT
C            = 1 TRIANGULAR
C            = 2 IN-LINE SQUARE
C            = 3 ROTATED SQUARE
C     RHOI - REFERENCE DENSITIES FOR TUBE FLUID, KG/M3
C     RHOS - REFERENCE DENSITIES FOR SHELL FLUID, KG/M3
C     VISCI - REFERENCE VISCOSITIES FOR TUBE FLUID, Ns/M2
C     VISCS - REFERENCE VISCOSITIES FOR SHELL FLUID, Ns/M2
C     XKI - REFERENCE CONDUCTIVITIES FOR TUBE FLUID, W/MK
C     XKS - REFERENCE CONDUCTIVITIES FOR SHELL FLUID, W/MK
C     CPI - REF. HEAT CAPACITIES FOR TUBE FLUID, J/KGK
C     CPS - REF. HEAT CAPACITIES FOR SHELL FLUID, J/KGK
C     TREFI - REFERENCE TEMPERATURES FOR TUBE FLUID, K
C     TREFS - REFERENCE TEMPERATURES FOR SHELL FLUID, K
C     XKW - THERMAL CONDUCTIVITY OF TUBE WALL, W/M.K
C     RDI - TUBE SIDE FOULING FACTOR, M2K/W
C     RDS - SHELL SIDE FOULING FACTOR, M2K/W
C     IST - STATE OF TUBE SIDE FLUID
```

```
C         = 1 LIQUID
C         = 2 GAS
C     ISS - STATE OF SHELL SIDE FLUID
C         = 1 LIQUID
C         = 2 GAS
C     ITMAX - MAXIMUM NUMBER OF ITERATIONS
C
C ***********************************************************************
C
      IMPLICIT REAL*8 (A-H,O-Z)
      REAL*8 LBC,L,LS,LC,LBIN,LBOUT,DS
      DIMENSION RHOI(2),RHOS(2),VISCI(2),VISCS(2),CPI(2),
     &          CPS(2),XKI(2),XKS(2),TREFI(2),TREFS(2)
C
C ... INPUT GEOMETRY DATA
C
      ITMAX = 1000
      NSS   = 0.D0
      NPASS = 4.D0
      LAYOUT= 1
      LBC   = 450.D0
      LS    = 27.D0
      LBIN  = 165.D0
      LBOUT = 165.D0
      DO    = 25.4D0
      DI    = 19.86D0
      PT    = 31.75D0
      EPS   = 0.025D0
C...
      TREFI(1)= 323.D0
      TREFI(2)= 283.D0
      TREFS(1)= 375.D0
      TREFS(2)= 289.D0
      RHOI(1) = 988.1D0
      RHOI(2) = 999.7D0
      RHOS(1) = 798.D0
      RHOS(2) = 885.D0
      VISCI(1)= 0.0006D0
      VISCI(2)= 0.00126D0
      VISCS(1)= 0.000258D0
      VISCS(2)= 0.000679D0
      XKI(1)= 0.64D0
      XKI(2)= 0.603D0
      XKS(1)= 0.126D0
      XKS(2)= 0.163D0
      CPI(1)= 4183.D0
      CPI(2)= 4195.D0
      CPS(1)= 1980.D0
      CPS(2)= 1675.D0
      XKW   = 45.D0
      RDI   = 0.00036D0
      RDS   = 0.00018D0
C...
      IST   = 1
      ISS   = 1
C...
      DOTL  = DO*(NT/0.175D0)**(1.D0/2.285D0)
      DSB   = (DOTL*10.D-3)+8.D0
      DS    = DOTL+DSB
```

```
      LC     = 0.25D0*DOTL
      R1O3   = 1.D0/3.D0
      R2O3   = 2.D0/3.D0
C...
      TOLEPS= 1.D-12
      TOLCHK= 1.D-06
C...
      RW     = (DO-DI)*1.D-3/(2.D0*XKW)
      A      = PI*1.D-3*DO*(L-2.D-3*LS)*DFLOAT(NT)
C
C ... CHECK DATA CONSISTENCY
C
      CPIM   = SPHEAT(CPI,TREFI,(TI1+TI2)*0.5D0)
      CPSM   = SPHEAT(CPS,TREFS,(TS1+TS2)*0.5D0)
      QI     = WI*CPIM*(TI2-TI1)
      QS     = WS*CPSM*(TS2-TS1)
      QRATIO= DABS(QI/QS)
      IF (DABS(1.D0-QRATIO).GT.TOLCHK) WRITE(NOUT,311)
      Q      = QI
      TIB    = (TI1+TI2)*0.5D0
C
C ... CALCULATE SHELL SIDE HEAT TRANSFER COEFFICIENT
C
      TSB    = (TS1+TS2)*0.5D0
      VISCSM= VISCOS(VISCS,TREFS,TSB,ISS)
      RHOSM = DENSTY(RHOS,TREFS,TSB,ISS)
      CPSM   = SPHEAT(CPS,TREFS,TSB)
      XKSM   = THCOND(XKS,TREFS,TSB)
      TW     = (TSB+TIB)*0.5D0
      TWNEW = TW
      ITER1 = 0
80    PHIS   = 1.D0
      IF (ISS.EQ.1) PHIS=(VISCSM/VISCOS(VISCS,TREFS,TW,1))**0.14D0
      HS     = HSHELL(DO,DS,L-2.D-3*LS,LBC,LBIN,LBOUT,LC,DOTL,DSB,PT,NT,
     &               NSS,WS,VISCSM,CPSM,XKSM,PHIS,LAYOUT,PI,R1O3,R2O3)



C
C ... ESTIMATE TUBE SIDE HEAT TRANSFER COEFFICIENT
C
      VISCIM= VISCOS(VISCI,TREFI,TIB,IST)
      RHOIM = DENSTY(RHOI,TREFI,TIB,IST)
      CPIM   = SPHEAT(CPI,TREFI,TIB)
      XKIM   = THCOND(XKI,TREFI,TIB)
      UI     = 4.D6*WI*DFLOAT(NPASS)/(PI*DI**2*RHOIM*DFLOAT(NT))
      REI    = 1.D-3*DI*UI*RHOIM/VISCIM
      PRI    = CPIM*VISCIM/XKIM
      PHIT   = 1.D0
      IF (IST.EQ.1) PHIT=(VISCIM/VISCOS(VISCI,TREFI,TW,1))**0.14D0
      HI     = HTUBE(REI,PRI,DI,L,XKIM,PHIT,R1O3,R2O3)
C
C ... ESTIMATE TUBE WALL TEMPERATURE
C
      TW     = TIB+HS/(HS+HI)*(TSB-TIB)
      IF (DABS((TW-TWNEW)/TW).LE.TOLEPS) GOTO 90
      TWNEW = TW
      ITER1 = ITER1+1
      IF (ITER1.LT.ITMAX) GOTO 80
```

```
      WRITE(NOUT,314)
      STOP
C
C ... CALCULATE HEAT LOAD FROM HEAT TRANSFER EQUATION
C
90    CONTINUE
      U     = 1.D0/(DO/(DI*HI)+1.D0/HS+RW+RDS+RDI)
      DT1   = TS1-TI2
      DT2   = TS2-TI1
      IF (DT1.GT.0.D0.AND.DT2.GT.0.D0) GOTO 100
      WRITE(NOUT,315)
      STOP
100   DELT  = (DT1-DT2)/DLOG(DT1/DT2)
      FT    = 1.D0
110   DELTM = DELT*FT
      AREQ  = QI/(U*DELTM)
      DA    = (A-AREQ)/A*100.D0
      DIF   = A-AREQ
      RETURN
C...
300   FORMAT(8F10.0)
301   FORMAT(20I3)
302   FORMAT(/5X,'SHELL AND TUBE EXCHANGER RATING'//)
303   FORMAT(' NUMBER OF TUBES=',I4/' NUMBER OF TUBE PASSES=',
     &I3/' NUMBER OF SEALING STRIPS=',I3/' TUBE LAYOUT=',I2/)
304   FORMAT(' SHELL INSIDE DIA.=',F7.2,' MM'/' BAFFLE CUT=',
     &F7.2,' MM'/' TUBE SHEET THICKNESS=',F7.2,' MM'/
     &' DIAMETRAL SHELL-BAFFLE CLEARANCE=',F7.2,' MM'/
     &' SHELL OUTER TUBE LIMIT=',F7.2,' MM'/)
305   FORMAT(' CENTRAL BAFFLE SPACING=',F7.2,' MM'/
     &' INLET BAFFLE SPACING=',F7.2,' MM'/
     &' OUTLET BAFFLE SPACING=',F7.2,' MM'/)
306   FORMAT(' TUBE LENGTH=',F8.4,' M'/' TUBE OUTER DIA.=',
     &F7.2,' MM'/' TUBE INNER DIA.=',F7.2,' MM'/
     &' TUBE PITCH=',F7.2,' MM'/' TUBE ROUGHNESS=',F7.3,' MM'/)
307   FORMAT(' PHYSICAL PROPERTIES AT TWO REF. TEMPERATURES'/
     &' TUBE FLUID:')
308   FORMAT(' SHELL FLUID:')
309   FORMAT(' REFERENCE TEMPERATURES,K',T30,2F12.1/
     &' DENSITY,KG/M^3',T30,2F12.1/' VISCOSITY,N.s/M^2',
     &T30,2E13.4/' THERMAL CONDUCTIVITY,W/M.K',T30,
     &2E13.4/' HEAT CAPACITY,J/KG.K',T30,2E13.4/)
310   FORMAT(' WALL THERMAL CONDUCTIVITY=',E12.4,' W/M.K'/
     &' TUBE SIDE FOULING FACTOR=',E12.4,' M^2.K/W'/
     &' SHELL SIDE FOULING FACTOR=',E12.4,' M^2.K/W'/)
311   FORMAT(' SHELL SIDE AND TUBE SIDE HEAT DUTY DIFFER BY',
     &/' MORE THAN TOLCHK %. QI IS TAKEN FOR CALCULATIONS'/)
312   FORMAT(' NO CONVERGENCE IN CALCULATING TI1')
313   FORMAT(' NO CONVERGENCE IN CALCULATING TI2')
314   FORMAT(' NO CONVERGENCE IN CALCULATING TW')
315   FORMAT(' TEMPERATURE CROSS OCCURS'/
     &' CALCULATIONS ABANDONED'/)
316   FORMAT(' TUBE SIDE:'/' INLET TEMPERATURE=',F10.4,' K'/
     &' OUTLET TEMPERATURE=',F10.4,' K'/' FLOW RATE=',
     &F8.4,' KG/s'/' HEAT TRANSFER COEFF.=',E12.4,
     &' W/M^2.K'//)
317   FORMAT(' SHELL SIDE:'/' INLET TEMPERATURE=',F10.4,' K'/
     &' OUTLET TEMPERATURE=',F10.4,' K'/' FLOW RATE=',
     &F8.4,' KG/s'/' HEAT TRANSFER COEFF.=',E12.4,
```

```
     &' W/M^2.K'//)
318   FORMAT(' NO CONVERGENCE IN HEAT TRANSFER AND ENERGY',
     &' BALANCES')
319   FORMAT(' CONVERGED IN',I5,' ITERATIONS'/)
320   FORMAT(' OVERALL HEAT TRANSFER COEFFICIENT=',E12.4,
     &' W/M^2.K'/' ACTUAL HEAT TRANSFER AREA=',
     &F7.2,' M^2'/' MEAN TEMPERATURE DIFFERENCE=',
     &F6.1,' K'/' SKIN TEMPERATURE=',F6.1,' K'/
     &' HEAT DUTY=',E13.5,' W'/)
321   FORMAT(' REQUIRED HEAT TRANSFER AREA=',F7.2,' M^2'/
     &' EXTENT OF OVER(UNDER) DESIGN=',F6.1,' PER CENT')
322   FORMAT(' SHELL SIDE PRESSURE DROP=',E12.4,' N/M^2'/
     &' TUBE SIDE PRESSURE DROP=',E12.4,' N/M^2'/)
      END
C
C     ------------------------------------------
      FUNCTION HTUBE (RE,PR,D,L,XK,PHI,R1O3,R2O3)
C     ------------------------------------------
C
C     SUBPROGRAM EVALUATES THE HEAT TRANSFER COEFFICIENT
C     FOR FORCED CONVECTION INSIDE TUBES
C     RE - REYNOLDS NUMBER
C     PR - PRANDTL NUMBER
C     D - TUBE INSIDE DIAMETER, MM
C     L - TUBE LENGTH, M
C     XK - FLUID THERMAL CONDUCTIVITY, W/M K
C     PHI - VISCOSITY CORRECTION FACTOR
C
      IMPLICIT REAL*8 (A-H,O-Z)
      REAL*8 L,NU
C...

      IF (RE.GT.2100.D0) GOTO 10
C
C ... LAMINAR FLOW
C
      GZ    = R E*PR*D*1.D-3/L
      IF (GZ.GT.100.D0) NU=1.86D0*GZ**R1O3*PHI
      IF (GZ.LE.100.D0) NU=(3.66D0+0.085D0*GZ*PHI/(1.D0+
     &                      0.047D0*GZ**R2O3))
      GOTO 20
C
C ... TRANSITION FLOW
C
10    IF (RE.LT.1.D4) NU=0.116D0*(RE**R2O3-125.D0)*PR**R1O3*
     &                   (1.D0+(D*1.D-3/L)**R2O3)*PHI
C
C ... TURBULENT FLOW
C
      IF (RE.GE.1.D4) NU=0.023D0*RE**0.8D0*PR**R1O3*PHI
C
20    HTUBE = NU*XK/(D*1.D-3)
C
      RETURN
      END
C
```

```
C     ------------------------------------------------------------
      FUNCTION HSHELL (D,DS,L,LBC,LBIN,LBOUT,LC,DOTL,DSB,PT,NT,
     &                 NSS,W,VISC,CP,XK,PHI,LAYOUT,PI,R103,R203)
C     ------------------------------------------------------------
C
C     SUBPROGRAM EVALUATES THE SHELL-SIDE HEAT TRANSFER
C     COEFFICIENT FOR FORCED CONVECTION IN A SHELL AND TUBE
C     HEAT EXCHANGER
C     D - TUBE OUTSIDE DIAMETER, MM
C     DS - SHELL INSIDE DIAMETER, MM
C     L - TUBE LENGTH, M
C     LBC - CENTRAL BAFFLE SPACING, MM
C     LBIN - INLET BAFFLE SPACING, MM
C     LBOUT - OUTLET BAFFLE SPACING, MM
C     LC - BAFFLE CUT, MM
C     DOTL - SHELL OUTER TUBE LIMIT, MM
C     DSB - DIAMETRAL SHELL-BAFFLE CLEARANCE, MM
C     PT - TUBE PITCH, MM
C     NT - TOTAL NUMBER OF TUBES IN THE BUNDLE
C     NSS - NUMBER PAIRS OF SEALING STRIPS
C     W - FLOW RATE IN SHELL, KG/s
C     VISC - VISCOSITY OF SHELL FLUID, Ns/M2
C     CP - HEAT CAPACITY OF SHELL FLUID, J/KG K
C     XK - THERMAL CONDUCTIVITY OF SHELL FLUID, W/M K
C     PHI - VISCOSITY CORRECTION FACTOR
C     LAYOUT - FLAG FOR TYPE OF TUBE LAYOUT
C            = 1 TRIANGULAR
C            = 2 IN-LINE SQUARE
C            = 3 ROTATED SQUARE
C
      IMPLICIT REAL*8 (A-H,O-Z)
      REAL*8 L,LBC,LC,NC,NCW,LBIN,LBOUT
C...
      DIMENSION A1(5,3),A2(5,3),A3(3),A4(3)
C...
      DATA A1 /0.321,0.321,0.593,1.36,1.4,0.37,0.107,0.408,0.9,
     &         0.97,0.37,0.37,0.73,0.498,1.55/,
     &     A2 /-0.388,-0.388,-0.477,-0.657,-0.667,-0.395,-0.266,
     &         -0.46,-0.631,-0.667,-0.396,-0.396,-0.5,-0.656,-0.667/,
     &     A3 /1.45,1.187,1.93/, A4 /0.519,0.37,0.5/
C...
      PRATIO= PT/D
      GOTO (10,20,30),LAYOUT
10    PP    = (DSQRT(3.D0)/2.D0)*PT
      PN    = PT*0.5D0
      GOTO 40
20    PP    = PT
      PN    = PT
      GOTO 40
30    PP    = PT/DSQRT(2.D0)
      PN    = PP
40    NC    = DS*(1.D0-2.D0*LC/DS)/PP
      IF (LAYOUT.EQ.1) PD=PT
      IF (LAYOUT.GT.1) PD=PN
      SM    = LBC*(DS-DOTL+(PT-D)*(DOTL-D)/PD)
      RES   = D*W*1.D3/(VISC*SM)
      PR    = CP*VISC/XK
```

```
C
C ... CALCULATE HEAT TRANSFER COEFFICIENT FOR AN IDEAL TUBE BANK
C
      IF (RES.GE.1.D4) J=1
      IF (RES.GE.1.D3.AND.RES.LT.1.D4) J=2
      IF (RES.GE.1.D2.AND.RES.LT.1.D3) J=3
      IF (RES.GE.1.D1.AND.RES.LT.1.D2) J=4
      IF (RES.LT.1.D1) J=5
      A     = A3(LAYOUT)/(1.D0+0.14D0*RES**A4(LAYOUT))
      HJ    = A1(J,LAYOUT)*(1.33D0/PRATIO)**A*RES**A2(J,LAYOUT)
      HSI   = HJ*CP*W/(SM*1.D-6)*PR**(-R2O3)*PHI
C
C ... BAFFLE CONFIGURATION CORRECTION FACTOR
C
      TERM  = (DS-2.D0*LC)/DOTL
      TERM1 = DACOS(TERM)
      FTC   = (PI+2.D0*TERM*DSIN(TERM1)-2.D0*TERM1)/PI
      PHIC  = FTC+0.54D0*(1.D0-FTC)**0.345D0
C
C ... BAFFLE LEAKAGE CORRECTION FACTOR
C
      STB   = 15.80642D0*D*(1.D0+FTC)*DFLOAT(NT)
      SSB   = DS*DSB*0.5D0*(PI-DACOS(1.D0-2.D0*LC/DS))
      R1    = (STB+SSB)/SM
      R2    = SSB/(SSB+STB)
      PHIL  = 0.44D0*(1.D0-R2)+(1.D0-0.44D0*(1.D0-R2))*DEXP(-2.2D0*R1)
C
C ... BUNDLE BYPASSING CORRECTION FACTOR
C
      FBP   = (DS-DOTL)*LBC/SM
      IF (RES.LE.1.D2) C1=1.35D0
      IF (RES.GT.1.D2) C1=1.25D0
      TERM  = DFLOAT(NSS)/NC
      IF (TERM.GE.0.5D0) GOTO 50
      IF (NSS.EQ.0) C2=0.D0
      IF (NSS.NE.0) C2=2.D0*(TERM**R1O3)
      PHIB  = DEXP(-C1*(1-C2)*FBP)
      GOTO 60
50    PHIB  = 1.D0
60    NB    = 1.D3*L/LBC-1
C
C ... ADVERSE TEMPERATURE GRADIENT BUILD-UP CORRECTION FACTOR
C
      IF (RES.GE.100.D0) GOTO 70
      NCW   = 0.81D0*LC/PP
      PHIRS = 1.51D0/((NC+NCW)*(DFLOAT(NB)+1.D0))**0.18D0
      IF (RES.LT.20.D0) PHIR=PHIRS
      IF (RES.GE.20.D0.AND.RES.LE.1.D2) PHIR=PHIRS-
     &                          (1.D0-PHIRS)*(0.25D0-0.0125D0*RES)
      IF (PHIR.LE.0.4D0) PHIR=PHIRS
      GOTO 80
70    PHIR  = 1.D0
C
C ... UNEQUAL INLET/OUTLET BAFFLE SPACING CORRECTION
C
80    AN    = 0.333D0
      IF (RES.GT.1.D2) AN=0.6D0
      PHIS  = ((DFLOAT(NB)-1.D0)+(LBIN/LBC)**(1.D0-AN)+(LBOUT/LBC)**
     &     (1.D0-AN))/(DFLOAT(NB)-1.D0+(LBIN+LBOUT)/LBC)
```

```
      HSHELL= HSI*PHIC*PHIL*PHIB*PHIR*PHIS
C...
      RETURN
      END
C...
C     ------------------------------------------------------
      FUNCTION DPSHEL (D,DS,L,LBC,LBIN,LBOUT,LC,DOTL,DSB,PT,
     &                 NT,NSS,W,RHO,VISC,PHI,LAYOUT,PI,R103)
C     ------------------------------------------------------
C
C     SUBPROGRAM CALCULATES THE SHELL-SIDE PRESSURE DROP
C     IN A SHELL AND TUBE EXCHANGER FOR SINGLE PHASE FLOW
C     D - TUBE OUTSIDE DIAMETER, MM
C     DS - SHELL INSIDE DIAMETER, MM
C     L - TUBE LENGTH, M
C     LBC - CENTRAL BAFFLE SPACING, MM
C     LBIN - INLET BAFFLE SPACING, MM
C     LBOUT - OUTLET BAFFLE SPACING, MM
C     LC - BAFFLE CUT, MM
C     DOTL - SHELL OUTER TUBE LIMIT, MM
C     DSB - DIAMETER SHELL-BAFFLE CLEARANCE, MM
C     PT - TUBE PITCH, MM
C     NT - TOTAL NUMBER OF TUBES IN THE BUNDLE
C     NSS - NUMBER PAIRS OF SEALING STRIPS
C     W - FLOW RATE IN SHELL, KG/s
C     VISC - FLUID VISCOSITY, N.s/M**2
C     PHI - VISCOSITY CORRECTION FACTOR
C     RHO - FLUID DENSITY, KG/M**3
C     LAYOUT - FLAG FOR TYPE OF TUBE LAYOUT
C            = 1 TRIANGULAR
C            = 2 IN-LINE SQUARE
C            = 3 ROTATED SQUARE
C
      IMPLICIT REAL*8 (A-H,O-Z)
      REAL*8 L,LBC,LC,NCW,NC,LBIN,LBOUT
C...
      DIMENSION B1(5,3),B2(5,3),B3(3),B4(3)
      DATA B1 /0.372,0.486,4.57,45.1,48.0,0.391,0.0815,6.09,
     &         32.1,35.0,0.303,0.333,3.5,26.2,32.0/,
     &     B2 /-0.123,-0.152,-0.476,-0.973,-1.,-0.148,0.022,
     &         -0.602,-0.963,-1.,-0.126,-0.136,-0.476,-0.913,-1./,
     &     B3 /7.0,6.3,6.59/, B4 /0.5,0.378,0.52/
C...
      PRATIO= PT/D
      GOTO (10,20,30),LAYOUT
10    PP    = (DSQRT(3.D0)/2.D0)*PT
      PN    = PT*0.5D0
      GOTO 40
20    PP    = PT
      PN    = PT
      GOTO 40
30    PP    = PT/DSQRT(2.D0)
      PN    = PP
C
C ... CALCULATE IDEAL TUBE-BANK FRICTION FACTOR
C
40    NC    = DS*(1.D0-2.D0*LC/DS)/PP
      IF (LAYOUT.EQ.1) PD=PT
      IF (LAYOUT.GT.1) PD=PN
```

```
      SM    = LBC*(DS-DOTL+(PT-D)*(DOTL-D)/PD)
      RES   = D*W*1.D3/(VISC*SM)
      IF (RES.GE.1.D4) J=1
      IF (RES.GE.1.D3.AND.RES.LT.1.D4) J=2
      IF (RES.GE.1.D2.AND.RES.LT.1.D3) J=3
      IF (RES.GE.1.D1.AND.RES.LT.1.D2) J=4
      IF (RES.LT.1.D1) J=5
      B     = B3(LAYOUT)/(1.D0+0.14D0*RES**B4(LAYOUT))
      FJ    = B1(J,LAYOUT)*(1.33D0/PRATIO)**B*RES**B2(J,LAYOUT)
      DPBI  = 2.D0*FJ*NC*(W/(SM*1.D-6))**2/(RHO*PHI)
C
C ... PRESSURE DROP FOR AN IDEAL WINDOW SECTION
C
      TERM  = (DS-2.D0*LC)/DOTL
      TERM1 = DACOS(TERM)
      FTC   = (PI+2.D0*TERM*DSIN(TERM1)-2.D0*TERM1)/PI
      TERM2 = 1.D0-2.D0*LC/DS
      SW    = (DS**2/4.D0)*(DACOS(TERM2)-TERM2*DSQRT(1.D0-TERM2**2))
     &                          -DFLOAT(NT)/8.D0*(1.D0-FTC)*PI*D**2
      DW    = 4.D0*SW/((PI/2.D0)*DFLOAT(NT)*(1.D0-FTC)*D+2.D0*DS*
     &                                              DACOS(TERM2))
      NCW   = 0.81D0*LC/PP
      GW    = (W**2)*1.D6/DSQRT(SM*SW)
      IF (RES.LE.1.D2) DPW=(0.026D0*VISC*(NCW/(PT-D)+
     &                      LBC/DW**2)+1.D0)*GW/RHO
      IF (RES.GT.1.D2) DPW=0.5D0*GW*(2.D0+0.6D0*NCW)/RHO
C
C ... CORRECTION FOR BAFFLE LEAKAGE EFFECT
C
      STB   = 15.80642D0*D*(1.D0+FTC)*DFLOAT(NT)
      SSB   = DS*DSB*0.5D0*(PI-DACOS(TERM2))
      R1    = (STB+SSB)/SM
      R2    = SSB/(SSB+STB)
      P     = -0.15D0*(1.D0+R2)+0.8D0
      RL    = DEXP(-1.33D0*(1.D0+R2)*R1**P)
C
C ... CORRECTION FOR BUNDLE BYPASS EFFECTC
C
      FBP   = (DS-DOTL)*LBC/SM
      IF (RES.LE.1.D2) C1=4.5D0
      IF (RES.GT.1.D2) C1=3.7D0
      TERM  = DFLOAT(NSS)/NC
      IF (TERM.GE.0.5D0) GOTO 50
      IF (NSS.EQ.0) C2=0.D0
      IF (NSS.NE.0) C2=2.D0*(TERM**R1O3)
      RB    = DEXP(-C1*(1-C2)*FBP)
      GOTO 60
50    RB    = 1.D0
C
C ... CORRECTION FOR UNEQUAL BAFFLE SPACING AT INLET/OUTLET
C
60    NB    = 1.D3*L/LBC-1
      AN    = 1.D0
      IF (RES.GT.100.D0) AN=0.2D0
      RS    = (LBIN/LBC)**(2.D0-AN)+(LBOUT/LBC)**(2.D0-AN)
```

```
C
C ... CALCULATE SHELL SIDE PRESSURE DROP
C
      DPSHEL= RB*DPBI*((DFLOAT(NB)-1.D0)*RL+
     &                      (1.D0+NCW/NC)*RS)+DFLOAT(NB)*RL*DPW
C...
      RETURN
      END
C
C     ------------------------------------
      FUNCTION VISCOS (VISC,TREF,T,ISTATE)
C     ------------------------------------
C
C     SUBPROGRAM EVALUATES VISCOCITY AT TEMPERATURE T FROM
C     VISCOSITIES AT TWO REFERENCE TEMPERATURES
C     TREF - REFERENCE TEMPERATURE VECTOR, K
C     VISC - REFERENCE VISCOSITY FACTOR, Ns/M2
C     T - TEMPERATURE AT WHICH VISCOSITY IS REQUIRED
C     ISTATE - FLAG FOR STATE OF FLUID
C            = 1 LIQUID (VISCOS=A*DEXP(B/T))
C            = 2 GAS (VISCOS=A+BT)
C
      IMPLICIT REAL*8 (A-H,O-Z)
      DIMENSION TREF(2),VISC(2),RHO(2),CP(2),XK(2)
C...
      IF (ISTATE.EQ.1) VISCOS=VISC(1)*DEXP(TREF(2)*(TREF(1)-T)/
     &                 (T*TREF(1)-TREF(2))*DLOG(VISC(2)/VISC(1)))
      IF (ISTATE.EQ.2) VISCOS=(VISC(2)*TREF(1)-VISC(1)*TREF(2)+
     &                 T*(VISC(1)-VISC(2)))/(TREF(1)-TREF(2))
C...
      RETURN
C
C     ------------------------
      ENTRY THCOND (XK,TREF,T)
C     ------------------------
C
C     EVALUATE THERMAL CONDUCTIVITY FROM VALUES AT TWO
C     REFERENCE TEMPERATURES
C     THCOND = A+B*T
C     XK - REFERENCE THERMAL CONDUCTIVITY VECTOR, W/M K
C
      THCOND = (XK(2)*TREF(1)-XK(1)*TREF(2)+T*(XK(1)
     &                                    -XK(2)))/(TREF(1)-TREF(2))
C...
      RETURN
C
C     ------------------------
      ENTRY SPHEAT (CP,TREF,T)
C     ------------------------
C
C     EVALUATE HEAT CAPACITY OF A FLUID GIVEN THE
C     VALUES AT TWO REFERENCE TEMPERATURES
C     SPHEAT = A+B*T
C     CP - REFERENCE HEAT CAPACITY VECTOR, J/KG K
C
      SPHEAT = (CP(2)*TREF(1)-CP(1)*TREF(2)+T*(CP(1)-CP(2)))
     &       /(TREF(1)-TREF(2))
C...
      RETURN
```

```
C
C     --------------------------------
      ENTRY DENSTY (RHO,TREF,T,ISTATE)
C     --------------------------------
C
C     EVALUATE DENSITY OF A FLUID AT TEMPERATURE T, GIVEN THE
C     DENSITY AT TWO REFERENCE TEMPERATURES
C     A SINGLE REFERENCE POINT IS ADEQUATE FOR GAS DENSITY
C     RHO - REFERENCE DENSITY VECTOR, KG/M3
C     ISTATE - FLAG FOR STATE OF FLUID
C            = 1 LIQUID (DENSTY=A+B*T)
C            = 2 GAS (DENSTY=A/T)
C
      GOTO (10,20),ISTATE
C...
10    DENSTY  = (RHO(2)*TREF(1)-RHO(1)*TREF(2)+T*(RHO(1)
     &                                   -RHO(2)))/(TREF(1)-TREF(2))
C...
      RETURN
C...
20    DENSTY  = RHO(1)*TREF(1)/T
      IF (DENSTY.EQ.0.D0) DENSTY=RHO(2)*TREF(2)/T
C...
      RETURN
      END
```

APPENDIX B

Listing of the Heat-Exchanger Network Static Optimization Program.

```
C ********************************************************************** C
C             HEAT-EXCHANGER NETWORK FLEXIBILITY ANALYSIS                C
C                        WITH BYPASS FRACTIONS                           C
C                     ANALYTICAL SOLUTION PROFILE                        C
C *  S. Ugur Akman                                    March 14, 1995 *  C
C ********************************************************************** C
      IMPLICIT REAL*8 (A-H,O-Z)
C
      PARAMETER (NDV = 6, NCON = 8, IGRAD = 0, NDVP=(NDV+1))
      PARAMETER (NRA = 10, NCOLA = 10, NRWK = 500, NRIWK = 250)
C
      PARAMETER (NRPT = 1)
C
      DIMENSION X(NDVP),VLB(NDVP),VUB(NDVP),G(NCON),IDG(NCON),
     &          IC(NRA),DF(NDVP),A(NRA,NCOLA),WK(NRWK),IWK(NRIWK)
C
      NO=6
      OPEN(NO,FILE='UHAOPT-0.OUT')
C
C ---------------------------------------------------------------------- C
C
C Initial guesses for decision variables (bypass fractions)
      DO 135 I=1,NDV
         X(I) = 0.D0
  135 CONTINUE
C
C Lower & upper bounds on decision variables
      DO 235 I=1,NDV
         VLB(I) = 0.D0
         VUB(I) = 0.995D0
  235 CONTINUE
C
C Constraint types ( g < 0 : nonlinear inequality constraints )
      DO 245 I=1,NCON
         IDG(I) = 0
  245 CONTINUE
C
C
```

```
C ADS Optimizer Options
      ISTRAT = 3
      IOPT   = 3
      IONED  = 3
      IPRINT = 2200
C
C
      DO 5000 K = 1 , NRPT
C
      INFO = -2
C     ----------------------------------------------------------------
      CALL ADS (INFO,ISTRAT,IOPT,IONED,IPRINT,IGRAD,NDV,NCON,X,VLB,VUB,
     &          OBJ,G,IDG,NAC,IC,DF,A,NRA,NCOLA,WK,NRWK,IWK,NRIWK)
C     ----------------------------------------------------------------
      WK( 3) = -1.D-5
      WK( 6) = 1.D-5
      WK( 8) = 1.D-10
      WK( 9) = 1.D-8
      WK(10) = 1.D-10
      WK(12) = 1.D-8
      WK(13) = 1.D-4
      WK(14) = 1.D-5
      WK(21) = 1.D-4
      WK(28) = 1.D+12
      WK(30) = 1.D-12
      WK(37) = 1.D-12
      IWK(3) = 100
      IWK(4) = 3
      IWK(5) = 3
      IWK(7) = 100
C
C     ----------------------------------------------------------------
1000  CALL ADS (INFO,ISTRAT,IOPT,IONED,IPRINT,IGRAD,NDV,NCON,X,VLB,VUB,
     &          OBJ,G,IDG,NAC,IC,DF,A,NRA,NCOLA,WK,NRWK,IWK,NRIWK)
C     ----------------------------------------------------------------
C
      IF (INFO.EQ.0) GOTO 2000
C
C ---------------------------------------------------------------------- C
C
C        ---------------------------------
         CALL HEN (X, G, OBJ, NDV, NCON, NO, 0)
C        ---------------------------------
C
         GOTO 1000
C
2000  CONTINUE
C
C ---------------------------------------------------------------------- C
C
C     ---------------------------------
      CALL HEN (X, G, OBJ, NDV, NCON, NO, 1)
C     ---------------------------------
C
C
      WRITE(6,991) OBJ
      WRITE(6,992) (X(I),I=1,NDV)
      WRITE(6,993) (G(I),I=1,NCON)
```

```
991   FORMAT(//,' O P T I M U M :',/,26('-'),//,' OBJ   =',E18.10)
992   FORMAT(/,' X(I)  =',/,(8X,(3E18.10)))
993   FORMAT(/,' G(I)  =',/,(8X,(3E18.10)))
C
C
      IF (K.NE.NRPT) THEN
         DO 635 I=1,NDV
            X(I) = X(I) + 0.01D0
  635    CONTINUE
      ENDIF
C
C
 5000 CONTINUE
C
      STOP
      END
C
C ******************************************************* C
      SUBROUTINE HEN (X, G, OBJ, NDV, NCON, NO, IOPT)
C ******************************************************* C
C ********************************************************************** C
C *  S. Ugur Akman                                        March 17, 1995 * C
C *                                                                      * C
C *         H E A T  -  E X C H A N G E R     N E T W O R K              * C
C *                                                                      * C
C ********************************************************************** C
C**********************************************************************C
C
      IMPLICIT REAL*8 (A-H,O-Z)
C
      PARAMETER (NHEX=3)
C
      DIMENSION WH(NHEX),WC(NHEX),U(NHEX),UA(NHEX),AHEX0(NHEX),
     & THI0(NHEX),TCI0(NHEX),THI(NHEX),TCI(NHEX),THO0(NHEX),TCO0(NHEX),
     & THO(NHEX),TCO(NHEX),THT0(NHEX),TCT0(NHEX),THT(NHEX),TCT(NHEX),
     & RH0(NHEX),RC0(NHEX),RH(NHEX),RC(NHEX),DTLM0(NHEX),DTLM(NHEX),
     & DRH(NHEX),DRC(NHEX),Q(NHEX),QH(NHEX),QC(NHEX)
      DIMENSION X(NDV),G(NCON)
C
C
      IF (ICALL.EQ.1) GOTO 10000
C
C Minimum Approach Temperature (reasonable value must be zero)
      DTMIN = 0.D0
C
C Input Overall Heat-Transfer Coefficients of HEXs
      U(1)  = 1000.D0
      U(2)  = 1000.D0
      U(3)  = 1000.D0
C
C Input Heat-Capacity-Flowrates of Streams in HEXs
      WH(1) = 1500.D0
      WC(1) = 2000.D0
      WH(2) = 1000.D0
      WC(2) = 2000.D0
      WH(3) = 1000.D0
      WC(3) = 3000.D0
C
```

```
C Nominal Supply (source-stream) Temperatures to HEN (before upset)
      THI0(1) = 620.D0
      TCI0(1) = 388.D0
      THI0(2) = 583.D0
      TCI0(3) = 313.D0
C
C Nominal Intermediate (interconnection) Temperatures of HEN (before upset)
      TCI0(2) = 553.D0
      THI0(3) = 563.D0
C
C Nominal Bypass Openings (bypass fraction)
      RH0(1) = 0.0D0
      RH0(2) = 0.0D0
      RH0(3) = 0.0D0
      RC0(1) = 0.0D0
      RC0(2) = 0.0D0
      RC0(3) = 0.0D0
C
C Nominal Outlet (target) Temperatures from HEXs (before upset)
      THO0(1) = 400.D0
      TCO0(1) = TCI0(2)
      THO0(2) = THI0(3)
      TCO0(2) = 563.D0
      THO0(3) = 323.D0
      TCO0(3) = 393.D0
C
      WRITE(NO,3330)
 3330 FORMAT(/////)
      DO 3 J=1,NHEX
         WRITE(NO,8000) J,THI0(J),J,THO0(J),J,TCO0(J),J,TCI0(J)
    3 CONTINUE
 8000 FORMAT(' THI0(',I1,') =',F10.4,5X,' THO0(',I1,') =',F10.4,/,
     &       ' TCO0(',I1,') =',F10.4,5X,' TCI0(',I1,') =',F10.4,/)
C
C Calculate Nominal Log-Mean Temperature Difference of HEXs (before upset)
      WRITE(NO,*) ' '
      DO 4 J=1,NHEX
         DTLM0(J) = ((THI0(J)-TCO0(J))-(THO0(J)-TCI0(J)))
     &            / DLOG((THI0(J)-TCO0(J))/(THO0(J)-TCI0(J)))
         WRITE(NO,9002) J,DTLM0(J)
    4 CONTINUE
 9002 FORMAT(' DTLM0(',I1,') =',F10.6)
C
C Calculate Nominal Areas of HEXs
      WRITE(NO,*) ' '
      DO 6 J=1,NHEX
         AHEX0(J) = (WH(J)*(THI0(J)-THO0(J)))/(U(J)*DTLM0(J))
         UA(J) = U(J)*AHEX0(J)
         WRITE(NO,9004) J,AHEX0(J)
    6 CONTINUE
 9004 FORMAT(' AHEX0(',I1,') =',F10.6)
C
```

```
C Calculate Nominal Temperatures of HEX Outlets (before bypass mixing)
C & Targets (after bypass mixing) (from Analytical Solution Profile)
      DO 725 J=1,NHEX
         VHR=WH(J)*(1.D0-RH0(J))
         VCR=WC(J)*(1.D0-RC0(J))
      IF(J.EQ.2) TCI0(2)=TCT0(1)
      IF(J.EQ.3) THI0(3)=THT0(2)
C     ------------------------------------------------------------
      CALL STST (J,VHR,VCR,UA(J),THI0(J),TCI0(J),THO0,TCO0,NHEX)
C     ------------------------------------------------------------
C     ------------------------------------------------------
      CALL MIX (J,RH0,RC0,THI0,TCI0,THO0,TCO0,THT0,TCT0,NHEX)
C     ------------------------------------------------------
  725 CONTINUE
C
      WRITE(NO,3100)
 3100 FORMAT(//,
     &' Nominal Temperatures of HEX Outlets (before bypass mixing) &',/,
     &' Targets (after bypass mixing) (Analytical Solution Profile)',/,
     &' (Before Disturbance)',/)
      DO 1725 J=1,NHEX
         WRITE(NO,3110) J,THO0(J),J,TCO0(J),J,THT0(J),J,TCT0(J)
 1725 CONTINUE
 3110 FORMAT(' THO0(',I1,') =',F10.4,5X,' TCO0(',I1,') =',F10.4,/,
     &       ' THT0(',I1,') =',F10.4,5X,' TCT0(',I1,') =',F10.4,/)
      WRITE(NO,3340)
 3340 FORMAT(/////)
C
C ------------------------------------------------------------------ C
C
C Input Source-Temperature (input) Disturbances
      write(*,*) ' '
      write(*,*) ' Enter Disturbance +/- d[THI(1)] [THI0(1)=620]'
      read(*,*) DTHI1
      write(*,*) ' Enter Disturbance +/- d[THI(2)] [THI0(2)=583]'
      read(*,*) DTHI2
      write(*,*) ' Enter Disturbance +/- d[TCI(1)] [TCI0(1)=388]'
      read(*,*) DTCI1
      write(*,*) ' Enter Disturbance +/- d[TCI(3)] [TCI0(3)=313]'
      read(*,*) DTCI3
      THI(1) = THI0(1) + DTHI1
      TCI(1) = TCI0(1) + DTCI1
      THI(2) = THI0(2) + DTHI2
      TCI(3) = TCI0(3) + DTCI3
C
C
C Input Control Ranges for Target-Stream Temperatures of HEN
      write(*,*) ' '
      write(*,*) ' Enter +/- Control Range for H-1 Target Temperature'
      read(*,*) TRNGH1
      write(*,*) ' Enter +/- Control Range for H-3 Target Temperature'
      read(*,*) TRNGH3
      write(*,*) ' Enter +/- Control Range for C-2 Target Temperature'
      read(*,*) TRNGC2
      write(*,*) ' Enter +/- Control Range for C-3 Target Temperature'
      read(*,*) TRNGC3
C
10000 CONTINUE
```

```
C
C ------------------------------------------------------------------ C
C
C Assign current optimal values of bypass fractions (from optimizer)
      RH(1) = X(1)
      RH(2) = X(2)
      RH(3) = X(3)
      RC(1) = X(4)
      RC(2) = X(5)
      RC(3) = X(6)
C
C
C Calculate Final Temperatures of HEX Outlets (before bypass mixing)
C & Targets (after bypass mixing) (from Analytical Solution Profile)
      DO 925 J=1,NHEX
         VHR=WH(J)*(1.D0-RH(J))
         VCR=WC(J)*(1.D0-RC(J))
      IF(J.EQ.2) TCI(2)=TCT(1)
      IF(J.EQ.3) THI(3)=THT(2)
C     ------------------------------------------------------
      CALL STST (J,VHR,VCR,UA(J),THI(J),TCI(J),THO,TCO,NHEX)
C     ------------------------------------------------------
C     ------------------------------------------------
      CALL MIX (J,RH,RC,THI,TCI,THO,TCO,THT,TCT,NHEX)
C     ------------------------------------------------
  925 CONTINUE
C
      IF (IOPT.EQ.0) GOTO 10100
C
      WRITE(NO,3200)
 3200 FORMAT(/////,
     &' (After Disturbance) Temperatures of HEXs :',/,
     &' Inlets                          THI(J) & TCI(J) :',/,
     &' Outlets (before bypass mixing) THO(J) & TCO(J) :',/,
     &' Targets (after  bypass mixing) THT(J) & TCT(J) :',/,
     &' (Analytical Solution Profile)',/)
      DO 1825 J=1,NHEX
         WRITE(NO,3210) J,THI(J),J,TCI(J),J,THO(J),J,TCO(J),
     &                  J,THT(J),J,TCT(J)
 1825 CONTINUE
 3210 FORMAT(' THI(',I1,') =',F10.4,5X,' TCI(',I1,') =',F10.4,/,
     &       ' THO(',I1,') =',F10.4,5X,' TCO(',I1,') =',F10.4,/,
     &       ' THT(',I1,') =',F10.4,5X,' TCT(',I1,') =',F10.4,/)
C
      WRITE(NO,1200) (THO0(J),J=1,NHEX),(TCO0(J),J=1,NHEX),
     &               (THT0(J),J=1,NHEX),(TCT0(J),J=1,NHEX)
 1200 FORMAT(//,
     &' Hot  Outlets before Upset (before bypass mixing):',/,3F10.4,//,
     &' Cold Outlets before Upset (before bypass mixing):',/,3F10.4,///,
     &' Hot  Outlets before Upset (after  bypass mixing):',/,3F10.4,//,
     &' Cold Outlets before Upset (after  bypass mixing):',/,3F10.4,/)
C
      WRITE(NO,1300) (THO(J),J=1,NHEX),(TCO(J),J=1,NHEX),
     &               (THT(J),J=1,NHEX),(TCT(J),J=1,NHEX)
 1300 FORMAT(//,
     &' Hot  Outlets after  Upset (before bypass mixing):',/,3F10.4,//,
     &' Cold Outlets after  Upset (before bypass mixing):',/,3F10.4,///,
     &' Hot  Outlets (targets) after Upset (after bypass mixing):',/,
```

```
     &  3F10.4,//,
     &' Cold Outlets (targets) after Upset (after bypass mixing):',/,
     &  3F10.4,/)
C
      WRITE(NO,1205) ((THO0(J)-THO(J)),J=1,NHEX),
     &               ((TCO0(J)-TCO(J)),J=1,NHEX)
 1205 FORMAT(//,
     &' Change (before-after upset) in Hot  Outlets',
     &' (before bypass mixing):',/,3F10.4,//,
     &' Change (before-after upset) in Cold Outlets',
     &' (before bypass mixing):',/,3F10.4,/)
C
      WRITE(NO,1215) ((THT0(J)-THT(J)),J=1,NHEX),
     &               ((TCT0(J)-TCT(J)),J=1,NHEX)
 1215 FORMAT(//,
     &' Change (before-after upset) in Hot  Targets:',/,3F10.4,//,
     &' Change (before-after upset) in Cold Targets:',/,3F10.4)
C
      WRITE(NO,645)
  645 FORMAT(////)
      DO 650 J=1,NHEX
         QH(J)   = WH(J)*(1.D0-RH(J))*(THI(J)-THO(J))
         QC(J)   = WC(J)*(1.D0-RC(J))*(TCO(J)-TCI(J))
         DTLM(J) = ((THI(J)-TCO(J))-(THO(J)-TCI(J)))
     &           / DLOG((THI(J)-TCO(J))/(THO(J)-TCI(J)))
         Q(J)    = UA(J)*DTLM(J)
         WRITE(NO,655) J,QH(J),J,QC(J),J,Q(J),J,DTLM(J)
  655 FORMAT(' QH(',I1,')=',F12.4,1X,' QC(',I1,')=',F12.4,1X,
     &       ' Q(',I1,')=',F12.4,1X,' DTLM(',I1,')=',F8.4)
  650 CONTINUE
C
      WRITE(NO,9645)
 9645 FORMAT(////)
C
      SUMRH=0.D0
      SUMRC=0.D0
      DO 9950 J=1,NHEX
         SUMRH = SUMRH + RH(J)
         SUMRC = SUMRC + RC(J)
         WRITE(NO,9980) J,RH(J),J,(WH(J)*RH(J)),J,RC(J),J,(WC(J)*RC(J))
 9950 CONTINUE
 9980 FORMAT(' RH(',I1,') =',F10.8,5X,'[WHRH(',I1,') =',F10.4,/,
     &       ' RC(',I1,') =',F10.8,5X,'[WCRC(',I1,') =',F10.4)
      WRITE(NO,9970) SUMRH,SUMRC,(SUMRH+SUMRC)
 9970 FORMAT(///,' SUM-RH = ',F10.6,/,' SUM-RC = ',F10.6,/,
     &           ' SUM-R  = ',F10.6)
C
C Evaluate to Check the Feasibility of the Implicit Constraints:
C Inequalities (Minimum Approach Temperature) Load Constraints ( g < 0 )
C Inequalities Disturbed-Input Load Constraints ( g < 0 )
      WRITE(NO,556)
  556 FORMAT(///,
     &' Check of the Feasibility of Implicit Constraints:',/,
     &'         Minimum-Approach Temperature Constraints:',/,
     &'            ( TCO(J)-THI(J)+DTMIN < 0 )',/,
     &'            ( TCI(J)-THO(J)+DTMIN < 0 )',/,
     &'         Disturbed-Input Constraints:',/,
     &'                  ( TCI(J)-THI(J) < 0 )',/)
```

```
      DO 555 J=1,NHEX
         WRITE(NO,558) J,J,(TCO(J)-THI(J)+DTMIN),
     &                  J,J,(TCI(J)-THO(J)+DTMIN),J,J,(TCI(J)-THI(J))
  555 CONTINUE
  558 FORMAT(' [TCO(',I1,')-THI(',I1,')+DTMIN < 0] :',F12.6,/,
     &       ' [TCI(',I1,')-THO(',I1,')+DTMIN < 0] :',F12.6,/,
     &       ' [TCI(',I1,')-THI(',I1,')       < 0] :',F12.6,/)
C
10100 CONTINUE
C
C ------------------------------------------------------------------- C
C
C Evaluate Inequality (Control Range) Constraints ( g < 0 )
      G(1) = THT(1)-(THT0(1)+TRNGH1)
      G(2) = (THT0(1)-TRNGH1)-THT(1)
      G(3) = TCT(2)-(TCT0(2)+TRNGC2)
      G(4) = (TCT0(2)-TRNGC2)-TCT(2)
      G(5) = THT(3)-(THT0(3)+TRNGH3)
      G(6) = (THT0(3)-TRNGH3)-THT(3)
      G(7) = TCT(3)-(TCT0(3)+TRNGC3)
      G(8) = (TCT0(3)-TRNGC3)-TCT(3)
C
C
C Evaluate the Objective Function
C
C      SUMRH = + RH(1) + RH(2) + RH(3)
C      SUMRC = + RC(1) + RC(2) + RC(3)
C
C      OBJ =
C     &     + SUMRH
C     &     + SUMRC
C
C
C      OBJ =
C     &     + DABS(THT(1)-THT0(1))
C     &     + DABS(TCT(2)-TCT0(2))
C     &     + DABS(THT(3)-THT0(3))
C     &     + DABS(TCT(3)-TCT0(3))
C
      OBJ =
     &     + (THT(1)-THT0(1))**2
     &     + (TCT(2)-TCT0(2))**2
     &     + (THT(3)-THT0(3))**2
     &     + (TCT(3)-TCT0(3))**2
C
C
      ICALL=1
C
      RETURN
      END
C
```

```
C ********************************************************** C
      SUBROUTINE STST (JHEX,WH,WC,UA,TH0,TC0,TH,TC,NHEX)
C ********************************************************** C
      IMPLICIT REAL*8 (A-H,O-Z)
C
      DIMENSION TH(NHEX),TC(NHEX)
C
      R=UA/WC-UA/WH
      RW=WH/WC
      EXPR=DEXP(R)
      RAT=(TC0-RW*TH0*EXPR)/(1.D0-RW*EXPR)
      TH(JHEX)=TH0*EXPR+RAT*(1.D0-EXPR)
      TC(JHEX)=RW*TH0+RAT*(1.D0-RW)
C
      RETURN
      END
C
C ********************************************************** C
      SUBROUTINE MIX (J,RH,RC,TH0,TC0,TH,TC,THT,TCT,NHEX)
C ********************************************************** C
      IMPLICIT REAL*8 (A-H,O-Z)
C
      DIMENSION RH(NHEX),RC(NHEX),
     & TH0(NHEX),TH(NHEX),THT(NHEX),TC0(NHEX),TC(NHEX),TCT(NHEX)
C
      THT(J)=TH0(J)*RH(J)+TH(J)*(1.D0-RH(J))
      TCT(J)=TC0(J)*RC(J)+TC(J)*(1.D0-RC(J))
C
      RETURN
      END
```

APPENDIX C

Listing of the Program for Open-Loop Control of Heat-Exchanger Network.

```
C*************************************************************************C
C ********************************************************************** C
C *  S. Uğur Akman - Cantürk Boyacı   Oct. 26, 1992 - Sept. 20, 1995 * C
C *                                                                    * C
C *                    H E A T  -  E X C H A N G E R                   * C
C *                          OPEN-LOOP CONTROL                         * C
C *                    [Solution by Finite Differences]                * C
C ********************************************************************** C
C*************************************************************************C
C
C
C        ACH     : INNER CROSSECTIONAL AREA OF A SINGLE TUBE, m^2
C        ACC     : TOTAL CROSSECTIONAL AREA OF THE SHELL, m^2
C
C        AH      : INNER SURFACE AREA OF A SINGLE TUBE/LENGTH, m^2
C        AC      : OUTER SURFACE AREA OF A SINGLE TUBE/LENGTH, m^2
C        AS      : INNER SURFACE AREA OF THE SHELL/LENGTH, m^2
C
C        VH      : VELOCITY OF THE TUBE-SIDE, m/sec
C        VC      : VELOCITY OF THE SHELL-SIDE, m/sec
C
C        TWA     : CROSSECTIONAL TUBE WALL AREA, m^2
C        SWA     : CROSSECTIONAL SHELL WALL AREA, m^2
C
C        HI      : INSIDE HEAT TRANSFER COEFFICIENT
C        HO      : OUTSIDE HEAT TRANSFER COEFFICIENT
C        HS      : SHELL-WALL HEAT TRANSFER COEFFICIENT
C
C        RHOT    : DENSITY OF TUBE & SHELL WALL METAL (STEEL)
C        CPT     : CP OF TUBE & SHELL WALL METAL (STEEL)
C
C...
      IMPLICIT REAL*8 (A-H,O-Z)
C...
      PARAMETER (NHEX=3, NZ=51, NODE=(NHEX*(4*NZ+2)))
      PARAMETER (LRW=50000, LIW=30)
C...
      DIMENSION UU(NODE),DUU(NODE),RWORK(LRW),IWORK(LIW)
      EXTERNAL PDE,JACPDE
C...
      NI=5
      NO=6
```

```
      NOT=8
      NOE=10
      OPEN(NO,FILE='GENERAL.OUT')
      OPEN(NOT,FILE='DEVIATION.OUT')
      OPEN(NOE,FILE='ERROR.OUT')
C...
C...
C   Read the Input Parameters for LSODES
C ---------------------------------------
      TIME0  =    0.0D0
      TSTOP  =  300.0D0
      TPRINT =    0.5D0
C...
C   Set the Optional Input Parameters of LSODES
C ---------------------------------------------
      MF     = 222
      RTOL   = 1.D-05
      ATOL   = 1.D-06
      H0     = 1.D-04
C...
      ITOL   = 1
      ITASK  = 4
      ISTATE = 1
      IOPT   = 1
      IWORK(6) = 5000
      RWORK(5) = H0
C...
      TIME=TIME0
C...
      WRITE(NO,801) TIME0,TSTOP,TPRINT,RTOL,ATOL,NODE
C...
C   Initialize the Vector of Dependent Variables
C ---------------------------------------------
C     ----------------------------------------
      CALL INITIAL (NODE, TIME, UU, DUU, NI, NO)
C     ----------------------------------------
C...
      TOUT=TIME0
C...
 1000 CONTINUE
C...
      RWORK(1)=TOUT
C...
C   Call the IVP Solver (LSODES) to Integrate Between TIME & TOUT
C ------------------------------------------------------------
C     ------------------------------------------------------------------
      CALL LSODES (PDE, NODE, UU, TIME, TOUT, ITOL, RTOL, ATOL, ITASK,
     &             ISTATE, IOPT, RWORK, LRW, IWORK, LIW, JACPDE ,MF)
C     ------------------------------------------------------------------
C...
C   Print the Results at the End of the Integration Interval
C -------------------------------------------------------
C     -------------------------------------------------------
      CALL PRINT (UU, TIME, TIME0, TSTOP, TPRINT, NI, NO, NOT, NOE)
C     -------------------------------------------------------
C...
```

```
C   Stop if Error is Reported by LSODES
C -------------------------------------
      IF (ISTATE.LT.0) THEN
         WRITE(NO,9999) ISTATE
         GO TO 3000
      ENDIF
C...
C   Call LSODES Again for the New Interval of Integration
C -------------------------------------------------------
      IF (TIME.GE.TSTOP) GO TO 2000
      TOUT=TOUT+TPRINT
      GO TO 1000
C...
 2000 CONTINUE
C...
      WRITE(NO,900)
      WRITE(NO,901) IWORK(11)
      WRITE(NO,902) IWORK(12)
      WRITE(NO,903) IWORK(13)
      WRITE(NO,904) IWORK(19)
      WRITE(NO,905) IWORK(20)
      WRITE(NO,906) IWORK(21)
      WRITE(NO,907) IWORK(17),IWORK(18)
C...
  801 FORMAT(///,10X,'Input-Parameters for LSODES',/,10X,52('='),//,
     &  10X,'Initial Value of Time ..... ',F10.2,/,
     &  10X,'Final Value of Time ........ ',F10.2,/,
     &  10X,'Print Interval of Time ..... ',F10.2,//,
     &  10X,'Relative Error Tolerance Parameter ..... ',1PE10.4,/,
     &  10X,'Absolute Error Tolerance Parameter ..... ',1PE10.4,//,
     &  10X,'Number of Ordinary Differential Equations ...  ',I4,/)
  900 FORMAT(1H1,////,10X,'Computational Statistics for  LSODES',/,
     &           10X,48('='),/)
  901 FORMAT(10X,'Number of Steps Taken ............ ',I8)
  902 FORMAT(10X,'Number of Function Evaluations ... ',I8)
  903 FORMAT(10X,'Number of Jacobian Evaluations ... ',I8,/)
  904 FORMAT(10X,'No. of Nonzero Elements in the Jacobian ... ',I4)
  905 FORMAT(10X,'No. of Extra Function Evaluations ',/,10X,
     &           '    Needed for Each Jacobian Evaluation ... ',I4)
  906 FORMAT(10X,'No. of Sparse LU Decompositions ........... ',I4,/)
  907 FORMAT(10X,'Required RWORK Size ... ',I5,/,10X,
     &           'Required IWORK Size ... ',I5,//)
 9999 FORMAT(///,' Error Halt... ISTATE =',I3,//)
C...
 3000 CONTINUE
C...
      STOP
      END
C...
C ******************************************************* C
      SUBROUTINE INITIAL (NODE, TIME, UU, DUU, NI, NO)
C ******************************************************* C
C...
      IMPLICIT REAL*8 (A-H,O-Z)
      REAL*8   L
C...
      PARAMETER (NHEX=3, NZ=51)
C...
      COMMON/U/ UTH(NHEX,NZ),UTC(NHEX,NZ),UTT(NHEX,NZ),UTS(NHEX,NZ)
```

```
      COMMON/PARAM/ L(NHEX), VH(NHEX), VC(NHEX), UH(NHEX), UC1(NHEX),
     &              UC2(NHEX),UT1(NHEX),UT2(NHEX),US(NHEX),TH0(NHEX),
     &              TC0(NHEX), UTH0(NHEX,NZ), UTC0(NHEX,NZ),
     &              UTT0(NHEX,NZ), UTS0(NHEX,NZ)
      COMMON/BYPASS/ RH(NHEX),RC(NHEX),RHO(NHEX),RCO(NHEX),to,
     &               THST(NHEX),TCST(NHEX),THUT(NHEX),TCUT(NHEX)
      DIMENSION UU(NODE),DUU(NODE),AH(NHEX),AC(NHEX),NT(NHEX),DS(NHEX),
     &          ACH(NHEX),ACC(NHEX),THI(NHEX),THO(NHEX),
     &          TCI(NHEX),TCO(NHEX),FH(NHEX),FC(NHEX),HI(NHEX),HO(NHEX),
     &          HS(NHEX),SWA(NHEX),AS(NHEX),TCH(NHEX),TCC(NHEX),
     &          TCT(NHEX),TICS(NHEX),TCCP(NHEX)
      COMMON/ASTST/ THS(NHEX,NZ),TCS(NHEX,NZ),
     &              THSU(NHEX,NZ),TCSU(NHEX,NZ),
     &              TTS(NHEX,NZ),TSS(NHEX,NZ),
     &              TTSU(NHEX,NZ),TSSU(NHEX,NZ), Z(NZ)
C...
C...
C   Read the Model Parameters
C ---------------------------
      THI(1)   =  620.D0
      THO(1)   =  385.D0
      TCI(1)   =  300.D0
      TCO(1)   =  417.5D0
      FH(1)    =  10000.D0
      FC(1)    =  20000.D0

      THI(2)   =  720.D0
      THO(2)   =  530.D0
      TCI(2)   =  417.5D0
      TCO(2)   =  560.D0
      FH(2)    =  15000.D0
      FC(2)    =  20000.D0

      THI(3)   =  530.D0
      THO(3)   =  410.D0
      TCI(3)   =  280.D0
      TCO(3)   =  340.D0
      FH(3)    =  15000.D0
      FC(3)    =  30000.D0

      RHOT     =  7833.78D0
      CPT      =  502.44D0

      DO 425 K=1,NHEX
C     ------------------------------------------------------------------
            CALL HEX (THI(K),THO(K),TCI(K),TCO(K),FH(K),FC(K),L(K),
     &                VH(K),VC(K),AH(K),AC(K),AS(K),ACH(K),ACC(K),
     &                NT(K),HO(K),HI(K),TWA,SWA(K),RHOT,CPT,TCH(K),
     &                TCC(K),TCT(K),TICS(K),TCCP(K),DS(K),K)
C     ------------------------------------------------------------------
            HO(K)   =  2000.D0
            HS(K)   =  2000.D0
            HI(K)   =  HO(K)*((AC(K))/AH(K))
C...
            WRITE(NO,*)'HEX #........> ',K
            WRITE(NO,*)'NT          : ',NT(K)
            WRITE(NO,*)'LENGTH      : ',L(K)
            WRITE(NO,*)'SHELL DIA.: ',DS(K)
            WRITE(NO,*)
```

```
            WRITE(NO,*)'VH         : ',VH(K)
            WRITE(NO,*)'VC         : ',VC(K)
            WRITE(NO,*)
            WRITE(NO,*)'AH , AH*L  : ',AH(K),AH(K)*L(K)
            WRITE(NO,*)'AC , AC*L  : ',AC(K),AC(K)*L(K)
            WRITE(NO,*)'AC*L*NT    : ',AC(K)*L(K)*NT(K)
            WRITE(NO,*)'AS , AS*L  : ',AS(K),AS(K)*L(K)
            WRITE(NO,*)
            WRITE(NO,*)'ACH        : ',ACH(K)
            WRITE(NO,*)'ACC        : ',ACC(K)
            WRITE(NO,*)
            WRITE(NO,*)'HI         : ',HI(K)
            WRITE(NO,*)'HO         : ',HO(K)
            WRITE(NO,*)'HS         : ',HS(K)
            WRITE(NO,*)
  425 CONTINUE
C...
      U     =   1000.0D0
      ROH   =   840.D0
      ROC   =   840.D0
      CPH   =   1046.7D0
      CPC   =   1046.7D0
C...
      RH(1) = 0.D0
      RH(2) = 0.D0
      RH(3) = 0.D0
      RC(1) = 0.D0
      RC(2) = 0.D0
      RC(3) = 0.D0
C...
      DO 2501 J=1,NHEX
         UH(J)  = HI(J)*AH(J)/(ROH*CPH*ACH(J))
         UC1(J) = HO(J)*AC(J)*NT(J)/(ROC*CPC*ACC(J))
         UC2(J) = HS(J)*AS(J)/(ROC*CPC*ACC(J))
         UT1(J) = HI(J)*AH(J)/(RHOT*CPT*TWA)
         UT2(J) = HO(J)*AC(J)/(RHOT*CPT*TWA)
         US(J)  = HS(J)*AS(J)/(RHOT*CPT*SWA(J))
         WRITE(NO,*) 'UH, UC1, UC2, UT1, UT2, US'
         WRITE(NO,*) J,UH(J),UC1(J),UC2(J),UT1(J),UT2(J),US(J)
2501  CONTINUE
C...
C...
C   Input Terminal (input) Temperatures
C -----------------------------------
      TH0(1) = 620.D0
      TC0(1) = 300.D0
      TH0(2) = 720.D0
      TC0(3) = 280.D0
C...
C...
      DO 825 I=1,NZ
         Z(I)=DFLOAT(I-1)/DFLOAT(NZ-1)
  825 CONTINUE
C...
C   Input Initial Temperature Profiles
C -----------------------------------
      WRITE(NO,1100)
 1100 FORMAT(///,' Steady-State Profiles before Upset :',/,38('-'),/)
C
```

```
      DO 725 J=1,NHEX
         VHR=VH(J)*(1.D0-RH(J))
         VCR=VC(J)*(1.D0-RC(J))
      IF(J.EQ.2) TC0(2)=TCST(1)
      IF(J.EQ.3) TH0(3)=THST(2)
C     ------------------------------------------------------------------
      CALL STST (J,L(J),Z,VHR,VCR,UH(J),UC1(J),UC2(J),UT1(J),UT2(J),
     &           US(J),TH0(J),TC0(J),THS,TCS,TTS,TSS,NO)
C     ------------------------------------------------------------------
C     ------------------------------------
      CALL MIXH (J,RH,TH0,THS,THST,NHEX,NZ)
      CALL MIXC (J,RC,TC0,TCS,TCST,NHEX,NZ)
C     ------------------------------------

      WRITE(NO,*) 'QH',J,(FH(J)*(TH0(J)-THS(J,NZ)))
      WRITE(NO,*) 'QC',J,(FC(J)*(TCS(J,1)-TC0(J)))

      DTLM=((TH0(J)-TCS(J,1))-(THS(J,NZ)-TC0(J)))
     &    /DLOG( (TH0(J)-TCS(J,1))/(THS(J,NZ)-TC0(J)) )
      WRITE(NO,*) 'DTLM',J,DTLM
      WRITE(NO,*) 'Q',U*AC(J)*L(J)*NT(J)*DTLM


  725 CONTINUE
C...
      WRITE(NO,3100)
 3100 FORMAT(///,' Target Temperatures before Upset :',/,36('-'),/)
      DO 1725 J=1,NHEX
         WRITE(NO,3110) J, THST(J), J, TCST(J)
 1725 CONTINUE
 3110 FORMAT(' THST(',I1,')',F10.4,5X,' TCST(',I1,')',F10.4)
C...
C...
      DO 35 J=1,NHEX
      DO 35 I=1,NZ
         UTH0(J,I)=THS(J,I)
         UTC0(J,I)=TCS(J,I)
         UTT0(J,I)=TTS(J,I)
         UTS0(J,I)=TSS(J,I)
   35 CONTINUE
C...
C...
C   Set the Initial Conditions (@ Time = 0, 0 < Z < L)
C -------------------------------------------------------
      DO 25 J=1,NHEX
      DO 25 I=1,NZ
         UTH(J,I)=UTH0(J,I)
         UTC(J,I)=UTC0(J,I)
         UTT(J,I)=UTT0(J,I)
         UTS(J,I)=UTS0(J,I)
   25 CONTINUE
C...
C...
C   Input Terminal (input) Disturbances
C -------------------------------------
      TH0(1) = TH0(1) + 0.D0
      TC0(1) = TC0(1) - 4.D0
      TH0(2) = TH0(2) + 0.D0
      TC0(3) = TC0(3) - 0.D0
```

```
C
C...
      RH(1) = 0.1991884263D-01
C      RH(1) = 0.D0
      RH(2) = 0.D0
      RH(3) = 0.D0
      RC(1) = 0.4684139883D-03
C      RC(1) = 0.D0
      RC(2) = 0.D0
      RC(3) = 0.5596164119D-01
C      RC(3) = 0.D0
C...
      DO 246 I=1,NHEX
         RHO(I)=RH(I)
         RCO(I)=RC(I)
  246 CONTINUE
C...
C   Calculate Final Temperature Profiles
C -------------------------------------
      WRITE(NO,1105)
 1105 FORMAT(///,' Steady-State Profiles after Upset  :',/,38('-'),/)
C
      DO 925 J=1,NHEX
         VHR=VH(J)*(1.D0-RH(J))
         VCR=VC(J)*(1.D0-RC(J))
      IF(J.EQ.2) TCO(2)=TCUT(1)
      IF(J.EQ.3) THO(3)=THUT(2)
C     ---------------------------------------
      CALL STST (J,L(J),Z,VHR,VCR,UH(J),UC1(J),UC2(J),UT1(J),
     &           UT2(J),US(J),THO(J),TCO(J),THSU,TCSU,TTSU,TSSU,NO)
C     ---------------------------------------
C     ---------------------------------------
      CALL MIXH (J,RH,THO,THSU,THUT,NHEX,NZ)
      CALL MIXC (J,RC,TCO,TCSU,TCUT,NHEX,NZ)
C     ---------------------------------------
  925 CONTINUE
C...
      WRITE(NO,3105)
 3105 FORMAT(///,' Target Temperatures after Upset  :',/,36('-'),/)
      DO 1925 J=1,NHEX
         WRITE(NO,3210) J, THUT(J), J, TCUT(J)
 1925 CONTINUE
 3210 FORMAT(' THUT(',I1,')',F10.4,5X,' TCUT(',I1,')',F10.4)
C...
      WRITE(NO,1200) (THS(J,NZ),J=1,NHEX),(TCS(J,1),J=1,NHEX),
     &               (THSU(J,NZ),J=1,NHEX),(TCSU(J,1),J=1,NHEX)
      WRITE(NO,1205) ((THS(J,NZ)-THSU(J,NZ)),J=1,NHEX),
     &               ((TCS(J,1)-TCSU(J,1)),J=1,NHEX)
 1200 FORMAT(//,' Hot  Stream Outputs at Steady State :',/,38('-'),
     &        /,3F10.4,//,
     &          ' Cold Stream Outputs at Steady State :',/,38('-'),
     &        /,3F10.4,///,
     &          ' Hot  Stream Outputs at Disturbance  :',/,38('-'),
     &        /,3F10.4,//,
     &          ' Cold Stream Outputs at Disturbance  :',/,38('-')
     &        /,3F10.4)
 1205 FORMAT(//,' Change in Hot  Stream Outputs       :',/,38('-'),
     &        /,3F10.4,//,
     &          ' Change in Cold Stream Outputs       :',/,38('-'),
```

```
     &        /,3F10.4,/)
C...
C   Transfer the Variables to the Vector of Dependent Variables in
LSODES
C -------------------------------------------------------------------
--
      DO 215 J=1,NHEX
         K=(4*(J-1)*NZ)
      DO 200 I=1,NZ
         UU(K+I) = UTH(J,I)
         UU(K+I+NZ) = UTC(J,I)
         UU(K+I+NZ+NZ) = UTT(J,I)
         UU(K+I+NZ+NZ+NZ) = UTS(J,I)
  200 CONTINUE
         UU((4*NHEX*NZ)+J) = 0.D0
         UU((4*NHEX*NZ+NHEX)+J) = 0.D0
  215 CONTINUE
C...
C     ------------------------------
      CALL PDE (NODE, TIME, UU, DUU)
C     ------------------------------
C...
C   Set the Vector of Temporal Derivatives in LSODES to Zero
C ------------------------------------------------------------
      DO 225 I=1,NODE
         DUU(I)=0.D0
  225 CONTINUE
C...
      RETURN
      END
C...
C ********************************************************************* C
      SUBROUTINE STST (JHEX,L,Z,VH,VC,UH,UC1,UC2,UT1,
     &                 UT2,US,TH0,TC0,THS,TCS,TTS,TSS,NO)
C ********************************************************************* C
      IMPLICIT REAL*8 (A-H,O-Z)
      REAL*8   L
C...
      PARAMETER (NHEX=3, NZ=51)
C
      DIMENSION THS(NHEX,NZ),TCS(NHEX,NZ),TTS(NHEX,NZ),TSS(NHEX,NZ),
     &          Z(NZ)
C...
      WRITE(NO,990) JHEX
C
      UHA=UH*UT2/(UT1+UT2)
      UCA=UC1*UT1/(UT1+UT2)
      RM=UCA/VC-UHA/VH
      A=(TC0-(VH/VC)*(UCA/UHA)*TH0*DEXP(RM*L))/
     &  (1.D0-(VH/VC)*(UCA/UHA)*DEXP(RM*L))
      DO 10 I=1,NZ
         ZL=Z(I)*L
         THS(JHEX,I)=TH0*DEXP(RM*ZL)+A*(1.D0-DEXP(RM*ZL))
         TCS(JHEX,I)=((VH*UCA)/(VC*UHA))*TH0*DEXP(RM*ZL)
     &              +A*(1.D0-((VH*UCA)/(VC*UHA))*DEXP(RM*ZL))
         TTS(JHEX,I)=(UT1/(UT1+UT2)*THS(JHEX,I)) + (UT2/(UT1+UT2))*
     &               TCS(JHEX,I)
         TSS(JHEX,I)=TCS(JHEX,I)
      WRITE(NO,992) Z(I),THS(JHEX,I),TCS(JHEX,I),TTS(JHEX,I),TSS(JHEX,I)
```

```
   10 CONTINUE
C...
  990 FORMAT(/,2X,'analytical solution for HEX(',I1,')',/,
     &          2X,'   Z/L          TH          TC',
     &             '          TT          TS')
  992 FORMAT(2X,F6.2,4F12.4)
C...
      RETURN
      END
C...
C ***************************************** C
      SUBROUTINE PDE (NODE, TIME, UU, DUU)
C ***************************************** C
      IMPLICIT REAL*8 (A-H,O-Z)
      REAL*8   L
C...
      PARAMETER (NHEX=3, NZ=51)
C...
      COMMON/U/ UTH(NHEX,NZ),UTC(NHEX,NZ),UTT(NHEX,NZ),UTS(NHEX,NZ)
      COMMON/PARAM/ L(NHEX), VH(NHEX), VC(NHEX), UH(NHEX), UC1(NHEX),
     &              UC2(NHEX),UT1(NHEX),UT2(NHEX),US(NHEX),TH0(NHEX),
     &              TC0(NHEX), UTH0(NHEX,NZ), UTC0(NHEX,NZ),
     &              UTT0(NHEX,NZ), UTS0(NHEX,NZ)
      COMMON/BYPASS/ RH(NHEX),RC(NHEX),RHO(NHEX),RCO(NHEX),to,
     &               THST(NHEX),TCST(NHEX),THUT(NHEX),TCUT(NHEX)
      COMMON/ASTST/ THS(NHEX,NZ),TCS(NHEX,NZ),
     &              THSU(NHEX,NZ),TCSU(NHEX,NZ),
     &              TTS(NHEX,NZ),TSS(NHEX,NZ),
     &              TTSU(NHEX,NZ),TSSU(NHEX,NZ), Z(NZ)
      DIMENSION UTHZ(NHEX,NZ),UTCZ(NHEX,NZ),DUTH(NHEX,NZ),DUTC(NHEX,NZ),
     &          DUTT(NHEX,NZ),DUTS(NHEX,NZ)
      DIMENSION UUTH(NZ),UUTC(NZ), UUTHZ(NZ),UUTCZ(NZ)
      DIMENSION THT(NHEX),TCT(NHEX)
      DIMENSION UU(NODE),DUU(NODE)
C...
C...
C   Set the Non-negativity Constraint for the Dependent Variables
C ---------------------------------------------------------------
      DO 35 I=1,NODE
         IF(UU(I).LT.0.D0) UU(I)=0.D0
   35 CONTINUE
C...
C   Transfer the Variables from LSODES
C ------------------------------------
      DO 125 J=1,NHEX
         K=(4*(J-1)*NZ)
      DO 100 I=1,NZ
         UTH(J,I) = UU(K+I)
         UTC(J,I) = UU(K+I+NZ)
         UTT(J,I) = UU(K+I+NZ+NZ)
         UTS(J,I) = UU(K+I+NZ+NZ+NZ)
  100 CONTINUE
  125 CONTINUE
C...
```

```
C   Set the Boundary Conditions
C -----------------------------
      DO 8900 J=1,NHEX
C        ------------------------------------
         CALL MIXH (J,RH,TH0,UTH,THT,NHEX,NZ)
         CALL MIXC (J,RC,TC0,UTC,TCT,NHEX,NZ)
C        ------------------------------------
 8900 CONTINUE
      UTH(1,1)  = TH0(1)
      UTC(1,NZ) = TC0(1)
      UTH(2,1)  = TH0(2)
      UTC(2,NZ) = TCT(1)
      UTH(3,1)  = THT(2)
      UTC(3,NZ) = TC0(3)
C...
C...
C   Evaluate the Spatial Derivatives
C ---------------------------------
      DO 175 J=1,NHEX
      DO 165 I=1,NZ
         UUTH(I)=UTH(J,I)
         UUTC(I)=UTC(J,I)
  165 CONTINUE
C     ------------------------------------------------
      CALL DSS020 (0.D0, L(J), NZ, UUTH, UUTHZ, +1.D0)
      CALL DSS020 (0.D0, L(J), NZ, UUTC, UUTCZ, -1.D0)
C     ------------------------------------------------
      DO 166 I=1,NZ
         UTHZ(J,I)=UUTHZ(I)
         UTCZ(J,I)=UUTCZ(I)
  166 CONTINUE
  175 CONTINUE
C...
C...
C   Assamble the Partial Differential Equations
C ---------------------------------------------
      DO 15 J=1,NHEX
         VHR=VH(J)*(1.D0-RH(J))
         VCR=VC(J)*(1.D0-RC(J))
      DO 10 I=1,NZ
C...
C   Partial Differential Equation for the Hot Fluid
C ---------------------------------------------------
      DUTH(J,I) = - (VHR)*UTHZ(J,I) - (UH(J))*(UTH(J,I)-UTT(J,I))
C...
C   Partial Differential Equation for the Cold Fluid
C ----------------------------------------------------
      DUTC(J,I) = + (VCR)*UTCZ(J,I) + (UC1(J))*(UTT(J,I)-UTC(J,I))
     &            + (UC2(J))*(UTS(J,I)-UTC(J,I))
C...
C   Partial Differential Equation for the Tube Wall
C ---------------------------------------------------
      DUTT(J,I) = + (UT1(J))*(UTH(J,I)-UTT(J,I))
     &            + (UT2(J))*(UTC(J,I)-UTT(J,I))
C...
C   Partial Differential Equation for the Shell Wall
C ----------------------------------------------------
      DUTS(J,I) = + (US(J))*(UTC(J,I)-UTS(J,I))
C...
```

```
   10 CONTINUE
   15 CONTINUE
C...
C...
C   Set the Temporl Derivatives at the Boundaries to Zero
C -------------------------------------------------------
      DO 18 J=1,NHEX
         DUTH(J,1)  = 0.D0
         DUTC(J,NZ) = 0.D0
   18 CONTINUE
C...
C...
      DO 205 J=1,NHEX
         K=(4*(J-1)*NZ)
      DO 200 I=1,NZ
         DUU(K+I) = DUTH(J,I)
         DUU(K+I+NZ) = DUTC(J,I)
         DUU(K+I+NZ+NZ) = DUTT(J,I)
         DUU(K+I+NZ+NZ+NZ) = DUTS(J,I)
  200 CONTINUE
         DUU((4*NHEX*NZ)+J) = DABS(THT(J)-THST(J))
         DUU((4*NHEX*NZ+NHEX)+J) = DABS(TCT(J)-TCST(J))
  205 CONTINUE
C...
      RETURN
      END
C...
C
*****************************************************************************
C
      SUBROUTINE PRINT (UU, TIME, TIME0, TSTOP, TPRINT, NI,NO,NOT,NOE)
C
*****************************************************************************
C
      IMPLICIT REAL*8 (A-H,O-Z)
      REAL*8   L
C...
      PARAMETER (NHEX=3, NZ=51, NODE=(NHEX*(4*NZ+2)))
C...
      COMMON/U/ UTH(NHEX,NZ),UTC(NHEX,NZ),UTT(NHEX,NZ),UTS(NHEX,NZ)
      COMMON/PARAM/ L(NHEX), VH(NHEX), VC(NHEX), UH(NHEX), UC1(NHEX),
     &              UC2(NHEX),UT1(NHEX),UT2(NHEX),US(NHEX),TH0(NHEX),
     &              TC0(NHEX), UTH0(NHEX,NZ), UTC0(NHEX,NZ),
     &              UTT0(NHEX,NZ), UTS0(NHEX,NZ)
      COMMON/BYPASS/ RH(NHEX),RC(NHEX),RHO(NHEX),RCO(NHEX),to,
     &               THST(NHEX),TCST(NHEX),THUT(NHEX),TCUT(NHEX)
      COMMON/ASTST/ THS(NHEX,NZ),TCS(NHEX,NZ),
     &              THSU(NHEX,NZ),TCSU(NHEX,NZ),
     &              TTS(NHEX,NZ),TSS(NHEX,NZ),
     &              TTSU(NHEX,NZ),TSSU(NHEX,NZ), Z(NZ)
      DIMENSION DTH(NHEX,NZ),DTC(NHEX,NZ),DTHU(NHEX,NZ),DTCU(NHEX,NZ)
      DIMENSION THT(NHEX),TCT(NHEX),
     &          DTHT(NHEX),DTCT(NHEX),DTHUT(NHEX),DTCUT(NHEX)
      DIMENSION DTT(NHEX,NZ),DTS(NHEX,NZ),DTTU(NHEX,NZ),DTSU(NHEX,NZ)
      DIMENSION ETH(NHEX),ETC(NHEX)
      DIMENSION UU(NODE)
C...
```

```
C...
      DO 35 I=1,NODE
         IF(UU(I).LT.0.D0) UU(I)=0.D0
   35 CONTINUE
C
      DO 125 J=1,NHEX
         K=(4*(J-1)*NZ)
      DO 100 I=1,NZ
         UTH(J,I) = UU(K+I)
         UTC(J,I) = UU(K+I+NZ)
         UTT(J,I) = UU(K+I+NZ+NZ)
         UTS(J,I) = UU(K+I+NZ+NZ+NZ)
  100 CONTINUE
         ETH(J) = UU((4*NHEX*NZ)+J)
         ETC(J) = UU((4*NHEX*NZ+NHEX)+J)
  125 CONTINUE
C
C   Set the Boundary Conditions
C -----------------------------
      DO 8900 J=1,NHEX
C        ------------------------------------
         CALL MIXH (J,RH,TH0,UTH,THT,NHEX,NZ)
         CALL MIXC (J,RC,TC0,UTC,TCT,NHEX,NZ)
C        ------------------------------------
 8900 CONTINUE
      UTH(1,1)  = TH0(1)
      UTC(1,NZ) = TC0(1)
      UTH(2,1)  = TH0(2)
      UTC(2,NZ) = TCT(1)
      UTH(3,1)  = THT(2)
      UTC(3,NZ) = TC0(3)
C
C...
      IF (TIME.EQ.TIME0) THEN
      WRITE(NO,1)
      WRITE(NOT,90)
      WRITE(17,192)
      WRITE(NOE,92)
C...
      NL=2*(NZ-1)/10
C...
      ENDIF
C...
C
      DO 210 J=1,NHEX
         DTHT(J)=THT(J)-THST(J)
         DTCT(J)=TCT(J)-TCST(J)
         DTHUT(J)=THT(J)-THUT(J)
         DTCUT(J)=TCT(J)-TCUT(J)
      DO 210 I=1,NZ
         DTH(J,I)=UTH(J,I)-THS(J,I)
         DTC(J,I)=UTC(J,I)-TCS(J,I)
         DTHU(J,I)=UTH(J,I)-THSU(J,I)
         DTCU(J,I)=UTC(J,I)-TCSU(J,I)
         DTT(J,I)=UTT(J,I)-TTS(J,I)
         DTS(J,I)=UTS(J,I)-TSS(J,I)
         DTTU(J,I)=UTT(J,I)-TTSU(J,I)
         DTSU(J,I)=UTS(J,I)-TSSU(J,I)
  210 CONTINUE
```

```
C
C...
      WRITE(NO,2) TIME,
     &            (THT(J),J=1,NHEX),(TCT(J),J=1,NHEX),
     &            (DTHT(J),J=1,NHEX),(DTCT(J),J=1,NHEX),
     &            (ETH(J),J=1,NHEX),(ETC(J),J=1,NHEX),
     &            (RH(J),J=1,NHEX),(RHO(J),J=1,NHEX),
     &            (RC(J),J=1,NHEX),(RCO(J),J=1,NHEX)
      WRITE(NO,3) (Z(I),I=1,NZ,NL)
      WRITE(NO,4)
      DO 110 J=1,NHEX
         WRITE(NO,5) J,(UTH(J,I),I=1,NZ,NL)
         WRITE(NO,7) (DTH(J,I),I=1,NZ,NL)
         WRITE(NO,9) (DTHU(J,I),I=1,NZ,NL)
         WRITE(NO,6) J,(UTC(J,I),I=1,NZ,NL)
         WRITE(NO,8) (DTC(J,I),I=1,NZ,NL)
         WRITE(NO,10) (DTCU(J,I),I=1,NZ,NL)
         WRITE(NO,96) J,(UTT(J,I),I=1,NZ,NL)
         WRITE(NO,98) (DTT(J,I),I=1,NZ,NL)
         WRITE(NO,910) (DTTU(J,I),I=1,NZ,NL)
         WRITE(NO,86) J,(UTS(J,I),I=1,NZ,NL)
         WRITE(NO,88) (DTS(J,I),I=1,NZ,NL)
         WRITE(NO,810) (DTSU(J,I),I=1,NZ,NL)
         WRITE(NO,*) ' '
  110 CONTINUE
C...
      WRITE(NOT,91) TIME,(DTHT(J),J=1,NHEX),(DTCT(J),J=1,NHEX),
     &                   (DTHUT(J),J=1,NHEX),(DTCUT(J),J=1,NHEX)
      WRITE(NOE,95) TIME,(ETH(J),J=1,NHEX),(ETC(J),J=1,NHEX)
      WRITE(17,191) TIME,DTH(1,NZ),DTC(1,1),DTT(1,NZ),DTS(1,1)
C...
    1 FORMAT(1H1,///,10X,' H E N    R e s u l t s',/,10X,24('-'),//)
    2 FORMAT(/,' Time    =',1X,F10.2,//,
     &         ' Hot Targets  :',3F10.4,/,
     &         ' Cold Targets :',3F10.4,/,
     &         ' +/- H_Targets:',3F10.4,/,
     &         ' +/- C_Targets:',3F10.4,/,
     &         ' ErrInt H     :',3(2X,F8.2),/,
     &         ' ErrInt C     :',3(2X,F8.2),/,
     &         ' RH           :',3(2X,F10.5),/,
     &         ' RHO          :',3(2X,F10.5),/,
     &         ' RC           :',3(2X,F10.5),/,
     &         ' RCO          :',3(2X,F10.5),/)
    3 FORMAT(  ' Z       =',21(7X,F4.2))
    4 FORMAT(1X,75('-'))
    5 FORMAT(  ' TH-',I1,'    =',21(F11.4))
    6 FORMAT(  ' TC-',I1,'    =',21(F11.4))
   96 FORMAT(  ' TT-',I1,'    =',21(F11.4))
   86 FORMAT(  ' TS-',I1,'    =',21(F11.4))
    7 FORMAT(  ' TH-THS  =',21(F11.4))
    8 FORMAT(  ' TC-TCS  =',21(F11.4))
   98 FORMAT(  ' TT-TTS  =',21(F11.4))
   88 FORMAT(  ' TS-TSS  =',21(F11.4))
    9 FORMAT(  ' TH-THSU =',21(F11.4))
   10 FORMAT(  ' TC-TCSU =',21(F11.4))
  910 FORMAT(  ' TT-TTSU =',21(F11.4))
  810 FORMAT(  ' TS-TSSU =',21(F11.4))
   90 FORMAT(' TIME     DTH_1   DTH_2   DTH_3   DTC_1   DTC_2   DTC_3',
     &          '  DTHU_1  DTHU_2  DTHU_3  DTCU_1  DTCU_2  DTCU_3')
```

```
   92 FORMAT(' TIME        ETH_1      ETH_2      ETH_3',
     &               '      ETC_1      ETC_2      ETC_3')
   91 FORMAT(F6.2,2X,12F8.3)
  192 FORMAT(' TIME      DTH_1    DTC_1    DTT_1    DTS_1')
  191 FORMAT(F6.2,2X,4F8.3)
   95 FORMAT(F6.2,2X,6F10.2)
C...
      RETURN
      END
C...
C ********************************************** C
      SUBROUTINE MIXH (J,RH,TH0,TH,THT,NHEX,NZ)
C ********************************************** C
      IMPLICIT REAL*8 (A-H,O-Z)
C...
      DIMENSION RH(NHEX),TH0(NHEX),TH(NHEX,NZ),THT(NHEX)
C...
      THT(J)=TH0(J)*RH(J)+TH(J,NZ)*(1.D0-RH(J))
C...
      RETURN
      END
C...
C ********************************************** C
      SUBROUTINE MIXC (J,RC,TC0,TC,TCT,NHEX,NZ)
C ********************************************** C
      IMPLICIT REAL*8 (A-H,O-Z)
C...
      DIMENSION RC(NHEX),TC0(NHEX),TC(NHEX,NZ),TCT(NHEX)
C...
      TCT(J)=TC0(J)*RC(J)+TC(J,1)*(1.D0-RC(J))
C...
      RETURN
      END
C...
C ********************************************************** C
      SUBROUTINE JACPDE (NODE, TIME, UU, J, IA, JA, PDJ)
C ********************************************************** C
      IMPLICIT REAL*8 (A-H,O-Z)
      DIMENSION UU(NODE),IA(1),JA(1),PDJ(1)
      RETURN
      END
```

APPENDIX D

Listing of the Program for Closed-Loop Control of Heat-Exchanger Network.

```
C*********************************************************************C
C ******************************************************************* C
C *  S. Uğur Akman - Cantürk Boyacı   Oct. 26, 1992 - Sept. 20, 1995 * C
C *                                                                   * C
C *                     H E A T  -  E X C H A N G E R                 * C
C *                          CLOSED-LOOP CONTROL                      * C
C *                    [Solution by Finite Differences]               * C
C ******************************************************************* C
C*********************************************************************C
C
C
C        ACH     : INNER CROSSECTIONAL AREA OF A SINGLE TUBE, m2
C        ACC     : TOTAL CROSSECTIONAL AREA OF THE SHELL, m2
C
C        AH      : INNER SURFACE AREA OF A SINGLE TUBE/LENGTH, m2
C        AC      : OUTER SURFACE AREA OF A SINGLE TUBE/LENGTH, m2
C        AS      : INNER SURFACE AREA OF THE SHELL/LENGTH, m2
C
C        VH      : VELOCITY OF THE TUBE-SIDE, m/sec
C        VC      : VELOCITY OF THE SHELL-SIDE, m/sec
C
C        TWA     : CROSSECTIONAL TUBE WALL AREA, m2
C        SWA     : CROSSECTIONAL SHELL WALL AREA, m2
C
C        HI      : INSIDE HEAT TRANSFER COEFFICIENT
C        HO      : OUTSIDE HEAT TRANSFER COEFFICIENT
C        HS      : SHELL-WALL HEAT TRANSFER COEFFICIENT
C
C        RHOT    : DENSITY OF TUBE & SHELL WALL METAL (STEEL)
C        CPT     : CP OF TUBE & SHELL WALL METAL (STEEL)
C
C...
      IMPLICIT REAL*8 (A-H,O-Z)
C...
      PARAMETER (NHEX=3, NZ=51, NODE=(NHEX*(4*NZ+2)))
      PARAMETER (LRW=50000, LIW=30)
C...
      DIMENSION UU(NODE),DUU(NODE),RWORK(LRW),IWORK(LIW)
      EXTERNAL PDE,JACPDE
C...
      NI=5
      NO=6
```

```
      NOT=8
      NOE=10
      OPEN(NO,FILE='GENERAL.OUT')
      OPEN(NOT,FILE='DEVIATION.OUT')
      OPEN(NOE,FILE='ERROR.OUT')
C...
C...
C   Read the Input Parameters for LSODES
C ------------------------------------
      TIME0  =    0.0D0
      TSTOP  =  300.0D0
      TPRINT =    0.5D0
C...
C   Set the Optional Input Parameters of LSODES
C ------------------------------------------
      MF     = 222
      RTOL   = 1.D-05
      ATOL   = 1.D-06
      H0     = 1.D-04
C...
      ITOL   = 1
      ITASK  = 4
      ISTATE = 1
      IOPT   = 1
      IWORK(6) = 5000
      RWORK(5) = H0
C...
      TIME=TIME0
C...
      WRITE(NO,801) TIME0,TSTOP,TPRINT,RTOL,ATOL,NODE
C...
C   Initialize the Vector of Dependent Variables
C -------------------------------------------
C     ---------------------------------------
      CALL INITIAL (NODE, TIME, UU, DUU, NI, NO)
C     ---------------------------------------
C...
      TOUT=TIME0
C...
 1000 CONTINUE
C...
      RWORK(1)=TOUT
C...
C   Call the IVP Solver (LSODES) to Integrate Between TIME & TOUT
C -------------------------------------------------------------
C     -----------------------------------------------------------------
      CALL LSODES (PDE, NODE, UU, TIME, TOUT, ITOL, RTOL, ATOL, ITASK,
     &             ISTATE, IOPT, RWORK, LRW, IWORK, LIW, JACPDE ,MF)
C     -----------------------------------------------------------------
C...
C   Print the Results at the End of the Integration Interval
C -------------------------------------------------------
C     -------------------------------------------------------
      CALL PRINT (UU, TIME, TIME0, TSTOP, TPRINT, NI, NO, NOT, NOE)
C     -------------------------------------------------------
C...
```

```
C   Stop if Error is Reported by LSODES
C ------------------------------------
      IF (ISTATE.LT.0) THEN
         WRITE(NO,9999) ISTATE
         GO TO 3000
      ENDIF
C...
C   Call LSODES Again for the New Interval of Integration
C ------------------------------------------------------
      IF (TIME.GE.TSTOP) GO TO 2000
      TOUT=TOUT+TPRINT
      GO TO 1000
C...
 2000 CONTINUE
C...
      WRITE(NO,900)
      WRITE(NO,901) IWORK(11)
      WRITE(NO,902) IWORK(12)
      WRITE(NO,903) IWORK(13)
      WRITE(NO,904) IWORK(19)
      WRITE(NO,905) IWORK(20)
      WRITE(NO,906) IWORK(21)
      WRITE(NO,907) IWORK(17),IWORK(18)
C...
  801 FORMAT(///,10X,'Input-Parameters for LSODES',/,10X,52('='),//,
     &  10X,'Initial Value of Time ..... ',F10.2,/,
     &  10X,'Final Value of Time ........ ',F10.2,/,
     &  10X,'Print Interval of Time ..... ',F10.2,//,
     &  10X,'Relative Error Tolerance Parameter ..... ',1PE10.4,/,
     &  10X,'Absolute Error Tolerance Parameter ..... ',1PE10.4,//,
     &  10X,'Number of Ordinary Differential Equations ...  ',I4,/)
  900 FORMAT(1H1,////,10X,'Computational Statistics for  LSODES',/,
     &           10X,48('='),/)
  901 FORMAT(10X,'Number of Steps Taken ..... ',I8)
  902 FORMAT(10X,'Number of Function Evaluations ... ',I8)
  903 FORMAT(10X,'Number of Jacobian Evaluations ... ',I8,/)
  904 FORMAT(10X,'No. of Nonzero Elements in the Jacobian ... ',I4)
  905 FORMAT(10X,'No. of Extra Function Evaluations ',/,10X,
     &           '    Needed for Each Jacobian Evaluation ... ',I4)
  906 FORMAT(10X,'No. of Sparse LU Decompositions ..... ',I4,/)
  907 FORMAT(10X,'Required RWORK Size ... ',I5,/,10X,
     &           'Required IWORK Size ... ',I5,//)
 9999 FORMAT(///,' Error Halt... ISTATE =',I3,//)
C...
 3000 CONTINUE
C...
      STOP
      END
C...
C ******************************************************* C
      SUBROUTINE INITIAL (NODE, TIME, UU, DUU, NI, NO)
C ******************************************************* C
C...
      IMPLICIT REAL*8 (A-H,O-Z)
      REAL*8   L
C...
      PARAMETER (NHEX=3, NZ=51)
C...
      COMMON/U/ UTH(NHEX,NZ),UTC(NHEX,NZ),UTT(NHEX,NZ),UTS(NHEX,NZ)
```

```
      COMMON/PARAM/ L(NHEX), VH(NHEX), VC(NHEX), UH(NHEX), UC1(NHEX),
     &              UC2(NHEX),UT1(NHEX),UT2(NHEX),US(NHEX),TH0(NHEX),
     &              TC0(NHEX), UTH0(NHEX,NZ), UTC0(NHEX,NZ),
     &              UTT0(NHEX,NZ), UTS0(NHEX,NZ)
      COMMON/BYPASS/ RH(NHEX),RC(NHEX),RHO(NHEX),RCO(NHEX),to,
     &               THST(NHEX),TCST(NHEX),THUT(NHEX),TCUT(NHEX)
      DIMENSION UU(NODE),DUU(NODE),AH(NHEX),AC(NHEX),NT(NHEX),DS(NHEX),
     &          ACH(NHEX),ACC(NHEX),THI(NHEX),THO(NHEX),
     &          TCI(NHEX),TCO(NHEX),FH(NHEX),FC(NHEX),HI(NHEX),HO(NHEX),
     &          HS(NHEX),SWA(NHEX),AS(NHEX),TCH(NHEX),TCC(NHEX),
     &          TCT(NHEX),TICS(NHEX),TCCP(NHEX)
      COMMON/ASTST/ THS(NHEX,NZ),TCS(NHEX,NZ),
     &              THSU(NHEX,NZ),TCSU(NHEX,NZ),
     &              TTS(NHEX,NZ),TSS(NHEX,NZ),
     &              TTSU(NHEX,NZ),TSSU(NHEX,NZ), Z(NZ)
C...
C...
C   Read the Model Parameters
C ---------------------------
      THI(1)  =  620.D0
      THO(1)  =  385.D0
      TCI(1)  =  300.D0
      TCO(1)  =  417.5D0
      FH(1)   =  10000.D0
      FC(1)   =  20000.D0

      THI(2)  =  720.D0
      THO(2)  =  530.D0
      TCI(2)  =  417.5D0
      TCO(2)  =  560.D0
      FH(2)   =  15000.D0
      FC(2)   =  20000.D0

      THI(3)  =  530.D0
      THO(3)  =  410.D0
      TCI(3)  =  280.D0
      TCO(3)  =  340.D0
      FH(3)   =  15000.D0
      FC(3)   =  30000.D0

      RHOT    =  7833.78D0
      CPT     =  502.44D0

      DO 425 K=1,NHEX
C     ------------------------------------------------------------------------
            CALL HEX (THI(K),THO(K),TCI(K),TCO(K),FH(K),FC(K),L(K),
     &                VH(K),VC(K),AH(K),AC(K),AS(K),ACH(K),ACC(K),
     &                NT(K),HO(K),HI(K),TWA,SWA(K),RHOT,CPT,TCH(K),
     &                TCC(K),TCT(K),TICS(K),TCCP(K),DS(K),K)
C     ------------------------------------------------------------------------
            HO(K)  =  2000.D0
            HS(K)  =  2000.D0
            HI(K)  =  HO(K)*((AC(K))/AH(K))
C...
            WRITE(NO,*)'HEX #........> ',K
            WRITE(NO,*)'NT          : ',NT(K)
            WRITE(NO,*)'LENGTH      : ',L(K)
            WRITE(NO,*)'SHELL DIA.: ',DS(K)
            WRITE(NO,*)
```

```
            WRITE(NO,*)'VH          : ',VH(K)
            WRITE(NO,*)'VC          : ',VC(K)
            WRITE(NO,*)
            WRITE(NO,*)'AH , AH*L   : ',AH(K),AH(K)*L(K)
            WRITE(NO,*)'AC , AC*L   : ',AC(K),AC(K)*L(K)
            WRITE(NO,*)'AC*L*NT     : ',AC(K)*L(K)*NT(K)
            WRITE(NO,*)'AS , AS*L   : ',AS(K),AS(K)*L(K)
            WRITE(NO,*)
            WRITE(NO,*)'ACH         : ',ACH(K)
            WRITE(NO,*)'ACC         : ',ACC(K)
            WRITE(NO,*)
            WRITE(NO,*)'HI          : ',HI(K)
            WRITE(NO,*)'HO          : ',HO(K)
            WRITE(NO,*)'HS          : ',HS(K)
            WRITE(NO,*)
  425 CONTINUE
C...
      U     =   1000.0D0
      ROH   =   840.D0
      ROC   =   840.D0
      CPH   =   1046.7D0
      CPC   =   1046.7D0
C...
      RH(1) = 0.D0
      RH(2) = 0.D0
      RH(3) = 0.D0
      RC(1) = 0.D0
      RC(2) = 0.D0
      RC(3) = 0.D0
C...
      DO 2501 J=1,NHEX
         UH(J)  = HI(J)*AH(J)/(ROH*CPH*ACH(J))
         UC1(J) = HO(J)*AC(J)*NT(J)/(ROC*CPC*ACC(J))
         UC2(J) = HS(J)*AS(J)/(ROC*CPC*ACC(J))
         UT1(J) = HI(J)*AH(J)/(RHOT*CPT*TWA)
         UT2(J) = HO(J)*AC(J)/(RHOT*CPT*TWA)
         US(J)  = HS(J)*AS(J)/(RHOT*CPT*SWA(J))
         WRITE(NO,*) 'UH, UC1, UC2, UT1, UT2, US'
         WRITE(NO,*) J,UH(J),UC1(J),UC2(J),UT1(J),UT2(J),US(J)
2501  CONTINUE
C...
C...
C   Input Terminal (input) Temperatures
C -----------------------------------
      TH0(1) = 620.D0
      TC0(1) = 300.D0
      TH0(2) = 720.D0
      TC0(3) = 280.D0
C...
C...
      DO 825 I=1,NZ
         Z(I)=DFLOAT(I-1)/DFLOAT(NZ-1)
  825 CONTINUE
C...
C   Input Initial Temperature Profiles
C -----------------------------------
      WRITE(NO,1100)
 1100 FORMAT(///,' Steady-State Profiles before Upset :',/,38('-'),/)
C
```

```
      DO 725 J=1,NHEX
         VHR=VH(J)*(1.D0-RH(J))
         VCR=VC(J)*(1.D0-RC(J))
      IF(J.EQ.2) TC0(2)=TCST(1)
      IF(J.EQ.3) TH0(3)=THST(2)
C     ------------------------------------------------------------------
      CALL STST (J,L(J),Z,VHR,VCR,UH(J),UC1(J),UC2(J),UT1(J),UT2(J),
     &           US(J),TH0(J),TC0(J),THS,TCS,TTS,TSS,NO)
C     ------------------------------------------------------------------
C     -------------------------------------
      CALL MIXH (J,RH,TH0,THS,THST,NHEX,NZ)
      CALL MIXC (J,RC,TC0,TCS,TCST,NHEX,NZ)
C     -------------------------------------

      WRITE(NO,*) 'QH',J,(FH(J)*(TH0(J)-THS(J,NZ)))
      WRITE(NO,*) 'QC',J,(FC(J)*(TCS(J,1)-TC0(J)))

      DTLM=((TH0(J)-TCS(J,1))-(THS(J,NZ)-TC0(J)))
     &     /DLOG( (TH0(J)-TCS(J,1))/(THS(J,NZ)-TC0(J)) )
      WRITE(NO,*) 'DTLM',J,DTLM
      WRITE(NO,*) 'Q',U*AC(J)*L(J)*NT(J)*DTLM


  725 CONTINUE
C...
      WRITE(NO,3100)
 3100 FORMAT(///,' Target Temperatures before Upset :',/,36('-'),/)
      DO 1725 J=1,NHEX
         WRITE(NO,3110) J, THST(J), J, TCST(J)
 1725 CONTINUE
 3110 FORMAT(' THST(',I1,')',F10.4,5X,' TCST(',I1,')',F10.4)
C...
C...
      DO 35 J=1,NHEX
      DO 35 I=1,NZ
         UTH0(J,I)=THS(J,I)
         UTC0(J,I)=TCS(J,I)
         UTT0(J,I)=TTS(J,I)
         UTS0(J,I)=TSS(J,I)
   35 CONTINUE
C...
C...
C   Set the Initial Conditions (@ Time = 0, 0 < Z < L)
C -----------------------------------------------------
      DO 25 J=1,NHEX
      DO 25 I=1,NZ
         UTH(J,I)=UTH0(J,I)
         UTC(J,I)=UTC0(J,I)
         UTT(J,I)=UTT0(J,I)
         UTS(J,I)=UTS0(J,I)
   25 CONTINUE
C...
C...
C   Input Terminal (input) Disturbances
C -----------------------------------
      TH0(1) = TH0(1) + 0.D0
      TC0(1) = TC0(1) - 4.D0
      TH0(2) = TH0(2) + 0.D0
      TC0(3) = TC0(3) - 0.D0
```

```
C
C...
      RH(1) = 0.1991884263D-01
C      RH(1) = 0.D0
      RH(2) = 0.D0
      RH(3) = 0.D0
      RC(1) = 0.4684139883D-03
C      RC(1) = 0.D0
      RC(2) = 0.D0
      RC(3) = 0.5596164119D-01
C      RC(3) = 0.D0
C...
      DO 246 I=1,NHEX
         RHO(I)=RH(I)
         RCO(I)=RC(I)
  246 CONTINUE
C...
C   Calculate Final Temperature Profiles
C -------------------------------------
      WRITE(NO,1105)
 1105 FORMAT(///,' Steady-State Profiles after Upset  :',/,38('-'),/)
C
      DO 925 J=1,NHEX
         VHR=VH(J)*(1.D0-RH(J))
         VCR=VC(J)*(1.D0-RC(J))
      IF(J.EQ.2) TC0(2)=TCUT(1)
      IF(J.EQ.3) TH0(3)=THUT(2)
C     ---------------------------------------
      CALL STST (J,L(J),Z,VHR,VCR,UH(J),UC1(J),UC2(J),UT1(J),
     &           UT2(J),US(J),TH0(J),TC0(J),THSU,TCSU,TTSU,TSSU,NO)
C     ---------------------------------------
C     ---------------------------------------
      CALL MIXH (J,RH,TH0,THSU,THUT,NHEX,NZ)
      CALL MIXC (J,RC,TC0,TCSU,TCUT,NHEX,NZ)
C     ---------------------------------------
  925 CONTINUE
C...
      WRITE(NO,3105)
 3105 FORMAT(///,' Target Temperatures after Upset  :',/,36('-'),/)
      DO 1925 J=1,NHEX
         WRITE(NO,3210) J, THUT(J), J, TCUT(J)
 1925 CONTINUE
 3210 FORMAT(' THUT(',I1,')',F10.4,5X,' TCUT(',I1,')',F10.4)
C...
      WRITE(NO,1200) (THS(J,NZ),J=1,NHEX),(TCS(J,1),J=1,NHEX),
     &               (THSU(J,NZ),J=1,NHEX),(TCSU(J,1),J=1,NHEX)
      WRITE(NO,1205) ((THS(J,NZ)-THSU(J,NZ)),J=1,NHEX),
     &               ((TCS(J,1)-TCSU(J,1)),J=1,NHEX)
 1200 FORMAT(//,' Hot  Stream Outputs at Steady State :',/,38('-'),
     &        /,3F10.4,//,
     &          ' Cold Stream Outputs at Steady State :',/,38('-'),
     &        /,3F10.4,///,
     &          ' Hot  Stream Outputs at Disturbance  :',/,38('-'),
     &        /,3F10.4,//,
     &          ' Cold Stream Outputs at Disturbance  :',/,38('-')
     &        /,3F10.4)
 1205 FORMAT(//,' Change in Hot  Stream Outputs       :',/,38('-'),
     &        /,3F10.4,//,
     &          ' Change in Cold Stream Outputs       :',/,38('-'),
```

```
     &        /,3F10.4,/)
C...
C   Transfer the Variables to the Vector of Dependent Variables in
LSODES
C -------------------------------------------------------------------------
--
      DO 215 J=1,NHEX
         K=(4*(J-1)*NZ)
      DO 200 I=1,NZ
         UU(K+I) = UTH(J,I)
         UU(K+I+NZ) = UTC(J,I)
         UU(K+I+NZ+NZ) = UTT(J,I)
         UU(K+I+NZ+NZ+NZ) = UTS(J,I)
  200 CONTINUE
         UU((4*NHEX*NZ)+J) = 0.D0
         UU((4*NHEX*NZ+NHEX)+J) = 0.D0
  215 CONTINUE
C...
C     ------------------------------
      CALL PDE (NODE, TIME, UU, DUU)
C     ------------------------------
C...
C   Set the Vector of Temporal Derivatives in LSODES to Zero
C ------------------------------------------------------------
      DO 225 I=1,NODE
         DUU(I)=0.D0
  225 CONTINUE
C...
      RETURN
      END
C...
C ********************************************************************* C
      SUBROUTINE STST (JHEX,L,Z,VH,VC,UH,UC1,UC2,UT1,
     &                 UT2,US,TH0,TC0,THS,TCS,TTS,TSS,NO)
C ********************************************************************* C
      IMPLICIT REAL*8 (A-H,O-Z)
      REAL*8   L
C...
      PARAMETER (NHEX=3, NZ=51)
C
      DIMENSION THS(NHEX,NZ),TCS(NHEX,NZ),TTS(NHEX,NZ),TSS(NHEX,NZ),
     &          Z(NZ)
C...
      WRITE(NO,990) JHEX
C
      UHA=UH*UT2/(UT1+UT2)
      UCA=UC1*UT1/(UT1+UT2)
      RM=UCA/VC-UHA/VH
      A=(TC0-(VH/VC)*(UCA/UHA)*TH0*DEXP(RM*L))/
     &  (1.D0-(VH/VC)*(UCA/UHA)*DEXP(RM*L))
      DO 10 I=1,NZ
         ZL=Z(I)*L
         THS(JHEX,I)=TH0*DEXP(RM*ZL)+A*(1.D0-DEXP(RM*ZL))
         TCS(JHEX,I)=((VH*UCA)/(VC*UHA))*TH0*DEXP(RM*ZL)
     &              +A*(1.D0-((VH*UCA)/(VC*UHA))*DEXP(RM*ZL))
         TTS(JHEX,I)=(UT1/(UT1+UT2)*THS(JHEX,I)) + (UT2/(UT1+UT2))*
     &               TCS(JHEX,I)
         TSS(JHEX,I)=TCS(JHEX,I)
      WRITE(NO,992) Z(I),THS(JHEX,I),TCS(JHEX,I),TTS(JHEX,I),TSS(JHEX,I)
```

```
   10 CONTINUE
C...
  990 FORMAT(/,2X,'analytical solution for HEX(',I1,')',/,
     &         2X,'   Z/L          TH          TC',
     &            '          TT          TS')
  992 FORMAT(2X,F6.2,4F12.4)
C...
      RETURN
      END
C...
C ***************************************** C
      SUBROUTINE PDE (NODE, TIME, UU, DUU)
C ***************************************** C
      IMPLICIT REAL*8 (A-H,O-Z)
      REAL*8   L
C...
      PARAMETER (NHEX=3, NZ=51)
C...
      COMMON/U/ UTH(NHEX,NZ),UTC(NHEX,NZ),UTT(NHEX,NZ),UTS(NHEX,NZ)
      COMMON/PARAM/ L(NHEX), VH(NHEX), VC(NHEX), UH(NHEX), UC1(NHEX),
     &              UC2(NHEX),UT1(NHEX),UT2(NHEX),US(NHEX),TH0(NHEX),
     &              TC0(NHEX), UTH0(NHEX,NZ), UTC0(NHEX,NZ),
     &              UTT0(NHEX,NZ), UTS0(NHEX,NZ)
      COMMON/BYPASS/ RH(NHEX),RC(NHEX),RHO(NHEX),RCO(NHEX),to,
     &               THST(NHEX),TCST(NHEX),THUT(NHEX),TCUT(NHEX)
      COMMON/ASTST/ THS(NHEX,NZ),TCS(NHEX,NZ),
     &              THSU(NHEX,NZ),TCSU(NHEX,NZ),
     &              TTS(NHEX,NZ),TSS(NHEX,NZ),
     &              TTSU(NHEX,NZ),TSSU(NHEX,NZ), Z(NZ)
      DIMENSION UTHZ(NHEX,NZ),UTCZ(NHEX,NZ),DUTH(NHEX,NZ),DUTC(NHEX,NZ),
     &          DUTT(NHEX,NZ),DUTS(NHEX,NZ)
      DIMENSION UUTH(NZ),UUTC(NZ), UUTHZ(NZ),UUTCZ(NZ)
      DIMENSION THT(NHEX),TCT(NHEX)
      DIMENSION UU(NODE),DUU(NODE)
C...
C...
C   Set the Non-negativity Constraint for the Dependent Variables
C ---------------------------------------------------------------
      DO 35 I=1,NODE
         IF(UU(I).LT.0.D0) UU(I)=0.D0
   35 CONTINUE
C...
C   Transfer the Variables from LSODES
C ------------------------------------
      DO 125 J=1,NHEX
         K=(4*(J-1)*NZ)
      DO 100 I=1,NZ
         UTH(J,I) = UU(K+I)
         UTC(J,I) = UU(K+I+NZ)
         UTT(J,I) = UU(K+I+NZ+NZ)
         UTS(J,I) = UU(K+I+NZ+NZ+NZ)
  100 CONTINUE
  125 CONTINUE
C...
C    FEED-BACK CONTROL APPLICATION
         RH(1) = RHO(1)*((THT(1)-THST(1))/(THUT(1)-THST(1)))
         RC(1) = RCO(1)*((THT(1)-THST(1))/(THUT(1)-THST(1)))
         RC(3) = RCO(3)*((THT(3)-THST(3))/(THUT(3)-THST(3)))
C
```

```
C   Set the Boundary Conditions
C -----------------------------
      DO 8900 J=1,NHEX
C        ------------------------------------
         CALL MIXH (J,RH,TH0,UTH,THT,NHEX,NZ)
         CALL MIXC (J,RC,TC0,UTC,TCT,NHEX,NZ)
C        ------------------------------------
 8900 CONTINUE
      UTH(1,1)  = TH0(1)
      UTC(1,NZ) = TC0(1)
      UTH(2,1)  = TH0(2)
      UTC(2,NZ) = TCT(1)
      UTH(3,1)  = THT(2)
      UTC(3,NZ) = TC0(3)
C...
C...
C   Evaluate the Spatial Derivatives
C ---------------------------------
      DO 175 J=1,NHEX
      DO 165 I=1,NZ
         UUTH(I)=UTH(J,I)
         UUTC(I)=UTC(J,I)
  165 CONTINUE
C     ------------------------------------------------
      CALL DSS020 (0.D0, L(J), NZ, UUTH, UUTHZ, +1.D0)
      CALL DSS020 (0.D0, L(J), NZ, UUTC, UUTCZ, -1.D0)
C     ------------------------------------------------
      DO 166 I=1,NZ
         UTHZ(J,I)=UUTHZ(I)
         UTCZ(J,I)=UUTCZ(I)
  166 CONTINUE
  175 CONTINUE
C...
C...
C   Assamble the Partial Differential Equations
C ---------------------------------------------
      DO 15 J=1,NHEX
         VHR=VH(J)*(1.D0-RH(J))
         VCR=VC(J)*(1.D0-RC(J))
      DO 10 I=1,NZ
C...
C   Partial Differential Equation for the Hot Fluid
C ------------------------------------------------
      DUTH(J,I) = - (VHR)*UTHZ(J,I) - (UH(J))*(UTH(J,I)-UTT(J,I))
C...
C   Partial Differential Equation for the Cold Fluid
C -------------------------------------------------
      DUTC(J,I) = + (VCR)*UTCZ(J,I) + (UC1(J))*(UTT(J,I)-UTC(J,I))
     &            + (UC2(J))*(UTS(J,I)-UTC(J,I))
C...
C   Partial Differential Equation for the Tube Wall
C ------------------------------------------------
      DUTT(J,I) = + (UT1(J))*(UTH(J,I)-UTT(J,I))
     &            + (UT2(J))*(UTC(J,I)-UTT(J,I))
C...
C   Partial Differential Equation for the Shell Wall
C -------------------------------------------------
      DUTS(J,I) = + (US(J))*(UTC(J,I)-UTS(J,I))
C...
```

```
   10 CONTINUE
   15 CONTINUE
C...
C...
C   Set the Temporl Derivatives at the Boundaries to Zero
C -------------------------------------------------------
      DO 18 J=1,NHEX
         DUTH(J,1)  = 0.D0
         DUTC(J,NZ) = 0.D0
   18 CONTINUE
C...
C...
      DO 205 J=1,NHEX
         K=(4*(J-1)*NZ)
      DO 200 I=1,NZ
         DUU(K+I) = DUTH(J,I)
         DUU(K+I+NZ) = DUTC(J,I)
         DUU(K+I+NZ+NZ) = DUTT(J,I)
         DUU(K+I+NZ+NZ+NZ) = DUTS(J,I)
  200 CONTINUE
         DUU((4*NHEX*NZ)+J) = DABS(THT(J)-THST(J))
         DUU((4*NHEX*NZ+NHEX)+J) = DABS(TCT(J)-TCST(J))
  205 CONTINUE
C...
      RETURN
      END
C...
C
*****************************************************************************
C
      SUBROUTINE PRINT (UU, TIME, TIME0, TSTOP, TPRINT, NI,NO,NOT,NOE)
C
*****************************************************************************
C
      IMPLICIT REAL*8 (A-H,O-Z)
      REAL*8   L
C...
      PARAMETER (NHEX=3, NZ=51, NODE=(NHEX*(4*NZ+2)))
C...
      COMMON/U/ UTH(NHEX,NZ),UTC(NHEX,NZ),UTT(NHEX,NZ),UTS(NHEX,NZ)
      COMMON/PARAM/ L(NHEX), VH(NHEX), VC(NHEX), UH(NHEX), UC1(NHEX),
     &              UC2(NHEX),UT1(NHEX),UT2(NHEX),US(NHEX),TH0(NHEX),
     &              TC0(NHEX), UTH0(NHEX,NZ), UTC0(NHEX,NZ),
     &              UTT0(NHEX,NZ), UTS0(NHEX,NZ)
      COMMON/BYPASS/ RH(NHEX),RC(NHEX),RHO(NHEX),RCO(NHEX),to,
     &               THST(NHEX),TCST(NHEX),THUT(NHEX),TCUT(NHEX)
      COMMON/ASTST/ THS(NHEX,NZ),TCS(NHEX,NZ),
     &              THSU(NHEX,NZ),TCSU(NHEX,NZ),
     &              TTS(NHEX,NZ),TSS(NHEX,NZ),
     &              TTSU(NHEX,NZ),TSSU(NHEX,NZ), Z(NZ)
      DIMENSION DTH(NHEX,NZ),DTC(NHEX,NZ),DTHU(NHEX,NZ),DTCU(NHEX,NZ)
      DIMENSION THT(NHEX),TCT(NHEX),
     &          DTHT(NHEX),DTCT(NHEX),DTHUT(NHEX),DTCUT(NHEX)
      DIMENSION DTT(NHEX,NZ),DTS(NHEX,NZ),DTTU(NHEX,NZ),DTSU(NHEX,NZ)
      DIMENSION ETH(NHEX),ETC(NHEX)
      DIMENSION UU(NODE)
C...
```

```
C...
      DO 35 I=1,NODE
         IF(UU(I).LT.0.D0) UU(I)=0.D0
   35 CONTINUE
C
      DO 125 J=1,NHEX
         K=(4*(J-1)*NZ)
      DO 100 I=1,NZ
         UTH(J,I) = UU(K+I)
         UTC(J,I) = UU(K+I+NZ)
         UTT(J,I) = UU(K+I+NZ+NZ)
         UTS(J,I) = UU(K+I+NZ+NZ+NZ)
  100 CONTINUE
         ETH(J) = UU((4*NHEX*NZ)+J)
         ETC(J) = UU((4*NHEX*NZ+NHEX)+J)
  125 CONTINUE
C
C   Set the Boundary Conditions
C -----------------------------
      DO 8900 J=1,NHEX
C        ------------------------------------
         CALL MIXH (J,RH,TH0,UTH,THT,NHEX,NZ)
         CALL MIXC (J,RC,TC0,UTC,TCT,NHEX,NZ)
C        ------------------------------------
 8900 CONTINUE
      UTH(1,1)  = TH0(1)
      UTC(1,NZ) = TC0(1)
      UTH(2,1)  = TH0(2)
      UTC(2,NZ) = TCT(1)
      UTH(3,1)  = THT(2)
      UTC(3,NZ) = TC0(3)
C
C...
      IF (TIME.EQ.TIME0) THEN
      WRITE(NO,1)
      WRITE(NOT,90)
      WRITE(17,192)
      WRITE(NOE,92)
C...
      NL=2*(NZ-1)/10
C...
      ENDIF
C...
C
      DO 210 J=1,NHEX
         DTHT(J)=THT(J)-THST(J)
         DTCT(J)=TCT(J)-TCST(J)
         DTHUT(J)=THT(J)-THUT(J)
         DTCUT(J)=TCT(J)-TCUT(J)
      DO 210 I=1,NZ
         DTH(J,I)=UTH(J,I)-THS(J,I)
         DTC(J,I)=UTC(J,I)-TCS(J,I)
         DTHU(J,I)=UTH(J,I)-THSU(J,I)
         DTCU(J,I)=UTC(J,I)-TCSU(J,I)
         DTT(J,I)=UTT(J,I)-TTS(J,I)
         DTS(J,I)=UTS(J,I)-TSS(J,I)
         DTTU(J,I)=UTT(J,I)-TTSU(J,I)
         DTSU(J,I)=UTS(J,I)-TSSU(J,I)
  210 CONTINUE
```

```
C
C...
      WRITE(NO,2) TIME,
     &            (THT(J),J=1,NHEX),(TCT(J),J=1,NHEX),
     &            (DTHT(J),J=1,NHEX),(DTCT(J),J=1,NHEX),
     &            (ETH(J),J=1,NHEX),(ETC(J),J=1,NHEX),
     &            (RH(J),J=1,NHEX),(RHO(J),J=1,NHEX),
     &            (RC(J),J=1,NHEX),(RCO(J),J=1,NHEX)
      WRITE(NO,3) (Z(I),I=1,NZ,NL)
      WRITE(NO,4)
      DO 110 J=1,NHEX
         WRITE(NO,5) J,(UTH(J,I),I=1,NZ,NL)
         WRITE(NO,7) (DTH(J,I),I=1,NZ,NL)
         WRITE(NO,9) (DTHU(J,I),I=1,NZ,NL)
         WRITE(NO,6) J,(UTC(J,I),I=1,NZ,NL)
         WRITE(NO,8) (DTC(J,I),I=1,NZ,NL)
         WRITE(NO,10) (DTCU(J,I),I=1,NZ,NL)
         WRITE(NO,96) J,(UTT(J,I),I=1,NZ,NL)
         WRITE(NO,98) (DTT(J,I),I=1,NZ,NL)
         WRITE(NO,910) (DTTU(J,I),I=1,NZ,NL)
         WRITE(NO,86) J,(UTS(J,I),I=1,NZ,NL)
         WRITE(NO,88) (DTS(J,I),I=1,NZ,NL)
         WRITE(NO,810) (DTSU(J,I),I=1,NZ,NL)
         WRITE(NO,*) ' '
  110 CONTINUE
C...
      WRITE(NOT,91) TIME,(DTHT(J),J=1,NHEX),(DTCT(J),J=1,NHEX),
     &                   (DTHUT(J),J=1,NHEX),(DTCUT(J),J=1,NHEX)
      WRITE(NOE,95) TIME,(ETH(J),J=1,NHEX),(ETC(J),J=1,NHEX)
      WRITE(17,191) TIME,DTH(1,NZ),DTC(1,1),DTT(1,NZ),DTS(1,1)
C...
    1 FORMAT(1H1,///,10X,' H E N    R e s u l t s',/,10X,24('-'),//)
    2 FORMAT(/,' Time    =',1X,F10.2,//,
     &         ' Hot Targets  :',3F10.4,/,
     &         ' Cold Targets :',3F10.4,/,
     &         ' +/- H_Targets:',3F10.4,/,
     &         ' +/- C_Targets:',3F10.4,/,
     &         ' ErrInt H     :',3(2X,F8.2),/,
     &         ' ErrInt C     :',3(2X,F8.2),/,
     &         ' RH           :',3(2X,F10.5),/,
     &         ' RHO          :',3(2X,F10.5),/,
     &         ' RC           :',3(2X,F10.5),/,
     &         ' RCO          :',3(2X,F10.5),/)
    3 FORMAT(  ' Z       =',21(7X,F4.2))
    4 FORMAT(1X,75('-'))
    5 FORMAT(  ' TH-',I1,'    =',21(F11.4))
    6 FORMAT(  ' TC-',I1,'    =',21(F11.4))
   96 FORMAT(  ' TT-',I1,'    =',21(F11.4))
   86 FORMAT(  ' TS-',I1,'    =',21(F11.4))
    7 FORMAT(  ' TH-THS  =',21(F11.4))
    8 FORMAT(  ' TC-TCS  =',21(F11.4))
   98 FORMAT(  ' TT-TTS  =',21(F11.4))
   88 FORMAT(  ' TS-TSS  =',21(F11.4))
    9 FORMAT(  ' TH-THSU =',21(F11.4))
   10 FORMAT(  ' TC-TCSU =',21(F11.4))
  910 FORMAT(  ' TT-TTSU =',21(F11.4))
  810 FORMAT(  ' TS-TSSU =',21(F11.4))
   90 FORMAT(' TIME     DTH_1   DTH_2   DTH_3   DTC_1   DTC_2   DTC_3',
     &          '  DTHU_1  DTHU_2  DTHU_3  DTCU_1  DTCU_2  DTCU_3')
```

```
   92 FORMAT(' TIME        ETH_1      ETH_2      ETH_3',
     &               '      ETC_1      ETC_2      ETC_3')
   91 FORMAT(F6.2,2X,12F8.3)
  192 FORMAT(' TIME     DTH_1    DTC_1    DTT_1    DTS_1')
  191 FORMAT(F6.2,2X,4F8.3)
   95 FORMAT(F6.2,2X,6F10.2)
C...
      RETURN
      END
C...
C ********************************************** C
      SUBROUTINE MIXH (J,RH,TH0,TH,THT,NHEX,NZ)
C ********************************************** C
      IMPLICIT REAL*8 (A-H,O-Z)
C...
      DIMENSION RH(NHEX),TH0(NHEX),TH(NHEX,NZ),THT(NHEX)
C...
      THT(J)=TH0(J)*RH(J)+TH(J,NZ)*(1.D0-RH(J))
C...
      RETURN
      END
C...
C ********************************************** C
      SUBROUTINE MIXC (J,RC,TC0,TC,TCT,NHEX,NZ)
C ********************************************** C
      IMPLICIT REAL*8 (A-H,O-Z)
C...
      DIMENSION RC(NHEX),TC0(NHEX),TC(NHEX,NZ),TCT(NHEX)
C...
      TCT(J)=TC0(J)*RC(J)+TC(J,1)*(1.D0-RC(J))
C...
      RETURN
      END
C...
C ********************************************************** C
      SUBROUTINE JACPDE (NODE, TIME, UU, J, IA, JA, PDJ)
C ********************************************************** C
      IMPLICIT REAL*8 (A-H,O-Z)
      DIMENSION UU(NODE),IA(1),JA(1),PDJ(1)
      RETURN
      END
```

REFERENCES

1. Hohmann, E. C., "Optimum Networks for Heat Exchange," Ph.D. Dissertation, University of South California, 1971.

2. Raghavan, S., "Heat Exchanger Network Synthesis: A Thermodynamic Approach," Ph.D. Dissertation, Purdue University, 1977.

3. Linnhoff, B., D. W. Townsend, D. Boland, G. F. Hewitt, B. E. A. Thomas, A. R. Guy and R. H. Marsland, *A User Guide on Process Integration for the Efficient Use of Energy*, Pergamon Press, New York, 1982.

4. Nishida, Y. A. Liu and L. Lapidus, "Studies in Chemical Process Design and Synthesis: III. A Simple and Practical Approach to the Optimal Synthesis of Heat Exchanger Networks," *Journal of American Institute of Chemical Engineers*, Vol. 23, pp. 77-93, 1977.

5. Konukman, A. E. Ş., U. Akman, H. Ütebay and M. C. Çamurdan, "Effects of Bypass-Stream Manipulations on Disturbance-Propagation Paths in Heat-Exchanger Networks," *DOĞA-Turkish Journal of Engineering and Environmental Sciences*, Vol. 19, pp. 43-51, 1995.

6. Mathisen K. W., S. Skogestad and E. A. Wolf, "Controllability of Heat Exchanger Networks," *paper 152n presented at Annual Meeting of the American Institute of Chemical Engineers*, LA, 14-19 November, 1991.

7. Mathisen K. W., S. Skogestad and T. Gunderson, "Optimal Bypass Placement in Heat Exchanger Networks," *paper 67e presented at Spring Meeting of the American Institute of Chemical Engineers*, New Orleans, 29 March-2 April, 1992.

8. Mathisen K. W. and S. Skogestad, "Design, Operation and Control of Resilient Heat Exchanger Networks," *paper 141g presented at Annual Meeting of the American Institute of Chemical Engineers*, Miami, 1-6 November, 1992.

9. Mathisen K. W., "Integrated Design and Control of Heat Exchanger Networks," Ph.D. Dissertation, University of Trondheim, 1994.

10. Konukman, A. E. Ş., U. Akman and M. C. Çamurdan, "Optimum Design of Controllable Heat Exchanger Networks Under Multi-Directional Resiliency-Target Constraints," *Computers and Chemical Engineering*, Vol. 19, pp. 149-154, 1995.

11. Raman, R., *Chemical Process Computations*, Elsevier Applied Science Publishers, New York, 1985.

12 Sinnot, R. K., J. M. Coulson and J. F. Richardson, *Chemical Engineering*, Vol. 6, Pergamon Press, New York, 1989.

13. Friedly, J. C., *Dynamic Behavior of Processes*, Prentice-Hall Inc., New Jersey, 1972.

14. Schiesser, W. E., and M. B. Carver, "Biased Upwind Difference Approximations for First-Order Hyperbolic (Convective) Partial Differential Equations," *paper 73d presented at Annual Meeting of the American Institute of Chemical Engineers*, New Orleans, 16-18 November, 1980.

15. Konukman, A. E. Ş., U. Akman and M. C. Çamurdan, "Optimum Design of Resilient and Controllable Heat Exchanger Networks," *Proceedings of the First National Chemical Engineering Congress*, Ankara, ODTÜ, 13-16 September 1994, Vol. 2, pp. 342-349, Ankara, Özdemir Basımevi, 1994.

16. Perry, R. H., and D. Green, *Perry's Chemical Engineers' Handbook*, Sixth Edition, McGraw-Hill, Singapore, 1984.

17. Ma, X. H., H. A. Preisig and R. M. Wood, "What Determines the Accuracy of the Low-Order Models for Heat Exchangers ?," *paper 130b presented at Annual Meeting of the American Institute of Chemical Engineers*, Miami, 2-6 November, 1992.

18. Edgar, T. F., and D. M. Himmelblau, *Optimization of Chemical Processes,* McGraw-Hill, New York, 1988.

19. Vanderplaats G. N., ADS-A Fortran Program For Automated Design Synthesis-Version 1.00, NASA Contractor Report 172460, Monterey, October 1984.

20 Yee, T. F. and I. E. Grossmann, "Simultaneous Optimization Models for Heat Integration - II. Heat Exchanger Network Synthesis," *Computers and Chemical Engineering*, Vol. 10, pp. 1165-1183, 1990.